

University of Windsor

Scholarship at UWindor

Electronic Theses and Dissertations

Theses, Dissertations, and Major Papers

2010

Calculation of Unsteady Loudness in the Presence of Gaps Through Application of the Multiple Look Theory

Helen Ule
University of Windsor

Follow this and additional works at: <https://scholar.uwindsor.ca/etd>

Recommended Citation

Ule, Helen, "Calculation of Unsteady Loudness in the Presence of Gaps Through Application of the Multiple Look Theory" (2010). *Electronic Theses and Dissertations*. 469.
<https://scholar.uwindsor.ca/etd/469>

This online database contains the full-text of PhD dissertations and Masters' theses of University of Windsor students from 1954 forward. These documents are made available for personal study and research purposes only, in accordance with the Canadian Copyright Act and the Creative Commons license—CC BY-NC-ND (Attribution, Non-Commercial, No Derivative Works). Under this license, works must always be attributed to the copyright holder (original author), cannot be used for any commercial purposes, and may not be altered. Any other use would require the permission of the copyright holder. Students may inquire about withdrawing their dissertation and/or thesis from this database. For additional inquiries, please contact the repository administrator via email (scholarship@uwindsor.ca) or by telephone at 519-253-3000ext. 3208.

Calculation of Unsteady Loudness in the Presence of Gaps Through Application of the Multiple
Look Theory

by

Helen Ule

A Dissertation
Submitted to the Faculty of Graduate Studies
through the Department of
Mechanical, Automotive and Materials Engineering
in Partial Fulfillment of the Requirements for the
Degree of Doctor of Philosophy at the
University of Windsor

Windsor, Ontario, Canada
2010

© 2010 Helen Ule

Calculation of Unsteady Loudness in the Presence of Gaps Through Application of the Multiple
Look Theory

by

Helen Ule

APPROVED BY:

Dr. Laura Wilber, External Examiner
Northwestern University

Dr. Nihar Biswas
Department of Civil and Environmental Engineering

Dr. Peter Frise
Department of Mechanical, Automotive and Materials Engineering

Dr. Edwin Tam
Department of Mechanical, Automotive and Materials Engineering

Dr. Colin Novak, Co-Advisor
Department of Mechanical, Automotive and Materials Engineering

Dr. Robert Gaspar, Co-Advisor
Department of Mechanical, Automotive and Materials Engineering

Dr. Thecla Damianakis, Chair of Defense
School of Social Work

September 28, 2010

DECLARATION OF ORIGINALITY

I hereby certify that I am the sole author of this dissertation and that no part of this dissertation has been published or submitted for publication.

I certify that, to the best of my knowledge, my dissertation does not infringe upon anyone's copyright nor violate any proprietary rights and that any ideas, techniques, quotations, or any other material from the work of other people included in my dissertation, published or otherwise, are fully acknowledged in accordance with the standard referencing practices. Furthermore, to the extent that I have included copyrighted material that surpasses the bounds of fair dealing within the meaning of the Canada Copyright Act, I certify that I have obtained a written permission from the copyright owner(s) to include such material(s) in my dissertation and have included copies of such copyright clearances to my appendix.

I declare that this is a true copy of my dissertation, including any final revisions, as approved by my thesis committee and the Graduate Studies office, and that this dissertation has not been submitted for a higher degree to any other University or Institution.

Abstract

Experimental studies have shown that for short gaps between 2 to 5 ms, the perceived loudness is higher than for uninterrupted noise presented to the ear. Other studies have also shown that the present temporal integration models for the calculation of time varying loudness do not adequately account for short duration phenomena.

It has been proposed that the multiple look approach is a more applicable method for describing these short term circumstances. This approach breaks a sound into small durations or looks having length of 1 ms which allows for the intelligent processing of the looks and decision making depending on the nature of the stimulus. However, present technologies (i.e. FFT) are not adequate to deal with short duration sounds across the entire frequency spectra. A compromised approach is taken here to account for perceived loudness levels for sounds in the presence of gaps while using an integration model. This approach is referred to as a multiple look gap adjustment model.

A model and software code was developed to take a recorded sound presented to the ear and process it into individual looks which are then examined for the presence of gaps ranging in length between 1 to 10 ms. If gaps are found, an appropriate gap adjustment is applied to the sound. The modified stimulus is subsequently evaluated for loudness level using a model which relies on temporal integration.

The multiple look model was tested using several sounds including mechanical and speech sounds and was found to perform as intended. While recommendations for improvement and further study are included, the application of the model has shown particular merit for perceptual analysis of sounds involving speech.

Dedication

I would like to dedicate this Doctoral dissertation to my Mother, Ivi Ule, and in loving memory of my father, Janez Ule. Also included are the friends closest to my heart. Thank you for all of your love, support, and sacrifice throughout my life.

Acknowledgments

I would like to acknowledge the inspirational instruction, guidance and support of my co-advisor Dr. Colin Novak for whom I could not have completed this effort without his assistance, tolerance, and enthusiasm.

I would also like my co-advisor Dr. Robert Gaspar who has always had time to listen to my thoughts, concerns and desires, no matter how elementary.

My sincerest thanks are given to my other dissertation committee members, Dr. Peter Frise, Dr. Edwin Tam, Dr. Nihar Biswas and the external examiner, Dr. Laura Ann Wilber.

Heartfelt gratitude is extended to all my friends for their support during this period of my life, especially my long time friend Paul Fedory for his guidance and expertise in computer programming languages.

Acknowledgement is also given for the generous support and assistance to my academic pursuits by Bruel & Kjaer.

Table of Contents

DECLARATION OF ORIGINALITY	III
ABSTRACT	IV
DEDICATION	V
ACKNOWLEDGMENTS	VI
LIST OF FIGURES	IX
LIST OF TABLES	XI
NOMENCLATURE	XII
I INTRODUCTION	1
II BACKGROUND	8
2.1 ANATOMY OF THE HUMAN AUDITORY SYSTEM	8
2.1.1 Outer Ear.....	9
2.1.2 Middle Ear.....	10
2.1.3 Inner Ear	11
2.2 CHARACTERISTICS OF LOUDNESS.....	14
2.3 MODELING LOUDNESS	17
III LITERATURE SURVEY	21
3.1 LOUDNESS MODELS.....	21
3.1.1 Stationary Loudness Models.....	23
3.1.2 Unsteady Loudness Models	36
3.2 LOUDNESS USING TEMPORAL INTEGRATION.....	41
3.3 RESEARCH SUPPORTING MULTIPLE LOOK APPROACH FOR LOUDNESS	45
3.4 SUMMARY	52
IV THEORY	57
4.1 TEMPORAL INTEGRATION.....	58
4.2 MULTIPLE LOOK.....	60
4.3 UNSTEADY LOUDNESS MODEL	63
V APPROACH	67
5.1 PROPOSED MODEL.....	68
5.2 TEST PROCEDURE	76
VI DISCUSSION OF RESULTS	80
6.1 STATIONARY PURE TONE SOUNDS	80
6.2 STATIONARY MECHANICAL SOUNDS.....	85
6.3 TIME VARYING (UNSTEADY) SOUNDS.....	89
VII CONCLUSIONS AND RECOMMENDATIONS	93
7.1 CONCLUSIONS	93
7.2 CONTRIBUTIONS.....	94

7.3 RECOMMENDATIONS	96
BIBLIOGRAPHY	98
REFERENCE A	104
REFERENCE B	116
REFERENCE C	169
VITA AUCTORIS	178

List of Figures

Figure 1: (a) Schematic Illustration Demonstrating the Concept of Frequency Masking where One Sound Component is Masked by a Lower Amplitude Sound and (b) Schematic Illustration Temporal Masking where a Brief Sound Followed by a gap and then a Second Sound is Masked (Defoe, 2007).	3
Figure 2: ISO 226:2003 Equal Loudness Contours which illustrate the extreme frequency dependence on perceived loudness (International Organization for Standardization, 2003).	4
Figure 3: Schematic of the ear showing the main anatomical components of the outer, middle and inner ear (Science Kids).....	9
Figure 4: The transfer function, or frequency response, of the outer ear, including the resonance effects of the auditory canal at approximately 4 kHz (Everest & Pohlmann, Master Handbook of Acoustics, 2009).	10
Figure 5: Schematic of the cochlea stretched out showing the path of excitation through the cochlear fluid and along the basilar membrane (Hearing Aids Central.com).....	12
Figure 6: Relative position of excitation along the basilar membrane with respect to frequency. Low frequency excitation is located at the base of the membrane while high frequency excitation is found at the apex near the round window (Howard & Angus, Acoustics and Psychoacoustics, 2006).	12
Figure 7: a) Idealized critical band filter envelope of excitation along the basilar membrane showing an assumed frequency bandwidth shape, b) idealized bank of several critical filter envelopes (Howard & Angus, Acoustics and Psychoacoustics, 2006).	14
Figure 8: a) Three sounds having the same sound pressure level but varying bandwidths centred about 1 kHz, b) Subjective loudness for equal sound pressure levels showing an increase in loudness for bandwidths greater than 160 Hz (Everest & Pohlmann, Master Handbook of Acoustics, 2009).	16
Figure 9: Effect of duration on the perceived loudness for a steady tone where the loudness of the tone linearly increases for durations up to 200 ms after which the loudness becomes steady (Howard & Angus, Acoustics and Psychoacoustics, 2006).	17
Figure 10: Schematic of Specific Loudness Plot, or Loudness Value per Critical Bark Band measured in sone. Also Illustrated is the Area under the Specific Loudness Curve N' which is Directly Proportional to the Total Perceived Loudness (Bruel & Kjaer).	28
Figure 11: Masking patterns of narrow-band noise centred at 1 kHz with a bandwidth of 160 Hz at different levels LCB (Bruel & Kjaer).	29
Figure 12: Comparison of Zwicker's Critical Bandwidths to Glasberg and Moore's Equivalent Rectangular Bandwidths which demonstrate the low frequency errors resulting from Zwicker's listening experiments (Seeber, 2008).	34
Figure 13: Perceived difference in sound level in dB of two pulses with varying separation times and a single pulse showing an increased detectability for shorter separation times in ms (Viemeister & Wakefield, 1991).....	47

Figure 14: Schematic illustration of Viemeister’s experiment where pip signals are presented individually and simultaneously within two 10 ms gaps in the presence of a varying masker noise signal (Viemeister & Wakefield, 1991). 49

Figure 15: Graphical representation of the transfer function representing the effects of the outer and middle ear on the time waveform input. The result of this filter is a representation of the sound at the cochlea (Moore, Glasberg, & Baer, A Model for the Prediction of Thresholds, Loudness and Partial Loudness, 1997)..... 64

Figure 16: Sinusoidal representation of a 1 ms WAV file comprised of 32 samples which are given by hexadecimal values. Defined are the amplitudes for the Peak and RMS pressures of the sound wave 69

Figure 17: Flow chart illustrating the proposed model from input of WAV file, conversion to 1 ms looks and search and adjustment procedure for the presence of gaps. The adjusted file is subsequently reversed back to a WAV file format suitable for the calculation of loudness..... 72

Figure 18: Photograph of the experimental set up in the Semi-Anechoic room showing the Bruel & Kjaer acquisition system, amplifier loudspeaker and microphone. The test sounds are generated by the PULSE sound generator and played by the loudspeaker and subsequently recorded through the microphone. The acquisition system then prepares the WAV file for the multiple look gap correction and loudness programs. 78

Figure 19: Time domain plot for the 90 dB sinusoidal test sound without the modifications of inserted gaps in the signal 81

Figure 20: Time domain plot for the 90 dB sinusoidal test sound with the addition of inserted gaps in the signal with position and gap durations as specified in Table 4 81

Figure 21: Output of the multiple look program which shows the number of gaps found in the 90 dB gapped input file and the corresponding durations. Also given is the calculated loudness level using the integrated Cambridge model..... 85

Figure 22: Time domain plot for the white noise test signal without the modifications of inserted gaps in the signal used for the calculation of loudness level with and without the multiple look model 86

Figure 23: Time domain plot for the white noise test signal with the addition of inserted gaps in the signal with position and gap durations as specified in Table 4 used for the calculation of loudness level with and without the multiple look model. 86

Figure 24: Time domain plot for the warble sound used for the calculation of loudness level with and without the multiple look model. 87

Figure 25: Time domain plot for the recorded diesel engine sound used for the calculation of loudness level with and without the multiple look model. 87

Figure 26: Time domain plot for the spoken sentence, “Suzie sold seashells by the seashore”, chosen for its smooth cadence and expected lack of gaps. 90

Figure 27: Time domain plot for the spoken sentence, “Clickity clack, the train went down the track”, chosen for its rougher cadence and expected gaps in the signal. 90

List of Tables

Table 1: Zwicker's 24 critical bands having unit of Bark and the corresponding bandwidth and centre frequencies having units of Hz	27
Table 2: Evolution of the significant work leading to the development of both stationary and unsteady loudness models, including the significance of each milestone.	40
Table 3: Detection correction levels for applied for corresponding gap durations to the 1 ms looks	71
Table 4: Position in signal duration having inserted gap, the length of the gap and corresponding adjustment	82
Table 5: Loudness level for 1000 Hz sinusoidal signals without inserted gaps calculated using DIN 45631, Cambridge model and with multiple look gap correction model	83
Table 6: Loudness level for 1000 Hz sinusoidal signals with gaps inserted calculated using DIN 45631, Cambridge model and with multiple look gap correction model	83
Table 7: Loudness levels for steady mechanical sounds (white noise, warble and diesel) calculated using the Cambridge model and multiple look gap correction model.	88
Table 8: Loudness levels for time varying sinusoidal sweep and speech sounds calculated using the Cambridge model and multiple look gap correction model.	91

Nomenclature

AGC	automatic gain control
ANSI	American National Standards Institute
dB	decibel
CPB	constant percentage bandwidth
DIN	Deutsches Institut fur Normung
DSP	Digital Signal Processing
ERB	Equivalent Rectangular Bandwidths
f_T	Frequency of test tone
F	represents the fraction of the difference between the summation of all the loudness within a given band and the maximum band loudness
FFT	Fast Fourier Transform
h_r	height of water in container (from example in Chapter 4)
h_{r0}	initial height of water in the container (from example in Chapter 4)
$h_r(t)$	response to a sound with duration t (from example in Chapter 4)
HATS	head and torso simulator
Hz	Hertz
ISO	International Standards Organization
kHz	Kilohertz, 1000 Hertz
I	rate of water leaking out (from example in Chapter 4)
I_T	level of test tone
ms	milliseconds, 1/10 second
N	loudness
ns	nanoseconds
R	rate of rain (from example in Chapter 4)
RPM	revolutions per minute
S	loudness
S_m	maximum loudness
S_t	total loudness
SPL	sound pressure level
STEP	spectral-temporal excitation patterns
t	duration (from example in Chapter 4)
t_i	integration time constant (from example in Chapter 4)
TVL	time varying loudness
WAV	Windows Wave (audio format/file extension)
τ	leak rate (from example in Chapter 4)

I Introduction

The ability to hear and discriminate sounds is a critical sensory mechanism in humans as it enables them to communicate and to react to auditory stimuli within their environment. Communication is necessary for the maintenance of social relationships and the ability to detect and analyze sounds within the environment. It is critical to an individual's ability to understand its surroundings and to its overall quality of life.

The physical manifestation of sound is that of vibrations of air molecules propagating through a medium. The human auditory system has the complex task of transforming this sound into something meaningful. The auditory system is a complex one for which much is still not understood in regard to the extensive processing of the physical stimulus of sound into a psychoacoustic perception of the stimulus.

From an engineering perspective, the goal is often to finding the source mechanisms of a sound in the hope of altering them to either attenuate the noise or improve its quality from a perceptual perspective. The latter is referred to as the science of psychoacoustics or sound quality. In order to perform this task adequately it is also important that engineers understand the mechanisms of the human auditory system that influence these perceptions; that is, the relationships between the sound characteristics entering the ear and the perceptual sensations which they produce. Unfortunately it is difficult to understand both what the auditory system does and how it works. This is because the perceptual components of hearing a sound cannot entirely be explained by a simple understanding of the anatomy of the auditory system. Much of what is known about the perception of sound has been surmised by scientists

and engineers through psychophysical experiments for which the results have been used to model the perception and discrimination of sound. It is from these observed results that engineers have developed the mathematical models to predict the sound quality attributes of sounds. That is, they attempt to predict the perceived sound quality of a sound in the hopes of either determining a best sound from an array of product samples or perhaps to modify the sound to improve its quality.

The most fundamental of all of the psychoacoustic metrics is loudness, a model for which many other metrics rely on for the basis of their calculation algorithms. Loudness is said to be a metric which closely matches the perceived intensity of a sound, however, this should not be confused with the physical quantity of sound intensity. Loudness is a psychological quantity measured by a human listener. "On physical grounds alone, one expects that loudness should be different from intensity because the ear does not transmit all frequencies equally, i.e. it does not have a flat frequency response." (Hartmann, 1998) This nonlinearity in frequency is due to the geometry of the outer ear, resonances within the human ear canal and bone conduction. This results in a transfer function having resonances in the 3 kHz to 12 kHz frequency range. In other words, the magnitude of the acoustic stimulus input to the nervous system does not depend on a physical quantity of intensity alone and is instead largely frequency dependant. It is this fact which has lead to the development of the equal loudness contours first plotted by Fletcher and Munson at the Bell Laboratories (Fletcher & Munson, 1933) .

Another characteristic of loudness which involves frequency is frequency masking. Here, a sound or a frequency component of a lower amplitude sound is covered by another sound, or component of a sound with a similar frequency makeup. If a sound is unsteady in nature, another type of masking which can occur is called temporal or time masking. This can occur

when one sound, or component of a single sound, follows very closely after another in time. Figures 1(a) and 1(b) are schematic illustrations of frequency and temporal masking respectively (Defoe, 2007). The concept of temporal masking will be shown to be a very important component of this dissertation as it is associated with the perception of loudness for unsteady sounds.

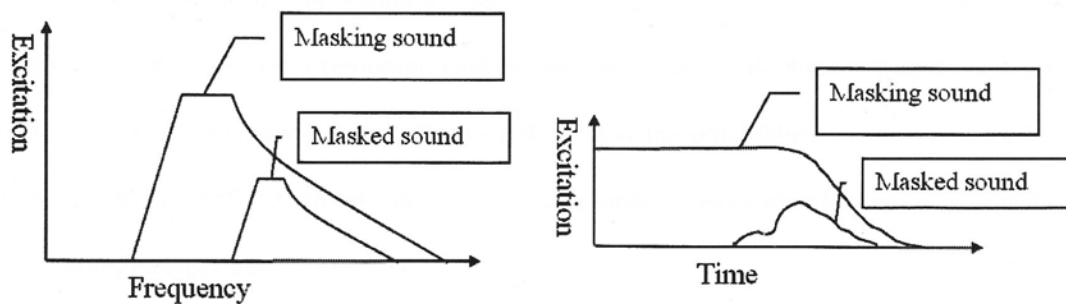


Figure 1: (a) Schematic Illustration Demonstrating the Concept of Frequency Masking where One Sound Component is Masked by a Lower Amplitude Sound and (b) Schematic Illustration Temporal Masking where a Brief Sound Followed by a gap and then a Second Sound is Masked (Defoe, 2007).

Examination of the standardized ISO 226:2003 equal loudness contours given in Figure 2 illustrates the frequency dependence on the perception of sound due to the nonlinearity of the human auditory system at the low and high frequency extremes. The initial equal loudness contours which were later standardized were developed using jury testing techniques. For this, pure tones sounds were played to jurors who were asked to rate the loudness of successive tones at varying sound pressure amplitudes and frequencies compared to a 1000 Hz reference tone. The unit given to loudness on the equal loudness plots is the phon (pronounced as fawn). The reference line for the equal loudness contour is defined as the 40 phon line. For this plot, a 1000 Hz tone will have both a loudness of 40 phons and a sound pressure level of 40 dB. As the frequency is decreased it is observed that the equal loudness contour for the 40 dB line begins

to slope upwards illustrating a decrease in ability of the human ear to perceive sounds at these lower frequencies. A similar trend is illustrated as the frequency increases above 1 kHz. The exception to this is a dip or enhanced acuteness to sound within the frequency range of approximately 4000 Hz. This is due to resonances within the human ear canal which act as a quarter wave resonator. Examination of the 40 phon line at 100 Hz shows that the sound pressure level of a sound would need to be approximately 65 dB to sound as equally loud as the 1000 Hz at 40 dB.

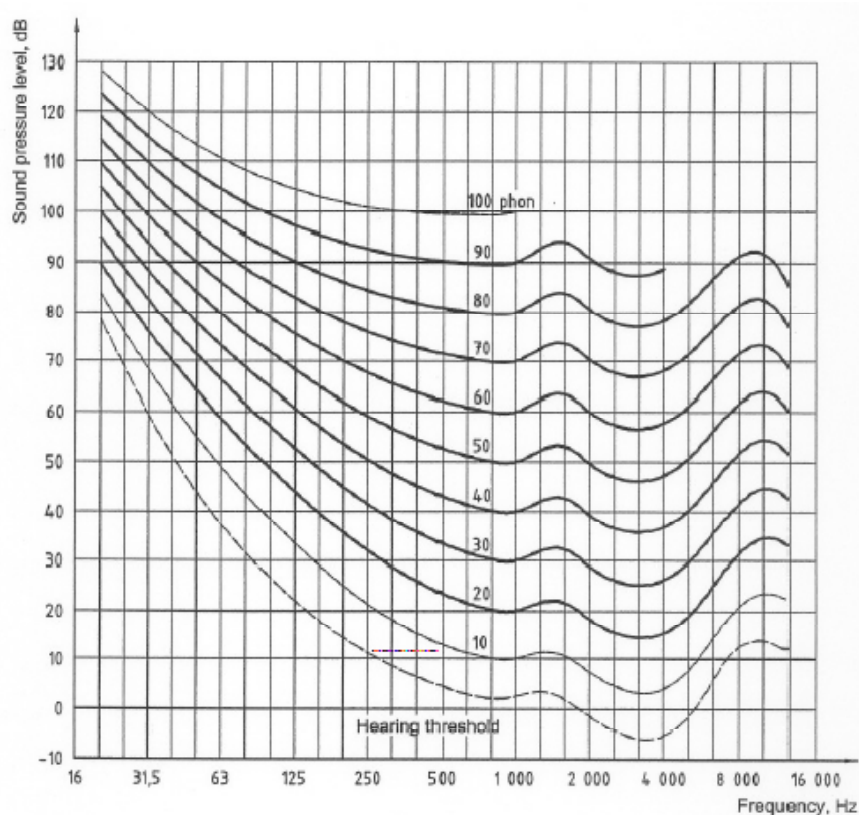


Figure 2: ISO 226:2003 Equal Loudness Contours which illustrate the extreme frequency dependence on perceived loudness (International Organization for Standardization, 2003).

Loudness in phons can also be expressed as loudness level with the unit of sones where the 40 phon line represents 1 sone. For an increase in loudness by 10 phons, a double in loudness level is realized. For example, 40 phons is 1 sone, 50 phons are 2 sones, 60 phons are 4 sones etc.

It should be noted that the representation of loudness using the equal loudness contours is rather simplistic in that it is a representation of pure tones only and not of more realistic complex sounds found in real life experience. For the estimation of loudness for real sounds, complex loudness models are needed. These models are divided into two fundamental types, being loudness models for stationary or steady sounds which do not change with time and more complex non-stationary models used for the calculation of loudness of unsteady sounds. Several calculation techniques for both types can be found in the literature and are discussed in greater detail in Chapter 3. It should be recognized that the mechanisms underlying the perception of loudness are not all fully understood and that these models are only best approximations and are still fought with uncertainties and assumptions.

The focus of this dissertation is on the more complex determination of loudness for unsteady sounds. To date, the generally accepted approaches to the calculation of unsteady loudness use the method referred to as temporal or long term integration where the intensity of the unsteady signals are integrated over time. Psychoacoustic studies have found this method to be acceptable for sounds which do not change significantly over durations of approximately 100 ms or longer. However, it has been known for many years (Exner, 1876) that the absolute thresholds of sounds are strongly dependent upon duration as well as frequency. Experiments have shown that the perceived absolute thresholds are increased for sounds which are short in duration or in the presence of gaps. The use of temporal integration methods cannot account

for the short duration data, and therefore, cannot be considered to be good predictors of loudness for all signal types.

An alternative theory which is thought by some to be a better representative auditory model of the human hearing system is called the multiple look approach. The premise of the multiple look theory is that the auditory system takes many samples or “looks” of a stimulus and stores them into memory for later processing. The specific processing performed is dependent on the makeup of the signal contained in the successive look. For the case where gap or burst of information is present, the short term looks are processed immediately as an auditory perception. If the signal is steadier in nature, the looks are instead stored for a longer period and then processed as an integrated signal over time, synonymous with the concept of a leaky integrator model.

The caveat of the multiple look approach is that it cannot be adequately implemented using present day technology over the full auditory frequency range given the limitations of present day digital signal processing techniques. That is, the DSP cannot adequately sample short duration signals with a low enough frequency resolution to cover the full auditory range.

The objective of this work is to develop an alternative model which will account for the hearing phenomena demonstrated by the experiments supporting the multiple look theory while at the same time be viable to implement in light of the present day limitations of signal processing capabilities. The proposed model is a hybrid multiple look approach which uses level correction factors in conjunction with temporal integration methods in order to adequately represent the perceived loudness levels in the presence of gaps in a stimulus signal.

In addition to the solution statement above, the scope leading to the objective is to ensure flexibility and wide use adaptability of the model. As will be detailed further in this report, it is intended that the multiple look model developed will be integrated into existing and future loudness models using integration theory. As such, the model developed here should be easy to integrate into any of these loudness models. While this work is focused on the hearing phenomenon of gap detection, the algorithm should be easily adaptable to other attributes such as burst detection. The code should be open and allow for modifications to its parameters and correction values in order to accommodate new empirical data in the future. Finally, the method developed model should be well suited to be used for other psychoacoustic metric such as speech intelligibility.

The layout of this dissertation is as follows. Given the nature of the material presented in the literature review section, some background information is first provided in Chapter 2. The intent is to provide fundamental information in regard to how the auditory system functions as well as a more thorough description of the mechanisms related to the perception of loudness and how it is modeled. This information is necessary for the non audiologist in preparation for Chapter 3 which is a traditional presentation of the literature review which identifies the present state of art. Chapter 4 provides the background theory of the calculation processes which is necessary to bridge the gap between Chapter 2 and the methodology details given in Chapter 5. A detailed description of the multiple look gap correction model developed in the dissertation as well as the experimental setup is given in Chapter 5 followed by a presentation of the results in Chapter 6. Finally, a discussion of the conclusions and recommendations for future work will be provided in the final chapter.

II Background

Acoustics is a well developed science of the study of sound from a physical perspective. It deals with the quantification of the physical parameters of sound power or sound pressure. Psychoacoustics is the study of how we perceive sounds. This includes the quantification of how good or how bad a noise source sounds is perceived to be by an individual listener. In order to study psychoacoustics, it is necessary to first understand the physiology and workings of the human ear. This chapter will describe the main anatomical structure of the human ear as well as how these mechanisms are related to how humans perceive sounds. Also described will be the psychoacoustic metric of loudness including the link between the functional components of the ear and this perceptual metric. The discussions on loudness will include models that are for both stationary sounds which do not change with time as well as unsteady sounds. It should be noted though that much of the present understanding of hearing perception is based on listening experiments where controlled sounds are introduced to listeners and their responses are correlated to the inputs. While the responses to these experiments cannot often be described by the physiology of the hearing system in term of physical means, they do provide a foundation to the understanding of hearing perception and psychoacoustics.

2.1 Anatomy of the Human Auditory System

The anatomy of the human ear is divided into three fundamental sections as illustrated in Figure 3. These three sections are comprised of the outer ear which acts not only as a receptor device but has other important functions including sound localization. The middle ear acts as a mechanical amplifier of the sound waves which reach the tympanic membrane, or eardrum. The inner ear performs many of the functions which dictate hearing perception. A more detailed description of each of these components which make up the ear is given below.

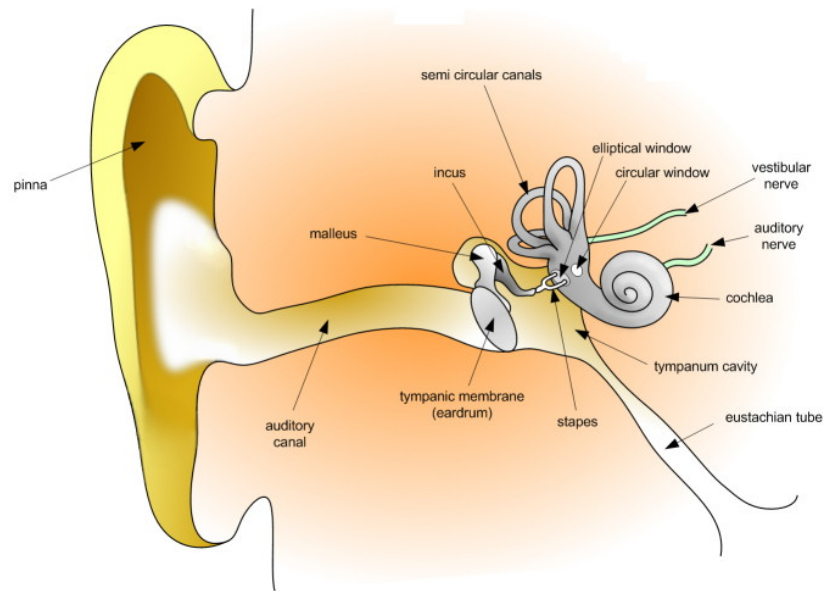


Figure 3: Schematic of the ear showing the main anatomical components of the outer, middle and inner ear (Science Kids).

2.1.1 Outer Ear

The outer ear consists of the pinna, concha and the auditory, or ear canal. The pinna is the external tissue which is comprised of grooves and depressions. The pinna acts as a noise collection device which has a similar effect to holding your open hand around your ear to direct noise into the ear. The main depression or cavity before the auditory canal is the concha. Together the pinna and concha aid in the effort of sound localization to determine the front to back and up and down positioning of a sound source. The auditory canal directs the sound to the tympanic membrane while at the same time offering some protection to the membrane. The approximately 25 mm long auditory canal, as well as the pinna and concha modify the frequency response of incoming sounds as shown in the transfer function in Figure 4. The auditory canal has

the most significant effect by amplifying sounds by several decibels in vicinity of the 4 kHz frequency range. It does so by acting as a quarter wave resonator, very much like an organ tube. The sound waves strike and cause the tympanic membrane, a very thin elastic boundary separating the outer and middle ear, to vibrate. The displacement of the ear drum is 10^{-3} nm at threshold of hearing (about 3/100 diameters of the hydrogen atom) and 10^3 nm at the threshold of pain.

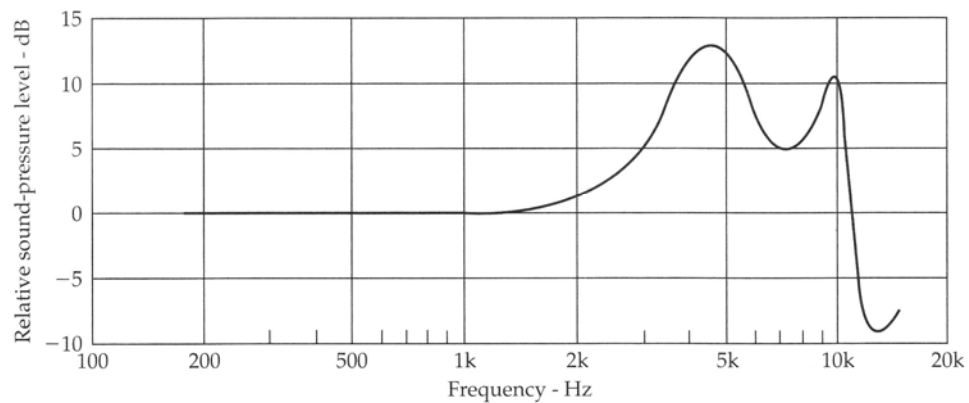


Figure 4: The transfer function, or frequency response, of the outer ear, including the resonance effects of the auditory canal at approximately 4 kHz (Everest & Pohlmann, Master Handbook of Acoustics, 2009).

2.1.2 Middle Ear

The middle ear is comprised of three tiny bones called the ossicles which is made up of the malleus, the incus and the stapes. Just as the malleus is fixed to the tympanic membrane, so is the stapes to the oval window at the boundary to the inner ear. The purpose of the middle ear is to transmit the excitation of the tympanic membrane to the relatively incompressible cochlear fluid inside known as perilymph without significant energy loss. Given that the energy transfer is from air to a liquid, a significant impedance change must be overcome. In this case, the impedance ratio is

approximately 4000:1. This is accomplished in two ways. The first is the mechanical advantage realized from the ossicles which act as three mechanical levers. The second is from the area difference between the tympanic membrane and the footplate of the stapes on the oval window. As a result, the pressure increase from the input to the malleus at the tympanic membrane to the output at the foot of the stapes into the oval window is approximately 33.8 times. A second function of the middle ear is to protect the auditory system from excessively loud sounds. This is accomplished by two muscles called the tensor tympani and the stapedius which contract and stiffen the ossicles system when exposed to sounds in excess of 75 dB pressure level. This phenomenon is known as the 'acoustic reflex' and provides approximately 12 to 14 dB of attenuation for frequencies below 1000 Hz.

2.1.3 Inner Ear

The inner ear is comprised of a snail shaped bone structure which is about the size of a pea called the cochlea. The function of the cochlea is to convert the mechanical vibrations induced into the cochlea by the stapes at the oval window into nerve impulses or firings to the brain to be processed into acoustic impressions.

The fluid filled cochlea is approximately 25 mm long and coiled about 2.75 turns. It is divided along its length by two membranes called Reissener's membrane and the basilar membrane. Shown in Figure 5 is a schematic of the cochlea stretched out which shows the position of input vibration at the stapes into the cochlea. This energy then propagates along the length of the cochlea then down and back again to the round window causing an outward movement resulting in a pressure release. It is on the basilar membrane that standing waves are set up along its length and are positioned

depending on the frequency of the pressure excitation. As shown in Figure 6, low frequency excitations are located near the end of the basilar membrane while high frequency excitation has maximum amplitude at the apex near the oval window.

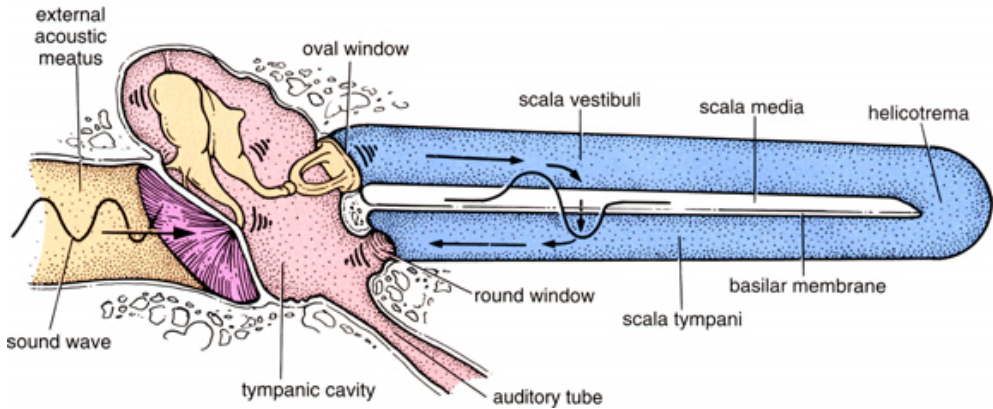


Figure 5: Schematic of the cochlea stretched out showing the path of excitation through the cochlear fluid and along the basilar membrane (Hearing Aids Central.com).

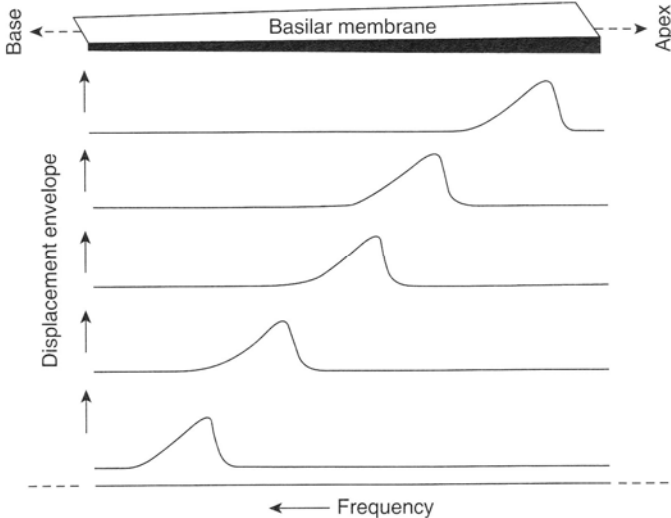


Figure 6: Relative position of excitation along the basilar membrane with respect to frequency. Low frequency excitation is located at the base of the membrane while high frequency excitation is found at the apex near the round window (Howard & Angus, Acoustics and Psychoacoustics, 2006).

Located along the basilar membrane are thousands of hair-like structures containing tiny hair bundles called stereocilia. When waves are set up on the basilar membrane, the stereocilia are bent which in turn results in discharges of electrical signal which initiate neural discharges to the auditory nerve and then to the brain. The firing of a neural discharge will initiate the firing of an adjacent fibre. It is believed that the loudness of a sound is proportional to the number of nerve fibres excited and repetition rate of the firing. It should be noted that a thorough understanding of how the inner ear and brain works is not yet known (Everest & Pohlmann, Master Handbook of Acoustics, 2009).

For a future understanding of loudness perception, it should be understood how the excitations along the basilar membrane relate to perceived frequency. The response is very much like a constant percentage band filter on an acoustic analyzer where the frequency response is divided into bands or envelopes with the width of each envelope increasing by the same percentage of the centre frequency of the band. For a one third octave analyzer, the width of each frequency band is a constant 23 percent of the band's centre frequency. The response along the basilar membrane acts in a very similar manner. Here, each band is often referred to as critical band (also referred to as Bark bands). Other theories exist which differ somewhat in the shape of the bandwidth windows. One such alternative is given by Glasberg and Moore who defined the bandwidths by Equivalent Rectangular Bandwidths (ERBs) (Glasberg & Moore, 1990). More detail to the different approaches is given in Chapter 3. Shown in Figure 7 is an idealized frequency response on the basilar membrane for a localized frequency excitation as well as a broadband excitation. The exact widths and locations of the

critical band centre frequencies is still unknown and gives rise to the different theories and approaches for the calculation of loudness.

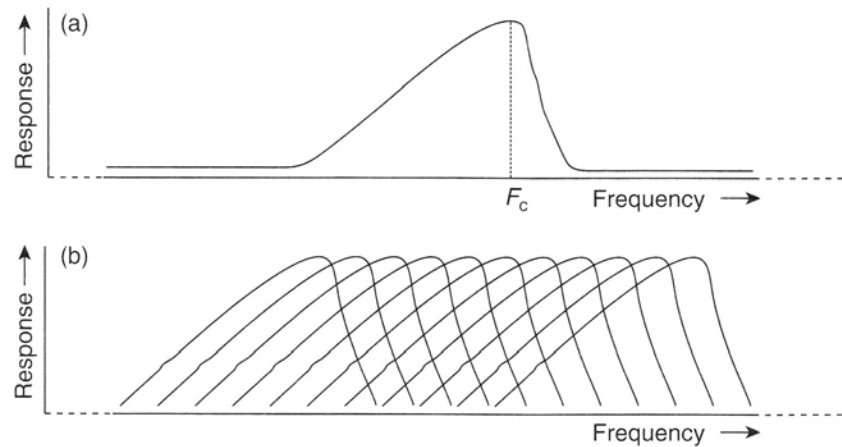


Figure 7: a) Idealized critical band filter envelope of excitation along the basilar membrane showing an assumed frequency bandwidth shape, b) idealized bank of several critical filter envelopes (Howard & Angus, Acoustics and Psychoacoustics, 2006).

2.2 Characteristics of Loudness

As described in Chapter 1, the work done by Fletcher and Munson (Fletcher & Munson, 1933) on the equal loudness curves (Figure 2) provided the foundation for the later development of models for the calculation of loudness. The unit for loudness which corresponds to the subjective impression of the intensity of a sound is the sone. The sone is defined as a subjective unit because a doubling of perceived loudness of a sound corresponds to a doubling of the amount of sones for the sound. Loudness is not a pure physical measurement as in the case of a sound pressure level having units of dB. Loudness is a subjective prediction which includes the

complex auditory responses to a sound stimulus including, for example, frequency masking, and for the case of unsteady sounds, time masking.

Discussion of loudness perception with respect to the equal loudness curves is restricted to the impressions of pure tone frequencies. Broadband sounds also have an effect on loudness which is different from pure tones. For example, the broadband sound of a passing bus of sound pressure level equal to that of a pure tone sound will sound much louder. Presented in Figure 8(a) are three sounds having equal sound pressure level but different bandwidths as described by Everest and Pohlmann (Everest & Pohlmann, Master Handbook of Acoustics, 2009). The heights representing the sound intensity per Hz vary such that they all have equal areas. However, as shown in Figure 8(b), the three sounds do not have equal loudness. The perceived loudness of the sounds increases for increased bandwidths greater than 160 Hz. This has been determined experimentally through listening tests. The reason for the increased threshold of perceived loudness for bandwidths greater than 160 Hz is due to the fact that 160 Hz is the approximated critical bandwidth for the human auditory system at 1 kHz. In other words, for sounds having bandwidths greater than 160 Hz, the spread of excitation would be across multiple critical bandwidths which results in a perceived increase of loudness.

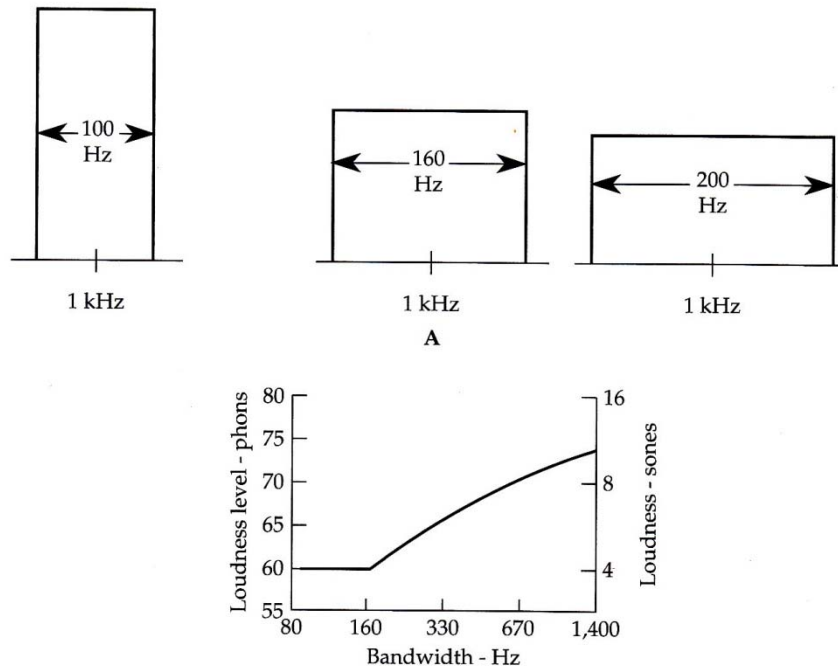


Figure 8: a) Three sounds having the same sound pressure level but varying bandwidths centred about 1 kHz, b) Subjective loudness for equal sound pressure levels showing an increase in loudness for bandwidths greater than 160 Hz (Everest & Pohlmann, Master Handbook of Acoustics, 2009).

In addition to the amplitude and frequency of a sound, the duration for which the sound occurs also affects the loudness of the sound. Shown in Figure 9 is an illustration of loudness with respect to time for a steady tone. For a steady sound it can take approximately 200 ms to reach full loudness. For unsteady sounds, the relationship between loudness and duration is more complicated. The presence of short duration bursts in the sound can have the effect of masking other sounds which occur as late as 20 ms after the burst. Conversely, the presence of a gap in a sound has been shown to increase the perceived thresholds of adjacent sounds by up to 4 dB and for as long as 10 ms.

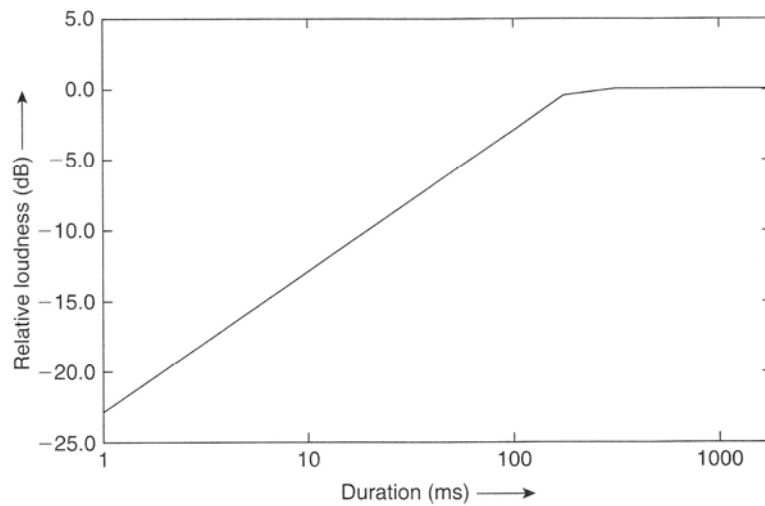


Figure 9: Effect of duration on the perceived loudness for a steady tone where the loudness of the tone linearly increases for durations up to 200 ms after which the loudness becomes steady (Howard & Angus, Acoustics and Psychoacoustics, 2006).

2.3 Modeling Loudness

Given the descriptions above which detail the complexity of the auditory system, it is easy to appreciate the difficulty in developing a model for the calculation of loudness. This is certainly true enough for stationary sounds but the degree of complexity is increased many times for the prediction of loudness for unsteady sounds. The effect that the time component has on perceived loudness and the mechanisms which influence it are still not greatly understood. What is known from the many listening experiments since the 1930s are just some of the phenomena that the time component of a sound has on how we perceive these unsteady sounds.

Many models for the calculation of steady loudness have been developed over the years, each new model having an increased complexity in procedure and a corresponding better correlation to the listening experiments. The different models also have a similar fundamental

methodology, from the input of the steady sound signal to the loudness output result. Where the differences between the different models lie is very much in the details and accuracy of the individual steps; details which have been improved on over the years as the understanding of the auditory system has increased as well as improved technology to process sounds due to faster computers and complex digital signal processing technologies.

While greater detail of the various models which have been developed over time will be presented in Chapter 3, a brief outline of the common steps of the calculation of loudness are given as follows:

- The sound is inputted into the model as a spectrum of the steady sound. Earlier models accepted octave spectra while the more modern (and accurate) models use third octave spectra or critical band levels as the input of choice. More complicated models allow the user to define the conditions of the acquisition of the input data as either free field, diffuse field or in some cases binaural.
- A transfer function representing the outer and middle ear is applied to the input spectra. This is one area where knowledge of these transfer functions has improved over the years. A very common error found in the practice of calculating loudness is that if the input signal is initially acquired using a binaural head and torso simulator (HATS), the application of the transfer function of either the outer or outer and middle ear (depending on manufacturer of the HATS) should be omitted. This is because the design of the HATS is intended to include the effects of the transfer function during acquisition of the sound.

- The excitation pattern at the cochlea is determined. This is another aspect of the model which has shown improvement given better knowledge of the excitation pattern from listening experiments.
- The excitation is then transformed into a specific loudness plot where the loudness in sones per critical band is plotted across the frequency range of hearing.
- The final step is to integrate the specific loudness curve to get the overall loudness of the input spectra.

While most of the loudness models in existence are designed for stationary sounds, a few models have also been developed for the calculation of loudness for unsteady sounds. It is worthwhile noting that the application of steady loudness models has at times been inappropriately applied to unsteady sounds. Some commercial software programs simply apply a stationary loudness model to short samples of time and have been marketed as unsteady loudness models. These software though do not give results which correlate well to human listening experiments as the stationary models cannot account for the temporal aspects of hearing perception. The real unsteady loudness models do account for the temporal effects of hearing through various methods. The most common of these is the integration of the signal over time. The more precise models will employ several integration techniques including short term integration for samples as short as 1 ms followed by long term integration for signal as long as 10 ms, 50 ms or several hundred milliseconds. One of the integration techniques commonly applied is called a 'leaky integrator' which will be discussed in more detail in Chapter 4. There is much debate though on the applicability of these integration techniques and whether the human auditory system really uses such a straight forward summation of energy. This has lead to alternative theories for which the multiple look approach is the most widely accepted. This theory suggests that sound is sampled by the auditory system in very short

durations, or 'looks' and then either applies the looks immediately to subsequent looks for more continuous sounds or instead stores this information for later processing in the case of more discontinuous sounds. More detail in regard to the studies supporting the multiple look theory and how it can be applied in practice to the calculation of loudness is given in the next chapters.

III Literature Survey

Much remains to be understood of all the processes associated with the human auditory system. While the physiology of the ear is well known, an all encompassing model which accurately predicts the perceptual results of all given stimuli remains to be found. The knowledge of how humans perceive certain sounds is based on listening experiments which have been developed and carried out over many years, mostly since the 1930s. From these experiments, several models have been developed to predict the perceived intensity of sounds. Adequate models used in practice for stationary sounds have been available since the early 1970s (Zwicker, Fastl, & Dallmayr, 1984) (International Organization for Standardization, 1975) and models for non stationary sounds in the past few years (Deutsches Institut für Normung, 2007) (Glasberg & Moore, 2002).

This chapter will provide a thorough understanding of loudness through discussion of the development of this metric pursued by researchers. Other research necessary for the understanding of the premise of this dissertation includes the review of work in the development of the various loudness models including the integration techniques as well as the experimental results which support the multiple look approach.

3.1 Loudness Models

The most common metrics used to quantify sound is the sound pressure level or sound power level. These are physical quantities which can easily be measured using electronic instruments. Loudness by contrast is a psychological quantity which is much more difficult to measure as any instrument intended to do so would need to emulate the processes and encoding of the human auditory system. While understanding of the probable physiological mechanisms of this

encoding exist in general, questions still remain in regard to specific perceptions including subtle vowel recognition, varying tonal colourization and impulsiveness (Hartmann, 1998).

Mechanisms external to the auditory system also influence the perceived loudness of sounds. The body's upper torso, chin, nose and the soft tissue of the outer ear, or pinna, have the effect of either increasing or attenuating a sound at different frequencies before it reaches the tympanic membrane. These transfer functions as well as the transfer function of the middle ear have influence on the magnitude of the auditory neural impulses sent to the brain and do not depend on intensity alone (Hartmann, 1998).

The calculation of loudness can be broken into two fundamental approaches. The first being the calculation of loudness for sounds which are stationary or steady in nature. That is, for sounds which do not change with respect to time. An example of a steady sound might be the sound of an engine operating at a constant RPM. A sustained pure tone with constant amplitude is also a stationary sound. As such, the early work in the development of the equal loudness contours and the subsequent loudness models based on these contours fall under the category of stationary models. The second group of loudness models are able to predict the perception of loudness for unsteady sounds. Examples of unsteady sounds include an automobile engine during a run up, process machinery noise and human speech. Unsteady loudness models have not been in existence for very long with the first usable metrics appearing in the literature within the past few years. Given the significant differences between how steady and unsteady loudness is calculated, the evolution of each of the two loudness model approaches will be discussed separately.

3.1.1 Stationary Loudness Models

While the above discussed observations of hearing sensation have been observed in the literature since the 19th Century (Exner, 1876), the first published work of great significance still today is the work of Fletcher and Munson's "Loudness, Its Definitions and Measurement" (Fletcher & Munson, 1933). This work, performed at the Bell Laboratories, was intended to study telephone receiver noise using subjective tests culminated in the equal loudness contours similar to the much later improved contours illustrated Figure 2 in the previous chapter. These contours, along with the work of Kingsbury in 1927 (Kingsbury, 1927) were the first to provide a good insight into the nonlinearity of auditory perception. The Fletcher and Munson experiments used telephone receivers to subject jurors to various intensity levels of pure tone sounds who were asked to judge on the relative loudness of the tones. Given that the tests were not under ideal free field conditions, transfer functions were used to correct the playback for the various frequencies which resulted in some error in the data. While their work was confined to the study of steady sounds, Fletcher and Munson recognized the difference in resulting perception between steady and unsteady sounds. They are also recognized for introducing the symbol N used to represent loudness. Also of great significance to future work is the fact that Fletcher and Munson recognized that the human ear reacts to stimuli in bands of frequency instead of pure tones, although the widths of these bands were incorrectly assumed at the time. Despite the inaccuracies and inappropriate assumptions, the work conducted at the Bell Laboratory made a significant contribution to the knowledge of loudness perception and the eventual development of a loudness model.

The Fletcher and Munson work was later followed up in 1937 by the work of Churcher and King and then Zwicker and Feldtkeller in 1955 (Churcher & King, 1937) (Zwicker & Feldtkeller, 1955). These also included experimentally obtained equal loudness contours. Unfortunately, none of the results between the three studies matched with each other. In recognition of this, Robinson and Dadson (Robinson & Dadson, 1956) at the National Physics Laboratories performed an extensive investigation in 1956 to correct for the mistakes and assumptions in the previous studies which became the first international standard for equal loudness contours, ISO/R 226:1961. The Robinson and Dadson's study also included an increased dynamic range to 130 dB and extended frequency range between 25 Hz and 15 kHz. The standardized curves though were for free field conditions only and could not be used to predict loudness for sounds within a diffuse field.

Mintz and Tyzzer (Mintz & Tyzzer, 1952) proposed a graphical approach to calculate loudness in 1952 which was based on the equal loudness contours developed by Fletcher and Munson. Similar to more modern calculation models, the Mintz and Tyzzer procedure used octave band inputs rather than the various constant band widths proposed by Fletcher and Munson. This was in recognition of the filtering process of the auditory system. For their procedure, the octave band data was plotted against curves from which the loudness was determined. The loudness for each octave was then summed to predict an overall loudness value. The significant shortcoming of this model was that it did not account for any masking effects and as a result produced acceptable results for sounds which had flat frequency spectra only.

Stevens (Stevens, 1956) developed a loudness computation model in 1956 which was also limited to sounds which that exhibited “approximately continuous spectra”. This was similar to the Mintz and Tyzzer model and limited its usability significantly. This model also accounted for the effects of frequency masking which Stevens referred to as “inhibition” and accommodated octave, half octave and third octave data as input. The basic premise behind Stevens’ model is given by the following equation;

$$S_t = S_m + F(\sum S - S_m) \quad (1)$$

Stevens redefined the variable representing loudness in his equation as S where S_t is the total loudness, S_m is the maximum loudness and F represents the fraction of the difference between the summation of all the loudness within a given band and the maximum band loudness. The variable F was dependant on the fraction of octave band data type. That is, F was taken to be 0.3, 0.2 or 0.13 for octave, half octave or third octave band data respectively. Loudness is then obtained as a function of sound pressure level for a given band using the equal loudness contour plots.

Stevens later improved his model (Stevens, 1961) with a simplified version where the equal loudness contours used to determine the loudness as a function of sound pressure level were now a series of interconnecting linear lines. The value for F was also changed to 0.15 for the case of third octave input data. The result was a model which compared more favourably to jury data and one which is easier to calculate. This improved version of the Stevens model later became a British standard, BS 4198:1967 (British Standards, 1967).

Zwicker published work (Zwicker, Flottorp, & Stevens, 1957) (Zwicker, 1961) which proposed the use of critical, or Bark bands, as the inherent filter network of the auditory system as opposed to third octaves. Through psychoacoustic experiments, Zwicker was able to show that the perceived loudness of a pair of tones of diverging frequency remained constant until a critical frequency value was achieved. After the critical frequency tone was surpassed, the perceived loudness of the higher frequency tone would also increase for frequencies up to approximately 4 kHz. After that, the loudness would instead decrease. The trending would follow the equal loudness contours; however, the establishment of the critical bands and their lower and upper frequencies was a major step forward in the understanding of auditory filter position along the basilar membrane within the cochlea of the ear. It is the excitation of the 24 various critical bands (or Bark bands identified as Bark 1 through 24) along the basilar membrane that the auditory system interprets as an appropriately corresponding frequency. Zwicker later redefined the critical bands below 500 Hz as having constant bandwidths of 100 Hz as opposed to the approximate constant 21% bandwidth (21% CPB) for all bands above 500 Hz. Shown in Table 1 are the 24 critical bands and the corresponding frequency bandwidths and centre frequencies for each. It is interesting to note that the 21% relative bandwidth above 500 Hz is very near to the 23% relative bandwidth defined for third octave filters. This implies that the human auditory system is very near to a third octave filter set for the upper frequencies. Alternatively, equation 2 can also be used to calculate the critical bandwidth surrounding a given center frequency.

$$\Delta f = 25 + 75 \left[1 + 1.4 \left(\frac{f_t}{1000} \right)^2 \right]^{0.69} \quad (2)$$

Table 1: Zwicker's 24 critical bands having unit of Bark and the corresponding bandwidth and centre frequencies having units of Hz

Bark Band #	Center Freq.	Bandwidth	Start	Stop	Equiv. 1/3 Octave Bands
1	50	100	0	100	1.25 - 100
2	150	100	100	200	100 - 200
3	250	100	200	300	200 - 315
4	350	100	300	400	315 - 400
5	450	110	395	505	400 - 500
6	570	120	510	630	500 - 630
7	700	140	630	770	630 - 800
8	840	150	765	915	800
9	1000	160	920	1080	1000
10	1170	190	1075	1265	1250
11	1370	210	1265	1475	1250
12	1600	240	1480	1720	1600
13	1850	280	1710	1990	2000
14	2150	320	1990	2310	2000
15	2500	380	2310	2690	2500
16	2900	450	2675	3125	3150
17	3400	550	3125	3675	3150
18	4000	700	3650	4350	4000
19	4800	900	4350	5250	5000
20	5800	1100	5250	6350	6300
21	7000	1300	6350	7650	6300
22	8500	1800	7600	9400	8000
23	10500	2500	9250	11750	10k
24	13500	3500	11750	15250	12.5k

Zwicker with Paulus (Paulus & Zwicker, 1972) would later published a 1972 paper describing a model which included a FORTRAN computer code for calculating loudness which used the critical bandwidth filter set developed earlier by Zwicker. This paper provided the basis for what would become the most widely used loudness model for stationary sounds for nearly 30 years thereafter. The model was able to accommodate

both free field and diffuse sound fields and included the effects of simultaneous frequency masking. The model involved several steps which began with the input of the sound spectrum as either third octave data or critical band levels. If the former were used, the program was able to approximate the critical band levels by combining the third octave data into ranges which approximated the critical bands. Next, transfer functions representing the outer and middle ear are applied to the input spectrum followed by the determination of the excitation pattern at the cochlea. The excitation pattern is then transformed into a specific loudness plot. A schematic example of specific loudness for a single tone is illustrated in Figure 10. The x axis is the critical band rate and the y axis is the specific loudness having units of sone/Bark. The final step is to integrate the specific loudness curve to get the overall loudness of the input spectra, also shown in the figure below.

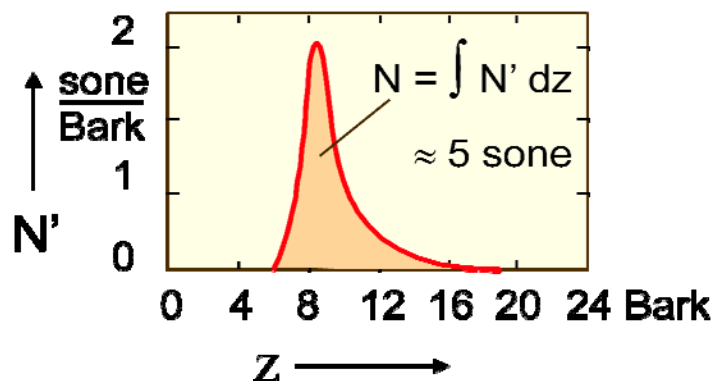


Figure 10: Schematic of Specific Loudness Plot, or Loudness Value per Critical Bark Band measured in sone. Also Illustrated is the Area under the Specific Loudness Curve N' which is Directly Proportional to the Total Perceived Loudness (Bruel & Kjaer).

The concept of the specific loudness is important also for the understanding of frequency masking as shown in Figure 11. Illustrated are the masking patterns of a narrow-band noise centred at 1 kHz with a bandwidth of 160 Hz. The lowest curve represents the equal loudness contour for the threshold in quiet. The other curves illustrate masking patterns for different levels of the 1 kHz narrow-band noise. For example, a test tone f_T at 2 kHz with a level L_T of 40 dB and below is masked if the noise level L_{CB} is above 80 dB. At low levels of the narrow band masker, the masking pattern has a symmetrical shape. However, when increasing the masker level above 40 dB, the lower level is shifted in parallel, whereas the upper slope gets flatter and flatter. This effect is called the “non-linear upward spread of masking”.

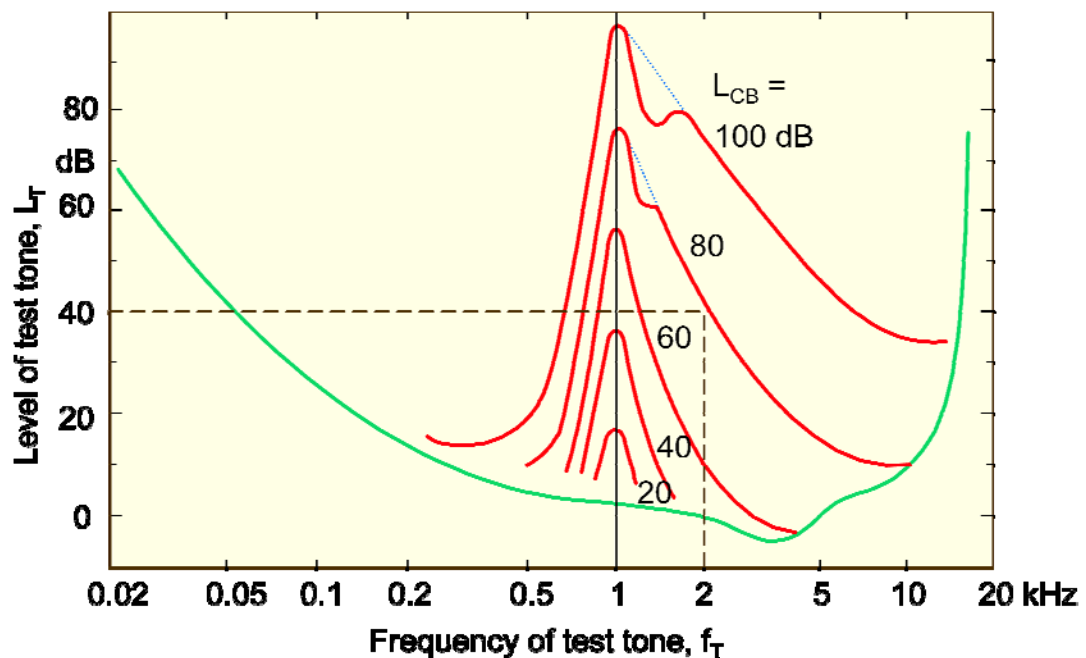


Figure 11: Masking patterns of narrow-band noise centred at 1 kHz with a bandwidth of 160 Hz at different levels L_{CB} (Bruel & Kjaer).

The first standard for the calculation of loudness was the ISO 532:1975, "Method for calculating loudness level" (International Organization for Standardization, 1975) which included both a Method A and a Method B component. This standard is for steady sounds only and is still in use at the time of this dissertation with a revision not expected for a few more years yet. While the two approaches are intended to calculate the same metric, the standard warns that user discrepancies as great as 5 phons may be realized between the two methods.

Method A from ISO 532:1975 is based on the work of Stevens (Stevens, 1961) and employs the use of equations and corresponding coefficient lookup tables. The method is also restricted to the input of octave band input data only as opposed to half and third octave input as originally intended by Stevens. Method A is also restricted for use within diffuse sound fields and input signals having relatively flat spectrums. Because of these restrictions, along with poor resolution of the calculated loudness value, it is a mostly disregarded method.

Method B is based on the procedure detailed by Zwicker and Paulus (Paulus & Zwicker, 1972). This method can be used for both diffuse and free field conditions with a third octave spectrum measured using a single microphone. The predicted loudness value though is representative of a binaural diotic (two ears with the same signal presented to both ears) loudness. Unfortunately the method did not include the FORTRAN program given in the earlier 1972 publication. The approach is instead a graphical one where the third octave data is transferred to a set of charts which results in the specific loudness plot versus frequency. Subsequent specific loudness plots for each consecutive band are also presented from left to right representing increases in loudness by vertical lines and decreases by downward curved slopes. Once each band has been plotted, an

overall specific loudness plot is given for the entire spectrum. It is the area under this plot that is summed across the spectrum to give a total loudness in phons or total loudness level in sones.

Given the tediousness of the graphical approach prescribed in the ISO 532:1975 Method B approach, Zwicker published an updated version of his 1972 computer program, this time in BASIC (Zwicker, Fastl, & Dallmayr, 1984). This newer version of the computer code accepted third octave data only as input, and not optional critical band values as the graphical method did which made it well suited to more increasingly available analyzers and hand held sound level meters.

The Deutsches Institut für Normung (German Institute for Standardization) released an updated and slightly improved version of the ISO 532/B approach in 1991. This standard was the DIN 45631 (Deutsches Institut für Normung, 1991). The changes given in the new version included data files which had been modified using the data given in the graphical look up tables of the 1975 ISO standard. The result of this was a better correlation to the ISO 226:1987 equal loudness contours in the lower frequency range, especially below 300 Hz (Charbonneau, Novak, & Ule, Comparison of Loudness Calculation Procedure Results to Equal Loudness Contours, 2009) (Charbonneau, Novak, & Ule, Loudness Prediction Model Comparison Using the Equal Loudness Contours, 2009). The standard also includes the BASIC computer code which was also released the same year by Zwicker (Zwicker, Fastl, Widmann, Kurakata, Kuwano, & Namba, 1991).

The next advancement in stationary loudness models was the 1996 paper by Moore and Glasberg (Moore & Glasberg, 1996). The fundamental approach was still similar to Zwicker's. The procedure involved application of the outer and middle ear transfer

functions on the third octave input spectra followed by the calculation of the excitation pattern. While similar to Zwicker's, the updated transfer functions were revised to reflect the results of earlier work by Moore and Glasberg (Glasberg & Moore, 1990). Next, the specific loudness contour is determined and is finally integrated to determine the overall loudness. The most significant change imposed by the Moore and Glasberg work was the introduction of an entirely different auditory filter shape to calculate the excitation patterns based on Equivalent Rectangular Bandwidths (ERBs) instead of the critical bandwidths developed by Zwicker. The accepted approach at one time was to approximate the auditory filter shapes by use of a power-spectrum model. Moore and Glasberg found through experimental testing that this produced errors when given specific masking patterns (Moore & Glasberg, 1987). They observed that listeners performed loudness comparisons over several filter sets rather than a single auditory filter as previously assumed. To prevent this, Moore and Glasberg conducted their experiments using notched-noise masking data where the targeted noise bands are presented along with a probe tone used to direct the listener's attention to prevent "off frequency listening".

From the experiment, Moore and Glasberg determined that for a normal hearing individual, the auditory filter shape is quite asymmetrical, with the lower branch generally rising less sharply than the upper. From the summary of the auditory filter shape, they derived the ERB values of the auditory filters across the audible frequency spectrum.

Later work resulted in an increase of the accuracy of the filter shapes (Glasberg & Moore, 1990). By updating the model with an equal loudness contour correction and limiting the frequency shift to 20% of the centre frequency, they were able to improve

on their previous filter estimations. This relationship, given in Equation 3, defines the ERB value in Hz for a given centre frequency (F) in kHz. In theory, this equation approximates the location of frequency dependant excitation along the basilar membrane and thus represents each segment as an individual ERB.

$$ERB = 24.7(4.37(F) + 1) \text{ (Glasberg \& Moore, 1990)} \quad (3)$$

Glasberg and Moore's 1990 paper also facilitated the use of ERB units to scale the frequency coordinates which is similar to Zwicker's unit of Bark. Equation 4 allows a user to specify the ERB Number for a given centre frequency value (F) in kHz. By doing so, spectra data can be presented using bandwidths which corresponds to those present in the auditory system (Moore & Glasberg, 1987).

$$\# \text{ of ERB} = 21.4 \log_{10}(4.37(F) + 1) \text{ (Glasberg \& Moore, 1990)} \quad (4)$$

Shown in Figure 12 is a comparison of Zwicker's critical bandwidths to Glasberg and Moore's ERB as presented by Seeber (Seeber, 2008). Studies have shown that Zwicker's loudness model deviates most from the equal loudness contours at frequencies below 500 Hz (Charbonneau, Novak, & Ule, 2009). This is also the frequency region where the two auditory filter shape models differ most. Sek and Moore suggested that this was because Zwicker's approach was heavily influenced by critical modulation frequencies resulting from the use of complex tone signals in the listening experiments used to determine the filter shapes (Sek & Moore, 1994). To determine his critical bandwidths, Zwicker's experiment involved the presentation of a pair of tones to a juror which are

continually separated in frequency until an increase in loudness was noticed (Zwicker, Flottorp, & Stevens, 1957). It was suggested by Sek and Moore that the low frequency tones were modulating with each other resulting in error. Their experiments which used only one tone eliminated the possibility of tonal modulation interference and instead resulted in auditory bandwidths which continued to decrease as illustrated in the Figure 12.

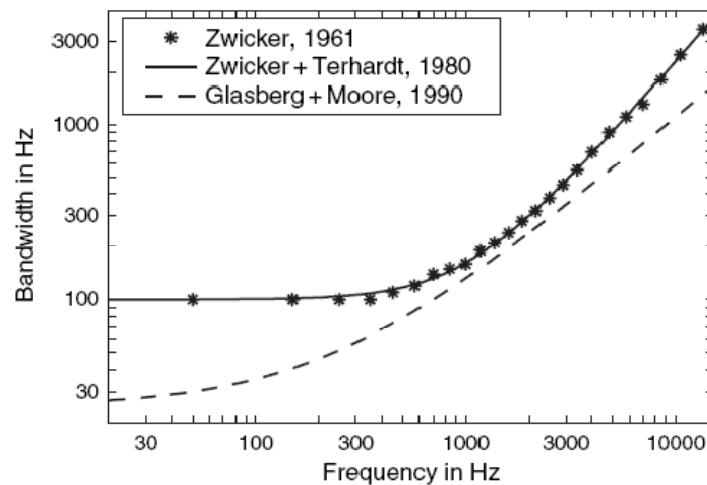


Figure 12: Comparison of Zwicker’s Critical Bandwidths to Glasberg and Moore’s Equivalent Rectangular Bandwidths which demonstrate the low frequency errors resulting from Zwicker’s listening experiments (Seeber, 2008).

Moore, Glasberg and Baer published an updated model which revised how the model accounted for binaural loudness and also had better correlation to updated equal loudness contours (Moore, Glasberg, & Baer, 1997). The model predicted a steeper slope in the lower frequency regions of the contours. This was later verified by a study performed by Suzuki and Takeshima’s (Suzuki & Takeshima, 2004). This loudness model would also eventually become standardized as ANSI S3.4:2005 (American Institute of Physics, 2005). For binaural diotic listening, the model would double the calculated loudness. For the case of dichotic presentation, the total loudness is given as the sum of

the loudness for the two independent sounds. This, along with the matching to the newer equal loudness contours resulted in the calculation of binaural loudness having a non-zero value at threshold for some frequencies. This correlates with human auditory experiments given that broadband signals whose components are below the threshold of hearing can result in a positive loudness. This 1997 model is also more flexible than previous models in that input spectrum can be specified as third-octave levels or levels at specified frequency bands. Broadband pink or white noise with levels or combinations of noises with tonal components can also be accommodated. For the sound field presentation, either monaural or binaural sound fields can be chosen to be represented as free field, diffuse field, or headphone with a specified frequency response to accommodate known headphones. The ANSI S3.4-2005 standard also makes reference to an available compiled computer program called ANSILLOUD for which an updated version called LOUD2006A can be found on the University of Cambridge – Auditory Perception Group website (Glasberg & Moore, LOUD2006A.exe - Loudness Model Calculated According to ANSI S3.4 2007).

To account for yet another update to the equal loudness contours (ISO 226:2003) (International Organization for Standardization, 2003), Glasberg and Moore updated their model again in 2006 (Glasberg & Moore, 2006). This required a revision to the hearing threshold values. This was achieved by a modification to the transfer function for the middle-ear. These changes resulted in an update to the present standard, ANSI S3.4:2007 (American National Standards Institute, 2007). An updated computer program (LOUD2006A) was developed and included with the 2007 standard and is also available on the web (Glasberg & Moore, LOUD2006A.exe - Loudness Model Calculated According to ANSI S3.4 2007).

3.1.2 Unsteady Loudness Models

The discussions of loudness calculation models have thus far have been restricted to models designed for the evaluation of stationary sounds which are steady with respect to time. These models are relatively simple and are easy to correlate to the results of auditory experiments. This is partially due to the fact that the designs of experiments which focus on steady sounds are fairly simple to implement, often using pure tones, and have good repeatability. The development of these steady models has given much insight to the present understanding of hearing perception and to the workings of the auditory system. Most real sounds encountered in daily life though are unsteady in nature. Examples include traffic noise, machinery noise on a factory floor or speech and other forms of communication. For these sounds, an alternative loudness method is necessary to include the temporal, or time effects, of the human auditory system. These effects can be very complex and add a significant degree of complexity to the process of determining the loudness for these time varying sounds. The following section focuses of the development of these unsteady loudness models.

Vogel proposed an unsteady loudness model in 1975 which was also designed to predict roughness, a psychoacoustic measurement of the annoyance of modulating sounds (Vogel, 1975). It should be noted that like roughness, many psychoacoustic metrics require first the calculation of loudness. Vogel's model followed the methodology of Zwicker's stationary model by calculating specific loudness across the critical band rate in slices of time. This is analogous to a Campbell or waterfall plot. The shortcoming of this approach is that it did not account for the actual temporal effects of the auditory system such as time masking, pre-masking, threshold shifts etc.

Zwicker published in 1977 an extension to his stationary loudness model to account for time-varying sounds (Zwicker, 1977). Due to the increased complexity of the required input of a transient sound for this model, as opposed to a simple third octave spectrum, the model was one more of theory than practicality given the limitations of signal processing capabilities of the day. In his model, Zwicker did not include the auditory effect of pre-masking and instead emphasized auditory post-masking. Also considered were the latency effects of low frequency stimuli, amplitude-modulated sounds, narrow-band noise at high centre frequencies, and like Vogel, frequency-modulated sounds. To account for the third dimension of time, in addition to critical band and specific loudness, Zwicker's model required a summation of loudness across both frequency and time. For this, spectral integration is performed first, followed by temporal integration. From here, time constants set up to match the temporal masking characteristics of the ear are applied. The result is a loudness versus time function for which the peak value generally corresponds to the subjective sensation of overall loudness. An analysis is also given which compares the results obtained using Zwicker's model to previously published subjective test and finds a favourable agreement. A follow up paper with an update to one of the graphs in the original 1977 paper was published a year later (Zwicker, 1977).

Ogura, Suzuki and Sone published a 1993 paper which compared several approaches for predicting time varying loudness. They concluded that out of the available approaches, Zwicker's 1977 loudness meter provided the best results but only with modifications proposed by the authors. They proposed longer rise and decay time constants in the temporal integration operation. This was further investigated by Stecker and Hafter who examined the effects of rise and decay times of a sound on perceived loudness

(Stecker & Hafter, 2000). They concluded that slow rise/fast decay sounds were perceived to be louder than fast rise/slow decay sounds. These results were consistent with statements by Zwicker in his 1977 paper.

The next significant advancement in the development of an unsteady loudness model was by Glasberg and Moore in their 2002 paper (Glasberg & Moore, 2002). This work was somewhat of an extension of their stationary loudness procedure with the significant difference being that the 2002 model would accept discrete spectral components in the form of a digitally recorded 16 bit WAV file as input. This allowed for much greater resolution or detail in the input signal compared to the much coarser third octave data (Glasberg & Moore, 2002). The output of the time varying loudness (TVL) model was both a both short-term and long-term loudness level. The authors described the usefulness of having both values using the example of speech as a noise source. They related short-term loudness as being useful for the measure of the intensity of a speech syllable. Long-term loudness on the other hand would be useful for the measure of the intensity of a much longer speech signal such as a sentence (Glasberg & Moore, 2002).

In order for the TVL model to accommodate the full audible frequency range and not lose resolution at higher frequencies for short duration signals, the model's use of six parallel FFTs to calculate spectral information over six bandwidths, calculated over decreasing lengths of time, for obtaining spectral information in increasing frequency ranges. The ranges of the bandwidths are 20 to 80 Hz, 80 to 500 Hz, 500 to 1250 Hz, 1250 to 2540 Hz, 2540 to 4050 Hz, and 4050 to 15000 Hz each having segment durations of 64, 32, 16, 8, 4, and 2 ms, respectively. The excitation pattern and instantaneous loudness levels are then calculated in the same fashion as their stationary model. The

short term loudness is calculated by temporally averaging the instantaneous levels, thus providing a running average for the signal. The long term loudness is subsequently calculated by temporal averaging of the short-term loudness. While this model has shown to provide good correlation to the latest 2003 equal loudness contours (Charbonneau, Novak, & Ule, 2009), the use of temporal averaging does not provide adequate prediction for noise bursts or sounds in the presence of gaps (Viemeister & Wakefield, 1991).

A second popular non stationary loudness model is the DIN 45631/A1 which was approved for release in 2010 (Deutsches Institut für Normung, 2007). Like the previous model which was based on the early studies by Glasberg and Moore this German standard is based on the 1977 work by Zwicker (Zwicker, 1977).

Zwicker's research on temporally varying sounds extended his 1972 stationary loudness work by adding the temporal loudness characteristics of phase effects, physiological noise, amplitude modulation, and frequency modulation. Eventually Zwicker determined that the phase effects on his temporal analysis were minimal and subsequently ignored them to simplify the model. The DIN standard also incorporates more up to date transfer functions curves which have been developed by others including Fastl (Fastl & Zwicker, 2007).

The DIN approach divides sound duration into three groups and treats them differently. For tones less than 100ms in length, the perceived loudness is decreased by a factor of two. Sounds having a length greater than 200 ms are classified as long lasting bursts and subsequently have the highest perceived level and the longest decay. The perceived loudness of tone bursts is determined to be the peak loudness value found over the period of the burst. This again is counter to the thinking of some of the more

up to date research (Viemeister & Wakefield, 1991) (Moore, 2003) (Pedersen & Ellermeir, 2005) (Pedersen B. , 2006). This model also ignores the effect of pre-masking which is thought to not be as influential as post-masking on loudness. This is supported by the perceived slow signal decay in a signal compared to the high rise rate. The model is said to be capable of describing tone bursts, amplitude and frequency modulated signals, narrow band noise, and speech.

Given in Table 2 is a summary of the significant work leading to the development of the various loudness models presented above. Detailed is the evolution of the equal loudness contours which eventually lead to models for both stationary and unsteady loudness as well as a description of the significance of each publication.

Table 2: Evolution of the significant work leading to the development of both stationary and unsteady loudness models, including the significance of each milestone.

Author/Associated Standard	Date	Stationary/ Non stationary	Brief Summary
Fletcher/Munson	1933	Stationary	-developed equal loudness contour graphs with jury tests -recognized that the human ear reacts to stimuli in bands of frequency instead of pure tones
Mintz/Tyzzar	1952	Stationary	-developed a graphical method to calculate loudness which recognized the bandwidth filters of the auditory system by using octaves -model did not account for any masking effects
Stevens	1956	Stationary	-model did account for frequency masking but was good for broadband sounds only
Stevens/ ISO 532A	1961	Stationary	-used octave values -used graphical technique with equal loudness contours -became British Standard 1967
Zwicker	1961	Stationary	-developed the most commonly used loudness model which uses critical, or Bark bands, to represent our hearing filters instead of third octave bands in Hz
Zwicker	1972	Stationary	-included a computer program (Fortran)

Zwicker/ ISO 532B	1975	Stationary	-diffuse/free fields; 1/3 octave input; binaural diotic -graphical method
Zwicker	1982	Stationary	-BASIC program
Zwicker/ DIN 45631	1991	Stationary	-DIN adopted the BASIC method
Moore/Glasberg	1996	Stationary	-used different filter for the ear which they called Equivalent Rectangular Bandwidths instead of Zwicker's critical bands -improved transfer function for the outer and middle ear
Moore/Glasberg/ ANSI S3.4:2005	1997	Stationary	-updated binaural loudness calculation -better correlation to equal loudness contours at the lower frequencies -input of third octaves; free/diffuse or headphone -ANSILOUD program
Moore/Glasberg/ ANSI S.3.4:2007	2006	Stationary	-updated with new ISO 226:2003 equal loudness contour data -updated transfer functions of outer and middle ear -LOUD2006 program
Vogel	1975	Non stationary	-results were like a Campbell plot -temporal masking included
Zwicker / DIN 45631:A1	1977	Non stationary	-performed a summation across both frequency and time -no pre-masking effects taken into account
Glasburg/Moore	2002	Non stationary	-allowed input of WAV file -outputted a short term and long term loudness value
Fastle / DIN 45631:A1	2007	Non stationary	-developed new transfer functions from Zwicker's previous ones used

3.2 Loudness using Temporal Integration

The concept of a temporal integration period was originally coined by Munson in 1947 to explain the reason for increase in perceived loudness with increasing signal duration (Munson, 1947).

The practiced theory of temporal perception has been that absolute thresholds of hearing are strongly dependant on the duration of the stimulus signal, at least for sounds lasting between 200 to 300 ms and that the auditory system is able to summate an internal representation of a signal over this period (Oxenham & Moore, 1994) (Moore, 2004). In fact, it is usually taken that

the sound intensity necessary for detection increases as the duration of the sound decreases (Zwislocki, 1960). As will be discussed later, this is true only to a minimum duration span. Early work in the 1940s by Hugh, Garner and Miller suggested that for certain durations of time, the auditory system appears to integrate acoustic energy over time (Viemeister & Wakefield, 1991). From the time of this early research until the early 1990s, the exclusive model for the temporal calculation of sounds has been taken as the time, or temporal integration model. While this section will describe some of the research and models which follow the theory of temporal integration, a more detailed description of the mechanisms of time integration will be given in the next chapter.

Moore described auditory temporal integration as a simple accumulation of acoustic stimuli over time, or energy integration which is used for the detection or discrimination of sounds (Moore, 2003). This assumption has been based on observations that the absolute threshold for detecting sounds, usually described in decibels (dB) of sound pressure level (SPL), decreases with increasing duration of the sound (Plomp & Bouman, 1959). This increase in performance has been modeled as a simple accumulation of intensity over time. Green described this behaviour in 1960 for the case of absolute threshold as the auditory system's energy integrator (Green, Auditory Detection of a Noise Signal, 1960) (Dallos & Olsen, 1964). Penner argued against the theory of the auditory system integrating energy over time. He surmised that it is neural activity which is instead combined over time as opposed to acoustic energy (Penner, 1972).

In addition to the general lack of consensus as to exactly what is combined over time, disagreement also exists as to how it is combined (Moore, 2003). Most agree that the auditory system does not in actuality integrate the acoustic stimuli in the same sense as a mathematical

integration operation. Despite this, existing time varying loudness models use what is referred to as a “leaky integrator” approach. This can be likened to determining the mass of water versus time based on its accumulation as it is being poured into a container; only the container has holes in it at various heights which allow the water to leak out. A more thorough description of this concept is given in Chapter 4.

An early loudness model which used a leaky integration approach was described by Stone (Stone, Moore, & Glasberg, 1997). The described real time loudness meter was a rather unsophisticated model which utilized early digital signal processing techniques. The model only included a very simple form of temporal integration and unlike the more modern loudness models did not account for the loudness impact of amplitude modulated sounds. The integration technique was a simple mathematical procedure which integrated a running tally of specific loudness but also accounted for the energy loss (thus the leaky concept of the integration) to account for any temporal masking effects.

The goal of another loudness application using a temporal integrator is to limit the ability of the modeled auditory system to detect rapid stimulus changes in certain tasks including gap detection, decrement approximation and the detection of amplitude modulation (Oxenham & Moore, 1994). This was accomplished by estimating the shape or weighting function of the temporal window from auditory tests and applying the weighted window in the loudness prediction. While such a temporal window model can adequately account for the data acquired from a number of such experiments, problems still remain (Moore, Glasberg, Plack, & Biswas, 1988). These include the inability to detect masking effects or signal duration for samples longer than 20 ms where empirical data showed otherwise. Another consequence of this approach is the failure to predict the additivity of non simultaneous maskers such as pre and

post masking within a given temporal window. Nonetheless, the integrator model did prove most useful for sounds with amplitude modulation and was eventually applied in a modified sense by Moore in his 2002 loudness model (Glasberg & Moore, 2002).

Glasberg and Moore's 2002 paper described a method for calculating loudness for unsteady sounds which used a more complicated form of temporal integration (Glasberg & Moore, 2002). Their model calculates both a continuous short term loudness followed by long term loudness using the results of the former. The temporal integration for the short term loudness component is essentially an averaging of the instantaneous loudness. The model does this in a manner which is analogous to the way that a control signal is generated in an automatic gain control (AGC) circuit which has a very steep attack time and a more gradual release time. The model calculates a short term estimate of loudness for every 1 ms of a time signal and while also keeping a running average of these short term estimates. If the running average is greater than the previous calculated instantaneous loudness, which corresponds to an attack, then the steep time constant is applied. If, on the other hand, the instantaneous loudness is less than the short term loudness, then a corresponding release time constant is applied. This approach means the short term loudness can increase quickly at the onset of a sound and also decays slower when the sound is turned off. The slower decay corresponds to the latency of neural activity along the basilar membrane in the ear and is also approximates the phenomenon of forward masking. As stated previously, the long term loudness is calculated using the short term loudness, again using an integration approach similar to an AGC circuit only with modified time constants. Here, the magnitude of the long term loudness is compared to the short term loudness to determine whether the sound is at the onset or decay. Because the above process involves the integration of the temporal impressions of very short durations of the sound, it is very capable of handling any unsteady sound. However, as described in the previous section, the model later uses six

simultaneous FFT calculations to evaluate the spectral influence on the sound. In order to achieve adequate spectral resolution, the processing of much longer signal durations is required. This in turn results in the long term integration time constants to become relatively long compared to the time resolution of the auditory system.

It is reported that the recently released DIN unsteady loudness model implements both spectral integration and temporal integration sound input to calculate loudness (Deutsches Institut für Normung, 2007). The procedure is based on Zwicker's early work (Zwicker, 1977). The standard though is written in German only and not available in English so no further details other than those in Zwicker's 1977 paper are available.

3.3 Research Supporting Multiple Look Approach for Loudness

The review of unsteady loudness has thus far been for models which use temporal integration techniques. This approach involves the accumulation of sound information over time to improve discrimination and account for known auditory effects which are known to be associated with time varying sounds such as masking and varying threshold levels with signal length. Despite these observations, listening experiments have shown that the auditory system does not use a process which is wholly synonymous with temporal integration. For example, it is unlikely that the auditory system would integrate over time for a task as simple as the detection of a pure tone presented in quiet. It has been suggested (Moore, 2003) that it may be more appropriate to consider the auditory process as a combination of information from multiple independent "looks". This section will review the evidence which supports the concept of multiple looks and how it may be a better representation of internal stimuli. This evidence will ultimately also support the approach taken in this dissertation.

The concept of the multiple looks theory is that the auditory system takes sequential samples, or looks, of the sound information and either immediately processes the information as a perception or stores the information for future processing. The decision to process or store the information is dependent on the nature of the stimuli. If for example the sound has large sudden increases or decreases in amplitude or gaps in the flow of the stimuli, then the sounds are processed immediately as independent samples. This is applicable for sounds which change over short durations from 1 ms to approximately 5 to 10 ms. If, on the other hand the sound is more continuous over a much longer time period then the “looks” are instead thought to be integrated over time.

The first real justification of the multiple look theory was published by Viemeister and Wakefield in 1991 which demonstrated the validity of the theory through two very important experiments (Viemeister & Wakefield, 1991). Their first experiment measured the detectability in quiet of two very short pulse signals compared to a single pulse. The results averaged over all the tests subjects is given in Figure 13 which demonstrates the threshold of detectability of the two pulse pair with increasing separation distance compared to a single pulse stimulus. It is demonstrated that for a separation of 1 ms that the level of detectability is 4 dB lower than for a single pulse. In other words the single pulse sound would need to be 4 dB greater to have the same perceived loudness as the two equal amplitude pulse pair. For separations larger than about 5 ms, the detectabilities are averaged to have a level of approximately 1.6 dB lower than those for a single pulse. The significant point of the data presented in Figure 13 is that the detectability levels increase with separations larger than 1 ms but then stop increasing once the separation has reach 5 ms. These results are inconsistent with those obtained using a long time constant leaking integrator. The results are consistent with the concept of the multiple look model. For the two pulse tones separated by small separations, the pulses fall within a brief temporal

window of the look and are combined together which results in greater acoustic input than that for a single pulse even though they are of equal amplitude of the single pulse. As the separation is increased, and assuming a non rectangular temporal window, only a partial combining of the acoustic information of the two independent pulses is achieved, and thus the looks are considered to be partially independent resulting in a smaller difference in detectability from a single pulse. So in other words, when multiple inputs are combined within a single look better performance is achieved than for a single pulse alone or when the multiple inputs are spread far enough apart that they become themselves independent looks and are treated as two single pulses.

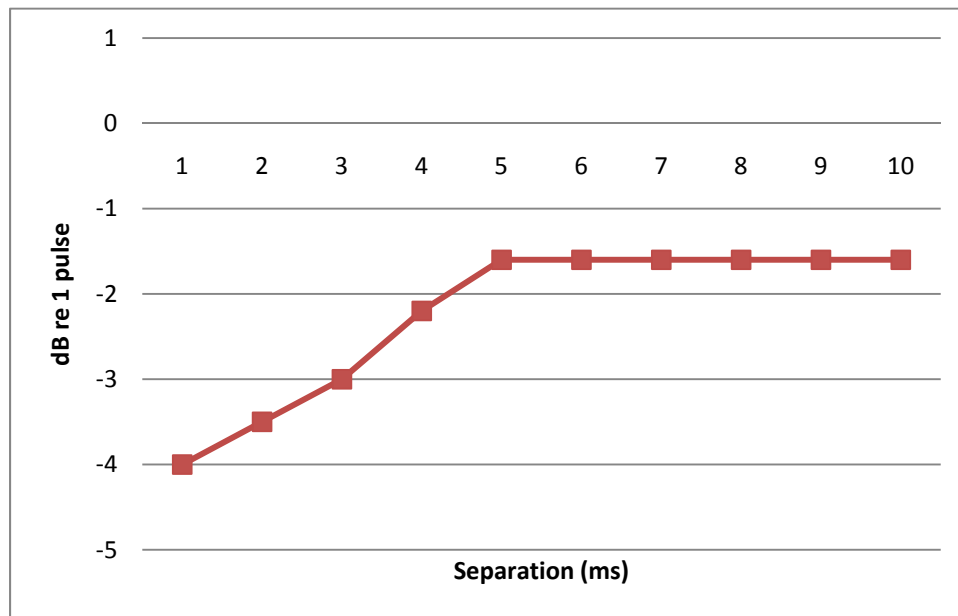


Figure 13: Perceived difference in sound level in dB of two pulses with varying separation times and a single pulse showing an increased detectability for shorter separation times in ms (Viemeister & Wakefield, 1991).

The results of the above experiment are inconsistent with the classic models of temporal integration published previously. Viemeister posed the question as to whether a single look integration model could be developed that employs integration and is yet consistent with his results. If a single look model is applied to the pulse pair scenario the results presented above

implies that energy from both pulses is either fully or at least partially combined. This would suggest then that any energy present between the pulse pairs would also have to be combined or integrated. To test for this an experiment could be performed where energy in the form of a masker is presented between a pulse pair, as opposed to quiet in the first experiment, which would result in a decrease in performance as the energy between the pulses would also be integrated. However, if the pulses are treated as independent looks, and not combined in a long term integration process, an increase of detectability of the pulses would be maintained.

The above hypothesis was tested in Viemeister's second listening experiment which is schematically illustrated in Figure 14 which illustrates the stimulus window for a single observation interval. Two 10 ms gaps in a continuous noise are presented 100 ms apart. Present within either the first, the second or both gaps simultaneously is a 1 kHz pip tone with a 5 ms rise and decay time. The noise level within the 50 ms interval centred between the gaps was also either raised or lowered by 6 dB increments or left unchanged. It was found that the threshold for detecting the simultaneous pairs of pip tones was consistently 2.5 dB lower than that for either of the two tones presented independently. For this, the listeners must have combined the information from the independent looks of the two pip tones. Had this been performed using temporal integration over the time interval, the results would have been affected by the presence of the noise between the gaps. It was also found that the perceived levels for the single and pair of pip sounds were for the most part unaffected by the presence and level of the noise between the gaps. These results support the idea of multiple looks and are inconsistent with the process of simple long term integration for the detection of the pip signals as presented in the experiment. In fact, no long term integration appears to occur at all and instead the data is consistent with the idea that the observer is taking multiple short term looks at the input signal and then combines the information from the looks in an intelligent or

decisive manner. In his experimental approach Viemeister was specific in his design of experiment to explicitly, “contrast these two approaches (integration versus multiple look) as clearly as possible and hence the use of brief elemental signals where the meaning of a *look* can be associated with each pulse and therefore is relatively unambiguous”.

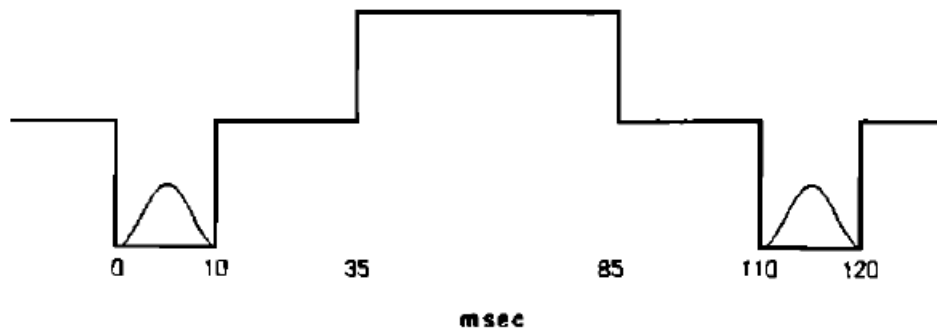


Figure 14: Schematic illustration of Viemeister’s experiment where pip signals are presented individually and simultaneously within two 10 ms gaps in the presence of a varying masker noise signal (Viemeister & Wakefield, 1991).

In his discussion, Viemeister posed the question as to whether the multiple look model can account for the known phenomena associated with temporal integration including long duration signals, tones and noise bursts. He concluded that, “almost any temporal integration data can be described. Indeed, the classical integration models can be subsumed as a subset of multiple look models.”

Moore published a paper in 2003 which discussed the relationship between the evidence supporting the multiple look theory and the phenomena of spectral-temporal excitation patterns (STEP), or the internal representations of stimuli (Glasberg & Moore, 2002). It was proposed that the central mechanisms of the auditory system make intelligent use of the

information contained within the looks in the STEP to enhance signal detection, discrimination, identification, etc. The idea is that the results of detection and discrimination experiments can be explained by using the concept that templates exist which are based on the internal representation of a stimulus, for example speech, and that decisions are made on the similarity of internal stored templates to a current stimulus. It is further surmised that information extracted from one part of a sound may influence the interpretation of information extracted from another part of the sound occurring at a different time. These theories can only be supported by the existence of the multiple look theory given that the information within looks is thought to be stored in memory. While the work by Moore was published in 2002, Viemeister suggested a similar use for these memory bits in his 1991 paper supporting the process of multiple look detection (Viemeister & Wakefield, 1991). Conversely, these same phenomena described by Moore cannot be explained by a simple accumulation process such as temporal integration.

Pedersen conducted several studies to investigate the temporal processing of the auditory system which resulted in data which supports multiple look theory. To study how listeners temporally integrate sounds to discriminate their loudness. In 2006 he published a paper which focused on how listeners apply weighting to various temporal segments of a sound when judging loudness. The outcome was a temporal weighting curve showing the importance of different temporal locations of the sound. It was shown that listeners emphasize onsets and offsets in their temporal weighting of a sound which showed that loudness integration is not a simple process as assumed in many loudness models. It was also demonstrated that listeners changed their pattern of temporal weighting if they are provided with feedback or a hint of the signal. This reinforces the work discussed in the previous paragraph by Moore. Also, a change in the spectral content in the middle of a sound, demonstrating the onset of a new event, was

shown to be weighted more heavily. Thus, it was shown that listeners pay attention to salient events within sounds, phenomena not possible with simple integration but only supported by a multiple look approach. He concluded that temporal variation is made available in the sensory system to allow for overall judgement of the properties of sound, such as loudness, and, “this information is weighted and analyzed in complex ways, which is not adequately described as a simple summation process,” but can be explained by the multiple look theory (Pedersen & Ellermeir, 2005).

In another study which compares loudness of temporally varying sounds, it was found that listeners weigh onsets and offsets in a comparison task but generally the last sound is found to receive the greater weight, as a result of memory effects or distribution of attention. The results suggest that the two sounds are individually processed and thus the auditory system does not seem to integrate the two sounds as a continuous stream, but rather identifies the components as independent looks. The sounds used in the experiment were also used as the input to Glasberg and Moore’s 2002 loudness model which uses temporal integration. It was found that the temporal properties of this model did not predict the results of listening experiments (Pedersen B. , 2006).

Through his various studies on auditory temporal processing of different task types, Pedersen concluded that, “auditory temporal processing cannot be described by a single integrator device in the sensory system” (Pedersen B. , 2006). The question to then be asked is how do listeners arrive at loudness impressions. The answer to this is critical to the development of an accurate loudness model which can adequately represent the judgement of loudness for all cases of stimuli. “Current models assume that loudness integration is a summation process to a large extent, while the very different weighting curves found (in Pedersen’s work) suggest that the

envelope is evaluated in more complex ways as to judge (an overall loudness) level” (Pedersen B. , 2006). It has been argued by some that the most plausible answer to this is the multiple look approach. This is because the listening experiments have been able to disprove the applicability of an integration model for determining loudness impressions for most transient sounds other than the most temporally fundamental. Conversely, these same experiments have not been able to disprove the validity of the multiple look theory but instead support it either fully or in some cases at least peripherally.

The fundamental outcome that can be taken from the work of Viemeister and others is that the multiple look model better explains the results of cognitive listening experiments, especially those dealing with the impression of loudness for sounds. It is surmised that to be able to do this the process of multiple looks allows for the storing in memory of the sound data for each sample or *look* which then can be selectively accessed for future intelligent processing and decision making. It is this concept that allows the model to account for temporal resolution phenomena including modulation detection, gap detection, onset and offset weighting etc. A similar strong argument for a long term integrator model is not supported by these same studies.

3.4 Summary

As described in Chapter 2, much is understood about the physiology of the human hearing system. Less is understood though of the mechanisms associated with many hearing sensations, including loudness. It is often presumed that these sensations are highly individual but experiments have shown that for people with normal hearing, many sensations agree among listeners who have very different personalities, background and experiences. Because of this general agreement, it is also possible to predict them. The task of investigating the phenomena

and developing the tools to predict auditory sensations is given to the audiologist and is then often given to the engineers to apply the knowledge. Amongst the most fundamental of these tools is the psychoacoustic metric of loudness.

The early development of a loudness model is credited to Fletcher and Munson's paper, "Loudness, Its Definitions and Measurement" which included the first plot of the equal loudness contours (Fletcher & Munson, 1933). These contours provided insight into the perception of the intensity of sounds and more importantly related this perception to the physical parameter of sound pressure. The equal loudness plots have been updated several times and are presently standardized as ISO 226:2003 (International Organization for Standardization, 2003). Also of significance was Fletcher and Munson's recognition that the human ear reacts to sound in frequency bands instead of pure tones, a key element to future loudness models.

The first calculation model for loudness was proposed by Mintz and Tyzzer which plotted octave band data against curves from which loudness was determined (Mintz & Tyzzer, 1952). While their model lacked the inclusion of frequency masking effects, and thus good correlation to experiments, it did set a procedure for other more refined models to follow over the following years including that of Stevens. His model was more refined as it allowed for third octave input spectra which follows more closely the auditory filter characteristics of the ear and also accounted for frequency masking (Stevens, 1956). The model worked only reasonably well though for sounds with continuous spectra, thus eliminating most real world applications.

Zwicker developed the concept of critical bands which represent the filter envelopes of the auditory system (Zwicker, Flottorp, & Stevens, 1957) (Zwicker, 1961). This was critical for future loudness models in order to truly represent the auditory processing of the basilar membrane. The critical bands were to be further refined much later by Moore who renamed them as

Equivalent Rectangular Bandwidths (ERB) in 1987 (Moore & Glasberg, 1987). Zwicker's work would eventually lead to a steady loudness model in 1972 which would also eventually be adapted as the ISO standard 532B in 1975 (Paulus & Zwicker, 1972) (International Organization for Standardization, 1975). Improvements were later made to this model which bettered both the low frequency and low level prediction of loudness (Zwicker, Fastl, & Dallmayr, 1984). These improvements were eventually included in the 1991 DIN standard (Deutsches Institut für Normung, 1991).

The next innovation in loudness models was by Glasberg and Moore in 1996. Their model included updated transfer functions of the outer and middle ear as well as the application of the ERB filters (Moore & Glasberg, 1996). This model was eventually standardized by ANSI in 2005 and again updated in 2007 as ANSI s3.4 2007 (American Institute of Physics, 2005) (American National Standards Institute, 2007). Independent studies have shown that the Glasberg and Moore model has better correlation to the latest standardized equal loudness contours (Charbonneau, Novak, & Ule, Comparison of Loudness Calculation Procedure Results to Equal Loudness Contours, 2009) (Charbonneau, Novak, & Ule, Loudness Prediction Model Comparison Using the Equal Loudness Contours, 2009).

Most of the historical work has been directed toward loudness models for steady sounds, however, models for unsteady sounds have also been developed, but with much less success given the complexities associated with the modeling of the temporal components of the auditory system. A first model was proposed by Vogel which was not too successful as it was simply an extension of Zwicker's 1972 stationary loudness model (Vogel, 1975). Zwicker also proposed a time varying model himself, but given the complexity of the approach, it was not

very practical to implement. It did include the temporal effects of post-masking, but not pre masking (Zwicker, 1977).

The first real advancement in the development of a time varying model was by Glasberg and Moore in 2002 (Glasberg & Moore, 2002). Their model which uses both short term and long term integration of the time signal is capable of accounting for many temporal phenomena. It has not shown adequate prediction of burst sounds or sounds in the presence of gaps. Another method has been recently standardized by DIN (Deutsches Institut für Normung, 2007). However, this standard is available in German only, so a review of its contents has not been included.

The time varying loudness methods to date rely on temporal integration to combine the acoustic energy of the stimuli over time. Different integration models exist, including the “leaky integrator “ model but other studies have shown that the integrator approach cannot explain many temporal processing phenomenon of the auditory system (Viemeister & Wakefield, 1991) (Pedersen B. , 2006). It has been proposed instead by Veimeister that a more plausible model for the processing of time varying sounds is the multiple look approach (Viemeister & Wakefield, 1991). Through several experiments, he showed that sounds are processed by the auditory system in small samples about 1 ms in length and stored. It is thought that if the sounds are continuous then the samples are somehow integrated. If the sounds though are not continuous, have burst components or gaps, then the stored samples are processed in a manner other than by integration. Pederson and Moore have both suggested that the decision on how the sounds are processed is often based on experience (Pedersen & Ellermeir, 2005) (Moore, 2003).

It has been demonstrated that much work has been done over the past 80 years or so in the development of loudness models for stationary sounds. Progress has also been accomplished in

the initial development of time varying loudness models using time integration techniques. While this approach has shown good results for some unsteady sounds, others have shown that integration is not the likely mechanism employed by the auditory system. A more likely approach is some form of the multiple look approach. Given the above, the remaining chapters of this dissertation will focus on applying the knowledge gained thus far on the multiple look theory and applying this knowledge toward the development of an improved loudness calculation model.

IV Theory

Most sounds encountered in real life are not steady in nature and can instead be significantly time dependant. As such, the calculation of loudness for these unsteady sounds must also be a function of time. Examples of unsteady sounds include speech and music. Of particular interest to engineers is what is referred to as technical sounds which are often rhythmic or impulsive in nature and may be associated with an inadequate sound quality, especially when dealing with consumer products.

Depending on the temporal nature of a sound, whether it is a tone burst or short gap, the perceived loudness of the sound is often significantly different if the occurrence is less than 100 ms. Loudness for sounds having durations longer than that are usually independent of the duration (Fastl & Zwicker, 2007).

Given the above, the manner in which an unsteady loudness model treats the temporal component of a sound is critical. Some theories which were initially thought to be good models for the mechanisms of the auditory system have been subsequently found through experimentation to not be accurate for all types of sounds. As such, these approaches are now treated more as a “best available” approximation. Other approaches which seem to better represent these mechanisms are not as practical to implement. The following sections will provide a more detailed background to the underlying theories of these philosophies. Also given is a more detailed description of the Cambridge model which is one of the more popular approaches for calculating loudness. This more thorough description is necessary as the following chapter for approach will use this model and as such, a good understanding of its methodology is important.

4.1 Temporal Integration

The more common models which are able account for temporal resolution follow the idea that latency exists within the auditory system which limits temporal resolution. The true cause of latency, if it does in fact exist, is not known. Some thoughts are that it is related to inertial effects within the cochlea while others believe it is associated with the activities of auditory nerve. Others still believe that time latency does not really exist and instead the observations which lead to the conclusion of its existence are instead related to neural processing within the brain. Most loudness models follow the philosophy of the former. As a result, these models use temporal integration to sum the acoustic or neural energy of a sound over time.

Models using temporal integration can be divided into two groups. The first group, which covers the majority of the models, use an integration approach which occurs over a relatively long period of time, often up to a few hundred milliseconds. The running average approach, or leaky integrator, are included in this classification and are described first. The second group assumes a much shorter integration time. A third group may also be accepted which uses a combination of both short and long integration times.

Munson was the first to propose that the auditory system used some form of integration in 1947 when he suggested the use of a leaky integrator model (Munson, 1947). Hartman (Hartmann, 1998) provides a good description of the leaky integrator model by comparing it to the measure of the intensity of rain by measuring the rate at which it fills a container when left out in the rain. If for example there was 5 mm of rain in the container after 20 minutes, one would conclude that the rate of rainfall was 15 mm per hour, a measurement representing a perfect integration of the rain fall. This can be modelled by:

$$h_r = Rt_I \quad (5)$$

Here, h_r is the height of water in the container, R is the rate of rain and t is the integration time constant. If for instance it was necessary to measure the rate of rainfall on a continuous basis, and if the container were relatively small such that it would eventually fill up, one could drill small holes in the container to allow the rain to leak out at a controlled rate. The rate now at which the container would fill with rainwater is given by the following equation where l is given as the rate of water leaking out of the holes in the side of the container:

$$\frac{dh_r}{dt} = R - l \quad (6)$$

Now to better ensure that the container does not over flow, one could drill additional holes in the container such that more rain leaks out as the level of rainwater in the container becomes higher. The leak rate is proportional to the height of the water and the constant of proportionality, given by τ , which has the dimensions of time.

$$l = h_r/\tau \quad (7)$$

From equations 6 and 7, the differential equation for the height of rainwater in the container be given as:

$$\frac{dh_r}{dt} = R - h_r/\tau \quad (8)$$

Solving for the solution of the differential equation, where $h_{r,0}$ is the initial height of water in the container, we get:

$$h_r(t) = R\tau(1 - e^{-t/\tau}) + h_{r,0}e^{-t/\tau} \quad (9)$$

The above equation 6 describes the output with respect to time for a leaky integrator system. Using this concept, Plomp and Bouman (Plomp & Bouman, 1959) (Hartmann, 1998) assumed a constant time constant and surmised that loudness was an accumulation of neural spikes. In other words, the response to a stimulus over a period of time t is given by the accumulated number of spikes given by $h_r(t)$. Now, if one were to assume that loudness increases monotonically with neural spike count, then equation 9 supports the observation that loudness

grows with duration of a steady sound (up to a duration of approximately 200 ms). It is from this observation that many unsteady loudness models justify the use of the leaky integrator approach. If on the other hand the sound is much shorter in duration, the time constant used for longer sounds would be too large to be applied, or $t \ll \tau$. For this case, the models instead would simply apply the perfect integrator approach given in equation 5 above. This however, is a rather simplistic approach.

As stated earlier, a second classification of integrator models use a much shorter time constant. These models are usually designed to work for specific auditory tasks such as modulation detection, gap detection or non-simultaneous masking (Moore, Glasberg, Plack, & Biswas, 1988). The downfall of this integration approach is that these models greatly mispredict quasi steady and steady sounds. A first test after all for an unsteady loudness model would be its ability to adequately predict the loudness for a steady sound such as a steady pure tone. Here, the performance of such models would fall short.

More sophisticated models instead can use a number of varying time constants chosen depending on the length of the steady subset of the stimulus within the unsteady signal. The problem with this approach is that that the time constants are assumed and fit well with quasi steady subsets of stimuli only, including sounds with modulation. This approach does not work well with sounds containing burst components or short duration gaps.

4.2 Multiple Look

Upon having a better understanding of the integration approach, a resolution-integration paradox becomes apparent (Green, 1985). That is, several solutions exist for which none are satisfactory for all conditions. One solution to this is to use a completely different approach which avoids the necessity for sole integration of the time data. Listening experiments have shown that change in threshold, as well as other levels with respect to change in signal duration,

occur because a longer stimulus provide more opportunity or chances to detect the stimulus through repeated and/or multiple sampling. This concept is called multiple looks. An ideal implementation of such a model would be for it to accommodate a loudness calculation which includes all auditory mechanisms resulting from a temporally changing stimulus. Some of these include gap detection, burst detection, modulation detection and increasing threshold level detection with increasing stimulus duration.

A few methods for the application of multiple looks have been proposed over the years, although none have been implemented (Green & Swets, 1966) (Viemeister & Wakefield, 1991). Presented here is a proposed approach which has resulted from the background research for this dissertation. As will be described later, the following methodology does have implementation limitations as a result of limitations of the available technologies. As a result, a compromised model is detailed in the next chapter which describes the approach of this dissertation.

The process begins with the acquisition of a single channel of stimuli representing a binaural diotic signal which is sampled with sufficient resolution and sampling rate to satisfy the Nyquist theorem for the desired upper frequency range. The transfer function of sound through the outer ear and middle ear is then applied. A decision is required as to whether the model will accommodate frontal incidence only or also include random incidence, with application of the appropriate transfer function. A decision is also required as to the length of an individual look. Given today's sampling rate capabilities, a 1 ms look is recommended. Look durations less than 1 ms are believed to be smaller than actual auditory resolution (Fitzgibbons, 1983). Longer looks, particularly those greater than 3 ms, would result in temporal windows lacking sufficient resolution to constitute a look and would instead require integration with a short time constant.

The looks then undergo a frequency analysis dividing the signal into frequency spans matching the auditory critical bands. From here, the excitation pattern for each of the critical bands can be determined for the 1 ms sample. Care would need to be taken to ensure that an appropriate rise and decay rate for each excitation pattern is used as these are level dependant with low frequency slopes in the pattern becoming less steep with increasing level. The next step in the model is the calculation of the instantaneous loudness from the excitation patterns. The transformation from excitation to a specific loudness pattern involves a compressive nonlinearity such as a half wave rectification followed by a window with a short time constant. This is meant to resemble the compression that occurs in the cochlea (Yates, 1995) (Ruggero, Rich, Recio, Narayan, & Robles, 1997). The instantaneous loudness is now resolved as the area under the specific loudness pattern. This provides the loudness for the 1 ms look. The running output of these looks are then stored in short term memory which has its own decay characteristics and a time constant that is much longer than the look. This time constant may be as high as 200 ms. These memory allocations can be treated as a vector of the looks of the processed input. These looks can then be made available for appropriate computations and comparisons. The model can scan the vector to find envelope fluctuations representing modulation, significant bursts or gaps in the input. A decision can then be made as whether to process the data immediately, for example increasing the instantaneous loudness to the data immediately preceding a gap or perhaps taking relatively steady or unchanging instantaneous loudness over a sufficient period of say 10 ms and applying an appropriate integration technique. Another idealized application of a temporal resolution task involving integration would be for the detection of a tone. It is expected in this case that an observer would use all of the samples for a tone within an observation interval. As the duration of the tone increases, so

would the number of looks, thus resulting in an improvement in auditory performance or lower threshold up to the end of the 200 ms time constant.

From a philosophical perspective, the above procedure of application of the multiple look model is hypothesized to be feasible. It should be noted that components to the procedure which are critical to the modeling of loudness, including application of the ear transfer functions, determination of the excitation patterns, specific loudness and instantaneous loudness, are not unique to this model. While these steps are common to most all loudness models, they are independent from the temporal components of the calculation procedure. It is the proposed temporal treatment of the looks which is unique. From a practical perspective, implementation of the multiple look model does have its limitations. This is mainly due to the limitations associated with the available digital signal processing techniques associated with the frequency analysis of very short time signals, in this case 1 ms. These limitations will be discussed in greater detail in Chapter 5.

4.3 Unsteady Loudness Model

In order to have an adequate understanding of the approach given in this dissertation which will be detailed in the next chapter, a thorough understanding of the unsteady loudness model is required. The methodology for this model, which is referred to as the Cambridge model, was first detailed by Glasberg and Moore in 2002 (Glasberg & Moore, 2002).

The Cambridge model was initially a steady loudness calculator which was later adapted to also be able to predict loudness for time varying sounds. One of the short comings of the original model was that it required the input of the spectrum for the target sound in one third octave bands. The updated time varying model instead uses a time wave input of the sound, such as that acquired by a microphone and analyzer system.

The first step of the model is to impose a finite response filter which approximates the transfer function for the outer and middle ear. An illustration of the transfer function is given in Figure 15. By performing the filter operation on the initial waveform as opposed to modifying the magnitude values in a calculated Fast Fourier Transform (FFT), which is to be performed later, smearing of the low frequencies by the windowing operations are avoided. The result of the transform process is representative of the sound reaching the cochlea.

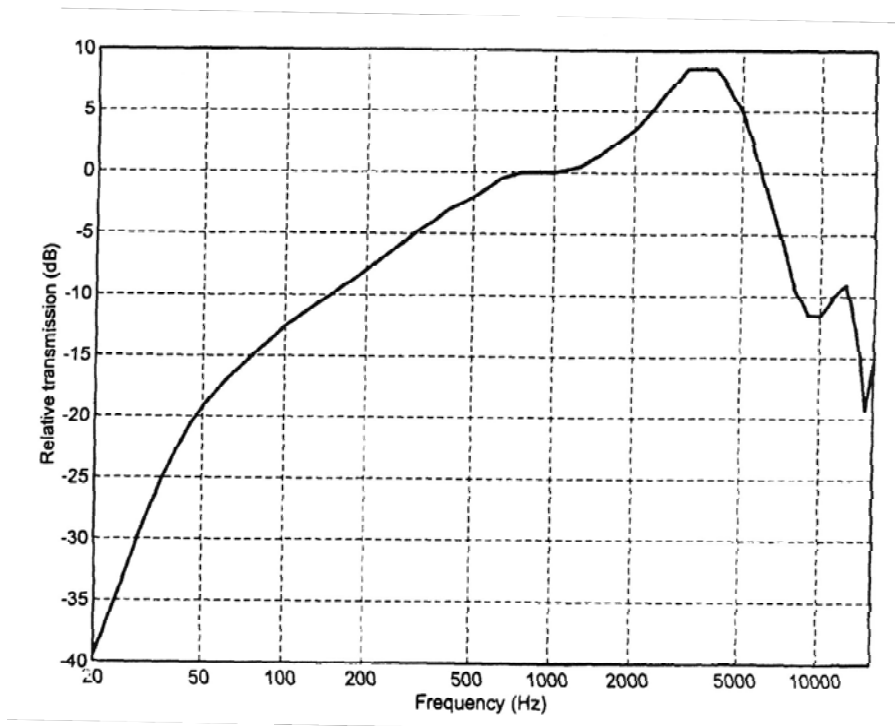


Figure 15: Graphical representation of the transfer function representing the effects of the outer and middle ear on the time waveform input. The result of this filter is a representation of the sound at the cochlea (Moore, Glasberg, & Baer, A Model for the Prediction of Thresholds, Loudness and Partial Loudness, 1997)

The next step is the calculation of the short term spectrum of the modified waveform using an FFT. Given that the frequency content of an expected waveform is spread across the audible frequency range, multiple FFTs are required to achieve adequate spectral resolution at the low frequency ranges. To accommodate this, six simultaneous FFT operations are performed in

parallel. To achieve adequate low frequency resolution a compromise was made by using relatively long time periods of the input signal of 64 ms. From this alone, a compromise in this method is already apparent given that the resulting excitation patterns derived from the 64 ms processed signal will be approximated to represent auditory stimuli in the order of one to several ms. A second compromise to the long signal length of the low frequency FFT is that amplitude modulations containing low frequency data will not be detected. For the higher centre frequencies, the time segments for the FFTs get shorter as the centre frequencies increase thus achieving improved temporal resolution which is more representative of the auditory system.

Next, calculation of an excitation pattern using the spectral results of the FFT analysis is performed. The outputs of Equivalent Rectangular Bandwidths (ERBs) are produced for the centre frequencies spaced at 25% of the ERBs. These excitation patterns represent the response along the basilar membrane across the audible frequency range as was described in Chapter 1.

The excitation patterns are then transformed to the specific loudness pattern. The specific loudness curves are integrated to approximate the total instantaneous loudness. This is similar to the calculation for loudness for a steady input sound.

The instantaneous loudness is then integrated in time to predict the temporal component of the perceived unsteady loudness. To include as many temporal phenomena as possible, the Cambridge model performs both a short term and long term integration process. The short term loudness is estimated from 1 ms time segments of the instantaneous loudness results. By comparing subsequent short term loudness values a decision is made as to whether the signal is changing rapidly in time, thus suggesting the presence of a burst signal and also accommodating high frequency amplitude modulations of the signal. This comparison is achieved by inspection

of the rise and decay rates of the 1 ms durations and allowing for the implementation of a short integration process with an appropriate short time constant. The long term loudness is calculated by temporally integrating the short term loudness results, thus also smoothing the response over time.

This model has been shown to provide excellent results for steady sounds by accurately predicting absolute threshold levels as well as loudness as a function of amplitude level and bandwidth. It has also shown good correlation to the equal loudness contours. For unsteady sounds, the model showed good correlation with empirical data in predicting the effect of increasing threshold levels, or detectability, with increases in duration as great as 200 ms. This can be attributed to an appropriate long term temporal integration process. The model was also able to adequately account for the long term loudness of amplitude modulated sounds. A good match to empirical data was shown to be possible for modulation rates from 2 to 1,000 Hz on a 4,000 Hz carrier. As alluded to above, the calibre of the model's ability to predict amplitude modulation for lower carrier rates is decreased. Limitations of the model are that it has not been shown to accommodate extremely short burst signals or the detection of gaps in the stimulus.

V Approach

Section 4.1 in the previous chapter described the fundamental theory for the more common temporal integration techniques used for the calculation of time varying loudness. It was shown that long term integration can be used with relatively good success for time varying sounds which are quasi-steady for durations of 10 ms or more and that short term integration can be useful for predicting some auditory observations including tone bursts. Also shown was the Cambridge model developed for the calculation of time varying loudness. This model uses both short and long term temporal integration to account for several auditory phenomena.

A description of a proposed procedure for calculating unsteady loudness using a multiple look model was also described. The caveat to this procedure is that it requires that a Fast Fourier Transform be applied to very short segments of the stimulus having lengths of approximately 1 or 2 ms. This is not possible given the limitation in frequency resolution that this would impose on the processed signal. A justification for this is given as follows:

Given that the input stimulus is a 16 bit WAV file having a frequency span of 25600 Hz, present day acquisition capabilities allows for a smallest number of samples or divisions of the signal to be 50. From this, the smallest frequency resolution possible is calculated as 25600 divided by 50, or 512 Hz. This translates into a minimum sample length being the inverse of 512 Hz which is 2 ms. In other words, the limitation of a state of the art acquisition is a minimum sample length of 2 ms with a lower frequency limit of 512 Hz. While an argument towards a compromise for using a signal length of 2 ms may be possible, having a lower frequency cut-off of 512 Hz is not justifiable. The lower extreme for the audible human frequency range is 20 Hz which is far below the above limitation of 512 Hz. Such a system would not be useful for practical analysis applications.

While the development of a true multiple look approach is desired, it was decided that for the research presented in this dissertation that a calculation method which is alternative to the present loudness models, but still retains both the spirit and ability to account for auditory phenomenon which the present models are incapable of, be developed. This hybrid approach is one which samples the stimulus signals as 1 ms looks and can processes the information to account for known auditory characteristics. It was further decided to focus on the specific characteristic of gap detection as this is one phenomenon which has been documented experimentally but has not been demonstrated to be included in any other loudness model. While extension of the proposed model could be made in the future to include other auditory traits, the focusing on one specific hearing aspect will also allow for easier demonstration without the need to account for multiple attributes. The following section is a description of the methodology of the proposed model. Subsequent sections will include details of the experimental setup and test parameters.

5.1 Proposed Model

The stated goal of this research is to develop a model using the philosophy, and thus advantages, of the multiple look theory to calculate loudness. The model is to include the auditory attributes associated with the presence of short duration gaps in the stimulus signal. Specifically, the model will account for the empirical data by Viemeister and others as was described in Chapter 3. Another goal for the proposed model is that it is designed such that it can be adapted to be used as an extension to most any time varying model and thus account for the short comings of these other models as well as compliment to the advantages and abilities of these models. In other words, this model would perform as an add-on to the loudness model and will target a specific auditory task through intelligent processing of the sampled looks.

The process begins with the input of a single channel of stimuli which represents the binaural diotic signal presented to the outer ear. The signal is sampled as a 16-bit resolution WAV file with a 32 kHz sampling rate. This will result in a file containing 32 samples for every 1 ms of stimulus data. The length for each look was chosen to be 1 ms. Studies have reported this to be the minimum length for audibility (Fitzgibbons, 1983).

As shown in Figure 16 for a steady sinusoidal wave, the 1 ms look is comprised of 32 samples, each representing the amplitude of the peak pressure of the wave. For the WAV file, each of the samples is given as a hexadecimal number. A calibration factor taken from the acquisition system is applied to each sample. The calibration factor scales the maximum value representing the full scale deflection of the acquisition file and fits this between the full scale deflection of the WAV file, or between the values of 32 768 and -32 768 for a 16 bit file.

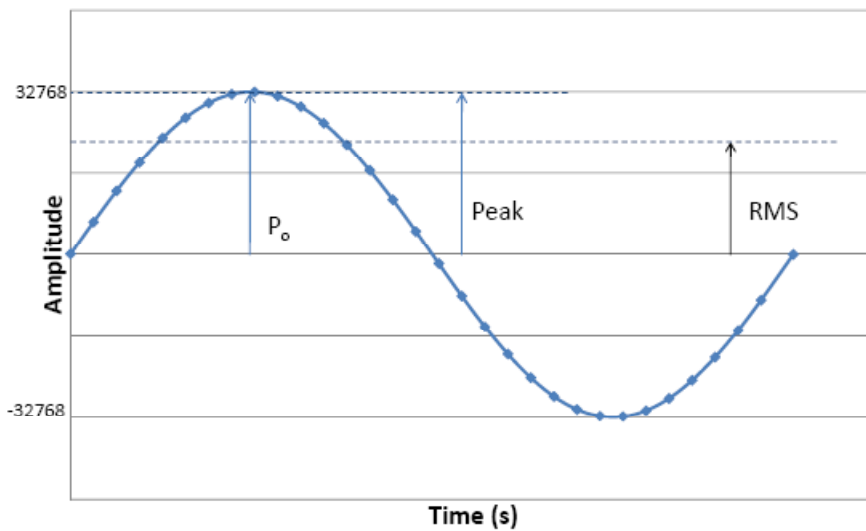


Figure 16: Sinusoidal representation of a 1 ms WAV file comprised of 32 samples which are given by hexadecimal values. Defined are the amplitudes for the Peak and RMS pressures of the sound wave

Each of the samples is next converted from a peak pressure value to a root mean square (RMS) value. This converts all samples to all positive hexadecimal values. Each RMS pressure is changed to a sound level having units of decibel (dB) using equation 10.

$$L = 20 \log \left(\frac{P_{RMS}}{2 \times 10^{-5}} \right) \quad (10)$$

Finally, in order to represent the 32 samples of sound level as a single 1 ms sound, a one millisecond equivalent sound level is calculated using equation 11. This is an energy mean of the noise level averaged over the 1 ms measurement period.

$$L_{eq} = 10 \log \left[\sum_{i=1}^N (f_i) (10^{L_{pi}/10}) \right] \quad (11)$$

Once the 1 ms sound levels have been calculated from the acquired WAV file, intelligent processing of the noise information can be performed. Specifically, the signal is scanned for the presence of any short duration gaps spanning in length from 1 ms to 5 ms. If a gap is found, a detectability shift is applied with amplitude dependant on the length of the gap. While this can be user defined, a gap is taken to be when there is a 25 dB drop in level from one millisecond sample to the next. The 25 dB drop for recognition of a gap is taken from Shailer's 1983 publication on '*Gap Detection as a Function of Frequency, Bandwidth and Level*' (Shailer & Moore, 1983). Once a drop is found, the next step is to determine the length of the gap. A loop is designed to perform this operation where the level for each look is compared to the look just prior to the presence of the gap. If the gap is found to be 1 ms long, an adjustment of 4 dB is applied to the adjacent sound. Similarly, adjustment values of 3.5, 3, 2.2 and 1.6 dB are applied if a gap of 2, 3, 4 or 5 to 10 ms respectively is found. These adjustment factors are illustrated in Table 3. If the gap is determined to be longer than 10 ms, no adjustment is applied and the gap is instead defined as a drop in level and the search parameter is reset.

Table 3: Detection correction levels for applied for corresponding gap durations to the 1 ms looks

Duration of Gap (ms)	Detectability Adjustment (+dB)
1	4.0
2	3.5
3	3.0
4	2.2
5 to 10	1.6
Greater than 10	0.0

Once the file has been entirely searched and all detectability shifts have been applied, the file WAV file must then be reconstructed into its original form for analysis of loudness. This involves a reversal of the previous procedure to where the Peak pressure values in hexadecimal format are obtained. A flow chart outlining the algorithm for the model is shown in Figure 17.

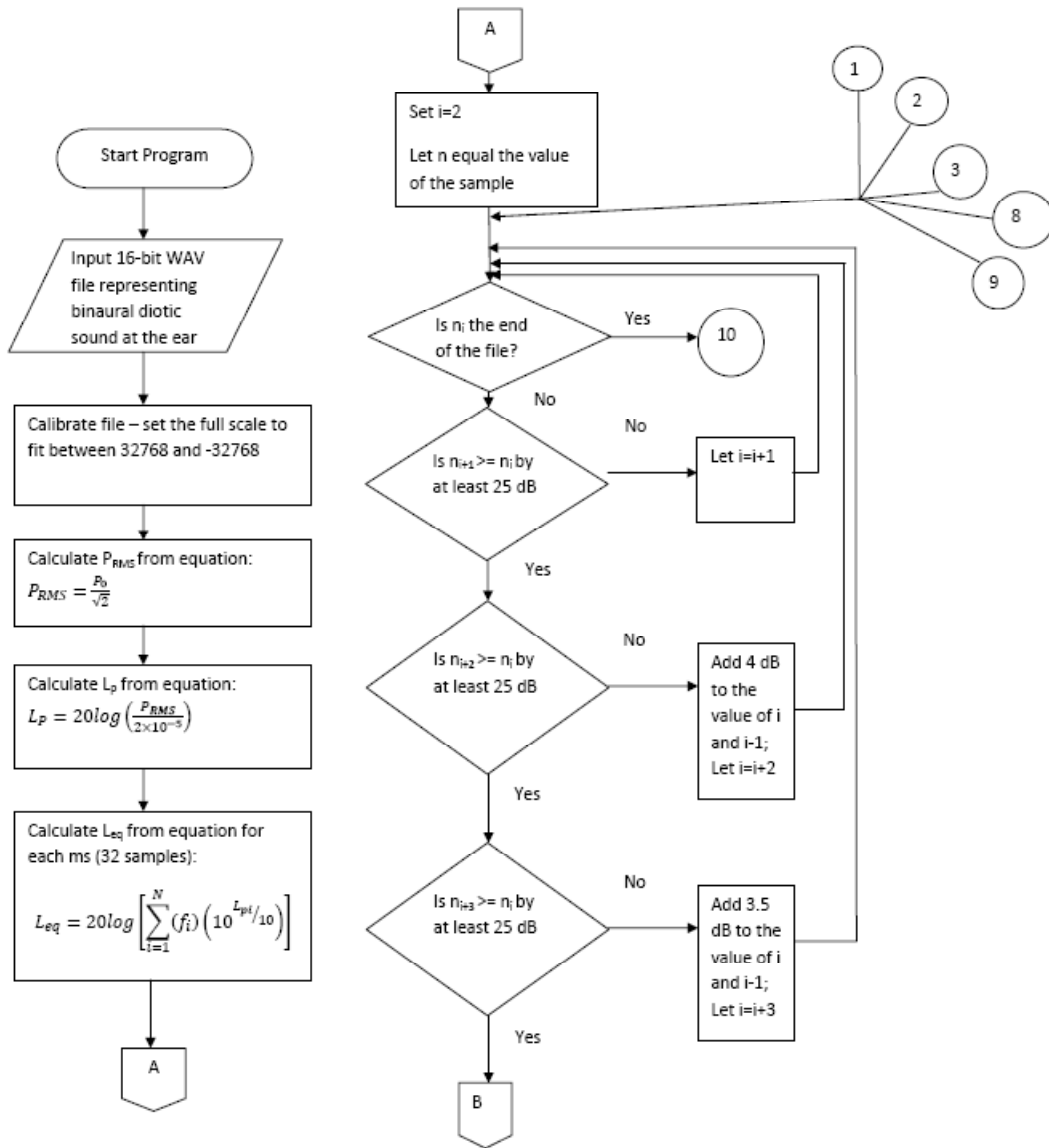


Figure 17: Flow chart illustrating the proposed model from input of WAV file, conversion to 1 ms looks and search and adjustment procedure for the presence of gaps. The adjusted file is subsequently reversed back to a WAV file format suitable for the calculation of loudness

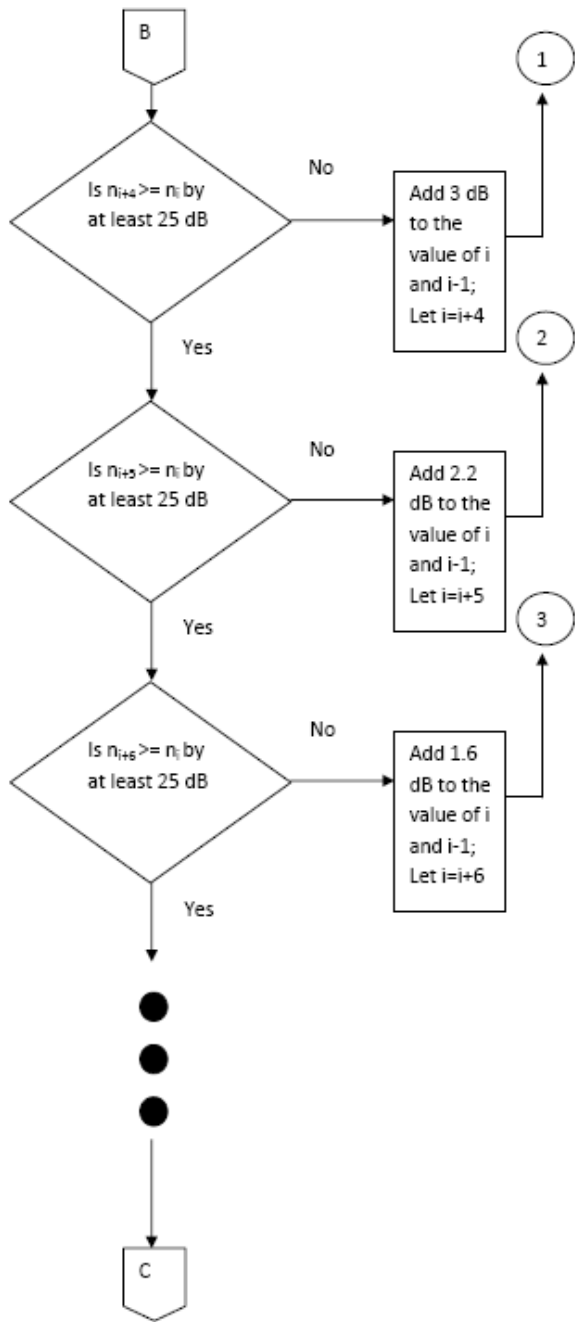


Figure 17 continued

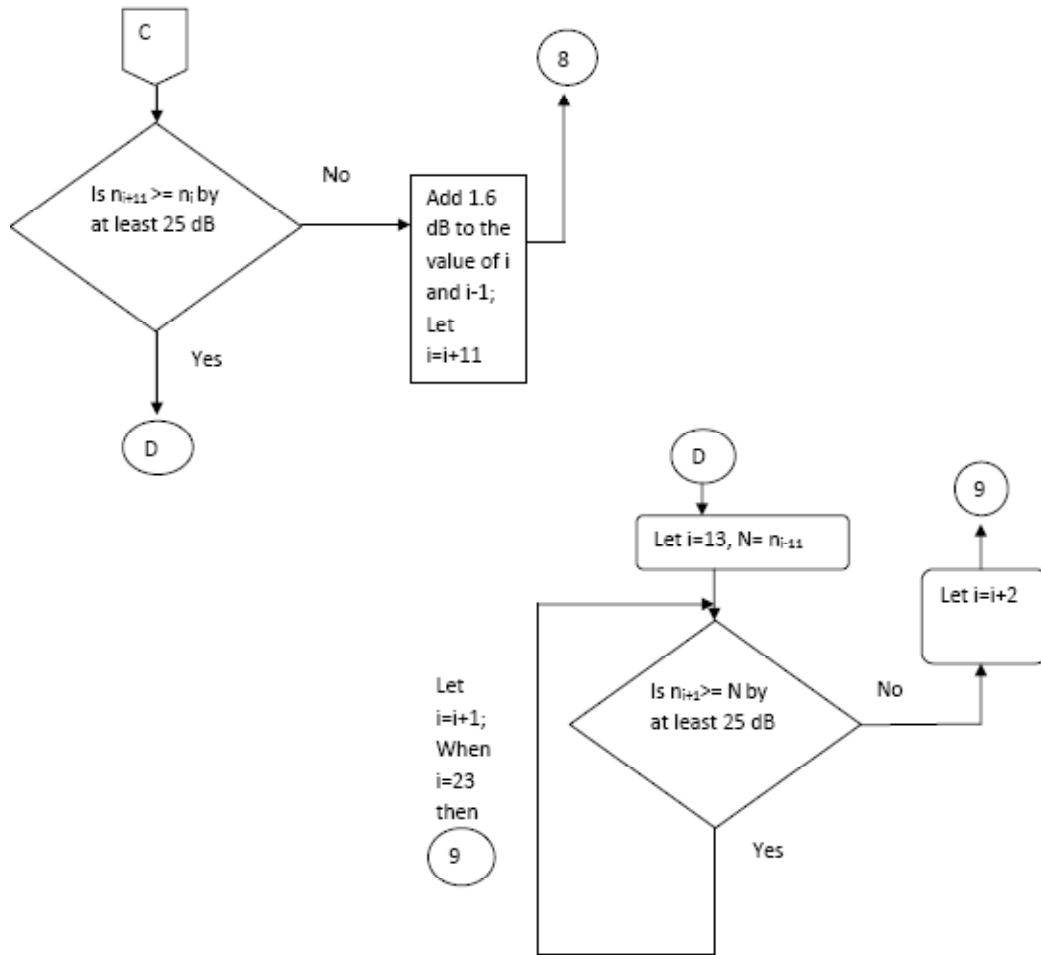


Figure 17 continued

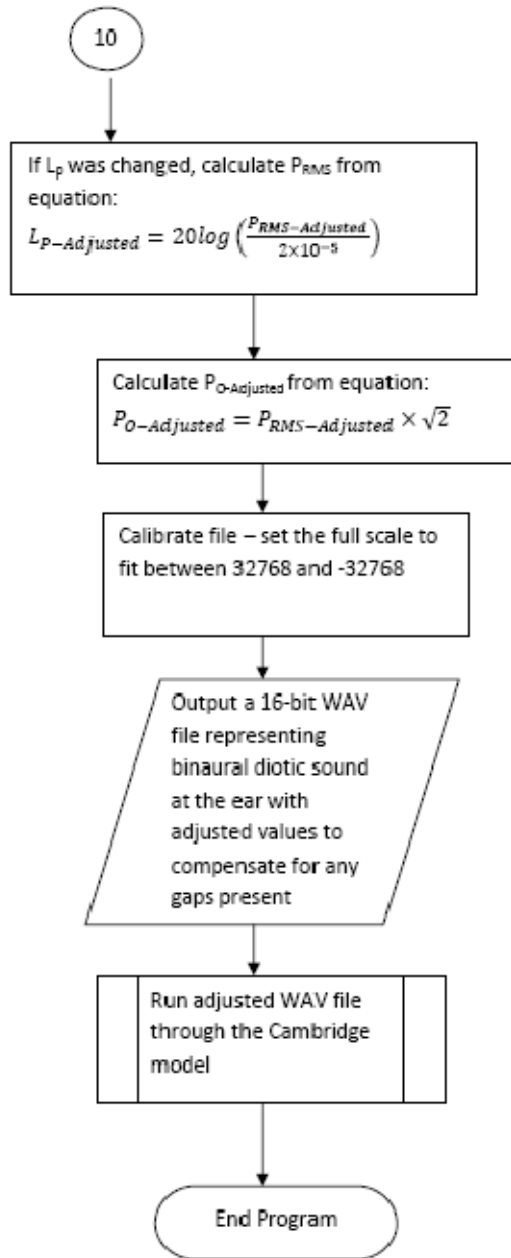


Figure 17 continued

A computer program was developed to perform the operations of the outlined model using the programming language of Ruby. Ruby is a general purpose object oriented language which was originated in the mid-1990s. This programming language was chosen for its simplicity and ease of programming as well as for the fact that it is easily integrated into other language codes. This was important given that one of the goals of this work was to be able to interface the multiple look gap correction model to any time varying loudness model. Another advantage of the use of Ruby for this research is that it is an open code. The auditory data used for the development of the multiple look gap correction model is based on the present state of art knowledge. It is possible that future studies may dictate the necessity for changes in threshold corrections values or duration limits. The open code format used here will very easily allow for such modification. A copy of the written source code for the multiple look gap correction model is provided in the appendix as Reference A.

5.2 Test Procedure

In order to test the proposed model, a test procedure was established using several recorded sounds including stationary and time varying pure tones, white noise, warble tones as well “real life” sounds including speech and mechanical sounds. Some of the sounds were altered so as to insert gaps in the signals of known location and duration to test and debug operation of the multiple look gap correction computer code.

The pure tones were used to establish that the input signals were in fact calibrated to the correct levels. This is facilitated by the fact that a known stationary pure tone signal at a measured sound level can be easily translated into a corresponding loudness or loudness level by cross referencing the two values on the equal loudness contour plots.

The white noise sounds were chosen to represent broadband stimuli. Given that such a signal is inherently constant and without gaps, voids in the data file of varying lengths were inserted and run through the gap detection program. The output was monitored to ensure that the appropriate level corrections were applied. The same was done for the time varying pure tone signals.

The warble tones are representative of variable sounds with short duration gaps. The mechanical sound was of a diesel engine which is another source which has characteristic gaps. Speech sounds can be either relatively smooth or have many sporadic gaps. Two sentences, "Clickity clack, the train goes down the track" and "Suzie sold seashells by the sea shore" were recorded and analysed. These two specific sentences were chosen to represent both a choppy and smooth speech sample respectively.

All the sounds were recorded in a semi-anechoic room having a background sound level of approximately 17 dBA. The main reason for using the chamber was to remove any potential influence on the recordings from outside sources of noise. The recording setup used a Bruel & Kjaer PULSE Type 3560C IDA^e Front end for both the signal generation and the recording of the sounds. The sounds were generated using the PULSE signal generator and send to a Bruel & Kjaer Type 4295 Omni source loudspeaker via a Type 2716 power amplifier for amplification of the signal. A Bruel & Kjaer Type 4190 microphone with a Type 2671 preamplifier was used to acquire the loudspeaker signal at a distance of 0.5 meters from the centreline of the vertically oriented driver. The output to the speaker from the generator was controlled and fined tuned by adjusting the voltage output of the signal generator. The resolution adjustment capability of the generator is one microvolt. The measurement setup was field calibrated before and after measurements using a Bruel & Kjaer Type 4231 sound calibrator. The technical data sheets

detailing the specifications for the acquisition equipment are provided in the appendix as Reference B. A photograph illustrating the equipment setup in the semi-anechoic room is given in Figure 18.



Figure 18: Photograph of the experimental set up in the Semi-Anechoic room showing the Bruel & Kjaer acquisition system, amplifier loudspeaker and microphone. The test sounds are generated by the PULSE sound generator and played by the loudspeaker and subsequently recorded through the microphone. The acquisition system then prepares the WAV file for the multiple look gap correction and loudness programs.

Once the test signals were recorded, and in some cases modified with reference gaps, they were processed into 16 bit WAV files suitable for input into the multiple look gap correction and subsequently loudness models. Outputs of the results are given in the next chapter. The time varying loudness model used to perform the loudness calculation was the Cambridge model

which was detailed in the previous chapter. As stated earlier, some of the test signals were also stationary sounds. While the Cambridge is purported to accurately calculate loudness for stationary sounds, the stationary test sounds were also processed for loudness using a program designed to follow the DIN 45631 steady loudness standard. While some differences are expected in the calculated stationary loudness values between the two models, these should be minimal. This is especially true for the 1000 Hz sinusoidal signals since all loudness values on the equal loudness curve are referenced to this frequency. These results are also given in the following chapter.

VI Discussion of Results

This chapter presents the results from the implementation of the multiple look gap correction model on the various test samples. The calculated loudness using the multiple look approach will be compared the corresponding loudness results from implementation of the Cambridge time varying loudness program for all files. The files derived from the stationary sound will also be compared to the DIN 45631 stationary loudness model. This is to provide a correlation between the time varying and non-time varying loudness models as well as to the multiple look adaptation. Presented also for each sample type is a high resolution time domain image of the sound file and sample outputs from the multiple look program which identifies the number and location of found gaps and the corresponding correction factors applied.

6.1 Stationary Pure Tone Sounds

As an initial test of the multiple look gap correction model, and its adaptation to the Cambridge time varying loudness model, pure sinusoidal tones were generated at 1000 Hz and tested using the various models. The advantage of using the 1000 Hz sinusoids is that the calculated loudness levels can be compared directly back to the equal loudness contours, given previously in Figure 2. That is, a 1000 Hz sinusoidal tone having a sound level of 90 dB will theoretically have a corresponding loudness level 90 phons. The sound levels tested included 60 dB, 65 dB, 70 dB, 73 dB, 80 dB, 85 dB, 90 dB and 94 dB (standard microphone calibration sound level).

The obvious thing to note is that a sinusoidal wave is a continuous sound wave and thus has no gaps. In order to use these signals, gaps were inserted into the wave in the centre of each 10 ms segment for the first 50 ms. The next 20 ms duration had no gaps inserted. The 70 ms signal was then repeated for a total signal length of 2000 ms. This exercise was also beneficial in the

initial debugging phase of the program as it allowed for inspection of the data output to ensure that the appropriate correction amplitudes were applied to the correct corresponding gaps. Illustrated in Figures 19 and 20 are the time domain plots for both the unmodified 90 dB sinusoidal sound as well as the corresponding plot with the inserted gaps. The similar plots for the other steady sinusoidal signals are provided in the Appendix as Reference C. For reference, the location of the inserted gaps and expected adjustment values is provided in Table 4.

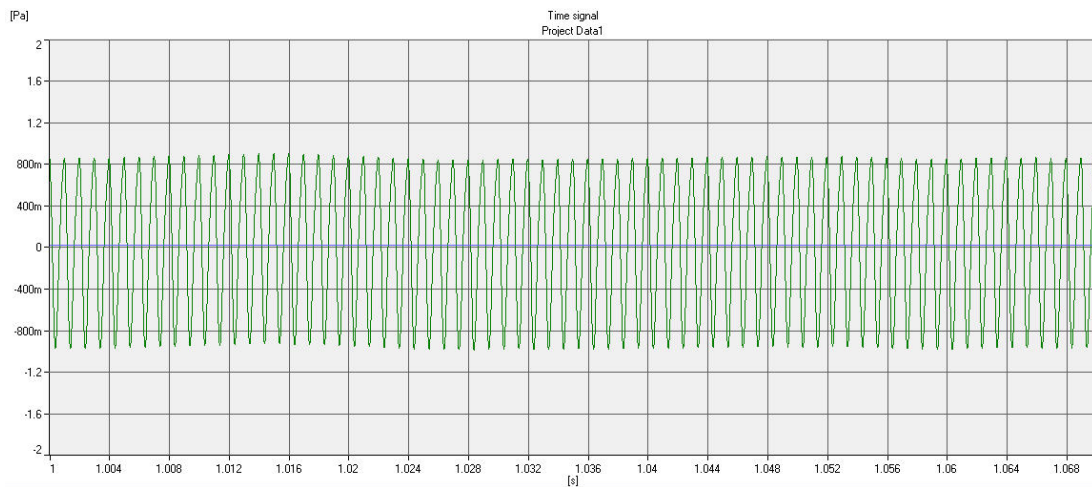


Figure 19: Time domain plot for the 90 dB sinusoidal test sound without the modifications of inserted gaps in the signal

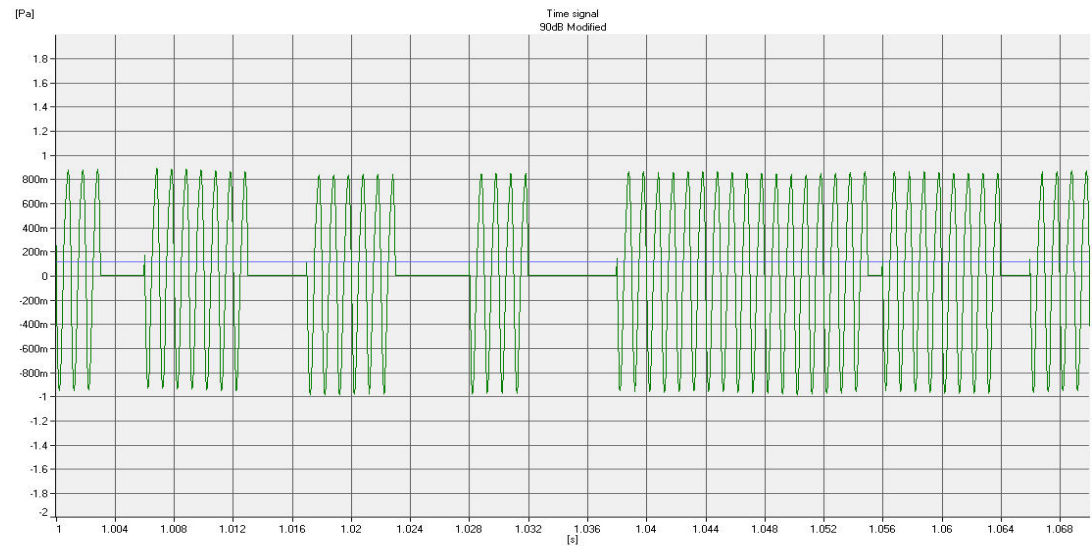


Figure 20: Time domain plot for the 90 dB sinusoidal test sound with the addition of inserted gaps in the signal with position and gap durations as specified in Table 4

Table 4: Position in signal duration having inserted gap, the length of the gap and corresponding adjustment

Segment in Signal for which Gap was Inserted (ms)	Length of Gap (ms)	Adjustment (dB)
1 to 10	1	4.0
11-20	2	3.5
21-30	3	3.0
31 -40	4	2.2
41 – 50	5	1.6
51 – 60	0	0.0
61 - 70	0	0.0

The test results for the steady sinusoidal signals without the inserted gaps are given in Table 5. The test results for the steady sinusoidal signals with the inserted gaps into the signals are given in Table 6. Listed are the sound level for the tones, the steady loudness level calculated using the method specified by the DIN 45631 standard, the calculated loudness level using the time varying Cambridge model and the loudness level using the multiple look gap correction model.

Table 5: Loudness level for 1000 Hz sinusoidal signals without inserted gaps calculated using DIN 45631, Cambridge model and with multiple look gap correction model

Signal Sound Pressure (dB)	Stationary Loudness Level (Phons) from DIN 45631	Time Varying Loudness Level (Phons) from Cambridge Model	Time Varying Loudness Level (Phons) using Multiple Look Gap Adjustments
60dB	55.2	58.2	58.2
65dB	65.4	65.5	65.5
70dB	72.3	71.5	71.5
73dB	74.9	74.2	74.2
80dB	81.8	79.7	79.7
85dB	87.2	84.8	84.7
90dB	93.7	90.3	90.3
94dB	98.2	94.7	94.7

Table 6: Loudness level for 1000 Hz sinusoidal signals with gaps inserted calculated using DIN 45631, Cambridge model and with multiple look gap correction model

Signal Sound Pressure (dB)	Stationary Loudness Level (Phons) from DIN 45631	Time Varying Loudness Level (Phons) from Cambridge Model	Time Varying Loudness Level (Phons) using Multiple Look Gap Adjustments
60dB	66.5	68.4	70.3
65dB	73.1	74.1	75.7
70dB	78.3	79.2	80.7
73dB	80.4	81.1	82.5
80dB	85.7	85.9	87.2
85dB	90.6	90.0	91.1
90dB	95.7	94.7	95.9
94dB	99.9	97.5	98.6

Inspection of Table 5 shows very good agreement between the Cambridge model results and the multiple look model incorporating the adjustments for gaps. In fact, the values between the two columns are for the most part identical. This should be of no surprise given that the signal is void of any gaps, and therefore, no adjustments should be expected. The numerical results for these two calculations are also in very good agreement with the signal sound pressure level.

That is, given that the stimulus is a pure tone at 1000 Hz, the resulting loudness levels should be the same as the inputted sound level. The differences realized between the two range between a relatively small 1.8 and 0.2. The loudness levels calculated using the DIN procedure for a steady signal did not do as well. The differences here between the input sound level and the loudness level are a more significant range from 4.8 to 0.4 with most of the difference at least 2.0. While this observation has little bearing on any direct conclusions to the multiple look model, it does raise some caution to the accuracy of the DIN model. This is supported in the literature (Charbonneau, Novak, & Ule, 2009).

Inspection of Table 6 shows a marked change in loudness level for all models. This is not surprising given that the “gapped” model does sound significantly different than the original sinusoidal wave and thus should not be expected to have the same loudness level. The important observation is that the multiple look model has a consistent 1 to 2 phon increase over the Cambridge model results. This is expected given the predictable gap duration and spacing that was applied. For reference, the summary output of the multiple look calculation with integration with the Cambridge model is given in Figure 21. The output shows not only the calculated loudness level but also provides a summary of the how many gaps were found and the corresponding durations. The conclusion that can be drawn here using a simple sinusoidal wave is that the resulting loudness level calculation follows intended adjustments set out by the development of the gap detection model. It can further be said that this was accomplished by intelligent decisions based on the content of the 1 ms looks. While results showing the expected outcome of the multiple look gap adjustment model is shown in both Table 4 and 5 when compared to the Cambridge model results, no listening tests were conducted in this work to further validate the developed model. It should also be noted that given the unreliability of the DIN models results, they are not included in any further comparisons.

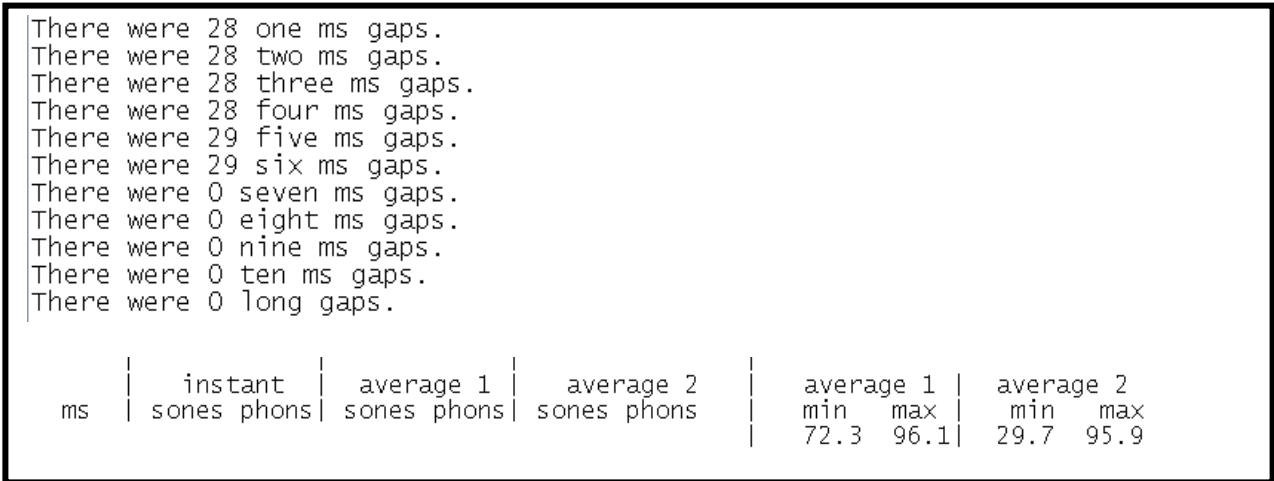


Figure 21: Output of the multiple look program which shows the number of gaps found in the 90 dB gapped input file and the corresponding durations. Also given is the calculated loudness level using the integrated Cambridge model

6.2 Stationary Mechanical Sounds

Stationary sounds classified as generated or mechanical sounds were also analysed using the different calculation models. The evaluated sounds included a generated white noise signal having a sound level of 70 dB, a warble sound having a sound level of 60 dB, and a diesel engine which was recorded with a sound level of 55 dB. The white noise signal is defined as a random signal with a flat power spectral density. In other words, the signal contains equal power within a fixed bandwidth at any center frequency. As was the case with the sinusoidal signals, white noise does not contain any natural gaps within the signal. As such, gaps were inserted into the signal in the same manner as was done with the pure tones and as was detailed in Table 4. The warble and diesel sounds inherently contain gaps within the signal so these were analysed in the natural format as they were recorded. Figures 22 and 23 illustrate approximately 2000 ms of the time plot for the white noise signal without and with the gaps inserted respectively. Similarly, Figure 24 is the time plot for the warble sound and Figure 25 is the same for the diesel engine recording.

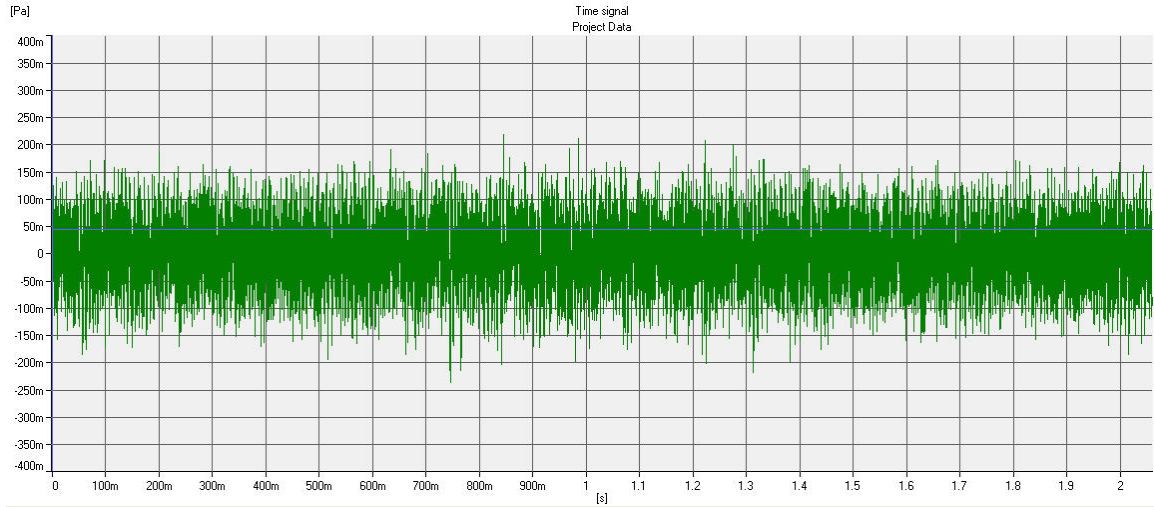


Figure 22: Time domain plot for the white noise test signal without the modifications of inserted gaps in the signal used for the calculation of loudness level with and without the multiple look model

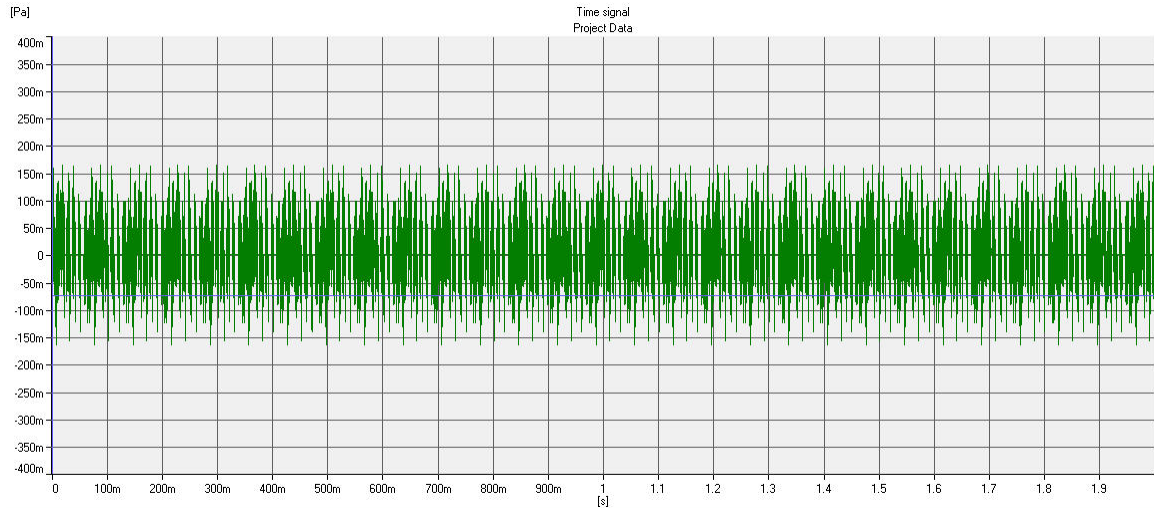


Figure 23: Time domain plot for the white noise test signal with the addition of inserted gaps in the signal with position and gap durations as specified in Table 4 used for the calculation of loudness level with and without the multiple look model.

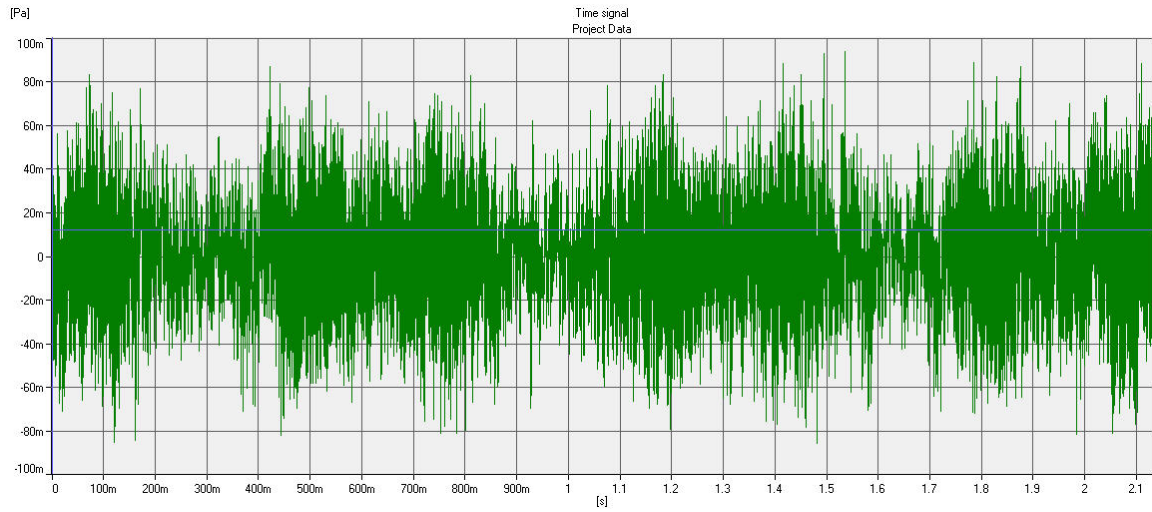


Figure 24: Time domain plot for the warble sound used for the calculation of loudness level with and without the multiple look model.

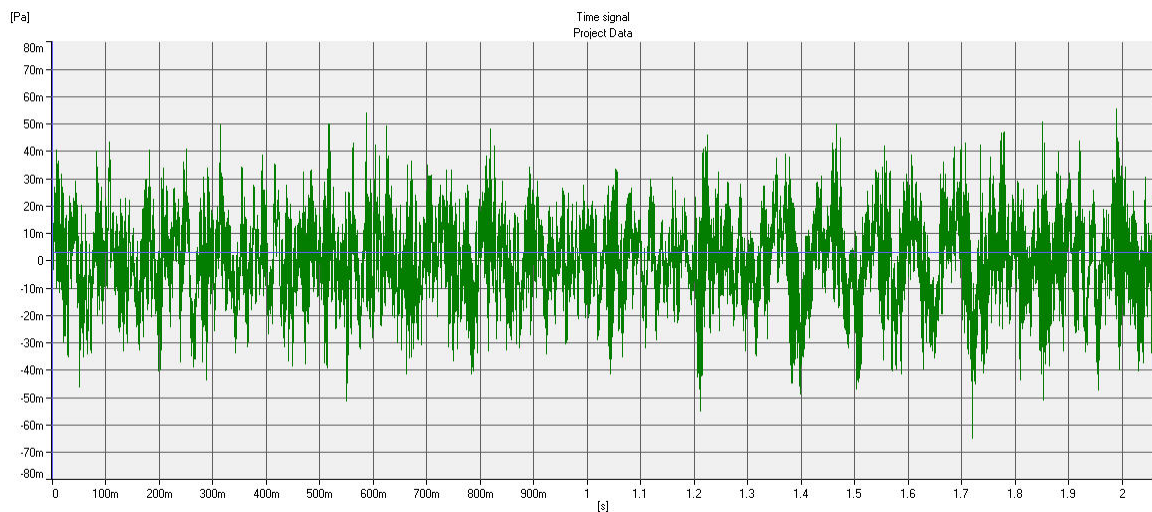


Figure 25: Time domain plot for the recorded diesel engine sound used for the calculation of loudness level with and without the multiple look model.

The calculated results for all the steady mechanical sounds are given in Table 7. Listed are the measured sound level for the sounds at which they were recorded and subsequently analysed. Also given are the steady loudness levels calculated for each signal using the method specified by the time varying Cambridge model and the loudness level using the multiple look gap correction model.

Table 7: Loudness levels for steady mechanical sounds (white noise, warble and diesel) calculated using the Cambridge model and multiple look gap correction model.

Signal Description	Time Varying Loudness Level (Phons) from Cambridge Model	Time Varying Loudness Level (Phons) using Multiple Look Gap Adjustments
White Noise without gaps	86.5	86.5
White Noise with gaps	85.0	85.6
Warble	79.0	79.1
Diesel Engine	70.7	70.6

As expected, the calculated loudness levels for the white noise signal containing no gaps was the same for both the Cambridge model alone and with the implementation of the multiple look gap adjustment model. At a minimum this is an indication that the multiple look model did not produce erroneous results.

For the white noise signal with the inserted gaps, an increase of 0.6 dB is realized by implementation of the multiple look model over the application of the Cambridge model alone. While an immediate application of this result cannot be given for this artificial sound, the result does provide the predicted outcome, thus showing merit to the model.

As was for the case of the white noise with the gap inserted, an increase in loudness level is also given for the warble sound, albeit a much smaller increase. This is not unexpected though if one

were to carefully inspect the time trace of the warble sound provided above in Figure 24. Unlike the white noise of sinusoidal signals with gaps, the time trace is relatively steady and full and more absent visually of numerous gaps.

The one sound sample that showed an anomaly was the result for the diesel engine. Upon closer post inspection of the time signal, it became evident that the signal while rough does not have any found gaps as defined by the multiple look gap adjustment algorithm. The anomaly in the results was the fact that the multiple look loudness level results actually shows a decrease in loudness level by 0.1 phons. While not at all significant, a decrease should not occur. A similar result was seen above in Table 5 for the steady 85 dB sinusoidal signal with no gap. It has been determined that an inaccuracy of up to 0.1 phons can occur during the regeneration of the modified file back into the 16 bit hexadecimal WAV format. This is due to the fact that the 32 samples within each look are treated as an average during the regeneration process. While not significant, the next chapter will include a recommendation to revise the treatment of the samples contained in the look to maintain a better resolution of the post adjusted data.

6.3 Time Varying (Unsteady) Sounds

Two time varying sounds were also analysed using the Cambridge time varying loudness model and the multiple look model. The two sounds evaluated were both spoken sentences. The evaluation of unsteady loudness for speech signals is a common for the application of speech recognition and intelligibility metrics. As such, they were included in this study. The first sentence was comprised of the phrase, "Suzie sold seashells by the seashore". This sentence was chosen for its smooth cadence and expected lack of gaps in the recorded signal. The second sentence was comprised of the phrase, "Clickity clack, the train went down the track". This

sentence was chosen specifically for its much rougher cadence and greater chance to have gaps within the recorded sentence. The time plots for the “Suzie” and “train” sentence are illustrated in Figures 26, and 27 respectively.

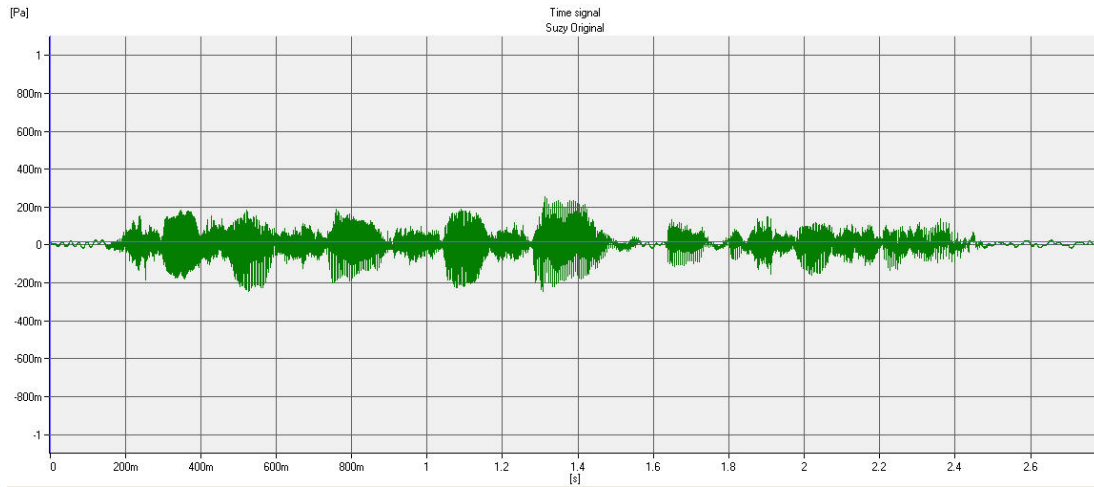


Figure 26: Time domain plot for the spoken sentence, “Suzie sold seashells by the seashore”, chosen for its smooth cadence and expected lack of gaps.

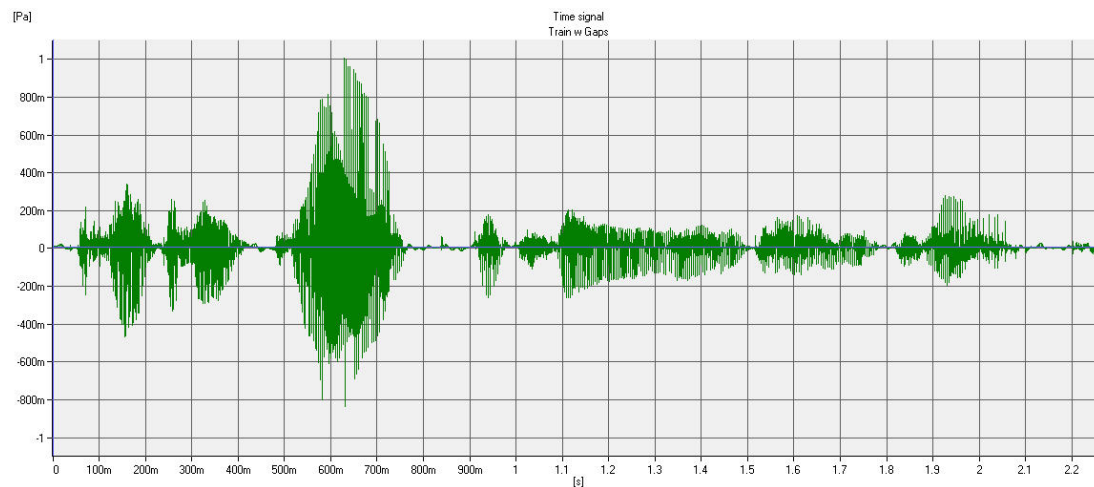


Figure 27: Time domain plot for the spoken sentence, “Clickity clack, the train went down the track”, chosen for its rougher cadence and expected gaps in the signal.

The calculated loudness level results for the two time varying sounds are given in Table 8. Given are the measured sound levels at which the sounds were recorded and subsequently analysed. Also given are the unsteady loudness levels calculated using the time varying Cambridge model and the loudness level using the multiple look gap correction model.

Table 8: Loudness levels for time varying sinusoidal sweep and speech sounds calculated using the Cambridge model and multiple look gap correction model.

Signal Description	Time Varying Loudness Level (Phons) from Cambridge Model	Time Varying Loudness Level (Phons) using Multiple Look Gap Adjustments
Spoken Sentence "Suzie"	84.0	84.0
Spoken Sentence "Train"	90.9	94.1

As stated above, the "Suzie sold seashells by the seashore" sentence is very smooth with the syllables joined together with a great degree of sibilance. This is evident by the loudness level result with both the Cambridge model and the multiple look gap adjustment model producing the same result. Such an outcome can be applied to the application and understanding of alternative psychoacoustic metrics, particularly those concerned with speech transmission, intelligibility and recognition. All of which are metrics for which their outcomes are related to the presence, or lack of, sibilance and alternatively harshness.

The second sentence, "Clickity clack, the train went down the track", resulted in a noticeable increase in loudness level with application of the multiple look gap adjustments. As with the first sentence, this result shows significant implication and usefulness to speech metrics. The

result also follows the perceived difference in loudness for this harder sentence when compared to the former.

Given the data presented in this chapter, it has been demonstrated that the multiple look gap adjustment program does have the ability to use the looks contained within a stimulus to identify the presence of gaps within the signal. Once found, an intelligent procedure is used to determine the length of the gap and apply the appropriate adjustment factor; one which follows the published empirical data.

VII Conclusions and Recommendations

This chapter provides a review of the conclusions that can be made based on the stated objectives and accompanying scope of this research. Also provided is a statement of the contributions that this work has made to the present state of the art. Finally, recommendations for future work and refinement of this research is also given.

7.1 Conclusions

Upon review of the results of this study, as well as recalling the stated objectives at the end of the introductory chapter of this dissertation, the following is a presentation of conclusions that have been reached.

1. The objective of this work was to develop a hybrid multiple look approach which uses level correction factors in conjunction with temporal integration methods in order to adequately represent the perceived loudness levels in the presence of gaps in a stimulus signal. A program was developed which divides the input signal into 1 ms looks, checks for the presence of gaps and makes the appropriate adjustments. The adjusted file is then converted to a state such that it can be applied to a loudness integration model.
2. As part of the scope to reach the stated objective, it was intended that the developed multiple look with gap correction abilities model would be integrated into an existing loudness model using integration theories. The model developed and presented in this work was used in conjunction with the Cambridge model for time varying loudness. It should be noted that the multiple look algorithm presented in this work can immediately be used with any time varying loudness model which accepts a WAV file as an input.

Integration into alternative file input structures can also be accomplished with minimal modification to the present code.

3. The focus of the multiple look model developed in this work was on the hearing phenomenon of gap detection. Other stimuli and resulting hearing sensations have been identified in the literature as not being adequately addressed by the present temporal integration models. Given that the fundamental aspect of this model included the division of the signal into short duration looks for intelligent decision making and processing, it can easily be adapted to include other phenomenon such as burst signal, something which is important to account for temporal pre-masking effects.
4. It was intended that any computer code developed in this study for the multiple look model would be open and be easily adaptable to allow for modifications to the programs parameters and correction values in order to accommodate any new empirical data in the future. The code used was a public domain Ruby language which is relatively simple to understand and edit with freely available editors. The code also does not require that it be compiled in order to execute the program, thus adding to its openness.
5. Finally, it was intended that any method developed should be well suited for use in other psychoacoustic metrics. Many existing metrics such as sharpness, fluctuation strength and roughness begin with the calculation of loudness. Given that the multiple look model has shown to improve present loudness models for the case of gaps being present in the input signal, inclusion of it in these other metrics would be similarly beneficial. The merit of using this model for speech has also been demonstrated in this dissertation.

7.2 Contributions

The following is a summary of the major contributions to the state of the art that can be attributed to the work presented in this dissertation.

1. While many experiments have been carried out in regard to the multiple look theory for the prediction of hearing perception, no model has yet been developed for application to the calculation of loudness. In this study, such a model was developed for the specific application for the adjustment of loudness for signals having the presence of gaps. The results presented have demonstrated merit to the application of this relatively overlooked, yet significant theory.
2. Much is still not known as to the many mechanisms associated for the perception of hearing sensations including loudness. The work presented in this dissertation not only expanded on the present knowledge of this psychoacoustic metric but also added to the present knowledge of the application of the multiple look theory, one which has not previously been applied.
3. The model developed has been designed to account for the hearing sensations associated with the presence of gaps in the stimulus signal. It was demonstrated that the application of this can be applied with success to many different types of signal including speech. Many metrics are presently available, such as speech intelligibility and articulation index however, these models have their shortcomings. The results of this work has shown that the presented model can be further applied to this specific application for the development of a new speech metric which includes the application of a loudness calculation using a multiple look approach.
4. While a primary objective of the model was to ensure applicability for speech sounds, this can be extended to include other sounds as well. Most notable would be mechanical sounds, environmental sounds such as traffic and any other stationary or unsteady sounds which can include short duration gaps.

7.3 Recommendations

The development of the multiple look model for the application of gap detection and adjustment for the calculation of loudness has demonstrated promise. The following is an identification of some of the areas where additional work can be undertaken to further this research.

1. The model and subsequent code developed using the multiple look theory was designed to integrate seamlessly with other loudness calculation software. As part of this, the program presented here was required to reconstruct the modified information contained within the individual looks back into a 16 bit WAV file for processing of loudness by the other calculation software. It was determined that during this reconstruction process that some temporal resolution of the 1 ms information can be lost. As a result, it was determined that in some circumstances an approximate 0.1 phon inaccuracy in loudness level can result in the final calculation. While this is not a significant value, improvements can be made and are being recommended to modify the treatment of the 32 hexadecimal format samples contained within each of the looks to eliminate this shortcoming in the software.
2. As was demonstrated in the results section of this dissertation, the perception of speech can be dependent on the content of the signal, including the presence of gaps. One of the applications where the multiple look model demonstrated particular promise was in the ability to analyse speech information. The understanding and application of evaluation models for speech recognition are ever increasing. This is particularly true given the aging demographic and increased interest in the treatment of hearing loss. Another application of the recognition of speech within automated systems such as voice activated electronics within automobiles. It is recommended that the application of multiple looks be expanded into the specific area of the recognition and treatment of speech as a stimulus.

The multiple look approach presented in this dissertation was specific to the application of the detection and adjustment for gaps present in the input signal presented to the ear. It was demonstrated in the literature review section that gap detection, while important, is not the only shortcoming associated with the present day loudness calculation models. This is especially true for those that rely on long term integration techniques for treatment of the temporal component of the sound. It is recommended that the model be expanded to include other distinct sound components. An example of this would be the inclusion of burst noise, an area which is important to the phenomenon of temporal pre-masking and one which is ignored by both the Cambridge model and the time varying method adapted by DIN as 45631-A1.

Bibliography

American Institute of Physics. (2005). ANSI S3.4-2005 Procedure for the Computation of Loudness of Steady Sounds. 42 . Melville, New York, USA.

American National Standards Institute. (2007). ANSI S3.4:2007 - American National Standard Procedure for the Computation of Loudness of Steady Sounds. Melville, New York, USA: Acoustical Society of America.

Berg, G. B. (1989). Analysis of Weights in Multiple Observation Tasks. *Journal of the Acoustical Society of America* , 85 (5), 1743-1746.

British Standards. (1967). Method for Calculating Loudness. 24 .

Bruel & Kjaer. (n.d.). Psychoacoustics - A Qualitative Description.

Buunen, T. J., & van Valkenburg, D. A. (1979). Auditory Detection of a Single Gap in Noise. *The Journal of the Acoustical Society of America* , 65 (Number 2), 534-537.

Charbonneau, J., Novak, C. J., & Ule, H. J. (2009). Comparison of Loudness Calculation Procedure Results to Equal Loudness Contours. *Internoise 2009*. Ottawa.

Charbonneau, J., Novak, C. J., & Ule, H. J. (2009). Loudness Prediction Model Comparison Using the Equal Loudness Contours. *Acoustics Week in Canada*. 37(3), pp. 64-65. Niagara-on-the-Lake: Canadian Acoustical Association.

Churcher, B. G., & King, A. J. (1937). The Performance of Noise Meters in Terms of the Primary Standard. *Journal of Electrical Engineering* , 81, 57-90.

Dallos, P. J., & Olsen, W. O. (1964). Integration of Energy at Threshold with Gradual Rise-Fall Tone Pips. *Journal of the Acoustical Society of America* , 36, 743-751.

Davis, A. (1995). *Hearing in Adults*. London: Whurr Publishers Ltd.

Defoe, J. (2007). *Evaluation of Loudness Calculation Techniques with Applications for Product Evaluation*. Windsor: University of Windsor.

Deutsches Institut für Normung. (1991). DIN 45631 - Procedure for Calculating Loudness Level and Loudness. Berlin, Germany: DIN.

Deutsches Institut für Normung. (2007). DIN 45631/A1 - Calculation of Loudness Level and Loudness from the Sound Spectrum - Zwicker Method - Amendment 1: Calculation of the Loudness of Time-Variant Sound. Berlin, Germany: Deutsches Institut für Normung.

Everest, F. A., & Pohlmann, K. C. (2009). *Master Handbook of Acoustics* (Fifth ed.). (J. Bass, Ed.) The McGraw-Hill Companies, Inc.

- Everest, F. A., & Pohlmann, K. C. (2009). *Master Handbook of Acoustics* (Fifth Edition ed.). (J. Bass, Ed.) The McGraw-Hill Companies, Inc.
- Exner, S. (1876). Zur Lehre von den Gehorsempfindungen. *Pflugers Archiv* , 13, 228-253.
- Fastl, H., & Zwicker, E. (2007). *Psycho-Acoustics: Facts and Models* (Third ed.). (T. Huang, M. Schroeder, & T. Kohonen, Eds.) Berlin: Springer.
- Fitzgibbons, P. J. (1983). Temporal Gap Detection in Noise as a Function of Frequency, Bandwidth, and Level. *The Journal of the Acoustical Society of America* , 74 (Number 1), 67-72.
- Fletcher, H., & Munson, W. A. (1933). Loudness, Its Definition, Measurement and Calculation. *The Journal of the Acoustical Society of America* , 5 (2), 82-108.
- Florentine, M., Buss, S., & Poulsen, T. (1996). Temporal Integration of Loudness as a Function of Level. *The Journal of the Acoustical Society of America* , 99 (3), 1633-1644.
- Forrest, T. G., & Green, D. M. (1987). Detection of Partially Filled Gaps in Noise and the Temporal Modulation Transfer Function. *The Journal of the Acoustical Society of America* , 82 (6), 1933-1943.
- Gjaevenes, K., & Rimstad, E. (1972). The Influence of Rise Time on Loudness. *The Journal of the Acoustical Society of America* , 51 (Number 4 (Part 2)), 1233-1239.
- Glasberg, B. R., & Moore, B. C. (2002). A Model of Loudness Applicable to Time-Varying Sounds. *The Journal of the Audio Engineering Society* , 50 (5), 331-342.
- Glasberg, B. R., & Moore, B. C. (1990). Derivation of Auditory Filter Shapes from Notched-Noise Data. *Hearing Research* , 47 (1-2), 103-138.
- Glasberg, B. R., & Moore, B. C. (n.d.). *LOUD2006A.exe - Loudness Model Calculated According to ANSI S3.4 2007*. Retrieved November 10, 2009, from Cambridge University Hearing Group - Auditory Demonstrations: <http://hearing.psychol.cam.ac.uk/Demos/demos.html>
- Glasberg, B. R., & Moore, B. C. (2006). Prediction of Absolute Thresholds and Equal-Loudness Contours Using a Modified Loudness Model (L). *Journal of the Acoustical Society of America* , 120 (2), 585-588.
- Green, D. M. (1960). Auditory Detection of a Noise Signal. *Journal of the Acoustical Society of America* , 32, 121-131.
- Green, D. M. (1985). Temporal Factors in Psychoacoustics. In A. Michelsen (Ed.), *Time Resolution in Auditory Systems* (pp. 122-140). Berlin: Springer-Verlag.
- Green, D. M., & Swets, J. A. (1966). *Signal Detection Theory and Psychoacoustics*. New York: Wiley.

Hartmann, W. M. (1998). *Signals, Sound, and Sensation* (1-56396-283-7 ed.). New York, New York, USA: Springer Science.

Hearing Aids Central.com. (n.d.). *How the Ear Works*. Retrieved August 20, 2010, from <http://www.hearingaidscentral.com/howtheearworks.asp>

Howard, D. M., & Angus, J. (2006). *Acoustics and Psychoacoustics* (Third ed.). Elsevier.

Howard, D. M., & Angus, J. (2006). *Acoustics and Psychoacoustics* (Third Edition ed.). Elsevier.

International Organization for Standardization. (1987). ISO226 Acoustics - Normal Equal-Loudness Contours. *Standard*. Geneva: International Organization for Standardization.

International Organization for Standardization. (2003). ISO226 Acoustics - Normal Equal-Loudness Contours. Geneva: International Organization for Standardization.

International Organization for Standardization. (1975). ISO532 Acoustics - Method for Calculating Loudness Level. Geneva: International Organization for Standardization.

ISO226 Acoustics - Normal Equal-Loudness Contours. (1961). ISO/R 226:1961 Normal Equal-Loudness Contours for Pure Tones and Normal Threshold of Hearing Under Free Field Listening Conditions. International Organization for Standardization.

Kingsbury, B. (1927). A Direct Comparison of the Loudness of Pure Tones. *Physics Review*, 29, 588.

McBride, R. L., Watson, A. J., & Cox, B. M. (1984). The Paired-Comparison Method as a Simple Difference Test. *Journal of Food Quality*, 6, 285-290.

Melnick, W. (1967). Comfort Level and Loudness Matching for Continuous and Interrupted Signals. *Journal of Speech and Hearing Research*, 99-109.

Miller, M. M. (1957). Noise Induced Vibration in Aircraft Structures. *The Journal of the Acoustical Society of America*, 29 (Number 1), 176-188.

Mintz, F., & Tyzzer, F. G. (1952). Loudness Chart for Octave-Band Data on Complex Sounds. *Journal of the Acoustical Society of America*, 24 (1), 80-82.

Miskolczy-Fodor, F. (1960). Relation between Loudness and Duration of Tonal Pulses. II. Response of Normal Ears to Sounds with Noise Sensation. *The Journal of the Acoustical Society of America*, 32 (Number 4), 482-486.

Moore, B. C. (2004). *An Introduction to the Psychology of Hearing* (Fifth ed.). London: Elsevier.

Moore, B. C. (2004). *An Introduction to the Psychology of Hearing* (Fifth Edition ed.). London: Elsevier.

- Moore, B. C. (2007). *An Introduction to the Psychology of Hearing* (Fifth ed.). Oxford, UK: Elsevier.
- Moore, B. C. (2007). *An Introduction to the Psychology of Hearing* (Fifth Edition ed.). Oxford, UK: Elsevier.
- Moore, B. C. (2003). Temporal Integration and Context Effects in Hearing. *Journal of Phonetics*, *31*, 563-574.
- Moore, B. C., & Glasberg, B. R. (1996). A Revision of Zwicker's Loudness Model. *Acustica - Acta Acustica*, *82* (2), 335-345.
- Moore, B. C., & Glasberg, B. R. (1987). Formulae Describing Frequency Selectivity as a Function of Frequency and Level, and Their Use in Calculating Excitation Patterns. *Hearing Research*, *28*, 209-225.
- Moore, B. C., Glasberg, B. R., & Baer, T. (1997). A Model for the Prediction of Thresholds, Loudness and Partial Loudness. *Journal of the Audio Engineering Society*, *45* (4), 224-240.
- Moore, B. C., Glasberg, B. R., Plack, C. J., & Biswas, A. K. (1988). The Shape of the Ear's Temporal Window. *Journal of the Acoustical Society of America*, *83*, 1102-1116.
- Munson, W. A. (1947). The Growth of Auditory Sensation. *Journal of the Acoustical Society of America*, *19*, 584-591.
- Oxenham, A. J., & Moore, B. C. (1994). Modeling the Additivity of Nonsimultaneous Masking. *Hearing Research*, *80*, 105-118.
- Paulus, E., & Zwicker, E. (1972). Programme Zur Automatischen Bestimmung Der Lautheit Aus Terzpegeln Oder Frequenzgruppenpegeln. *Acustica*, *27* (5), 253-266.
- Pedersen, B. (2006). *Auditory Temporal Resolution and Integration*. Aalborg: Aalborg University.
- Pedersen, B. (2006). Discrimination of Temporal Patterns on the Basis of Envelope and Fine-Structure Cues. *Auditory Temporal Resolution and Integration: Stages of Analyzing Time-Varying Sounds*, (pp. 85-96). Aalborg.
- Pedersen, B. (2006). Temporal Masking in the Auditory Identification of Envelope Patterns. *Auditory Temporal Resolution and Integration: Stages of Analyzing Time-Varying Sounds*, (pp. 67-82). Aalborg.
- Pedersen, B., & Ellermeier, W. (2005). Temporal Weighting in Loudness Judgements of Level-Fluctuating Sounds. *149th Meeting of the Acoustical Society of America* (pp. 13-23). Vancouver: Acoustical Society of America.
- Penner, M. J. (1972). Neural or Energy Summation in a Poisson Counting Model. *Journal of Mathematical Psychology*, *9*, 286-293.

- Plomp, R., & Bouman, M. A. (1959). Relation Between Hearing Threshold and Duration for Tone Pulses. *Journal of the Acoustical Society of America* , 31, 749-758.
- Pollack, I. (1958). Loudness of Periodically Interrupted White Noise. *The Journal of the Acoustical Society of America* , 30 (Number 3), 181-185.
- Pollack, I. (1951). On the Threshold and Loudness of Repeated Bursts of Noise. *The Journal of the Acoustical Society of America* , 23 (Number 6), 646-650.
- Robinson, D., & Dadson, R. (1956). A Re-Determination of the Equal-Loudness Relations for Pure Tones. *British Journal of Applied Physics* , 7, 166-181.
- Ruggero, M. A., Rich, N. C., Recio, A., Narayan, S. S., & Robles, L. (1997). Basilar-Membrane Responses to Tones at the Base of the Chinchilla Cochlea. *Journal of the Acoustical Society of America* , 101, 2151-2163.
- Science Kids. (n.d.). *Ear Diagram - Human Body Pictures & Images - Science for Kids*. Retrieved August 25, 2010, from <http://www.sciencekids.co.nz/pictures/humanbody/earDiagram.html>
- Seeber, B. U. (2008). Masking and Critical Bands. In B. U. Seeber, *Handbook of Signal Processing in Acoustics Volume I* (pp. 229-240). New York: Springer.
- Sek, A., & Moore, B. C. (1994). The Critical Modulation Frequency and its Relationship to Auditory Filtering at Low Frequencies. *Journal of the Acoustical Society of America* , 95 (5), 2606-2615.
- Shailer, M. J., & Moore, B. C. (1983). Gap Detection as a Function of Frequency, Bandwidth, and Level. *The Journal of the Acoustical Society of America* , 74 (Number 2), 467-473.
- Stecker, G. C., & Hafter, E. R. (2000). An Effect of Temporal Asymmetry on Loudness. *Journal of the Acoustical Society of America* , 107 (6), 3358-3368.
- Stevens, S. S. (1956). Calculation of Loudness of Complex-Noise. *Journal of the Acoustical Society of America* , 28 (5), 807-829.
- Stevens, S. S. (1961). Procedure for Calculating Loudness: Mark VI. *Journal of the Acoustical Society of America* , 33 (11), 1577-1585.
- Stone, M. A., Moore, B. C., & Glasberg, B. R. (1997). *A Real-Time DSP-Based Loudness Meter* (Vol. Contributions to Psychological Acoustics). (A. Schick, & M. Klatte, Eds.) Oldenburg, Germany: Bibliotheks und Informationssystem der Universitat Oldenburg.
- Susini, P., McAdams, S., & Smith, B. K. (2002). Global and Continuous Loudness Estimation of Time-Varying Levels. (D. Botteldooren, Ed.) *Acta Acoustica United with Acustica* , 88, 536-548.
- Suzuki, Y., & Takeshima, H. (2004). Equal Loudness Level Contours for Pure Tones. *Journal of the Acoustical Society of America* , 116 (2), 918-933.

- Viemeister, N. F., & Wakefield, G. H. (1991). Temporal Integration and Multiple Looks. *The Journal of Acoustical Society of America* , 90 (2), 858-865.
- Vogel, A. (1975). A Common Model for Loudness and Roughness. *Biological Cybernetics* , 18 (1), 31-40.
- Widmann, U., Lippold, R., & Fastl, H. (1998). A Computer Program Simulating Post-Masking for Applications in Sound Analysis Systems. *NOISE-CON 98* (pp. 451-456). Ypsilanti: Institute of Noise Control Engineering.
- Yates, G. K. (1995). *Cochlear Structure and Function*. (B. C. Moore, Ed.) San Diego, CA: Academic Press.
- Zwicker, E. (1977). Procedure for Calculating Loudness of Temporally Variable Sounds. *Journal of the Acoustical Society of America* , 62 (3), 675-682.
- Zwicker, E. (1961). Subdivision of the Audible Frequency Range into Critical Bands (Frequenzgruppen). *Journal of the Acoustical Society of America* , 33 (2), 248.
- Zwicker, E. (1958). Über Psychologische und Methodische Grundlagen der Lautheit. *Journal of the Acoustical Society of America* , 8, 237-258.
- Zwicker, E., & Feldtkeller, R. (1955). Über die Lautstärke von Gleichförmigen Geräuschen (On the loudness of stationary noises). *Acustica* , 5, 303-316.
- Zwicker, E., Fastl, H., & Dallmayr, C. (1984). BASIC - Program for Calculating the Loudness of Sounds From Their 1/3 Octave Band Spectra According to ISO 532B. *Acustica* , 55 (1), 63-67.
- Zwicker, E., Fastl, H., Widmann, E., Kurakata, K., Kuwano, S., & Namba, S. (1991). Program for Calculating Loudness According to DIN 45631 (ISO 532B). *Journal of the Acoustical Society of Japan* , 12 (1), 39-42.
- Zwicker, E., Flottorp, G., & Stevens, S. S. (1957). Critical Band Width in Loudness Summation. *Journal of the Acoustical Society of America* , 29 (5), 548-557.
- Zwislocki, J. J. (1960). Theory of Temporal Auditory Summation. *Journal of the Acoustical Society of America* , 32, 1046-1060.

Reference A

A. Written Source Code for the Multiple Look Gap Correction Model

Main.rb

```
require 'ThresholdCorrection'

File.open(ARGV[0], "rb") do |input_file|

  corrector = ThresholdCorrection.new(input_file)
  puts "The absolute raw max of this file is:
#{corrector.wave.absolute_raw_maximum}."
  if corrector.wave.pulse_factor.nil?
    puts "There's no pulse factor, sorry, can't run this file."
    break
  end

  corrector.calculate_time_equivalent_sound_levels
  corrector.calculate_adjustments

  #let's simulate adjusting everything by 4 dB.
  #corrector.adjustments = Array.new(corrector.ms_averages.length, 4.0)

  corrector.calculate_new_raw_values
  corrector.print_summary
  corrector.wave.write_file(ARGV[1])
end

system "tv1 -i #{ARGV[1]} -c 100 -s -3"
```

ThresholdCorrection.rb

```
class ThresholdCorrection
  require 'WaveFileParser'

  THRESHOLD_CUTOFF = 25.0
  GAP_LENGTH = 20

  # this makes the following things publicly accessible, outside of
  this file.
  attr_accessor :wave, :adjustments, :ms_averages, :one_gap, :two_gap,
:three_gap, :four_gap,
  :five_gap, :six_gap, :seven_gap, :eight_gap, :nine_gap, :ten_gap,
:long_gap

  # initialize is called when you when you go ThresholdCorrection.new
  # outside of this file
  def initialize(file)
    @wave = WaveFileParser.new(file)
    @wave.read_headers
    @wave.print_header_info
    @wave.read_data
    @wave.read_footer
    @one_gap, @two_gap, @three_gap, @four_gap,
    @five_gap, @six_gap, @seven_gap, @eight_gap, @nine_gap, @ten_gap,
@long_gap = Array.new(11, 0)
  end
end
```



```

    value_to_sum = (1.0 / 32.0) * (10.0 ** (dB / 10.0))
    sum += value_to_sum
    #puts "index: #{index}\ttraw: %.3f\tPrms: %.3f\tdB: %.3f\tvalue to
sum: %.3f\trunning sum: %.3f" % [raw_value, p_rms, dB, value_to_sum,
sum]
    #puts "index: #{index}\ttraw: %.3f\tPo: %.3f\tPrms: %.3f\tdB:
%.3f" % [raw_value, p_o, p_rms, dB]
    end
    sound_level = 10 * Math.log10(sum)
    sound_level
end

def calculate_adjustments
  if @ms_averages.any?
    @adjustments = Array.new(@ms_averages.length, 0.0)
    adjusted = false

    index = 2
    while index < @ms_averages.length

      if @ms_averages[index + 1] && ((@ms_averages[index] -
@ms_averages[index + 1]) >= THRESHOLD_CUTOFF)
        puts "ms #{index} is %.2fdB and ms #{index+1} is %.2fdB.
FOUND a difference of more than #{THRESHOLD_CUTOFF} dB." %
[@ms_averages[index], @ms_averages[index+1]]
        if @ms_averages[index + 2] && ((@ms_averages[index] -
@ms_averages[index + 2]) >= THRESHOLD_CUTOFF)
          puts "ms #{index} is %.2fdB and ms #{index+2} is %.2fdB.
FOUND a difference of more than #{THRESHOLD_CUTOFF} dB." %
[@ms_averages[index], @ms_averages[index+2]]
          if @ms_averages[index + 3] && ((@ms_averages[index] -
@ms_averages[index + 3]) >= THRESHOLD_CUTOFF)
            puts "ms #{index} is %.2fdB and ms #{index+3} is %.2fdB.
FOUND a difference of more than #{THRESHOLD_CUTOFF} dB." %
[@ms_averages[index], @ms_averages[index+3]]
            if @ms_averages[index + 4] && ((@ms_averages[index] -
@ms_averages[index + 4]) >= THRESHOLD_CUTOFF)
              puts "ms #{index} is %.2fdB and ms #{index+4} is
%.2fdB. FOUND a difference of more than #{THRESHOLD_CUTOFF} dB." %
[@ms_averages[index], @ms_averages[index+4]]
              if @ms_averages[index + 5] && ((@ms_averages[index] -
@ms_averages[index + 5]) >= THRESHOLD_CUTOFF)
                puts "ms #{index} is %.2fdB and ms #{index+5} is
%.2fdB. FOUND a difference of more than #{THRESHOLD_CUTOFF} dB." %
[@ms_averages[index], @ms_averages[index+5]]
                if @ms_averages[index + 6] && ((@ms_averages[index] -
@ms_averages[index + 6]) >= THRESHOLD_CUTOFF)
                  puts "ms #{index} is %.2fdB and ms #{index+6} is
%.2fdB. FOUND a difference of more than #{THRESHOLD_CUTOFF} dB." %
[@ms_averages[index], @ms_averages[index+6]]
                  if @ms_averages[index + 7] && ((@ms_averages[index]
- @ms_averages[index + 7]) >= THRESHOLD_CUTOFF)
                    puts "ms #{index} is %.2fdB and ms #{index+7} is
%.2fdB. FOUND a difference of more than #{THRESHOLD_CUTOFF} dB." %
[@ms_averages[index], @ms_averages[index+7]]
                    if @ms_averages[index + 8] &&
((@ms_averages[index] - @ms_averages[index + 8]) >= THRESHOLD_CUTOFF)

```

```

                puts "ms #{index} is %.2fdB and ms #{index+8}
is %.2fdB. FOUND a difference of more than #{THRESHOLD_CUTOFF} dB." %
[@ms_averages[index], @ms_averages[index+8]]
                if @ms_averages[index + 9] &&
((@ms_averages[index] - @ms_averages[index + 9]) >= THRESHOLD_CUTOFF)
                puts "ms #{index} is %.2fdB and ms #{index+9}
is %.2fdB. FOUND a difference of more than #{THRESHOLD_CUTOFF} dB." %
[@ms_averages[index], @ms_averages[index+9]]
                if @ms_averages[index + 10] &&
((@ms_averages[index] - @ms_averages[index + 10]) >= THRESHOLD_CUTOFF)
                puts "ms #{index} is %.2fdB and ms
#{index+10} is %.2fdB. FOUND a difference of more than
#{THRESHOLD_CUTOFF} dB." % [@ms_averages[index],
@ms_averages[index+10]]
                if @ms_averages[index + 11] &&
((@ms_averages[index] - @ms_averages[index + 11]) >= THRESHOLD_CUTOFF)
                puts "ms #{index} is %.2fdB and ms
#{index+11} is %.2fdB. FOUND a difference of more than
#{THRESHOLD_CUTOFF} dB." % [@ms_averages[index],
@ms_averages[index+11]]
                # long gap! so let's do the special loop
to get over it.
                gap_length = 12
                while (@ms_averages[index + gap_length]
&& ((@ms_averages[index] - @ms_averages[index + gap_length]) >=
THRESHOLD_CUTOFF))
                puts "Checking long gap: ms #{index} is
%.2fdB, ms #{index + gap_length} is %.2fdB." % [@ms_averages[index],
@ms_averages[index+gap_length]]
                if gap_length == GAP_LENGTH
                puts "Breaking out of a long gap
detection. Maximum gap allowance of #{GAP_LENGTH} has been reached."
                break
                end
                gap_length += 1
                end
                index += (gap_length + 3)
                @long_gap += 1
            else
                @adjustments[index] = 1.6
                @adjustments[index - 1] = 1.6
                puts "adjusting millisecond #{index-1}
and #{index} by 1.6 dB"
                index += 11
                @ten_gap += 1
                end
            else
                @adjustments[index] = 1.6
                @adjustments[index - 1] = 1.6
                puts "adjusting millisecond #{index-1} and
#{index} by 1.6 dB"
                index += 10
                @nine_gap += 1
                end
            else
                @adjustments[index] = 1.6
                @adjustments[index - 1] = 1.6

```

```

                                puts "adjusting millisecond #{index-1} and
#{index} by 1.6 dB"
                                index += 9
                                @eight_gap += 1
                                end
                                else
                                @adjustments[index] = 1.6
                                @adjustments[index - 1] = 1.6
                                puts "adjusting millisecond #{index-1} and
#{index} by 1.6 dB"
                                index += 8
                                @seven_gap += 1
                                end
                                else
                                @adjustments[index] = 1.6
                                @adjustments[index - 1] = 1.6
                                puts "adjusting millisecond #{index-1} and
#{index} by 1.6 dB"
                                index += 7
                                @six_gap += 1
                                end
                                else
                                @adjustments[index] = 1.6
                                @adjustments[index - 1] = 1.6
                                puts "adjusting millisecond #{index-1} and #{index}
by 1.6 dB"
                                index += 6
                                @five_gap += 1
                                end
                                else
                                @adjustments[index] = 2.2
                                @adjustments[index - 1] = 2.2
                                puts "adjusting millisecond #{index-1} and #{index}
by 2.2 dB"
                                index += 5
                                @four_gap += 1
                                end
                                else
                                @adjustments[index] = 3.0
                                @adjustments[index - 1] = 3.0
                                puts "adjusting millisecond #{index-1} and #{index} by
3.0 dB"
                                index += 4
                                @three_gap += 1
                                end
                                else
                                @adjustments[index] = 3.5
                                @adjustments[index - 1] = 3.5
                                puts "adjusting millisecond #{index-1} and #{index} by
3.5 dB"
                                index += 3
                                @two_gap += 1
                                end
                                else
                                @adjustments[index] = 4.0
                                @adjustments[index - 1] = 4.0

```

```

                puts "adjusting millisecond #{index-1} and #{index} by 4.0
dB"
                index += 2
                @one_gap += 1
            end
        else
            puts "ms #{index} is %.2fdB and ms #{index+1} is %.2fdB.
Didn't find a difference of more than #{THRESHOLD_CUTOFF} dB." %
[@ms_averages[index], @ms_averages[index+1]] if @ms_averages[index+1]
            index += 1
        end
    end
    @adjustments
end

def print_summary
    puts "There were #{@one_gap} one ms gaps."
    puts "There were #{@two_gap} two ms gaps."
    puts "There were #{@three_gap} three ms gaps."
    puts "There were #{@four_gap} four ms gaps."
    puts "There were #{@five_gap} five ms gaps."
    puts "There were #{@six_gap} six ms gaps."
    puts "There were #{@seven_gap} seven ms gaps."
    puts "There were #{@eight_gap} eight ms gaps."
    puts "There were #{@nine_gap} nine ms gaps."
    puts "There were #{@ten_gap} ten ms gaps."
    puts "There were #{@long_gap} long gaps."
end

def calculate_new_raw_values
    new_db_milliseconds = Array.new

    @wave.db_milliseconds.each_with_index do |ms_array, ms_index|
        new_ms_array = Array.new
        ms_array.each do |value|
            new_ms_array << value + @adjustments[ms_index]
        end
        new_db_milliseconds << new_ms_array
    end

    @wave.adjusted_db_milliseconds = new_db_milliseconds

    #1. (WAV value) * (factor from WAV footer/32768)= Po
    #2. Po/sqrt(2)=Prms
    #3. SPL=20*log(Prms/(2x10^-5)) where SPL is in dB

    new_raw_milliseconds = Array.new

    new_db_milliseconds.each_with_index do |ms_array, ms_index|
        new_ms_array = Array.new
        ms_array.each_with_index do |value, sample_index|
            prms = (2 * (10 ** -5)) * (10 ** (value / 20.0))
            p_o = prms * Math.sqrt(2.0)
            new_raw_value_float = p_o / (@wave.pulse_factor / 32767.0)
            new_raw_value = new_raw_value_float.round
        end
    end
end

```

```

        new_raw_value = new_raw_value * -1 if
@wave.raw_milliseconds[ms_index][sample_index] < 0

        #only print out where we made an adjustment
        if @wave.db_milliseconds[ms_index][sample_index] !=
@wave.adjusted_db_milliseconds[ms_index][sample_index]
            puts "ms: #{ms_index}, sample no. #{sample_index}\told raw:
#{@wave.raw_milliseconds[ms_index][sample_index]}\told dB: %.2f\tnew
dB: %.2f\tnew raw: #{new_raw_value}" %
                [@wave.db_milliseconds[ms_index][sample_index],
@wave.adjusted_db_milliseconds[ms_index][sample_index]]
            end
            new_ms_array << new_raw_value
        end
        new_raw_milliseconds << new_ms_array
    end

    @wave.adjusted_raw_milliseconds = new_raw_milliseconds
end

end

```

WaveFileParser

```

class WaveFileParser

    # this makes these variables accessible outside the class
    # inside the class they are prefixed with an @ symbol.
    attr_accessor :chunk_id, :chunksize, :format, :subchunklid,
:subchunklsize,
        :audioformat, :numchannels, :samplerate, :byterate, :blockalign,
        :bitpersample, :cbsize, :factid, :factsize, :factsamples,
:subchunk2id,
        :subchunk2size, :sample_count, :raw_milliseconds, :footer,
:pulse_factor_string,
        :pulse_factor, :bk_id, :bksize, :db_milliseconds,
:adjusted_db_milliseconds,
        :absolute_raw_maximum, :adjusted_raw_milliseconds

    # instance methods
    def initialize(file_obj)
        @file = file_obj
    end

    def read_two_byte_number
        @file.read(2).unpack("v").to_s.to_i unless @file.eof?
    end

    def read_four_byte_string
        @file.read(4).to_s unless @file.eof?
    end

    def read_four_byte_number
        @file.read(4).unpack("V").to_s.to_i unless @file.eof?
    end
end

```



```

def read_next_null_terminated_string
  found_null = false
  values = Array.new
  while(found_null == false)
    value = @file.read(1)

    #puts value != "\000" ? "value: #{value.to_s}." : "found a nil,
woot."

    if value == "\000" || @file.eof?
      found_null = true
      break
    end
    values << value
  end
  values
end

def read_headers
  @chunk_id = read_four_byte_string
  @chunksize = read_four_byte_number
  @format = read_four_byte_string
  @subchunk1id = read_four_byte_string
  @subchunk1size = read_four_byte_number
  @audioformat = read_two_byte_number
  @numchannels = read_two_byte_number
  @samplerate = read_four_byte_number
  @byterate = read_four_byte_number
  @blockalign = read_two_byte_number
  @bitspersample = read_two_byte_number

  if @subchunk1size.to_s == "18"
    @cbsize = read_two_byte_number
  end

  fact_present = false
  next_id = read_four_byte_string

  if next_id == "fact"
    fact_present = true
    @fact_id = "fact"
    @factsize = read_four_byte_number
    @factsamples = read_four_byte_number
  end

  if fact_present
    @subchunk2id = read_four_byte_string
  else
    @subchunk2id = next_id
  end

  @subchunk2size = read_four_byte_number
end

def print_header_info
  puts "chunk id: #{@chunk_id}"
  puts "chunk size: #{@chunksize}"
end

```

```

puts "format: #{@format}"
puts "subchunk1 id: #{@subchunk1id}"
puts "subchunk1 size: #{@subchunk1size}"
puts "audio format: #{@audioformat}"
puts "number of channels: #{@numchannels}"
puts "sample rate: #{@samplerate}"
puts "byte rate: #{@byterate}"
puts "block align: #{@blockalign}"
puts "bits per sample: #{@bitspersample}"

if @subchunk1size.to_s == "18"
  puts "cb size: #{@cbsize}"
end

if @fact_id
  puts "fact_id: #{@fact_id}"
  puts "fact size: #{@factsize}"
  puts "fact samples: #{@factsamples}"
end

puts "subchunk2 id: #{@subchunk2id}"
puts "subchunk2 size: #{@subchunk2size}"
end

def read_data
  @absolute_raw_maximum = 0
  if @numchannels == 1
    @raw_milliseconds = Array.new
    @sample_count = 0
    while (@sample_count <= ((@subchunk2size / 2) - 1) &&
!@file.eof?)
      @raw_milliseconds << read_ms
    end
    @raw_milliseconds
  end
end

def read_footer
  @footer = Array.new
  @bk_id = read_four_byte_string

  if @bk_id == "bkdk"

    puts "There's a pulse footer."
    @bksize = read_four_byte_number
    #puts "bkid: #{@bk_id}, bksize: #{@bksize}"

    while (!@file.eof)
      @footer << read_next_null_terminated_string.to_s
    end

    @pulse_factor_string = @footer[9]
    @pulse_factor = @pulse_factor_string.to_f
    puts "pulse factor: #{@pulse_factor.to_s}"

  elsif @bk_id.nil?
    puts "There's no pulse footer."
  end
end

```

```

    end
end

def write_file(filename)
  @file_to_write = File.new(filename, "wb+")
  write_headers
  write_data
  @file_to_write.close
end

private
def read_ms # this returns an array of 32 values
  array = Array.new
  for i in 0..31
    if @sample_count <= ((@subchunk2size / 2) - 1)
      sample = @file.read(2) unless @file.eof?
      sample = sample.unpack("s").to_s.to_i #unless
sample.is_a?(Fixnum)
      @absolute_raw_maximum = sample.abs if (@absolute_raw_maximum <
sample.abs)
      #puts "sample: #{sample}, sampleclass: #{sample.class.to_s}
sample count: #{@sample_count}, subchunk: #{@subchunk2size / 2}"
      array << sample
      @sample_count += 1
    end
  end
  array
end

def write_headers
  @file_to_write.write(@chunk_id)

  @file_to_write.write([@chunksizesize.to_s.to_i].pack("V"))

  @file_to_write.write(@format)
  @file_to_write.write(@subchunk1id)
  @file_to_write.write([@subchunk1size.to_s.to_i].pack("V"))
  @file_to_write.write([@audioformat.to_s.to_i].pack("v"))
  @file_to_write.write([@numchannels.to_s.to_i].pack("v"))
  @file_to_write.write([@samplerate.to_s.to_i].pack("V"))
  @file_to_write.write([@byterate.to_s.to_i].pack("V"))
  @file_to_write.write([@blockalign.to_s.to_i].pack("v"))
  @file_to_write.write([@bitpersample.to_s.to_i].pack("v"))

  if @subchunk1size.to_s == "18"
    @file_to_write.write([@cbsize.to_s.to_i].pack("v"))
  end

  if @fact_id
    @file_to_write.write("fact")
    @file_to_write.write([@factsizesize.to_s.to_i].pack("V"))
    @file_to_write.write([@factsamplesize.to_s.to_i].pack("V"))
  end

  @file_to_write.write(@subchunk2id)
  @file_to_write.write([@subchunk2size.to_s.to_i].pack("V"))

```

```
end

def write_data
  @adjusted_raw_milliseconds.each_with_index do |ms_array, ms_index|
    ms_array.each_with_index do |value, sample_index|
      @file_to_write.write([value.to_s.to_i].pack("v"))
    end
  end
end
end
end
```

Reference B

B. Technical Data Sheets Detailing the Specifications for the Acquisition Equipment



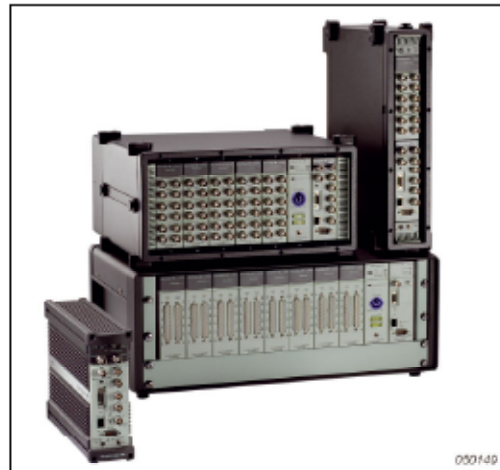
SYSTEM DATA

IDA^e Hardware Configurations for PULSE — Types 3560-B, 3560-C, 3560-D and 3560-E

PULSE™ is a versatile, task-oriented sound and vibration analysis system. It provides the platform for a range of PC-based measurement solutions from Brüel & Kjær. A PULSE system consists of a PC with LAN interface, PULSE software, Microsoft® Windows® operating system, Microsoft® Office, and data acquisition front-end hardware. Up to 10 front-ends can be combined into one measurement system with more than 300 input channels.

This System Data describes the hardware available for Data Acquisition Front-ends Types 3560-B, C, D and E.

PULSE Software as well as PULSE Pocket Analyzer Type 3560-L and the PULSE Lite software are described separately.



050149

USES AND FEATURES

USES

- Multiframe systems comprising up to 10 front-ends with synchronous sampling between front-ends for real-time measurements on more than 300 channels:
 - Type 3560-B: 5 input and 1 output channel
 - Type 3560-C: 2 modules. Up to 17 input and/or 3 generator output channels
 - Type 3560-D: 7 modules. Up to 65 input and/or 10 generator output channels
 - Type 3560-E: 10 modules. Up to 96 input and/or 16 generator output channels)
- Signal and system analysis using all PULSE application packages for, or example:
 - Time data acquisition
 - General noise and vibration measurements
 - Basic and advanced acoustics
 - Structural Analysis
 - Machine Diagnostics
 - Electroacoustic testing

FEATURES

- Dyn-X input modules with single, 160 dB input range
- Automatic detection of front-end hardware and transducers – supports IEEE 1451.4-capable transducers with TEDS (Transducer Electronic Data Sheet)
- Fully conditioned input and output channels for microphones and accelerometers, charge transducers, CCLD transducers and other transducers acting as voltage sources
- Full overload detection including out-of-band overload and indication of incorrect conditioning
- LAN interface allows the front-end to be placed close to the test object and reduces transducer cable length
- Rugged design for industrial use
- Battery (3560-B, C only)/external DC operated acquisition unit for field use
- Low-noise operation

Brüel & Kjær 

Introduction

PULSE is a versatile, task-oriented system for noise and vibration analysis. It provides the platform for a range of PC-based measurement solutions from Brüel & Kjær.

A PULSE system consists of a PC with LAN interface, PULSE software, Windows® 2000, XP or Windows Vista™, Microsoft® Office and IDA^e-based data acquisition front-end hardware. A system can contain more than 300 input channels located in up to 10 front-ends. The input/output conditioning modules perform signal conditioning and digitise the transducer signals. The IDA^e modules available for use in PULSE systems are shown in Fig. 1 and listed in the Ordering Information on page 23. Modules can be freely mixed in a single front-end or in a multiframe system. Further information on the controller and input/output modules is given in Table 1.

Fig. 1
Overview of the components available for use in a PULSE System with LAN Interface

Standard configurations for a wide variety of applications are described in the "PULSE Analyzers & Solutions" Catalogue both printed (BF 0209) and on www.bksv.com

For information on PULSE Pocket Analyzer Type 3560-L, see the separate Product Data (BP 1967)

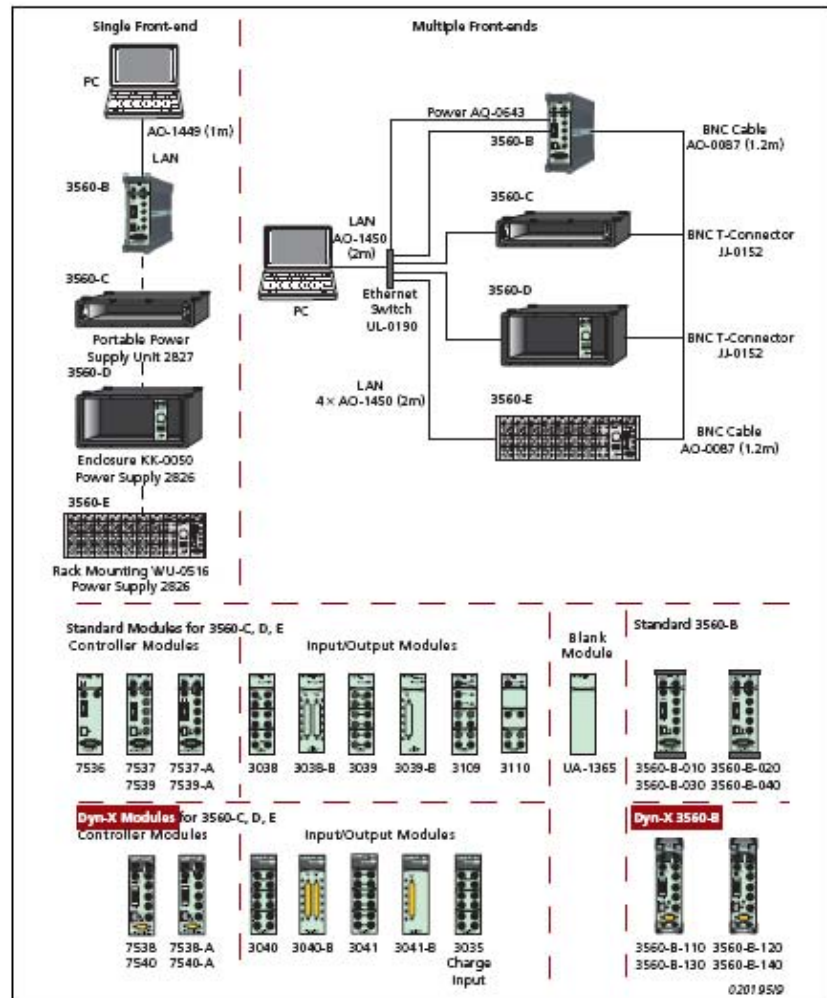


Table 1 Types and modules comprising PULSE front-ends

Type	Product Name	Frequency Range	Aux. Channels	Simultaneous Channels	Connectors	Input Type					
Type 3680-B											
3560-B-010	5-channel PULSE Data Acquisition Unit	0 Hz to 25.6 kHz	16 Aux Input ^d (10 samples/s) 2 Digital Output	5 Input 1 Sine Output	LEMO	Direct/CCLD ^a , ^b /Mic. Preamp. 1 Tacho Conditioning ^c					
3560-B-110					BNC	Direct/CCLD ^a 1 Tacho Conditioning ^c					
3560-B-020				5 Input 1 Generator Output	LEMO	Direct/CCLD ^a , ^b /Mic. Preamp. 1 Tacho Conditioning ^c					
3560-B-120					BNC	Direct/CCLD ^a 1 Tacho Conditioning ^c					
3560-B-030						LEMO				Direct/CCLD ^a , ^b /Mic. Preamp. 1 Tacho Conditioning ^c	
3560-B-130						BNC				Direct/CCLD ^a 1 Tacho Conditioning ^c	
3560-B-040											
3560-B-140											
Types 3680-C, D, E											
3105	Generator, 4/2-ch. Input/ Output Module	0 Hz to 25.6 kHz	-	4 Input 2 Generator Output	BNC and LEMO	Direct/CCLD ^a /Mic. Preamp. 1 Tacho Conditioning ^c	1 of these modules Up to 17 input channels	Up to 5 of these modules Up to 65 input channels	Up to 8 of these modules Up to 96 input channels		
3110	Generator, 2/1-ch. Input/ Output Module	0 Hz to 204.8 kHz		2 Input 1 Generator Output ^a							
3038	12-ch. Input Module	0 Hz to 25.6 kHz		-	12 Input	BNC				Direct/CCLD ^a 2 Tacho Conditioning ^b	
3040						2 × Sub-D				Direct/CCLD ^a /Mic. Preamp. ^b	
3038-B					6-ch. Input Module	6 Input				BNC and LEMO	Direct/CCLD ^a /Mic. Preamp. 1 Tacho Conditioning ^c
3040-B										Sub-D	Direct/CCLD ^a /Mic. Preamp. ^b
3039	6-ch. Charge & CCLD Input Module	0 Hz to 25.6 kHz		-	6 Input	BNT/BNC and TNC				Charge/Direct/CCLD ^a Tacho Conditioning on BNT Connector	
3041											
3039-B											
3041-B											
3035											
UA-1365	Blank Module										
7536	Controller Module	-									
7537	5/1-ch. Input/Output Controller Module	0 Hz to 25.6 kHz	16 Aux Input ^d (10 samples/s) 2 Digital Output	5 Input 1 Sine Output	LEMO	Direct/CCLD ^a , ^b /Mic. Preamp. 1 Tacho Conditioning ^c	1 of these modules	1 of these modules	1 of these modules		
7538				5 Input 1 Generator Output							
7539				5 Input 1 Sine Output	BNC	Direct/CCLD ^a 1 Tacho Conditioning ^c					
7540										5 Input 1 Generator Output	
7537-A											
7538-A											
7539-A											
7540-A											

a. Constant Current Line Drive for DeltaTron[®] and ICP[®] Accelerometers or Microphone Pre-amplifier
 b. Using adaptor cables
 c. All input channels can be used for tachometer operation

d. Only 12-channel currently supported in PULSE software
 e. Upper frequency @ 102.4 kHz
Dyn-X modules – See "Dyn-X Modules – Types 7538/38-A, 7540/40-A, 3035, 3040/40-B, 3041/41-B, 3560-B-110/120/130/140" on page 6.

PULSE Type 3560-B – Compact Data Acquisition Unit, up to 5 Input Channels

FEATURES

- Compact, robust casing for industrial and hard everyday use
- Battery operated (5 hours continuous) or DC powered (10 – 32 V)
- Silent operation to 35°C
- Cooling fans can be turned off for silent operation (will automatically restart if too hot)
- Synchronous sampling with other PULSE front-ends

Type 3560-B is a compact data acquisition system for battery/DC powered operation. The unit handles communication with the PC, measurement input and provides a sample clock. Eight versions are available, four standard and four Dyn-X – see the upper portion of Table 1.



A handle, UA-1689, is available for mounting on top of Type 3560-B, making it easier to carry.

PULSE Type 3560-C – Portable Data Acquisition Unit, up to 17 Input Channels

FEATURES

- Houses one input/output module and one controller module
- Robust casing for industrial and hard everyday use
- Rain cover for front panel allows passage of cables
- Battery operated or DC powered (10 – 32 V)
- Cooling fans can be turned off for silent operation (will automatically restart if too hot)
- Synchronous sampling with other PULSE front-ends

Type 3560-C is a portable data acquisition system with a battery/DC powered Type 2827 power supply unit. It can hold any combination of 1 Controller Module and 1 Input/Output Module (see Fig. 1 and Table 1). The controller module handles communication with the PC while the input/output module handles measurement input and provides a sample clock. As an example, a Type 3560-C fitted with a 5/1-ch. Input/Output Controller Module Type 7537 and a 12-ch. Input Module Type 3038 can measure up to 17 input channels.



050101

Environmental

To survive the harsh electrical environment found in, for example, cars, Type 3560-C has specifications that exceed the European EMC immunity requirements. ISO 7637-1 and 7637-2 “Road Vehicles – Electrical disturbance by conduction and coupling” requirements are met. Mechanical robustness is equally high, meeting MIL-STD-810C and IEC 60068-2-6.

Since all portable PULSE systems are built for outdoor use, they meet strict requirements for temperature and humidity. The operating temperature range extends from -10 to +50°C (+14 to 122°F). Type 3560-C will withstand rain if kept with the front panel facing upwards and the protection cover in place.

PULSE Type 3560-D – Multichannel Portable Data Acquisition Unit, up to 65 Input Channels

FEATURES

- Houses up to 5 input/output modules, Power Supply Type 2826 and one controller module
- Robust casing for industrial and hard everyday use
- DC powered (10 – 32 V) or via AC/DC convertor
- Main cooling fans can be turned off for nearly silent operation (will automatically restart if too hot)
- Synchronous sampling with other PULSE front-ends



050152

Type 3560-D is a data acquisition system comprising a frame that contains 7 modules. One of these must be the DC Power Supply Unit Type 2826, and one must be a Controller Module. The remaining 5 modules can be freely chosen from the I/O modules (see Fig. 1 and Table 1).^a

^a Note that one input module is always required, so the minimum input module configuration for Type 3560-D is: Type 2826 + Type 7536 + one input module; or Type 2826 + one of Types 7537, 7537-A, 7538, 7538-A, 7539, 7539-A, 7540, 7540-A

PULSE Type 3560-E – Multichannel Data Acquisition Unit, up to 96 Input Channels

FEATURES

- Comprises up to 8 input/output modules, Power Supply Type 2826 and one controller module
- DC powered (10 – 32 V) or via AC/DC convertor
- Optional Rack Mounting Enclosure KQ-0155, Air Guide EA-0540 and Fan Unit UH-1037
- Synchronous sampling with other PULSE front-ends



000153

Type 3560-E is a rack-mounted data acquisition system comprising 10 modules. One of these must be the DC Power Supply Unit Type 2826, and one must be a Controller Module. The remaining 8 modules can be freely chosen from the I/O modules (see Fig. 1)^a.

The system is delivered with a 19" Rack Mounting Kit, as shown above. A 19" Rack Enclosure KQ-0155, Air Guide EA-0540 and Fan Unit UH-1037 are available for rack-mounted systems.

Power Supply

Types 3560-B and 3560-C can either be powered by two internal Nickel-Metal Hydride batteries or from a 10 – 32 V DC power supply. A 100 – 240 V AC mains supply unit is included. The unit can be switched on and off from the front panel or, when using more than one front-end in one system, the on/off function can be controlled by another front-end using the Multiframe Control signal. A third possibility is to follow an external DC power supply, so that it switches on when the supply is connected.

When batteries are used^b, indicators on each side of the front panel indicate the condition of the batteries, allowing hot swap without interrupting measurement. When connected to an external DC supply, the batteries are charged automatically.

Types 3560-D and 3560-E can be powered from a 10 – 32 V DC power supply. An external 100 – 240 V AC mains supply unit, ZG-0430, is provided. The unit is a Type 2826 that can be switched on and off from the front panel or, when using more than one front-end in one system, the on/off function can be controlled by another front-end using the Multiframe Control signal. A third possibility is to follow an external DC power supply, so that it switches on when the supply is connected.

DC Output

To provide power for accessories such as a LAN switch or wireless LAN for interconnecting more front-ends, Types 3560-B, C and D have a 5 and 12 V DC output (LEMO FGG.00.302 connector) with fuse. Cables for these accessories must be ordered separately.

Silent Operation, Cooling

Type 3560-B is silent, operating without fans at ambient temperatures up to 35°C (95°F). Above this temperature the fans start up, but can be switched off from the PULSE software.

^a Note that one input module is always required, so the minimum input module configuration for Type 3560-E is: Type 2826 + Type 7536 + one input module; or Type 2826 + one of Types 7537, 7537-A, 7538, 7538-A, 7539, 7539-A, 7540, 7540-A

^b Batteries are not included.

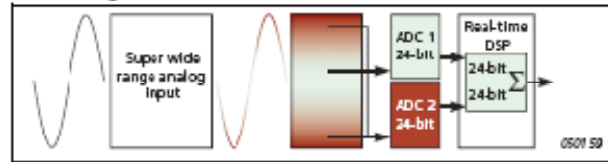
Types 3560-C and 3560-D: During operation fans keep the temperature of the unit within safety limits. In measurement situations where the fan noise^a can influence measurement results, the fans can be switched off from the PULSE software. If overheating threatens, the fans are automatically turned on again.

Dyn-X Modules – Types 7538/38-A, 7540/40-A, 3035, 3040/40-B, 3041/41-B, 3560-B-110/120/130/140

Fig. 2
Simplified block diagram of Dyn-X principle

Dyn-X technology – Exclusive Range from 0 to 160 dB

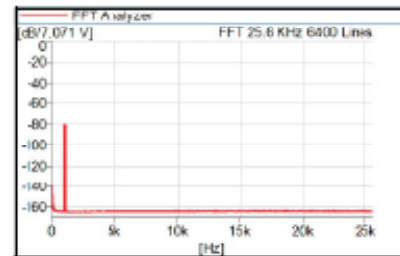
Dyn-X is an innovative range of state-of-the-art input modules with a single input range from 0 to 10 V_p and a useful analysis range exceeding 160 dB.



To date, high-quality transducers and preamplifiers have outperformed measuring equipment with regard to linearity and dynamic performance, being able to deliver a noise- and distortion-free signal over a dynamic signal range of 120 to 130 dB broadband and 160 dB narrow-band.

Fig. 3
160 dB analysis in one range. An FFT measuring a 1 kHz signal 80 dB below full-scale (7 V_{rms}). Note that noise and all spurious components measure 160 dB below full scale input

Now, with Dyn-X technology, the entire measurement and analysis chain for the first time matches or outperforms the transducer used for measurement. This eliminates the need for an input attenuator for ranging the analysis system input to the transducer output. All that you need to do to get excellent results is choose the right transducer.



Transducer Overload

Transducer max. output level can be entered in the software. If the input exceeds this level, then Dyn-X modules will give an overload warning on the front-end and in the PULSE Level Meter.

Accuracy, Safety and Efficiency

With no input range to set, you no longer have to worry about overloads, under-range measurements or discussions about the validation and verification of measurement results. And with no need for trial runs to ensure that the input range is correct, you have a far greater certainty of getting measurements right first time.

The measurement situations and applications below are examples of where the new Dyn-X technology can be usefully employed:

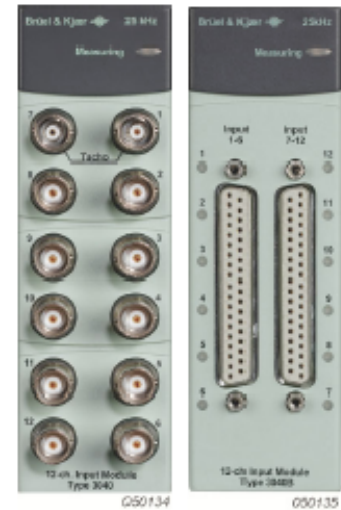
When you need to get the measurement right first time	<ul style="list-style-type: none"> Crash testing Destructive testing Heavy machinery – run up/ coast down 	When signal levels are unknown	<ul style="list-style-type: none"> Run up/down Field testing
Where there's minimal user interaction	<ul style="list-style-type: none"> Road testing Field testing 	When an overview of the whole measurement scenario is difficult	<ul style="list-style-type: none"> When measuring many channels When combining more signal types: Vibration, Sound, Temperature, Pressure, RPM, etc.
When time is limited	<ul style="list-style-type: none"> Test cells Wind tunnels Road testing Flight testing 		<ul style="list-style-type: none"> Test cells In-car testing Sound, vibration and other parameters involved
When testing is unattended	<ul style="list-style-type: none"> Production line Noise monitoring 	High-dynamic applications	<ul style="list-style-type: none"> Impulsive testing, room acoustics Run up/down Electroacoustics Structure measurements

a. See the Acoustic Noise Emission specifications for Types 3560-C (page 13) and 3560-D (page 13).

Input Channels

Available Input Modules

	Standard	Dyn-X
Input Modules		
12-ch. Input Module	3038, 3038-B	3040, 3040-B
6-ch. Input Module	3039, 3039-B	3041, 3041-B
6-ch. Charge & CCLD Input Module	–	3035
Input/Output Modules		
Generator, 4/2-ch. Input/Output Module	3109	–
Generator, 2/1-ch. Input/Output Module	3110	–
Input/Output Controller Modules		
5/1-ch. Input/Output Controller Modules	7537, 7537-A (3560-B-010/020)	7538, 7538-A (3560-B-110/120)
5/1-ch. Input/Output Controller Modules with Generator	7539, 7539-A (3560-B-030/040)	7540, 7540-A (3560-B-130/140)



USES

- Input channels for multichannel acoustic and vibration measurements

FEATURES

- Support IEEE 1451.4 capable transducers with TEDS
- Automatic DC offset compensation
- Overload indicator indicates incorrect conditioning and cable breaks on connected transducers
- Overload detection including out-of-band frequencies

Functions and features available in the modules are determined by software implemented and downloaded from PULSE LabShop.

Independent Channels

The input channels on a module can be set up independently; you can set up the high-pass filters and input gain separately and attach different types of transducers to different channels. The microphone polarization voltage can be switched on for all channels. (Note: Where polarization voltage is available, it is the same on all microphone channels in a module).

IEEE 1451.4 Transducers

Input modules supports IEEE 1451.4 capable transducers with standardised Transducer Electronic Data Sheets (TEDS). This feature allows automatic front-end and analyzer setup, based on information stored in the transducer. This information includes, for example, sensitivity, serial number, manufacturer and calibration date.

Transducer Conditioning Check

Input modules use two methods to detect transducer cable breaks or whether the wrong conditioning has been chosen. For microphones, their supply current is monitored. For DeltaTron® accelerometers (or microphones using DeltaTron® preamplifiers), the supply voltage is monitored. If conditioning errors such as a broken cable are detected, an error event is indicated as an overload on the specific channel.

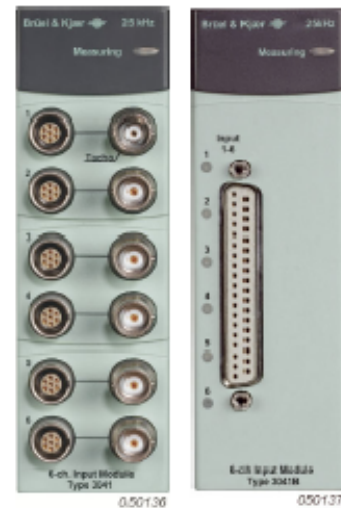


Table2 Overview of modules with input channels

Standard	-	3038	3038-B	3039	3038-B	3109	3110	7637	7637-A	
Dyn-X	3035	3040	3040-B	3041	3041-B	-	-	7638	7638-A	
								7640	7640-A	
Input Channels	6	12	12	6	6	4	2	5	5	
Frequency Range	25.6 kHz						204.8 kHz		25.6 kHz	
BNC (CCLD®Direct) ^a	5	10	-	5	-	4	-	-	5	
BNT (CCLD®Direct/Tacho) ^b	Ch. 1	Ch. 1 and 7	-	Ch. 1	-	Ch. 1	2	Ch. 1	Ch. 1	
TNC (Charge)	6	-	-	-	-	-	-	-	-	
LEMO (Preamp)	-	-	-	5	-	4	2	5	-	
37-pole D-sub	-	-	2	-	1	-	-	-	-	
Supports Charge Injection Calibration (CIC) check with LEMO microphone preamplifiers ^c	-	-	Yes ^d	Yes	Yes	Yes	Yes	Yes	Yes ^d	
Intensity Phase Matching	All BNT/DNC	5 + 6, 11 + 12	5 + 6, 11 + 12 ^d	5 + 6	5 + 5 ^d	Ch. 3 and 4	All	4 + 5	-	
		From 2005: All channels					From 2005: All channels			
		Dyn-X: All channels					Dyn-X: All channels			
AD converters	24-bit to 25.6 kHz					16-bit to 25.6 kHz	24-bit to 25.6 kHz, 16-bit to 204.8 kHz	24-bit to 25.6 kHz		
Floating/Non-floating	Yes					-	Yes			
Microphone Polarization	-	-	0 or 200 V						-	

a. Including DeltaTron® and ICP®

b. Charge operation can be obtained directly using Type 3035 or by using Charge to DeltaTron® Converter Type 2647 with other modules

c. Via dedicated application software and OLE interface

d. Via AQ-0602 17-pole In 6 x 1 FMO Adaptor Cable

6-ch. Charge & CCLD Input Module Type 3035

6-channel Charge & CCLD Input Module Type 3035 is designed specifically to allow the direct connection of charge transducers to a PULSE system. Each channel also has DeltaTron capability for IEPE transducers, and can also be used for direct input of voltages. Type 3035 compliments the other input modules in the PULSE IDA® range, and incorporates Dyn-X technology to give a useful measurement range of 160dB on each channel.

CCLD and Voltage Inputs

The voltage and DeltaTron inputs are via BNC connectors, and each channel has the same specification as the other Dyn-X input channels, such as those found on Types 3040 and 3041.

Charge Inputs

TNC connectors are provided for charge transducers. These provide the most stable charge contact for avoiding triboelectric noise from vibrations. TNC to microdot (10–32UNF) adaptors are included. The Dyn-X technology ensures optimal transducer support and ease of use and makes it possible to condition all charge transducers in only two input ranges (1 nC or 10 nC), while still providing state-of-the-art performance. Selectable dedicated high-pass (0.1, 1, 10 and 30 Hz) are provided, while low-pass filters (0.1, 1, 3, 10 and 30 krHz) allow efficient damping of the high accelerometer sensitivity at resonance, thus optimising the useful dynamic range.



081130

Output Channels

Available Generator Modules

	Standard	Dyn-X
Input/Output Modules		
Generator, 4/2-ch. Input/Output Module	3109	–
Generator, 2/1-ch. Input/Output Module	3110	–
Input/Output Controller Modules		
5/1-ch. Input/Output Controller Modules	7537, 7537-A (3560-B-010/020)	7538, 7538-A (3560-B-110/120)
5/1-ch. Input/Output Controller Modules with Generator	7539, 7539-A (3560-B-030/040)	7540, 7540-A (3560-B-130/140)



USES

- Generator output channels for system excitation for acoustic and vibration measurements

FEATURES

- Type 3109: 2 output channels: Full generator functionality to 25.6kHz
- Type 3110: 1 output channel: Full generator functionality to 102.4kHz
- Types 7539, 7539-A (3560-B-030/040), 7540, 7540-A (3560-B-130/140): 1 output channel: Full generator functionality to 25.6kHz
- Waveforms determined by PULSE software (see BU 0229)
- Types 7537, 7537-A (3560-B-010/020), 7538, 7538-A (3560-B-110/120): 1 output channel: Sine waveforms up to 25.6kHz; sine wave only

Type 3109

The two output channels on Type 3109 can be used as signal generators with a frequency range from 0 to 25.6kHz and can supply all the signals necessary for performing system analysis.

Type 3109 is designed around a powerful digital signal processor and a 24-bit D/A converter, and has exceptional flexibility, stability and accuracy. Output levels are adjustable in hardware, with maximum output ranging from 5 mV to 5 V RMS. Lower levels are possible by scaling the signal to the D/A converter. The signal is provided by a BNC connector and can be referred to ground or floating. It is possible to add a DC offset, but any unwanted DC offset is automatically removed.

Emergency Stop

The connector at the top of the module allows connection to an emergency stop control, allowing you to stop the generators immediately.

Type 3110

The output channel on Type 3110 can be used as signal generator with a frequency range from 0 to 102.4kHz and can supply all the signals necessary for performing system analysis. The generators are controlled from PULSE software.

Type 3110 is designed around a powerful digital signal processor and a 24-bit D/A converter, and has exceptional flexibility, stability and accuracy. The full dynamic output range is obtained from 7 mV to 7 V peak. Lower levels are possible by scaling the signal to the D/A converter. The signal is provided by a BNC connector and can be referred to ground or floating. It is possible to add a DC offset, but any unwanted DC offset is automatically removed.

Monitor Output

An input monitor signal is available on a BNC connector for each input channel. The signal is taken after the high-pass filter but before the anti-aliasing filter. The signal level is $2.236 V_p$ for full-scale input in any range. The signal is always referred to (chassis) ground.

Types 7539, 7539-A, 7540, 7540-A

The output channels on these modules can be used as signal generators with a frequency range from 0 to 25.6 kHz and can supply all the signals necessary for performing system analysis.

The modules are designed around a powerful digital signal processor and a 24-bit D/A converter, and have exceptional flexibility, stability and accuracy. The signal is provided by a BNC connector and can be referred to ground or floating. It is possible to add a DC offset, but any unwanted DC offset is automatically removed.

Types 7537, 7537-A, 7538, 7538-A

The output channels on these modules can be used as simple, high-quality sine tone generators with a frequency range from 0.001 to 25.6 kHz. The maximum output voltage is $5 V_{RMS}$ delivered in one output range through a 24-bit D/A converter. The signal is provided by a BNC connector, and may be referred to ground or floating.

Controller Modules

Available Controller Modules

	Standard	Dyn-X
100 Mbit Controller Module	7536	—
5/1-ch. Input/Output Controller Modules	7537, 7537-A (3560-B-010/020)	7538, 7538-A (3560-B-110/120)
5/1-ch. Input/Output Controller Modules with Generator	7539, 7539-A (3560-B-030/040)	7540, 7540-A (3560-B-130/140)

USES

- Communication interface between a PULSE Front-end and a PC running PULSE software, via LAN (Local Area Network)
- Measurement of voltage or physical parameters like position, wind speed or temperature via 12 auxiliary input channels

FEATURES

- Sets up and transmits data from input modules, provides sampling clock and synchronisation of front-ends
- Connection of remote control for sound intensity measurements via RS-232 interface
- Data transfer according to standard TCP/IP protocol



Synchronisation and Stacking

Controller Modules control and route all communication between the PC and the input/output modules, and transmit or receive synchronisation and clock signals to or from other front-ends. This enables up to 10 units to be combined to act as one multichannel system. It also enables all front-ends in a system to be turned on or off simultaneously.

RS-232

An RS-232 interface on the front panel allows communication with the optional Remote Control Unit ZH-0632 for sound intensity measurements. The interface is also used for setting up the LAN address and testing the front-end hardware.

Auxiliary Channels

12 DC channel^a, present on a single connector, are each sampled 10 times per second. The channels are single-ended and have six input ranges from 0.1 V to 31.6 V in 10 dB steps.



PULSE Software and Applications


The base software for a PULSE system is Noise and Vibration Analysis Type 7700 with both FFT and CPB analyzers, though separate FFT and CPB licenses are available as FFT Analysis Type 7770 and CPB Analysis Type 7771. On this base, you can install any other PULSE software and applications such as Data Recorder Type 7701 and Time Capture Type 7705. For descriptions of the PULSE software please refer to the separate System Data, BU 0229.

^a 4 additional auxiliary inputs are included for future use, and 2 open drain outputs, which allow for simple on/off control.

Compliance with Standards

(For environmental specifications and compliance with standards for PCs, see the specifications given by their respective manufacturers)

TYPES 3560-B-010, -020, -030, -040, -110, -120, -130, -140,
 TYPES 3560-C, 3560-D AND 3560-E WITH CONTROLLER MODULE TYPE 7536,
 INPUT/OUTPUT CONTROLLER MODULE TYPE 7537, 7537-A, 7538, 7538-A, 7539, 7539-A, 7540 OR 7540-A
 INPUT/OUTPUT MODULE TYPE 3035, 3038, 3038-B, 3039, 3039-B, 3040, 3040-B, 3041, 3041-B, 3109 OR 3110

	CE-mark indicates compliance with: EMC Directive and Low Voltage Directive. C-Tick mark indicates compliance with the EMC requirements of Australia and New Zealand.
Safety	EN/IEC 61010-1: Safety requirements for electrical equipment for measurement, control and laboratory use. UL 61010B-1: Standard for Safety – Electrical measuring and test equipment.
EMC Emission	EN/IEC 61000-6-3: Generic emission standard for residential, commercial and light industrial environments. EN/IEC 61000-6-4: Generic emission standard for industrial environments. CISPR 22: Radio disturbance characteristics of information technology equipment. Class B Limits. FCC Rules, Part 15: Complies with the limits for a Class B digital device.
EMC Immunity	EN/IEC 61000-6-1: Generic standards – Immunity for residential, commercial and light industrial environments. EN/IEC 61000-6-2: Generic standards – Immunity for industrial environments. EN/IEC 61326: Electrical equipment for measurement, control and laboratory use – EMC requirements. Note: The above is only guaranteed using accessories listed in this System Data.
Temperature	IEC 60068-2-1 & IEC 60068-2-2: Environmental Testing. Cold and Dry Heat. Operating Temperature: -10 to +50°C (14 to 122°F) Storage Temperature: -25 to +70°C (-13 to 158°F)
Humidity	IEC 60068-2-78: Damp Heat: 93% RH (non-condensing at 40°C (104°F))
Mechanical	Operating (peak values) MIL-STD-810C: Vibration: 12.7 mm, 15 ms ⁻² , 5–500 Hz Non-operating: IEC 60068-2-6: Vibration: 0.3 mm, 20 ms ⁻² , 10–500 Hz IEC 60068-2-27: Shock: 1000 ms ⁻² IEC 60068-2-29: Bump: 1000 bumps at: 250 ms ⁻²
Enclosure	IEC 60529: Protection provided by enclosures: 3560-B: IP 40; 3560-C: IP 32; 3560-D: IP 40; 3560-E: IP 20

EFFECT OF RADIATED/CONDUCTED RF, MAGNETIC FIELD AND VIBRATION

Radiated RF: 80–1000 MHz, 80% AM 1 kHz, 10 V/m
 Conducted RF: 0.15–80 MHz, 80% AM 1 kHz, 10 V
 Magnetic Field: 30 A/m, 50 Hz

Vibration: 5–500 Hz, 12.7 mm, 15 m/s²
 Input measured in 7.071 mV range with shorted input. All values are RMS. Conducted RF immunity on all channels is only guaranteed using an external connection from measuring ground to chassis terminal on Types 2826 or 2827

Input/Output	Radiated RF	Conducted RF	Magnetic Field	Vibration
Direct/OCLD	<10 μV	<130 μV	<4 μV	<80 μV
Preamplifier	<10 μV	< 25 μV	<8 μV	<80 μV
Generator	<80 μV	< 25 μV	<4 μV	< 5 μV
Charge	<130 fC	<130 fC	<10 fC	<80 fC

Specifications – PULSE Types 3560-B/C/D/E

Multi-analyzer Systems Type 3560-B, 3560-C, 3560-D and 3560-E with LAN interface are modular, expandable, multi-analysis systems that include the following components:

- Pentium® PC
- PULSE software

- Microsoft® Windows® 2000 or Windows® XP or Windows Vista™ operating system
- Microsoft® Office 2000, 2003, 2007 or XP
- Front-end comprising: Power Supply/Frame, Controller Module and a number of Input/Output Modules (see below)

Specifications – Portable PULSE Type 3560-B

POWER REQUIREMENTS

Fulfills the requirements of ISO 7637-1 and 7637-2 with batteries
 Voltage: 10 – 32 V DC

Power Consumption:

Nominal: 14 W
 Max.: 26 W (while charging battery)

Ext. Power Connector: LEMO coax., FFA.00.113, ground on shield

BATTERIES

Optional Accessories: 2 × DR35 NiMH or Ni 1030, 10.8 V (nominal)

Working Time (Continuous): 5 hours

Charging Time: 5 hours/battery

ACOUSTIC NOISE EMISSION (at 1 m)

Silent operation to 35°C (95°F) when not charging batteries. When charging batteries, fan operation may start at a lower ambient temperature

DC OUTPUT

+ 5V ± 0.5V; max. 0.4A (1A fused)
 +12V ± 1.0V; max. 0.4A (1A fused)
 Connector: LEMO FGG.00.302

DIMENSIONS (WITHOUT PROTECTIVE COVER)

Height: 182 mm (7.2")
 Width: 64 mm (2.5")
 Depth: 270 mm (10.6")
 Weight: 2.5 kg (5.5 lb.) without batteries

Specifications – Portable PULSE Type 3560-C**POWER SUPPLY/FRAME**

Type 2827

AVAILABLE MODULES

See "Ordering Information – PULSE Systems 3560-B, 3560-C, 3560-D, 3560-E" on page 23

POWER REQUIREMENTS

Fulfills the requirements of ISO 7637-1 and 7637-2 with batteries
 Voltage: 10 – 32V DC

Power Consumption:

Without DC output and when fitted with:
 1 × 7536 Controller Module
 1 × 3109 4/2-ch. or 3110 2/1-ch. Input/Output Module
 Nominal: 30 W

Max.: 42 W (while charging battery)

Ext. Power Connector: LEMO coax., FFA.00.113, ground on shield

BATTERIES

Optional Accessories: 2 × DR35 NiMH or NI 1030, 10.8 V (nominal)
 Working Time (Continuous): 2½ hours
 Charging Time: 6 hours/battery

ACOUSTIC NOISE EMISSION (at 1 m)

	dB SPL, A-weighted at 1 m	dB Lw, A-weighted
Fan Off	<17	<26
Normal (22°C)	32	40
Max.	33	41

DC OUTPUT

+5V ± 0.5V; max. 0.4A (1A fused)
 +12V ± 1.0V; max. 0.4A (1A fused)
 Connector: LEMO FGG.00.302

DIMENSIONS (WITHOUT PROTECTIVE COVER)

Height: 105 mm (4.1")
 Width: 376 mm (14.8")
 Depth: 300 mm (11.8")
 Weight: 5 kg (11 lb.) with Controller Module and Input/Output Module.
 When fitted with batteries, 6 kg (13 lb.)

Specifications – Multichannel Portable PULSE Type 3560-D**POWER SUPPLY**

Type 2826

FRAME (INCL. FAN UNIT)

KK-0050

AVAILABLE MODULES

See "Ordering Information – PULSE Systems 3560-B, 3560-C, 3560-D, 3560-E" on page 23

POWER REQUIREMENTS

Voltage: 10 – 32V DC
 Power Consumption:
 Without DC output and when fitted with:
 1 × 7530 Controller Module
 35 W nominal with 1 input module
 100 W nominal with 5 input modules

Ext. Power Connector: Neutrik® Powercon 3-pole

Max. No. of Tacho Probes: 4 in full frame

DC OUTPUT

+5V ± 0.5V; max. 0.4A (1A fused)
 +12V ± 1.0V; max. 0.4A (1A fused)
 Connector: LEMO FGG.00.302

ACOUSTIC NOISE EMISSION (at 1 m)

	dB SPL, A-weighted at 1 m	dB Lw, A-weighted
Fan Off	27	35
Normal (22°C)	30	38
Max.	42	50

DIMENSIONS

Height: 194 mm (7.6") with feet, 170 mm (6.7") without feet
 Width: 376 mm (14.8")
 Depth: 342 mm (13.5")

Specifications – Multichannel PULSE Type 3560-E**POWER SUPPLY**

Type 2826

RACK MOUNTING KIT

WU-0516

AVAILABLE MODULES

See "Ordering Information – PULSE Systems 3560-B, 3560-C, 3560-D, 3560-E" on page 23

POWER REQUIREMENTS

Voltage: 10 – 32V DC
 Power Consumption:
 When fitted with:
 1 × 7536 Controller Module

35 W nominal with 1 input module
 140 W nominal with 8 input modules
 Ext. Power Connector: Neutrik® Powercon 3-pole
 Max. No. of Tacho Probes: 2 in full frame

DIMENSIONS

Height: 134 mm (5.3") (3 standard rack-mounting units)
 Width: 482.6 mm (19")
 Depth: 300 mm (11.8")
 Weight: 8.7 kg (19 lb.) with Controller Module and 8 Input/Output Modules; 17.5 kg (38.5 lb.) with KQ-0155 and UH-1037

Specifications – Input Channels, Standard 24-bit and Dyn-X

		Standard 24-bit 7637/37-A/38/38-A, 3038/38-B/38/38-B 3680-B-010/020/030/040			Dyn-X 7638/38-A/40/40-A, 3035 (BNC/BNT) 3040/40-B/41/41-B, 3680-B-110/120/130/140			
Frequency Range		DC to 25.6 kHz						
A/D Conversion		24-bit			2 × 24-bit			
Data Transfer		24-bit 16-bit selectable						
Input Voltage Range		8 ranges: 7.071 mV _{peak} to 7.07 V _{peak} in 10 dB steps ^a , + 12 V _{peak}			1 range: 10 V _{peak}			
Input Signal Ground Coupling		Floating or single-ended (grounded to chassis)						
Input Impedance		Direct, Microphone: 1 MΩ <200 pF CCLD: >100 kΩ <200 pF						
Absolute Maximum Input		±35 V _{peak} without damage						
High-pass Filters		DC (f _L = 0)						
		-0.1 dB	-10%	-3 dB	Slope	-10%	-3 dB	Slope
		0.7 Hz high-pass filter	0.15 Hz	0.073 Hz	-20 dB/dec.	0.15 Hz	0.073 Hz	-20 dB/dec.
		7 Hz digital high-pass filter	1.45 Hz	0.707 Hz	-20 dB/dec.	1.45 Hz	0.707 Hz	-20 dB/dec.
		22.4 Hz high-pass filter	14.64 Hz	11.5 Hz	-60 dB/dec.	14.64 Hz	11.5 Hz	-60 dB/dec.
		Intensity filter	23.00 Hz	11.2 Hz	-20 dB/dec.	23.00 Hz	11.2 Hz	-20 dB/dec.
Absolute Amplitude Precision, 1 kHz, 1 V _{input}		±0.05 dB, typical ±0.01 dB						
Attenuator Linearity @ 1 kHz		±0.05 dB, typ. ±0.005 dB			-			
Amplitude Linearity (linearity in one range)		0 to 60 dB below full scale	±0.1 dB, typ. ±0.01 dB			±0.05 dB, typ. ±0.01 dB		
		60 to 80 dB below full scale	±0.2 dB, typ. ±0.02 dB			±0.05 dB, typ. ±0.01 dB		
		80 to 100 dB below full scale	typ. ±0.05 dB			±0.2 dB, typ. ±0.02 dB		
		100 to 120 dB below full scale	-			typ. ±0.02 dB		
		120 to 140 dB below full scale	-			typ. ±0.02 dB		
		140 to 160 dB below full scale	-			typ. ±1 dB		
Overall Frequency Response re 1 kHz, lower limit f _L to upper limit f _H		DC to max. 25.6 kHz: ±0.1 dB						
Noise:		Input Range	Guaranteed	Typical	Guaranteed	Typical		
Measured lin. 10 Hz to 25.6 kHz: μV _{RMS} (input terminated by 50 Ω or less)		7.071 mV	<2.5 (<16)	2.2 (<14)	Signal level <318 mV _{peak}		3 (<19)	
		22.36 mV	<3 (<19)	2.2 (<14)				
		70.71 mV	<4 (<25)	2.5 (<16)				
(Values in parentheses are specified in nV _{RMS} /√Hz)		223.6 mV	<6 (<38)	5.5 (<35)	Signal level >318 mV _{peak}		50 (<313)	
		707.1 mV	<17 (<107)	13 (<82)				
		2.236 V	<50 (<313)	33 (<207)				
		7.071 V	<150 (<940)	100 (<625)				
		12 V	<250 (<1570)	150 (<940)				
Spurious-free Dynamic Range (dB) re full scale input (input terminated by 50 Ω or less)		Input Range	Typical			Typical		
		7.071 mV	110 dB			160 dB		
		22.36 mV	110 dB					
		70.71 mV	120 dB					
		223.6 mV	130 dB					
		707.1 mV	130 dB					
		2.236 V	130 dB					
		7.071 V	130 dB					
		12 V	130 dB					
DC Offset re full scale		Guaranteed	Typical		Guaranteed	Typical		
		<-60 dB	-80 dB		<-60 dB	-80 dB		
Harmonic Distortion (all harmonics)		Guaranteed	Typical		Guaranteed	Typical		
		All Ranges				Guaranteed	Typical	
		-80 dB	-100 dB @ 1 kHz		-80 dB	-100 dB @ 1 kHz		

^a in rare cases in CCLD mode or when measuring signals with a high DC level in the 7 mV_{peak} and 22.36 mV_{peak} ranges with 0.7 Hz or 7 Hz high-pass filter settings, an overload might be indicated. If this occurs, increase the input voltage range.

Specifications – Input Channels, Standard 24-bit and Dyn-X (continued)

		Standard 24-bit 7637/37-A/38/38-A, 3038/38-B/38/38-B 3680-B-010/020/030/040			Dyn-X 7638/38-A/40/40-A, 3036 (BNC/BNT) 3040/40-B/41/41-B, 3680-B-110/120/130/140		
Crosstalk Between any two channels of a module or between any two channels in different modules	Frequency Range	Guaranteed	Typical	Frequency Range	Guaranteed	Typical	
	0 – 25.6 kHz	-100 dB	-140 dB	0 – 25.6 kHz	-100 dB	-140 dB	
Channel-to-Channel Match (same input range)	Guaranteed		Typical	Guaranteed		Typical	
	0.2 dB from lower frequency limit, f_L , to upper limit, f_U		± 0.01 dB	0.1 dB from lower frequency limit, f_L , to upper limit, f_U		± 0.01 dB	
Maximum Phase Difference (within one frame)	1.2* – 0.1* × (f/f _L) from f_L to $10 \times f_L$ (not valid for DC setting); 0.2* from $10 \times f_L$ to 1280 Hz (valid for DC setting); 0.1* + 0.1* × (f/1280) from 1280 Hz to 25.6 kHz			1.2* – 0.1* × (f/f _L) from f_L to $10 \times f_L$ (not valid for DC setting); 0.2* from $10 \times f_L$ to 6.4 kHz (valid for DC setting); 0.1* + 0.1* × (f/6400) from 6.4 kHz to 25.6 kHz			
Channel-to-Channel Match (any input range)	Guaranteed		Typical				
	0.2 dB from lower frequency limit, f_L , to upper limit, f_U		± 0.01 dB				
Maximum Phase Difference (within one frame)	1.2* – 0.1* × (f/f _L) from f_L to $10 \times f_L$ (not valid for DC setting); 0.2* from $10 \times f_L$ to 640 Hz (valid for DC setting); 0.1* + 0.1* × (f/640) from 640 Hz to 6.4 kHz						
Sound Intensity Phase Match (only for using Intensity filter)	Complies with IEC 1043 standard Class 1 and ANSI S1.12-1995 Class 1 using Brüel&Kjær Sound Intensity Probes (0.017" @ 50 Hz)						
	Channels Matched	7637, 7638: 4 and 5 3038, 3039 B: 5 and 6 3038, 3038 B: 5 and 6, 11 and 12 From 2005: All channels			All channels		
	Frequency Range	Guaranteed Phase Match	Typical Phase Match	Guaranteed Phase Match	Typical Phase Match		
	50 Hz – 250 Hz	$\pm 0.017^*$	$\pm 0.005^*$	$\pm 0.017^*$	$\pm 0.005^*$		
	250 Hz – 2.5 kHz	$0.017^* \times (f/250)$	$\pm 0.005^*$	$0.017^* \times (f/250)$	$\pm 0.005^*$		
2.5 kHz – 6.4 kHz	$\pm 0.17^*$	$\pm 0.08^*$	$\pm 0.17^*$	$\pm 0.08^*$			
Common Mode Rejection	Guaranteed		Typical	Guaranteed		Typical	
	0 – 120 Hz		70 dB	80 dB	70 dB	80 dB	
	120 Hz – 1 kHz		55 dB	60 dB	55 dB	60 dB	
	1 kHz – 25.6 kHz		30 dB	40 dB	30 dB	40 dB	
Absolute Max. Common Mode Voltage		$\pm 5 V_{peak}$ without damage $\pm 3 V_{peak}$ without clipping If common mode voltage exceeds the max. value, care must be taken to limit the signal ground current in order to prevent damage. Maximum is 100 mA. The instrument will limit the voltage to the stated max. "without damage" common mode value					
Anti-aliasing Filter At least 90 dB attenuation of those frequencies which can cause aliasing	Filter Type	3rd order Butterworth					
	-0.1 dB @	25.6 kHz					
	-3 dB @	100 kHz					
	Slope	-18 dB/octave					
Supply for Microphone Preamplifiers	$\pm 14.0 V$, 10 mA per channel (max. 20 mA if only 1 to 3 channels used)						
Supply for Microphone Polarization	200 V $\pm 1 V$, or 0 V						
Supply for DeltaTron/ICP®/CCLD	4 mA from 24 V source If any DeltaTron/ICP®/CCLD-coupled channel is paralleled with another channel, this must also be DeltaTron/ICP®/CCLD-coupled. Otherwise the signal might be clipped by the paralleled channel						
Tacho Supply (on BNT connectors)	6.5 V, max. 100 mA						
Analog Special Functions	Microphone Charge Injection Calibration: All modules with 7-pin LEMO support CIC via dedicated application software and OLE interface Analog Self-test: Functional Check Transducers: Supports IEEE 1451.4 capable transducers with standardised TEDS						
Overload Detection ^b	Signal overload CCLD overload: Detection of cable break or short-circuit + detection of CCLD transducer working point fault Microphone preamplifier overload: Detection of microphone preamplifier current consumption too high or too low Common mode voltage overload						

^b In Direct AC mode, care must be taken when measuring signals with a very high DC component – a DC + AC level exceeding approximately 12 V can be clipped and an overload will not be indicated

Specifications – Charge Input Channels, Dyn-X (all specifications for transducer capacitance = 1 nF)

		Dyn-X 3036 (TNC Charge Inputs) [†]		
Frequency Range		0.1 Hz to 25.6 kHz		
A/D Conversion		2 × 24-bit		
Data Transfer		24-bit		
Input Range		2 ranges: 10 nC _{peak} /1 nC _{peak}		
Input Signal Ground Coupling		Floating or single-ended (grounded to chassis)		
Absolute Maximum Input		±300 nC _{peak} without damage		
High-pass Filters ^b		DC (f _L = 0) Not available		
	–10%	–10%	–3 dB	Slope
	0.1 Hz high-pass filter	0.1 Hz	0.065 Hz	–40 dB/dec.
	1 Hz high-pass filter	1.0 Hz	0.65 Hz	–40 dB/dec.
	10 Hz high-pass filter	10.0 Hz	7.88 Hz	–60 dB/dec.
	30 Hz high-pass filter	30.0 Hz	23.63 Hz	–40 dB/dec.
Low-pass Filters		–10%	–10%	–3 dB
	100 Hz low-pass filter	100 Hz	143 Hz	–40 dB/dec.
	1 kHz low-pass filter	1.0 kHz	1.43 kHz	–40 dB/dec.
	3 kHz low-pass filter	3.0 kHz	4.31 kHz	–40 dB/dec.
	10 kHz low-pass filter	10.0 kHz	14.3 kHz	–40 dB/dec.
	30 kHz low-pass filter	30.0 kHz	43.1 kHz	–40 dB/dec.
	low-pass filter bypassed	See Anti-aliasing Filter		
Absolute Amplitude Precision, 1 kHz, 1 V _{input}		±0.05 dB, typ. ±0.01 dB		
Attenuator Linearity @ 1 kHz		±0.05 dB, typ. ±0.005 dB		
Amplitude Linearity (linearity in one range)		±0.05 dB, typ. ±0.01 dB		
	0 to 60 dB below full scale	±0.05 dB, typ. ±0.01 dB		
	60 to 80 dB below full scale	±0.05 dB, typ. ±0.01 dB		
	80 to 100 dB below full scale	±0.2 dB, typ. ±0.02 dB		
	100 to 120 dB below full scale	typ. ±0.02 dB		
	120 to 140 dB below full scale	typ. ±0.02 dB		
	140 to 160 dB below full scale	typ. ±1 dB		
Overall Frequency Response re 1 kHz, lower limit f _L to upper limit f _U		Min. 0.1 Hz to max. 25.6 kHz: ±0.1 dB, –10% at f _L and f _U		
Noise: Measured lin. 10 Hz to 25.6 kHz: fC _{rms} (input terminated by 1 nF)		Input Range	Signal Level	Guaranteed
		1 nC	<315 pC _{peak}	<5 (<32)
		1 nC	>315 pC _{peak}	<15 (<94)
	(Values in parentheses are specified in aC _{rms} /√Hz [a = 10 ⁻¹⁸])	10 nC	<3150 pC _{peak}	<15 (<94)
		10 nC	>3150 pC _{peak}	<65 (<407)
Spurious-free Dynamic Range (dB) re full scale input (input terminated by 1 nF)		Input Range	Typical	
		1 nC _{peak}	140 dB	
		10 nC _{peak}	150 dB	
DC Offset re full scale		Not applicable		
Harmonic Distortion (all harmonics, all ranges)		Guaranteed	Typical	
		–80 dB	–100 dB @ 1 kHz	
Crosstalk Between any two channels of a module or between any two channels in different modules		Frequency Range	Guaranteed	Typical
		0 – 25.6 kHz	–95 dB	–120 dB
Channel-to-Channel Match (same input range) ^b		Guaranteed		
	Maximum Gain Difference	0.1 dB from 3 × lower frequency limit, f _L to 1/3 upper limit, f _U 0.8 dB at f _L , 0.4 dB at f _U		Typical ±0.01 dB
	Maximum Phase Difference (within one frame)	0.4° from 10 × f _L to 0.1 × f _U 0.2° + 2° × (ff _U) from 0.1 × f _U to f _U For f _L = 10 Hz or 30 Hz: 1.4° - 0.1° × (ff _U) from f _L to 10 × f _L For f _L = 0.1 Hz or 1 Hz: 5.4° - 0.5° × (ff _U) from f _L to 10 × f _L		

Specifications – Charge Input Channels, Dyn-X (continued) (all specifications for transducer capacitance = 1 nF)

		Dyn-X 3036 (TNC Charge Inputs) ^a	
		Guaranteed	Typical
Channel-to-Channel Match (any input range) ^b	Maximum Gain Difference	0.2 dB from $3 \times$ lower frequency limit, f_L , to $1/3$ upper limit, f_U 1 dB at f_L , 0.5 dB at f_U	± 0.02 dB
	Maximum Phase Difference (within one frame)	0.4° from $10 \times f_L$ to $0.1 \times f_U$ $0.2^\circ + 2^\circ \times (f/f_U)$ from $0.1 \times f_U$ to f_U For $f_L = 10$ Hz or 30 Hz: $1.4^\circ - 0.1^\circ \times (f/f_L)$ from f_L to $10 \times f_L$ For $f_L = 0.1$ Hz or 1 Hz: $5.4^\circ - 0.5^\circ \times (f/f_L)$ from f_L to $10 \times f_L$	
Common Mode Rejection		Guaranteed	Typical
	0 – 120 Hz	50 dB	55 dB
	120 Hz – 1 kHz	50 dB	55 dB
1 kHz – 25.6 kHz	40 dB	50 dB	
Absolute Max. Common Mode Voltage		$\pm 5 V_{\text{peak}}$ without damage	
		$\pm 3 V_{\text{peak}}$ without clipping	
		If common mode voltage exceeds the max. value, care must be taken to limit the signal ground current in order to prevent damage. Maximum is 100 mA. The instrument will limit the voltage to the stated max. "without damage" common mode value.	
Anti-aliasing Filter At least 90 dB attenuation of those frequencies which can cause aliasing	Filter Type	3rd order Butterworth	
	-0.1 dB @	25.6 kHz	
	-3 dB @	100 kHz	
	Slope	-18 dB/octave	
Tacho Supply (on BNC connectors)		-	
Analog Special Functions		Analog Self-test: Functional Check	
Overload Detection ^c		Signal overload Common mode voltage overload DC servo out of range	

a. For OCLD and AC inputs see "Specifications – Input Channels, Standard 24-bit and Dyn-X" on page 14

b. For specifications with 0.7, 7 and 22.4 Hz high-pass filters, see the corresponding specifications for BNC/BNT Dyn-X channels

c. Note: All overloads in charge mode are indicated as "signal overload"

Specifications – Input Channels, Types 3109 and 3110

	3109			3110			
Frequency Range	DC to 25.6 kHz			DC to 25.6 kHz		DC to 204.8 kHz	
A/D Conversion	16-bit			24-bit		16-bit for frequency range > 25.6 kHz	
Data Transfer	16-bit			24-bit 16-bit selectable		16-bit	
Input Voltage Range	7 ranges: 7.071 mV _{peak} to 7.071 V _{peak} in 10 dB steps			8 ranges: 7.071 mV _{peak} to 22.34 V _{peak} in 10 dB steps			
Input Signal Ground Coupling	Floating with 100 Ω to chassis			Floating or single-ended (grounded to chassis)			
Input Impedance	Direct, Microphone: 1 MΩ < 200 pF						
	OCLD: > 100 kΩ < 200 pF						
Absolute Maximum Input	$\pm 50 V_{\text{peak}}$ (± 30 V DC) without damage			$\pm 35 V_{\text{peak}}$ without damage			
High-pass Filters	DC ($f_L = 0$)						
	-0.1 dB	-10%	-3 dB	Slope	-10%	-3 dB	Slope
	0.7 Hz high-pass filter	0.15 Hz	0.073 Hz	-20 dB/dec.	0.15 Hz	0.073 Hz	-20 dB/dec.
	7 Hz digital high-pass filter	1.45 Hz	0.707 Hz	-20 dB/dec.	1.45 Hz	0.707 Hz	-20 dB/dec.
	22.4 Hz high-pass filter	14.64 Hz	11.5 Hz	-60 dB/dec.	14.64 Hz	11.5 Hz	-60 dB/dec.
Intensity filter	23.00 Hz	11.2 Hz	-20 dB/dec.	23.00 Hz	11.2 Hz	-20 dB/dec.	
Absolute Amplitude Precision, 1 kHz, 1 V _{input}	± 0.1 dB			± 0.05 dB, typ. ± 0.005 dB			
Attenuator Linearity @ 1 kHz	± 0.1 dB			± 0.05 dB, typ. ± 0.005 dB			

Specifications – Input Channels, Types 3109 and 3110 (continued)

		3109	3110						
Amplitude Linearity (linearity in one range)	0 to 40 dB below full scale	±0.1 dB	-						
	40 to 60 dB below full scale	±0.4 dB	-						
	0 to 60 dB below full scale	-	±0.1 dB, typ. ±0.01 dB						
	60 to 80 dB below full scale	±1 dB	±0.2 dB, typ. ±0.02 dB						
80 to 100 dB below full scale		-	Typ. ±0.05 dB						
Overall Frequency Response re 1 kHz, f_L to f_H		DC to max. 25.6 kHz ±0.1 dB	DC to max. 204.8 kHz ±0.1 dB, f_L to 25.6 kHz +0.1/-0.2 dB, f_L to 102.4 kHz +0.1/-0.5 dB, f_L to 204.8 kHz						
Noise: μV_{rms} (input terminated by 50 Ω or less) (Values in parentheses are specified in nV/Hz)	Input Range	Measured lin. 10 Hz to 25.6 kHz		Measured lin. 10 Hz to 25.6 kHz		Measured lin. 10 Hz to 204.8 kHz			
		Guaranteed		24-bit ADO		16-bit ADO			
				Guar.	Typ.	Guar.	Typ.	Guar.	Typ.
		1.071 mV	3 (19)	3 (12.5)	1.5 (10)	3 (12.5)	1.5 (10)	6 (13)	4 (9)
		22.36 mV	3 (19)	2 (12.5)	1.5 (10)	2 (12.5)	1.5 (10)	6 (13)	4 (9)
		10.71 mV	5 (32)	2.5 (16)	1.7 (11)	4 (25)	2 (12.5)	10 (22)	6 (13)
		223.6 mV	10 (63)	5 (32)	2.5 (16)	10 (63)	5 (32)	20 (125)	12 (75)
		107.1 mV	31 (194)	10 (63)	5 (32)	31 (194)	16 (113)	60 (375)	30 (188)
		2.236 V	100 (625)	30 (188)	15 (94)	100 (625)	50 (313)	180 (1125)	125 (781)
		7.071 V	316 (1980)	100 (625)	45 (282)	300 (1875)	150 (938)	500 (3125)	400 (2500)
22.4 V	-	300 (1875)	150 (938)	900 (5625)	500 (3125)	1500 (9375)	1200 (7500)		
Spurious-free Dynamic Range (dB) re full scale input (input terminated by 50 Ω or less)	Input Range	Guaranteed		DC to 25.6 kHz		DC to 204.8 kHz			
				Guaranteed	Typ.	Guaranteed			
		1.071 mV	80 dB or <1 μV , whichever is greater	90 dB	90 dB	90 dB			
		22.36 mV		90 dB	110 dB	90 dB			
		10.71 mV		90 dB	120 dB	90 dB			
		223.6 mV		90 dB	120 dB	90 dB			
		107.1 mV		90 dB	120 dB	90 dB			
		2.236 V		90 dB	120 dB	90 dB			
7.071 V	90 dB	120 dB		90 dB					
22.4 V	-	90 dB		120 dB	90 dB				
DC offset re full scale		Guaranteed		Guaranteed		Typical			
		<-60 dB		<-60 dB		-80 dB			
Harmonic Distortion (all harmonics)		Guaranteed		DC to 25.6 kHz		DC to 204.8 kHz			
				Guaranteed	Typ.	Guaranteed	Typ.		
		All Ranges		7 mV to 7 V Ranges					
		-80 dB or <1 μV , whichever is greater		-90 dB	-90 dB	-75 dB	-90 dB		
22 V Range									
		-70 dB	-80 dB	-70 dB	-80 dB				
Crosstalk Between any two channels of a module or between any two channels in different modules		Frequency Range	7 mV – 7 V Input Range	Frequency Range	7 mV – 7 V Input Range	22 V Input Range			
		0 – 2 kHz	-100 dB	0 – 2 kHz	-120 dB	-90 dB			
		2 – 12.8 kHz	-85 dB	2 – 12.8 kHz	-100 dB	-90 dB			
		12.8 – 20.4 kHz	90 dB	12.8 – 20.4 kHz	-100 dB	-90 dB			
				25.6 – 102.4 kHz	-100 dB	-90 dB			
		102.4 – 204.8 kHz	-90 dB	-80 dB					

Specifications – Input Channels, Types 3109 and 3110 (continued)

	3109		3110	
	Guaranteed	Typical	Guaranteed	Typical
Channel-to-Channel Match (same input range)				
Maximum Gain Difference	0.2 dB from lower frequency limit, f_L , to upper limit, f_U	–	0.1 dB from lower frequency limit, f_L , to upper limit, f_U	<0.01 dB
Maximum Phase Difference (within one frame)	1.2° – 0.1° × (f/f_L) from f_L to $10 \times f_L$ (not valid for DC setting); 0.2° from $10 \times f_L$ to 1280 Hz (valid for DC setting); 0.1° + 0.1° × ($f/1280$) from 1280 Hz to 25.6 kHz		1.2° – 0.1° × (f/f_L) from f_L to $10 \times f_L$ (–1.1° at f_L and 0.2° at $10 \times f_L$) (not valid for DC setting); 0.2° from $10 \times f_L$ to 6400 Hz (valid for DC setting); 0.4° × $f/6.4$ kHz – 0.2° from 6.4 kHz to 204.8 kHz (–1.4° at 25.6 kHz, 0.4° at 102.4 kHz and 1.2.5° at 204.8 kHz)	
Channel-to-Channel Match (any input range)				
Maximum Gain Difference	0.2 dB from lower frequency limit, f_L , to upper limit, f_U	–	0.1 dB from lower frequency limit, f_L , to upper limit, f_U	<0.05 dB
Maximum Phase Difference (within one frame)	1.2° – 0.1° × (f/f_L) from f_L to $10 \times f_L$ (not valid for DC setting); 0.2° from $10 \times f_L$ to 640 Hz (valid for DC setting); 0.1° + 0.1° × ($f/640$) from 640 Hz to 6.4 kHz		1.2° – 0.1° × (f/f_L) from f_L to $10 \times f_L$ (–1.1° at f_L and 0.2° at $10 \times f_L$) (not valid for DC setting); 0.2° from $10 \times f_L$ to 6400 Hz (valid for DC setting); 0.8° × $f/6.4$ kHz – 1.6° from 6.4 kHz to 204.8 kHz (–2.6° at 25.6 kHz, 12.2° at 102.4 kHz and 25° at 204.8 kHz)	
Sound Intensity Phase Match (only for using intensity filter)	Complies with IEC 1043 standard Class 1 and ANSI S1.12 – 1995 Class 1 using Brüel & Kjær Sound Intensity Probes (0.017" @ 50 Hz)			
Channels Measured	3 and 4		1 and 2	
Frequency Range	Guaranteed Phase Match		Guaranteed Phase Match	Typical Phase Match
50 Hz – 250 Hz	±0.017°		±0.017°	±0.005°
250 Hz – 2.5 kHz	0.017° × ($f/250$)		0.017° × ($f/250$)	±0.005°
2.5 kHz – 6.4 kHz	±0.17°		±0.17°	±0.08°
Common Mode Rejection	Guaranteed		7 mV – 7V Input Range	
			Guaranteed	Typical
0 – 120 Hz	40 dB, 50 dB at DC		70 dB	80 dB
120 Hz – 1 kHz	40 dB		55 dB	60 dB
1 kHz – 25.6 kHz			30 dB	40 dB
Absolute Max. Common Mode Voltage	±15 V _{peak} without damage		±5 V _{peak} without damage	
	±1.5 V _{peak} without clipping		±3 V _{peak} without clipping	
	If common mode voltage exceeds the max. value, care must be taken to limit the signal ground current in order to prevent damage. Maximum is 100 mA. The instrument will limit the voltage to the stated max. "without damage" common mode value			
Anti-aliasing Filter At least 50 dB attenuation of those frequencies which can cause aliasing	Filter Type	3rd order Butterworth	Freq. Range ≤26.6 kHz	Freq. Range >26.6 kHz
	–0.1 dB @	25.6 kHz	25.6 kHz	102.4 kHz
	3 dB @	100 kHz	100 kHz	400 kHz
	Slope	–18 dB/octave	–18 dB/octave	
Supply for Microphone Preamplifiers	±15.0 V, max. 10 mA per channel		±14.0 V, max. 20 mA per channel	
Supply for Microphone Polarization	200 V ±1 V, or 0 V			
Supply for DeltaTron/ICP®/CCLD	4 mA from 24 V source			
Tacho Supply (on BNT connectors)	6.5 V, max. 100 mA			
Analog Special Functions	Microphone Charge Injection Calibration (depending on software support) Analog Self-test Functional Check Transducers: Supports IEEE 1451.4 capable transducers with standardised TEDs			
Overload Detection	Signal overload CCLD overload: Detection of cable break or short-circuit + detection of CCLD transducer working point fault Microphone preamplifier overload: Detection of microphone preamplifier current consumption too high or too low Common mode voltage overload (Type 3110 only)			

Specifications – Output Channels, Standard 24-bit and Dyn-X

	Standard 24-bit 7637/37-A/38/38-A		Dyn-X 7638/38-A/40/40-A	
Output Connector	1 × BNC			
Output Coupling	DC			
Signal Ground Coupling	Floating or grounded to chassis			
D/A Conversion	24-bit			
D/C Offset	±1 mV @ 25°C and ±10 mV @ full temperature range (-60 dB re max. output)			
Output Voltage Range	1 μV _{peak} – 7 V _{peak}			
Output Impedance	50 Ω			
Frequency Range	0 Hz – 25.6 kHz			
Frequency Response re 1 kHz	±0.1 dB, 1 mHz to 25.6 kHz			
Frequency Accuracy	0.0025%			
Waveform	7637, 7637 A	7638, 7638 A	7638, 7638 A	7640, 7640 A
	Sine only	Software determined Arbitrary waveforms up to 2 Msamples	Sine only	Software determined Arbitrary waveforms up to 2 Msamples
Amplitude Linearity @ 1 kHz	Typical			
0 to 60 dB below full scale	±0.1 dB			
60 to 100 dB below full scale	±0.2 dB			
Noise μV _{rms} (nV/√Hz)	Guaranteed	Typical	Guaranteed	Typical
	<30 (<188)	20 (125)	<30 (<188)	20 (125)
Harmonic and Spurious Distortion Products 0 – 25.6 kHz	< 80 dB re full range output or 1 μV, whichever is greater		< 80 dB re full range output or 1 μV, whichever is greater	
Absolute Amplitude Precision @ 23°C, 1 kHz, 1 V _{rms}	Guaranteed ±0.1 dB		Guaranteed ±0.1 dB	
Crosstalk between any generator output and any channel on any module 0 – 2 kHz	Guaranteed	Typical	Guaranteed	Typical
	-100 dB	-114 dB	-100 dB	-114 dB
2 kHz – 25.6 kHz	-85 dB	-110 dB	-85 dB	-110 dB
Common Mode Rejection 1 Hz – 1 kHz	Guaranteed 60 dB		Guaranteed 60 dB	
Max. Common Mode Voltage	5 V _{peak} , DC – 80 MHz			
	If common mode voltage exceeds the max. value, care must be taken to limit the signal ground current in order to prevent damage. Maximum is 100 mA. The instrument will limit the voltage to the stated max. "without damage" common mode value			
Reconstruction Filter Type	Sixth order Butterworth			
Attenuation of mirror frequencies	>80 dB			

Specifications – Output Channels, Types 3109 and 3110

	3109	3110	
Output Connector	2 × BNC	1 × BNC	
Output Coupling	DC		
Signal Ground Coupling	Floating or grounded to chassis		
D/A Conversion	24-bit		
D/C Offset	-	Output Level	
		DC Offset	
		7 mV _{peak} – 70 mV _{peak}	100 μV
		70 mV _{peak} – 700 mV _{peak}	100 μV
	700 mV _{peak} – 7 V _{peak}	1 mV	
Output Voltage Range	7 μV _{peak} – 7 V _{peak}	1 μV _{peak} – 7 V _{peak}	
Output Impedance	50 Ω		
Frequency Range	0 Hz – 25.6 kHz	0 Hz – 102.4 kHz	
Frequency Response re 1 kHz	±0.1 dB, 1 mHz to 25.6 kHz	±0.1 dB, 1 mHz – 25.6 kHz +0.1/-0.3 dB, 1 mHz – 102.4 kHz Typical: ±0.05 dB	
Frequency Accuracy	0.0025%		
Waveform	Software determined. Arbitrary waveforms up to 2 Msamples		

Specifications – Output Channels, Types 3109 and 3110 (continued)

		3109		3110				
Amplitude Linearity @ 1 kHz		Guaranteed		Guaranteed	Typical			
	0 to 60 dB below full scale	±0.1 dB		±0.1 dB	±0.05 dB			
	60 to 100 dB below full scale	±0.2 dB		±0.2 dB	±0.1 dB			
	100 to 120 dB below full scale	±0.5 dB		±0.5 dB	±0.2 dB			
	120 to 140 dB below full scale	±1.0 dB		±1.0 dB	±0.5 dB			
Noise μV_{rms} (nV/√Hz)	Output Level	(10 Hz – 26.8 kHz)		(10 Hz – 26.8 kHz)		(10 Hz – 204.8 kHz)		
		Guaranteed		Guaranteed	Typ.	Guaranteed	Typ.	
		7 mV _{peak} – 70 mV _{peak}		3 (19)	3 (19) 2.5 (16)	15 (34) 9 (20)	15 (34) 9 (20)	15 (34) 9 (20)
		70 mV _{peak} – 700 mV _{peak}		20 (125)	10 (63) 5 (32)	50 (111) 20 (45)	50 (111) 20 (45)	50 (111) 20 (45)
700 mV _{peak} – 7 V _{peak}		200 (1250)	50 (313) 30 (188)	300 (664) 100 (222)	300 (664) 100 (222)	300 (664) 100 (222)		
Harmonic and Spurious Distortion Products	0 – 25.6 kHz	< 80 dB re full range output or 1 μV , whichever is greater		< 80 dB re full range output or 1 μV , whichever is greater, at 10 k Ω load				
	25.6 – 102.4 kHz	-		< 70 dB re full range output or 1 μV , whichever is greater				
	Typical @ 1 kHz			100 dB re full range output				
Absolute Amplitude Precision		Guaranteed		Guaranteed	Typical			
	@ 23°C, 1 kHz, 1 V _{rms}	±0.05 dB		±0.05 dB	±0.005 dB			
	@ 1 kHz, 1 mV – 7 V _{peak}	±0.1 dB		±0.1 dB	±0.05 dB			
Crosstalk between generator output and any channel on any module		Guaranteed		Guaranteed	Typical			
	0 – 2 kHz	-100 dB		-				
	2 kHz – 25.6 kHz	-85 dB		-				
	0 – 102.4 kHz	-		-120 or better than -90 dB re max. input voltage whichever is greater (worse)	-150 dB			
Common Mode Rejection		Guaranteed		Guaranteed	Typical			
	1 Hz – 1 kHz	50 dB		50 dB	50 dB			
	1 kHz – 25.6 kHz	40 dB		24 dB	30 dB			
	25.6 kHz – 102.4 kHz	-		10 dB	20 dB			
Max. Common Mode Voltage		1 V _{peak} , DC – 4 MHz 10 V _{peak} , 4 MHz – 80 MHz		5 V _{peak} , DC – 80 MHz				
Reconstruction Filter	Type	Seventh order Butterworth		Sixth order Butterworth				
	Attenuation of mirror frequencies	> 80 dB						
Monitor Output	Connectors	2 × BNC						
	Output Level	2.236 V _p for full scale input in any range, ±0.05 dB						
	Output Impedance	50 Ω						
	Harmonic Distortion	0 – 25.6 kHz: < -90 dB 25.6 kHz – 102.4 kHz: < -80 dB						
		DC Offset (Max.)	None		Input Range	DC Offset (Max.)		
				7.071 mV	150 mV			
				22.36 mV	50 mV			
				70.71 mV	15 mV			
				223.6 mV	5 mV			
				707.1 mV	1.5 mV			
			2.236 V	0.5 mV				
			7.071 V	0.5 mV				
			22.36 V	0.5 mV				
Signal Output		From last amplifier before anti-aliasing filter, but after analog high-pass filters						

Specifications – Controller Modules Types 7536, 7537, 7537-A, 7538, 7538-A, 7539, 7539-A, 7540, 7540-A and 5-channel PULSE Data Acquisition Units 3560-B-010, -020, -030, -040, -110, -120, -130, -140

LAN Interface

CONNECTOR

RJ45 (10baseT/100baseTX) connector complying with IEEE-802.3 100baseX

PROTOCOL

TCP/IP

ACQUISITION PERFORMANCE

Data Transfer Rate (No. of Channels × Bandwidth) from Front-end via LAN Interface, per frame:

16- and 24-bit modules/channels can be mixed
 460.8 kHz (24-bit data transfer), 691.2 kHz (16-bit data transfer).
 This corresponds approximately to:

Upper Frequency (kHz)	No. of Channels ^a	
	24-bit (460.8 kHz)	16-bit (691.2 kHz)
25.6	18	27 ^b
12.8	36	54
6.4	72	96 ^c

- a. If one or more Type 3030, 3109 or 3032 is included in the system, performance is reduced to 409.6 kHz, for example, 16 channels to 25.6 kHz
- b. If Type 7533 is included, 6 channels to 25.6 kHz (153.6 kHz)
- c. Theoretically, 108 channels, but limited by max. number of channels in one frame

100MBit LAN can comfortably support a data transfer rate of 1200 to 1400 kHz, so for large systems with multiple frames, Gigabit LAN may be required for both PC card and Ethernet switch

Data Transfer Rate via WLAN

Up to 600 kHz (16-bit data transfer) for IEEE 802.11g, 54 MBit connection, dependent on local transmission conditions

Multiframe Control

This must only be connected to other BNC Multiframe Control Sockets in Type 7536 or 7537

Aux

AUXILIARY I/O

Number of Input Channels: 12^a

Input Connector: 1 × High density 20-pole D-sub

Sampling Rate: 10 samples per second (no internal anti-aliasing filters)

Input Connections: Single-ended

Input Voltage Ranges: Six input ranges from 0.1V to 31.6V in 10 dB steps

Input Protection: 50V

Input Impedance: 1 MΩ || < 200 pF

Precision:

Range	Precision
31.6V	±0.5% of reading ±20mV offset
10V	±0.5% of reading ±7mV offset
3.16V	±0.5% of reading ±7mV offset
1V	±0.5% of reading ±4mV offset
316 mV	±0.5% of reading ±2mV offset
100 mV	±0.5% of reading ±2mV offset

COMPATIBILITY WITH EXISTING TYPE 7536 LAN MODULES

Type 7536 100MBit LAN modules, hardware version 12.0 and greater, are compatible and calibrated
 Type 7536, hardware version 11.02 and serial number 2352315 – 2352340 of version 12.0, are compatible but need recalibration
 Type 7536, hardware version 11.02, will not function properly without a simple hardware modification (less than 25 units affected). There is a potential for damage if these modules are used for Auxiliary Logging without the modification

RS-232 Interface

RS-232 OUTPUT

Fulfills EIA-562 (electrical) and EIA-574 (mechanical)

OUTPUT SUPPLY

5V, max. 50mA

- a. 16 input channels (12 currently supported in software) plus 2 output channels which allow simple on/off control

Ordering Information – PULSE Systems 3560-B, 3560-C, 3560-D, 3560-E

3560-B	3560-C	3560-D	3560-E
<p>Type 3560-B: Compact PULSE</p> <p>Also includes the following accessories:</p> <ul style="list-style-type: none"> ZG-0429: Mains Supply/Battery Charger AN-xxxx: Mains Cable for ZG-0429 (xxxx: country dependent) AO-0546: Power Supply Cable for in-car use 	<p>Consists of:</p> <p>Type 2827: Portable Data Acquisition Unit</p> <p>Also includes the following accessories:</p> <ul style="list-style-type: none"> ZG-0429: Mains Supply/Battery Charger AN-xxxx: Mains Cable for ZG-0429 (xxxx: country dependent) AO-0546: Power Supply Cable for in-car use DD-0552: Protection Cover DH-0541: Shoulder Strap 	<p>Consists of:</p> <p>KK-0050: Enclosure Incl. Fan Unit</p> <p>Type 2826: Power Supply</p> <p>Also includes the following accessories:</p> <ul style="list-style-type: none"> ZG-0430: Mains Supply AN-xxxx: Mains Cable for ZG-0430 (xxxx: country dependent) AQ-0647: DC Supply Cable (Battery to Type 2826) DH-0541: Shoulder Strap 	<p>Consists of:</p> <p>WU-0516: 19" Rack Mounting Kit</p> <p>Type 2826: Power Supply</p> <p>Also includes the following accessories:</p> <ul style="list-style-type: none"> ZG-0434: Mains Supply AN-xxxx: Mains Cable for ZG-0434 (xxxx: country dependent) <p>Requires:</p> <ul style="list-style-type: none"> UW-1037: 19" Fan Unit (Height: 1 standard rack-mounting unit)
<p>System Options</p> <p>Any PULSE software – see the System Data for PULSE software (BU0229)</p>			
<p>5-channel PULSE Data Acquisition Units</p> <p>Standard</p> <p>Type 3560-B-010: LEMO</p> <p>Type 3560-B-020: BNC</p> <p>Type 3560-B-030: LEMO, Generator</p> <p>Type 3560-B-040: BNC, Generator</p> <p>Dyn-X</p> <p>Type 3560-B-110: LEMO</p> <p>Type 3560-B-120: BNC</p> <p>Type 3560-B-130: LEMO, Generator</p> <p>Type 3560-B-140: BNC, Generator</p>	<p>One Controller Module from:</p> <p>Standard</p> <ul style="list-style-type: none"> Type 7536: Controller Module Type 7537: 5/1-ch. Input/Output Controller Module (LEMO) Type 7537-A: 5/1-ch. Input/Output Controller Module (BNC) Type 7538: 5/1-ch. Input/Output Controller Module with Generator (LEMO) Type 7538-A: 5/1-ch. Input/Output Controller Module with Generator (BNC) <p>Dyn-X</p> <ul style="list-style-type: none"> Type 7538: 5/1-ch. Input/Output Controller Module (LEMO) Type 7538-A: 5/1-ch. Input/Output Controller Module (BNC) Type 7540: 5/1-ch. Input/Output Controller Module with Generator (LEMO) Type 7540-A: 5/1-ch. Input/Output Controller Module with Generator (BNC) 	<p>Up to Five Input/Output Modules from:</p> <p>Standard</p> <ul style="list-style-type: none"> Type 3038: 12-ch. Input Module Type 3038-B: 12-ch. Input Module Type 3039: 6-ch. Input Module Type 3039-B: 6-ch. Input Module Type 3109: 4/2-ch. Input/Output Module Type 3110: 2/1-ch. Input/Output Module UA-1365: Blank Module <p>Dyn-X</p> <ul style="list-style-type: none"> Type 3035: 6-ch. Charge & COLD Input Module Type 3041: 6-ch. Input Module Type 3041-B: 6-ch. Input Module Type 3040: 12-ch. Input Module Type 3040-B: 12-ch. Input Module UA-1365: Blank Module 	<p>Up to Eight Input/Output Modules from:</p> <p>Standard</p> <ul style="list-style-type: none"> Type 3038: 12-ch. Input Module Type 3038-B: 12-ch. Input Module Type 3039: 6-ch. Input Module Type 3039-B: 6-ch. Input Module Type 3109: 4/2-ch. Input/Output Module Type 3110: 2/1-ch. Input/Output Module UA-1365: Blank Module <p>Dyn-X</p> <ul style="list-style-type: none"> Type 3035: 6-ch. Charge & COLD Input Module Type 3041: 6-ch. Input Module Type 3041-B: 6-ch. Input Module Type 3040: 12-ch. Input Module Type 3040-B: 12-ch. Input Module UA-1365: Blank Module
<p>Optional Accessories</p>			
<ul style="list-style-type: none"> UA-1689: Handle for Type 3560-B UA-1590: Battery Charger and Holder (2x) QB-0048: Battery, NiMH DR35 AQ-0642: Power Cable between UL-0196 and Type 3560-B AQ-0643: Power Cable between UL-0190 and Type 3560-B <p>Type 3560-B-010, -020, -110, -130</p> <ul style="list-style-type: none"> AO-0090: 7-pin LEMO to BNC male (1.2m) for floating ground AO-0091: 7-pin LEMO to BNC female (1.2m) for floating ground JJ-0081: BNC Adaptor, female to female 	<ul style="list-style-type: none"> UA-1590: Battery Charger and Holder (2x) QB-0048: Battery, NiMH DR35 UA-1556: Notebook Mounting Kit UA-1572: 19" Rack Mounting Kit for Type 2827 AQ-0642: Power Cable between UL-0196 and Type 3560-C AQ-0643: Power Cable between UL-0190 and Type 3560-C KE-0439: Gullcase for Type 3560-C and PC 	<ul style="list-style-type: none"> AO-0642: Power Cable between UL-0196 and Type 3560-D AQ-0643: Power Cable between UL-0190 and Type 3560-D AQ-0656: Power Supply Cable with car service plug for 3560-D UA-1556: Notebook Mounting Kit 	<ul style="list-style-type: none"> KK-0155: 19" Rack Enclosure EA-0540: Air Guide UW-1037: 19" Fan Unit (Height: 1 standard rack-mounting unit)
<p>Services</p>			
<ul style="list-style-type: none"> 3560-B-CAF: Portable PULSE Accredited Calibration 3560-B-CAI: Portable PULSE Accredited Initial Calibration 3560-B-CTF: Conformance test of 3560-B with certificate and measured values 3560-B-EW1: Extended Warranty for 3560-B, one year extension 	<ul style="list-style-type: none"> 3560-C-CAF: Portable PULSE Accredited Calibration 3560-C-CAI: Portable PULSE Accredited Initial Calibration 3560-C-CTF: Conformance test of 3560-C with certificate and measured values 3560-C-EW1: Extended Warranty for 3560-C, one year extension 	<ul style="list-style-type: none"> 3560-D-CAF: Portable PULSE Accredited Calibration 3560-D-CAI: Portable PULSE Accredited Initial Calibration 3560-D-CTF: Conformance test of 3560-D with certificate and measured values 3560-D-EW1: Extended Warranty for 3560-D, one year extension 	<ul style="list-style-type: none"> 3560-E-CAF: Portable PULSE Accredited Calibration 3560-E-CAI: Portable PULSE Accredited Initial Calibration 3560-E-CTF: Conformance test of 3560-E with certificate and measured values 3560-E-EW1: Extended warranty for 3560-E, one year extension
<ul style="list-style-type: none"> 3560-011: Installation and Configuration (at Brüel & Kjær) 3560-HL1: 3560 Software and Hardware Support, One year of Helpline Support <p>* Accredited calibration (CAF), Accredited Initial Calibration (CAI) and Conformance Test (CTF) are also available for individual input/output modules by appending the letters to the type number, for example, 3109-CTF. For further information, please contact your local Brüel & Kjær representative</p>			

ACCESSORIES FOR MODULES

7638, 7637, 7638, 7639, 7640, 7637-A, 7638-A, 7639-A, 7640-A	3036, 3038, 3039, 3040, 3041, 3038-B*, 3039-B*, 3040-B*, 3041-B*, 3109, 3110						
ACCESSORIES INCLUDED							
<ul style="list-style-type: none"> • AO-144B: LAN Interface Cable crossover with RJ45 (1 m) • AO-145 1: RG-232 Cable for PULSE Controller Module • JJ-0152: BNC T-connector • UA-1617: LAN Cable Relief 	Type 3036: <ul style="list-style-type: none"> • 6 × JP-0162: TNC to 10-32 UNF Plug 						
OPTIONAL ACCESSORIES							
Types 7637, 7638, 7639, 7640 only <ul style="list-style-type: none"> • AO-0090: 7-pin LEMO to BNC (1.2 m) for Floating GND • AO-0091: 7-pin LEMO to BNC female (1.2 m) for floating gnd. • JJ-0081: BNC Adaptor, female to female For Auxiliary Parameter Logging <ul style="list-style-type: none"> • AO-1472: 37-pin D-sub to Aux I/O • AO-0594: 16 BNC Female to 37-pin D-sub • AO-0595: 37-pin D-sub converter cable for DATA DI-75B 	<ul style="list-style-type: none"> • Type 2647: Charge to OCLD Amplifier • JP-0145: BNC to 10-32 UNF Plug Adaptor • AO-0526: 4-pin Microtech to 3 × BNC Cable • 3 × BNC to multiplug for triaxial transducers • WB-1497: 20 dB Attenuator Types 3038-B, 3039-B, 3040-B, 3041-B only <ul style="list-style-type: none"> • AO-0535: 37-pole D-sub to 6 Microdot for accelerometers • AO-0536: 37-pole D-sub to 2 plugs for triaxial accelerometers • AO-0602: 37-pole D-sub to 6 × 7-pin LEMO (allows CIC and polarization voltage with Type 3038-B) • AO-0603: 37-pole D-sub to 6 × BNC Socket • WB-1482: 0/20 dB Attenuator Adaptor for D-Sub connector 						
<p>*Note: The following adaptors should not be used with polarization voltage enabled on the B-versions:</p> <table> <tr> <td>AO-0432: 37-pole D-sub to 6 × 3-pin LEMO</td> <td>AO-0562: 37-pole D-sub to STGF/Beamforming Array</td> </tr> <tr> <td>WL-1261: 37-pole D-sub to 6 × 7-pin LEMO</td> <td>WL-1271: 37-pole D-sub to 6 × BNC Socket</td> </tr> <tr> <td>WL-1291: 37-pole D-sub to 6 × BNC Plug</td> <td></td> </tr> </table>		AO-0432: 37-pole D-sub to 6 × 3-pin LEMO	AO-0562: 37-pole D-sub to STGF/Beamforming Array	WL-1261: 37-pole D-sub to 6 × 7-pin LEMO	WL-1271: 37-pole D-sub to 6 × BNC Socket	WL-1291: 37-pole D-sub to 6 × BNC Plug	
AO-0432: 37-pole D-sub to 6 × 3-pin LEMO	AO-0562: 37-pole D-sub to STGF/Beamforming Array						
WL-1261: 37-pole D-sub to 6 × 7-pin LEMO	WL-1271: 37-pole D-sub to 6 × BNC Socket						
WL-1291: 37-pole D-sub to 6 × BNC Plug							

SOFTWARE

Please refer to the System Data for PULSE software (BU 0229)

NOTEBOOK PCs*

7200-D-xxx Dell® Standard Notebook
 7201-D-xxx Dell® High-end Notebook
 7204-A-xx Crete ROCKY II Plus EX Ruggedized Notebook
 xx specifies country: DE, DK, ES, FR, GB, IT, RU, SE, US
 y specifies inclusion of Microsoft® Office Pro: 1 – not included; 2 – included

TOWER PCs*

7202-D-xxx Dell® Optiplex GX280 Standard Desktop
 7203-B-xxx Dell® Precision 690 High-end Tower PC
 xx specifies country: DE, DK, ES, FR, GB, IT, RU, SE, US
 y specifies inclusion of Microsoft® Office Pro: 1 – not included; 2 – included

a. PCs are constantly updated. Contact your local dealer for latest information.

PC ACCESSORIES

UL-0200 Vehicle Adaptor (12 – 32 V) for Rocky II+
 UL-0213 Dell® 17" Flat Panel Display TFT
 UL-0217 Dell® 19" Flat Panel Display TFT

PC HARDWARE

AO-1450 LAN Interface Cable with RJ45
 UL-0167 Netgear® 8-port, 100 MBIT Switch (220 V only)
 UL-0190 Netgear® 5-port, 100 MBIT Switch (220 V only)
 or
 UL-0229 Netgear® 5-port, 1 GBIT Switch (220 V only)

A wide range of Brüel & Kjær Accelerometers, Microphones, Preamplifiers and Sound Intensity Probes is available for use with a Type 3560 system. The system supports IEEE 1451.4 capable transducers with standardised TEDS

See also the PULSE Catalogue (BF 0205) for information on standard system configurations

TRADEMARKS

Microsoft and Windows are registered trademarks and Windows Vista™ is either a registered trademark or trademark of Microsoft Corporation in the United States and/or other countries - ICP is a registered trademark of PCB Group - MATLAB is a registered trademark of The MathWorks, Inc. - SONY is a registered trademark of Sony Corporation - Intel, Intel InBusiness and Pentium are registered trademarks of Intel Corporation or its subsidiaries in the United States and/or other countries - HP and Omnibook are registered trademarks of Hewlett-Packard Company - Dell and Latitude are registered trademarks of Dell Computer Corporation - Neutrik is a registered trademark of the Neutrik Group worldwide - Netgear is a registered trademark of NetGear, Inc.

Brüel & Kjær reserves the right to change specifications and accessories without notice

HEADQUARTERS: DK-2850 Naerum - Denmark - Telephone: +45 4680 0500
 Fax: +45 4680 1405 - www.bksv.com - info@bksv.com

Australia (+61) 20889 8888 - Austria (+43) 1 865 74 00 - Brazil (+55) 11 5168 8161
 Canada (+1) 514 695 8225 - China (+86) 10 680 29808 - Czech Republic (+420) 2 6702 1100
 Finland (+358) 9 755 950 - France (+33) 1 69 90 71 00 - Germany (+49) 421 17 87 0
 Hong Kong (+852) 2548 7466 - Hungary (+36) 1 215 83 05 - Ireland (+353) 1 807 4063
 Italy (+39) 02 57 96 061 - Japan (+81) 3 5715 5512 - Republic of Korea (+82) 2 3473 0605
 Netherlands (+31) 318 55 9290 - Norway (+47) 66 77 11 55 - Poland (+48) 22 816 75 96
 Portugal (+351) 21 4169 040 - Singapore (+65) 377 4512 - Slovak Republic (+421) 25 443 0701
 Spain (+34) 91 850 0820 - Sweden (+46) 33 225 622 - Switzerland (+41) 44 88 07 035
 Taiwan (+886) 2 2502 7255 - United Kingdom (+44) 14 38 739 000 - USA (+1) 800 332 2040

Local representatives and service organisations worldwide

Brüel & Kjær 





PRODUCT DATA

½" Prepolarized Free-field Microphone — Type 4189

Type 4189 is designed for high-precision, free-field measurements where a microphone with high sensitivity is required. Being prepolarized, Type 4189 can be used with both DeltaTron® and classical preamplifiers.



080143

USES

- Precision sound measurement
- Premium class sound level meters
- Equipment complying with IEC 61672 class 1

FEATURES

- Sensitivity: 50 mV/Pa
- Frequency: 6.3 Hz – 20 kHz
- Dynamic Range: 14.6 – 146 dB
- Temperature: –30 to +150°C (–22 to +302°F)
- Polarization: Prepolarized

Use of Free-field Microphones

At higher frequencies, reflections and diffractions causes a pressure increase in front of the diaphragm of a microphone. If not corrected, for this would result in an increased output voltage. A free-field optimisation means that the frequency response of the microphone has been designed in such a way that the free-field response at 0 degrees incidence is flat. This microphone is optimised for use with the protection grid in place.

Free-field microphones are commonly used for sound measurement in an anechoic chamber or far away from reflecting buildings, etc. Another area for free-field microphones is for general electroacoustic measurements purposes like loudspeaker and microphone measurements.

Type 4189 is suited for use in class 1 Sound Level Meters and for all high-precision acoustic measurements where a robust and stable free-field microphone with an upper frequency of 20kHz is required.

Manufacturing and Stability

A press-fitted, stainless-steel diaphragm ensures superior long-term stability and mechanical robustness – Type 4189 will withstand the 1 m drop test of IEC 60068–2–32.

All Brüel & Kjær Measuring Microphones are assembled in a clean room. This ensures that the microphones maintain their inherent low noise floor and high stability,

even when used in environments with a combination of high humidity and high temperature.

Polarization Voltage

Being prepolarized, Type 4189 is especially well suited for battery operated equipment and operation in environments with high humidity.

TEDS Microphones

Type 4189 is available in TEDS combinations with either classical or DeltaTron type preamplifier. The TEDS microphone is considered one unit and has been sealed in a clean environment. The TEDS is programmed with the loaded sensitivity of the actual cartridge and the data is therefore readily available. The default TEDS template is to IEEE P1451.4 but TEDS to IEEE 1451.4 is available on request.

Individual Calibration Data

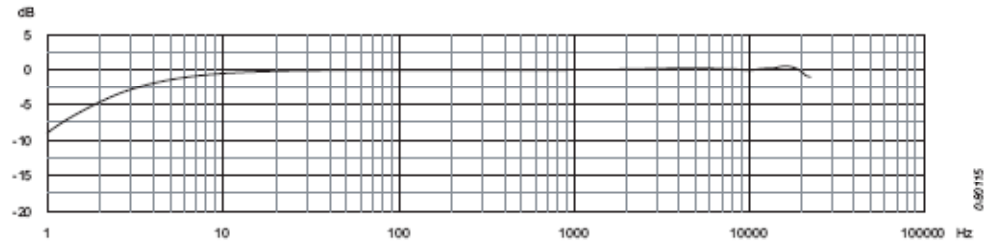
Each Type 4189 comes with an individual calibration chart including information about the open-circuit sensitivity, the frequency response in a free field as well as the electrostatic actuator response.

An enclosed mini-CD contains the individual calibration data at 1/12-octave frequencies plus a wealth of technical information, such as the influence of different accessories, response in different sound fields and much more. Using the CD data and the REq-X feature of PULSE™, a real-

Brüel & Kjær 

time correction for different measurement situations, can increase measurement accuracy.

Fig. 1 Typical free-field response of the microphone with protection grid. The low-frequency response is valid when the vent is exposed to the sound field



Specifications – 1/2" Free-field Microphone Type 4189 (valid from serial number 2495387)

IEC 61094-4 Type Designation: W52F
 Polarization Voltage: 0 V (pre-polarized)
 Open-circuit Sensitivity (250 Hz)^a: 50 mV/Pa, -28 dB ± 1.5 dB re 1 V/Pa
 0° Incidence Free-field Response^a: 10 Hz to 8 kHz: ± 1 dB
 6.3 Hz to 20 kHz ± 2 dB
 Lower Limiting Frequency (-3 dB)^a: 2 to 4 Hz
 Pressure Equalization Vent: Rear vented
 Diaphragm Resonance Frequency: 14 kHz (90° phase shift)
 Cartridge Capacitance^b: 14 pF at 250 Hz
 Equivalent Air Volume: 46 mm³ (250 Hz)
 Pistonphone Correction (Type 4228 with DP-0776) 0.00 dB
 Cartridge Thermal Noise: 14.6 dB(A), 15.3 dB(Lin)
 Upper Limit of Dynamic Range (3% Distortion): >146 dB SPL^b

Max. Sound Pressure Level: 158 dB (peak)

ENVIRONMENTAL

Operating Temperature Range: -30 to +150°C (-22 to +302°F)
 Storage Temperature: In Microphone Box: -30 to +70°C (-22 to +158°F)
 With Mini-CD: 5 to 50°C (41 to 122°F)
 Temperature Coefficient (250 Hz): -0.006 dB/K (-10 to +50°C, 14 to 122°F)
 Pressure Coefficient: -0.01 dB/kPa
 Operating Humidity Range: 0 to 100% RH (without condensation)
 Influence of Humidity: <0.1 dB in the absence of condensation
 Vibration Sensitivity (<1000 Hz): 62.5 dB equivalent SPL for 1m/s² axial vibration

Magnetic Field Sensitivity: 6 dB SPL for 80 A/m, 50 Hz field
 Estimated Long-term Stability: >1000 years/dB in dry air at 20°C (68°F)
 >2 hours/dB in dry air at 150°C (302°F)
 >40 years/dB in air at 20°C (68°F), 90% RH)
 >1 year/dB in air at 50°C (122°F), 90% RH)

DIMENSIONS

Diameter with Grid: 13.2 mm (0.52")
 Diameter without Grid: 12.7 mm (0.50")
 Height with Grid: 17.6 mm (0.69")
 Height without Grid: 16.3 mm (0.64")

Thread for Pre-amplifier Mounting: 11.7 mm-60 UNS

Note: All values are typical at 23°C (73.4°F), 101.3 kPa and 50% RH unless otherwise specified

a. Individually calibrated

b. 137 dB (peak) with DeltaTron preamplifier and 24 V supply and 140 dB (peak) with ±15 V supply

CE Compliance with EMC Directive

Ordering Information

Type 4189 1/2" Pre-polarized Free-field Microphone
 Includes the following accessories:
 • BC-0224: Calibration Chart^c
 • BC-5002: Microphone Mini-CD^c

TEDS COMBINATIONS

4189-A-021 1/2" Free-field Microphone with Preamplifier Type 2671
 4189-A-031 1/2" Free-field Microphone with Preamplifier Type 2699
 4189-B-001 1/2" Free-field Microphone with Preamplifier Type 2669-B

4189-C-001 1/2" Free-field Microphone with Preamplifier Type 2669-C
 4189-L-001 1/2" Free-field Microphone with Preamplifier Type 2669-L
 4189-W-003 1/2" Free-field Microphone with Preamplifier Type 2671-W-001

OPTIONAL ACCESSORIES

Type 2669 1/2" Microphone Preamplifier
 Type 2671 1/2" DeltaTron Preamplifier
 2671-W-001 1/2" DeltaTron Preamplifier (version with LLF < 1.2 Hz)
 Type 2699 1/2" DeltaTron Preamplifier, A-weighted
 Type 4231 Sound Calibrator
 Type 4228 Pistonphone

Type 4226 Multifunction Acoustic Calibrator
 DP-0776 Calibration Adaptor for 1/2" Microphones
 UA-0033 Electrostatic Actuator
 UA-1260 1/2" Angle Adaptor (approx. 80°)
 UA-0386 Nose Cone for 1/2" Microphone
 UA-0237 Windscreen for 1/2" microphone, 80 mm diameter
 UA-0469 Windscreen for 1/2" microphone, 65 mm diameter
 BA-5105 The Microphone Handbook

CALIBRATION SERVICES

4189-CAI Accredited Initial Calibration
 4189-CAF Accredited Calibration
 4189-CFF Factory Standard Calibration

Brüel & Kjær reserves the right to change specifications and accessories without notice

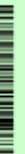
HEADQUARTERS: DK-2850 Naerum - Denmark - Telephone: +45 4580 0500
 Fax: +45 4580 5495 - www.bksv.com - info@bksv.com

Australia (+61) 29880 8888 - Austria (+43) 1 865 7400 - Brazil (+55) 11 5188 8161
 Canada (+1) 514 695 8225 - China (+86) 10 680 29005 - Czech Republic (+420) 2 6702 1100
 Finland (+358) 9 755 950 - France (+33) 1 69 90 71 00 - Germany (+49) 43 1 17 87 0
 Hong Kong (+852) 2548 7486 - Hungary (+36) 1 215 83 05 - Ireland (+353) 1 807 4063
 Italy (+39) 0257 66061 - Japan (+81) 3 6715 1512 - Republic of Korea (+82) 2 3473 0605
 Netherlands (+31) 316 55 9090 - Norway (+47) 66 77 11 55 - Poland (+48) 22 816 75 96
 Portugal (+351) 21 4169 040 - Singapore (+65) 6377 4512 - Slovak Republic (+421) 25 443 0701
 Spain (+34) 91 859 0620 - Sweden (+46) 33 225 522 - Switzerland (+41) 44 8807 036
 Taiwan (+886) 2 2502 7255 - United Kingdom (+44) 14 38 759 600 - USA (+1) 600 352 2040

Local representatives and service organisations worldwide

Brüel & Kjær

BPZ210-11 2008-06



PRODUCT DATA

DeltaTron[®] Microphone Preamplifier — Type 2671

DeltaTron[®] Microphone Preamplifier Type 2671 enables you to make acoustical measurements with a DeltaTron[®] input module. You can connect 1/2" prepolarized microphones to the preamplifier. The preamplifier's low output impedance allows problem-free use of long extension cables. The robust, compact design means that you can use Type 2671 over a wide range of environmental conditions.

USES

- Low price, multichannel sound measurement setups with 1/2" Brüel & Kjær Pre-polarized Condenser Microphones
- Multichannel signal analysis measurements
- Multichannel sound power measurements
- Industrial machinery noise measurements

FEATURES

- ICP[®] compatible
- BNC connector for easy installation and use with inexpensive BNC cables
- Connects directly to DeltaTron[®] sockets and to Brüel & Kjær microphone sockets with adaptor
- Low output impedance so that long extension cables can be used
- Falcon Range[®] product
- Supports "Smart Transducer Interface" IEEE1451.4 containing TEDS (Transducer Electronic Data Sheet)



Introduction

Preamplifier Type 2671 is very compact and operates over a wide range of temperature, humidity and other environmental conditions. It has a very high input impedance, presenting virtually no load to the microphone. The low output impedance means that you can connect long cables between the preamplifier and measurement equipment.

The main application for the preamplifier is in vibration setups with DeltaTron[®] or ICP[®] input modules where it is also desired to make acoustical measurements. It presents a very price competitive solution compared to a system with both vibration and acoustical inputs.

Description

DeltaTron[®] is a generic name for accelerometers and signal conditioning products from Brüel & Kjær. It identifies products that operate on a constant-current power supply and give output signals in the form of voltage modulation on the power supply line. One of the advantages of this system is that it allows you to use inexpensive BNC coaxial cables.

The preamplifier converts the DeltaTron[®] or ICP[®] constant-current line drive (CCLD) supply, which must be between 2 and 20mA (nominal 4mA), into a constant 12V DC level. The output signal from the microphone swings around this DC level. Since no polarization voltage is available, only prepolarized condenser microphones can be

used. The input impedance of Type 2671 is lowered to 1.5GΩ with the purpose of making a high-pass filter at 20Hz. This is done in order to compensate for filters which are often missing in the input modules (for example, A-weighting). Type 2671 is also available in a version without the high-pass filter, which has a flat response down to 2Hz, and in a version with built-in A-weighting, Type 2699.

TEDS

Support of TEDS means that the preamplifier can be used with the newly developed Smart Transducer interface according to IEEE1451.4. The ability to store and recall TEDS data drastically reduces test setup time and allows cost savings in most measurement situations.

Electromagnetic Compatibility (EMC)


Susceptibility of the preamplifier to radio-frequency electromagnetic radiation is low. The preamplifier complies with the requirements of EMC-directive 89/336/EEC. The product is in conformity with the following standards:

EN 50081-1 (1992): EMC - Generic emission standard. Residential, commercial and light industry.

EN 50082-1 (1992): EMC - Generic immunity standard. Residential, commercial and light industry.

The product has been tested and found to comply with:

2671

Brüel & Kjær 

prEN 50082-2 (Aug. 1994): EMC – Generic Immunity standard for industrial environments (final draft).

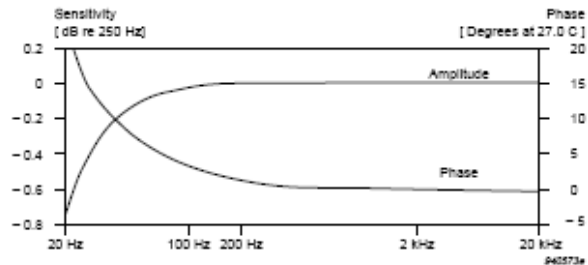
EN 50081-1 covers, e.g.:

- Radiated emission, 0.03 to 1 GHz
- Conducted emission, 0.15 to 30 MHz

prEN 50082-2 covers, e.g., the effects of:

- RF fields from 80 to 1000MHz at a field strength of 3 and 10 V/m with an amplitude modulation of 80%
- Electrostatic discharge, 4 and 8 kV
- Transient bursts at 1 kV
- Magnetic fields with a strength of 30 A/m at 50 Hz
- Pulse modulated radio frequency fields, 900 MHz at a field strength of 3 V/m and a duty cycle of 50%

Fig. 1
Typical frequency and phase response curves for Preamplifier Type 2671



Specifications – DeltaTron Microphone Preamplifier Type 2671

Frequency Response (re 250 Hz)
 200 Hz to 20 kHz, +0.2 dB, -0.2 dB
 20 Hz to 50 kHz, +0.2 dB, -2 dB
 Lower -3 dB limit at <12 Hz
 Upper -0.5 dB limit at >50 kHz
Attenuation: -0.3 dB (typical)
Gain Matching: 200 Hz to 10 kHz, 0.1 dB
Phase Linearity:
 1 kHz to 10 kHz, $\pm 1^\circ$
 100 Hz to 20 kHz, $< -3^\circ$, $+10^\circ$
Phase Matching:
 5° at 50 Hz
 2° at 100 Hz
Input Impedance: 1.5 GΩ || <0.4 pF
Output Impedance: <50 Ω
Max. Output Current:
 At 4 mA supply, 3 mA (peak)
 At 20 mA supply, 19 mA (peak)
Max. Output Voltage:
 7 V peak for f <20 kHz
 Corresponding to:
 141 dB SPL for microphone sensitivity of 30 mV/Pa
 138 dB SPL for microphone sensitivity of 50 mV/Pa
Max. DC Output Level: 12 V \pm 2 V over the specified operating temperature range
Distortion (THD):
 <-70 dB at 1.0 V_{out}, 1 kHz
 <-60 dB at 1.0 V_{out}, 10 kHz
Output Slew Rate: 2 V/μs (typical)
Noise:
 <4 μV A-weighted
 <15 μV Lin., 22.4 Hz to 22.4 kHz
Start-up Time: Signal within 0.1 dB within <10 s
Power Requirements: DeltaTron[®] supply, 2 to 20 mA, Nominal 4 mA
Connector Type: BNC socket
Dimensions: ∅12.7 mm × 85 mm (∅1/2" × 3.3") (including connector)
Thread for Preamplifier Mounting: 11.7 mm – 60 UNS

TRADEMARKS
 ICP is a registered trademark of PCB Piezotronics

Temperature Range:
 Operating: -20°C to +60°C (-4° to +140°F)
 Storage: -25°C to +70°C (-13° to +158°F)
 Humidity: 0 to 90% RH, non-condensing at 40°C (104°F)
 Shock: Max. 100g
 Influence of 80 A/m, 50 Hz Magnetic Field: Max. 4 μV

Note: the 1 mm hole on the side of Type 2671 is for acoustic ventilation and must not be blocked

The data above are valid for 4 mA supply, cable length <40 m and microphone capacitance = 12 pF, unless otherwise specified

Compliance with EMC Directive

Ordering Information

BNC to BNC coaxial cables
 AO 0429 1.2 m (3.9 ft.)
 AO 0142 3.0 m (9.8 ft.)
 AO 0430 10 m (32.8 ft.)

BNC to BNC double screened cables
 AO 0429 1.2 m (3.9 ft.)
 AO 0426 3.0 m (9.8 ft.)
 AO 00427 10 m (32.8 ft.)

Other cable lengths on request
 UA 00587 Portable Tripod, Includes Mounting Adaptor UA 0588 and two Extension Rods
 UA 0801 Light-weight Tripod
 UA 0588 Mounting Adaptor

Power Supply Adaptors
 Supplies constant current from microphone sockets
 ZS 00328 Brüel & Kjær 7-pin to BNC
 WB 1421 LEMO to BNC

Brüel & Kjær reserves the right to change specifications and accessories without notice

HEADQUARTERS: DK-2850 Narum · Denmark · Telephone: +45 4580 0500 · Fax: +45 4580 1405 · www.bksv.com · info@bksv.com

Australia (+61) 2 9880 8888 · Austria (+43) 1 865 74 00 · Brazil (+55) 11 5188-8186 · Canada (+1) 514 895-8225
 China (+86) 10 680 29096 · Czech Republic (+420) 2 6702 1100 · Finland (+358) 0-795 950 · France (+33) 1 69 90 71 00
 Germany (+49) 421 17 87 0 · Hong Kong (+852) 2548 7486 · Hungary (+36) 1 215 83 05 · Ireland (+353) 1 807 4083
 Italy (+39) 0257 68081 · Japan (+81) 3 3779 8671 · Republic of Korea (+82) 2 3475 0505 · Netherlands (+31) 318 55 9290
 Norway (+47) 66 77 11 55 · Poland (+48) 22 816 75 56 · Portugal (+351) 21 47 11 4 53 · Singapore (+65) 377 4512
 Slovak Republic (+421) 25 443 0701 · Spain (+34) 91 650 9620 · Sweden (+46) 8 445 8600 · Switzerland (+41) 1 880 70 35
 Taiwan (+886) 22 713 9303 · United Kingdom (+44) 14 38 735 000 · USA (+1) 800 332 2040
 Local representatives and service organisations worldwide

Brüel & Kjær

Rosendahl's Bogni-Kkari

03/03

BP 1446 - 14

PRODUCT DATA

Sound Sources for Building Acoustics: OmniPower™ Sound Source — Type 4292, OmniSource™ Sound Source — Type 4295, Tapping Machine — Type 3207, and Power Amplifiers — Type 2734-A and 2734-B

For proper building acoustics measurements, a sound source which fulfills the relevant standards (for example, ISO 140) is required. Brüel & Kjær offers a complete range of sound sources for building acoustics measurements, including Tapping Machine Type 3207, single-speaker omnidirectional OmniSource™ Type 4295 and 12-speaker omnidirectional OmniPower™ Type 4292. Power Amplifier Type 2734 can drive both OmniPower and OmniSource. Optional carrying cases for the sound sources are available, as well as wireless control systems for use with Hand-held Analyzer Type 2250 and the dual channel Type 2270.



Uses and Features

Uses

- Architectural and building acoustics
- Measurement of:
 - Airborne sound insulation
 - Reverberation time
 - Impact sound level

Features

- Part of a complete building acoustics system featuring Brüel & Kjær's Hand-held Analyzer Type 2250 or 2270
- Two omnidirectional noise sources
- Tapping machine for impact sound level measurements
- Remote operation via cable or wireless remote control
- Satisfies national and international standards
- Robust
- Easily portable

Brüel & Kjær 

Introduction

Architectural and building acoustic measurements require a range of noise sources for airborne noise and impact noise transmission measurements.

For airborne noise transmission measurements, an omnidirectional sound source is needed. Brüel & Kjær offers two solutions: OmniPower Sound Source Type 4292 and OmniSource Sound Source Type 4295.

For impact sound measurements, Brüel & Kjær offers Tapping Machine Type 3207, a robust and portable device that fulfils national and international standards.

These sound sources form a part of a complete measurement system along with a driving amplifier (for example Type 2734-A or 2734-B), a sound level analyzer (for example, Type 2250 or 2270), and a PC with Building Acoustic analysis and reporting software.

Brüel & Kjær supplies all of these items and a range of carrying cases for storage and transportation.

Product Line:

- OmniPower Type 4292, 12-speaker high-power omnidirectional sound source
- OmniSource Type 4295, lightweight single-speaker omnidirectional sound source
- Tapping Machine Type 3207
- Power Amplifier Type 2734-A or 2734-B, amplifiers for driving sound sources
- Flight Case KE-0449 and Carrying Cases KE-0364 and KE-0392 for packing and transporting equipment
- Cables and Wireless Remote Control accessories
- Battery Kit UA-1477 for Type 3207

Omnidirectional Sound Sources

For most building acoustics measurements, the sound source must radiate sound evenly in all directions to give reproducible and reliable results; therefore, the relevant building acoustics measurements standards (ISO 140 and ISO 3382) require the use of an omnidirectional sound source.

OmniPower Sound Source Type 4292

Fig. 1
OmniPower Sound
Source Type 4292



OmniPower Omnidirectional Sound Source Type 4292 (see Fig. 1) uses a cluster of 12 loudspeakers in a dodecahedral configuration that radiates sound evenly with a spherical distribution. All 12 speakers are connected in a series-parallel network to ensure both in-phase operation and an impedance that matches the power amplifier. The entire assembly weighs less than 14 kg and is fitted with a convenient lifting handle that does not measurably interfere with the sound field.

Powered by Power Amplifier Type 2734-A or 2734-B, the Sound Source can deliver a maximum sound power of 122 dB re 1 pW (100–3150 Hz). The high power output of Type 4292 makes it ideal for sound insulation measurements.

Type 4292 satisfies the requirements of DIN 52210, ISO 140 and ISO 3382 standards (see Fig. 2 through Fig. 5). Its directional response for the horizontal plane is shown in Fig. 6.

Fig. 2
 Frequency response
 for $1/3$ -octave sound
 power levels for
 OmniPower Type 4292
 using Power Amplifier
 Type 2734 and its
 internal pink noise
 generator

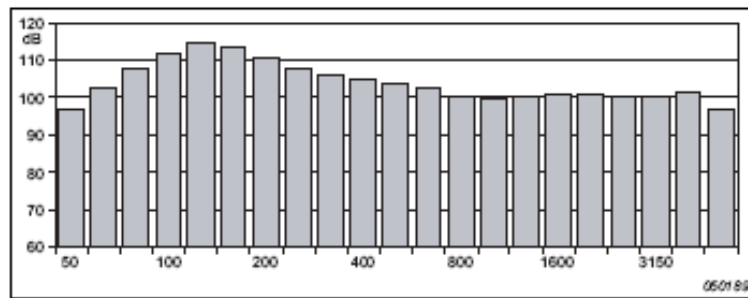


Fig. 3
 Frequency response
 for $1/3$ -octave sound
 power levels for
 OmniPower Type 4292
 using Power Amplifier
 Type 2734 and its
 internal pink noise
 generator

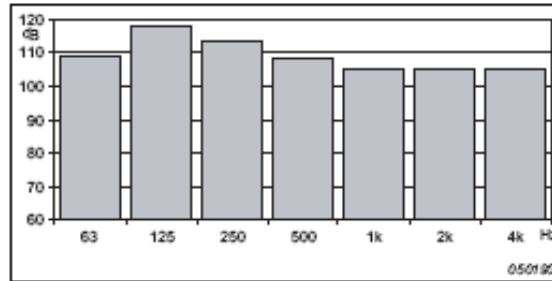


Fig. 4
 Directivity for
 OmniPower Type 4292
 according to ISO 140:
 maximum deviation
 from mean for 'gliding'
 30° arc. Upper and
 lower curves are the
 ISO 140 tolerances

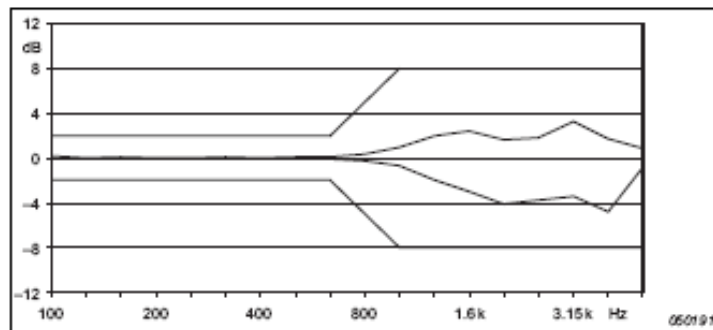


Fig. 5
 Directivity for
 OmniPower Type 4292
 according to ISO 3382:
 maximum deviation
 from mean for 'gliding'
 30° arc. Upper and
 lower curves are the
 ISO 3382 tolerances

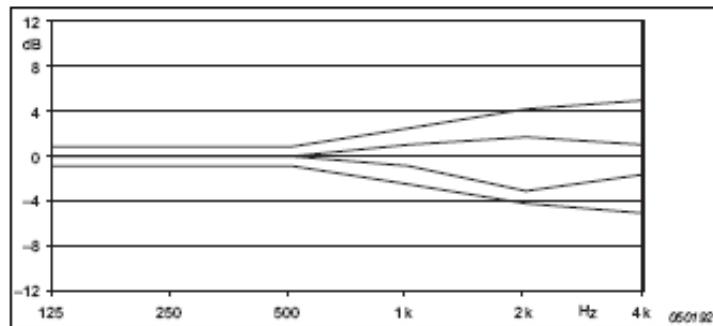


Fig. 6
 Type 4292's directional response for the horizontal plane, measured in 1/3-octaves. Below 1 kHz there is no significant deviation from omnidirectionality

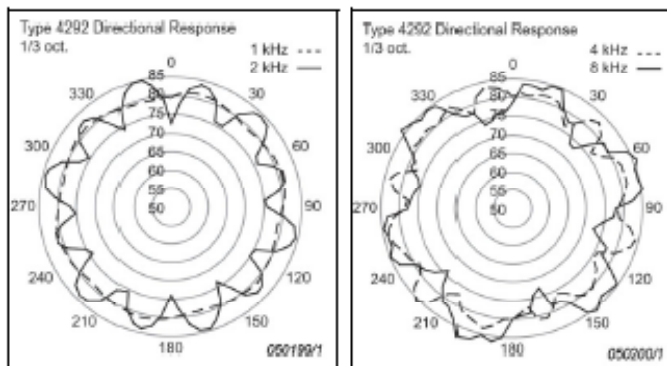
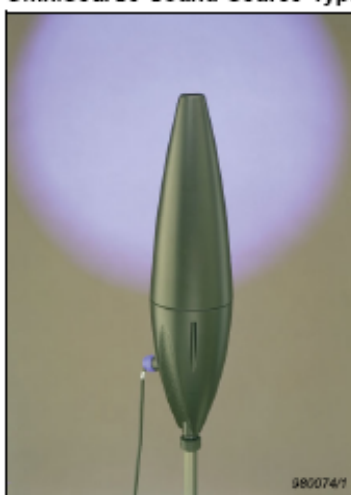


Fig. 7
 OmniSource Sound Source Type 4295



OmniSource Sound Source Type 4295

OmniSource Sound Source Type 4295 (see Fig. 7) presents a new solution to omnidirectional sound source design. Type 4295 is optimised for the measurement of room acoustic quantities such as reverberation time, sound distribution and spatial decay. The patented principle of the OmniSource Sound Source uses a single high-power loudspeaker, which directs the sound signal through a conical coupler to a circular orifice, and despite its compact dimensions and low weight, OmniSource Type 4295 is still capable of emitting a sound power of 105 dB re 1 pW (see Fig. 8 and Fig. 9).

The size of the orifice and the shape have been carefully engineered to radiate sound evenly in all directions. Thus, Type 4295 fulfils the national and international standards for omnidirectional sound sources (see Fig. 10 and Fig. 11). Type 4295's directional response for the plane through the axis is shown in Fig. 12.

Fig. 8
 Maximum 1/3-octave sound power levels for OmniSource Type 4295 using Power Amplifier Type 2734

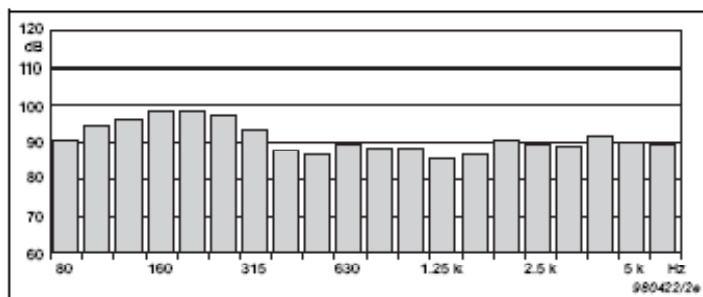


Fig. 9
 Maximum 1/4-octave sound power levels for OmniSource Type 4295 using Power Amplifier Type 2734

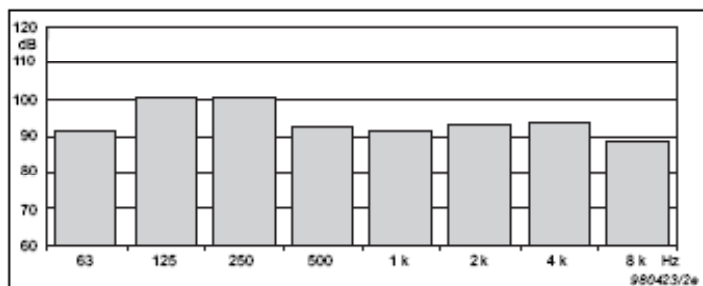


Fig. 10
Directivity for
OmniSource Type
4295 according to
ISO 140 maximum
deviation from mean
for 'gliding' 30° arc.
Upper and lower
curves are the
ISO tolerances

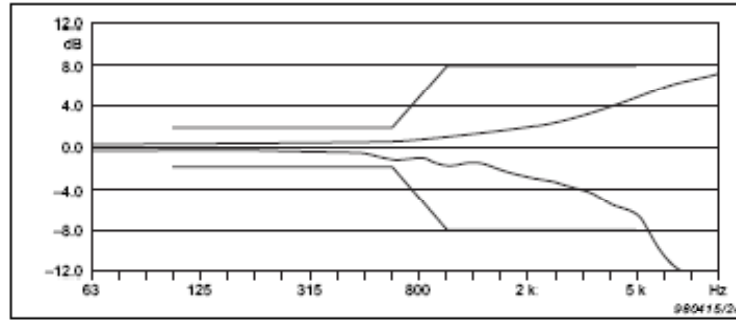


Fig. 11
Directivity for
OmniSource Type
4295 according to
ISO 3382: maximum
deviation from mean
for 'gliding' 30° arc.
Upper and lower
curves are the
ISO tolerances

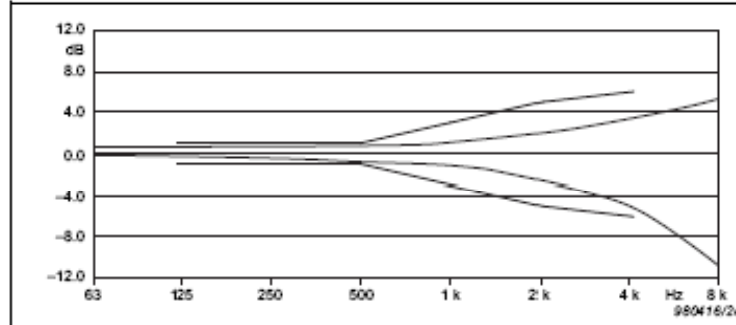
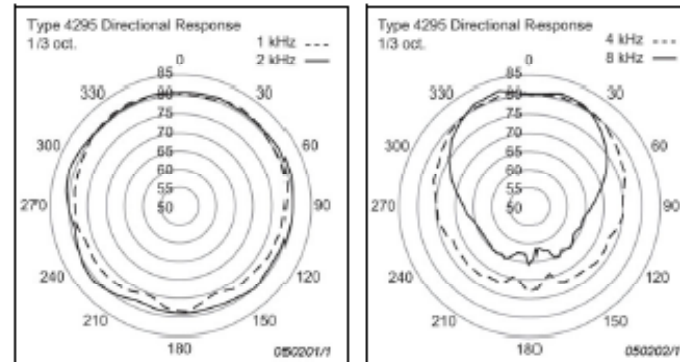


Fig. 12
Type 4295 directional
response for the plane
through the axis,
measured in 1/3-
octaves. Below 1 kHz
and in the plane
perpendicular to the
axis, there is no
significant deviation
from omnidirectionality



Impact Sound Source

Tapping Machine Type 3207

Tapping Machine Type 3207 is an impact sound generator (see Fig. 13). It can be used for impact sound measurements to national and international standards. The unit is available with an optional battery kit and a remote control.

Type 3207 uses five hammers each weighing 500 g and operating at 2 Hz dropping from a height of 40 mm, giving an operating frequency of 10 Hz. This fulfils national and international standards. The hammers are operated via tappets on a single shaft. The shaft is driven by a DC motor via a toothed belt and gearbox.

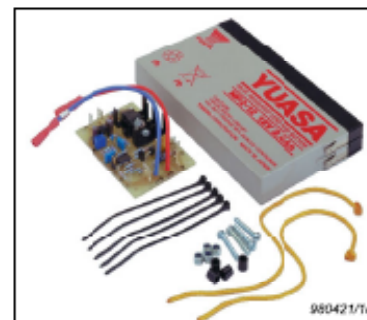
Fig. 13
Tapping Machine
Type 3207



The unit is based around a welded aluminium chassis. Both size and weight have been minimised for easy transportation. Three extendable legs support the unit during operation with rubber feet that are height adjustable with supplied gauges. This gives stable and level mounting during operation in accordance with the relevant standards.

The unit is powered via the supplied mains adaptor or the optional battery kit (see Fig.14), and can be remotely switched on and off via cable AQ-0633 or Wireless Remote Control Option UA-1476 (see Fig. 14).

Fig. 14
Accessories for
Tapping Machine.
Battery Kit
UA-1477 (right, and
Wireless Remote
Control UA-1476 (left),
which may also be
used to control the
internal generator of
Power Amplifier Type
2734



Power Amplifier Types 2734-A and 2734-B

Fig. 15
Top: Types 2734-A
and 2734-B are built
into robust flight cases
Middle: Type 2734-A
showing front mounted
controls and
connectors
Bottom: Type 2734-B
includes wireless audio
system UL-0256



Type 2734 is designed to power sound sources during building and room acoustic field measurements. Compact, light weight and built into a robust flight case, it is easy and safe to carry and transport to the measurement location. All connectors and controls are on the front for easy access.

It is simple to get the output level right and reproduce previous settings using the power amplifier's calibrator controls and level indicators. For flexibility, it has XLR, jack and BNC input sockets and BNC line and speaker output sockets. A sensitivity selector in 10 dB steps allows the amplifier to adapt to a variety of source signal levels and sound source ratings. Hand-held Analyzer Type 2250/2270's generator signal can be connected to the amplifier input, to provide the pink or white noise used in building acoustics.

In addition, Type 2734-B includes a wireless audio system (Fig. 23) to accommodate cable-free transmission of the building acoustics test signal, which could be white, pink or band-limited noise; or

swept sine. Wireless operation also makes source and receiver position changes more convenient. Type 2734-A can be upgraded to Type 2734-B by installing optional Wireless Audio System UL-0256.

Type 2734 has a built-in generator providing pink or white noise in the 50–5000 Hz range. It can be controlled from the front panel, or with the optional Wireless Remote Control UA-1476 (the same control used to control Tapping Machine Type 3207, Fig. 14). Transmitter UA-1476 has a pushkey for manual control, and a cable connection for automatic control from an analyzer.

Cases

Fig. 16
Carrying Case
KE-0392

Carrying Case KE-0392



OmniSource Sound Source Type 4295 has an optional, custom-designed carrying case with shoulder strap, KE-0392 (see Fig. 16), for easy storage and transportation. The case is foam lined and provides impact protection for the OmniSource inside.

Flight Case KE-0449

An optional transportation and storage case, KE-0449 is available for OmniPower Sound Source Type 4292 (see Fig. 17, left). It is custom designed, features a foam lining to protect Type 4292 and has two handles for ease of carriage.

Carrying Case KE-0364

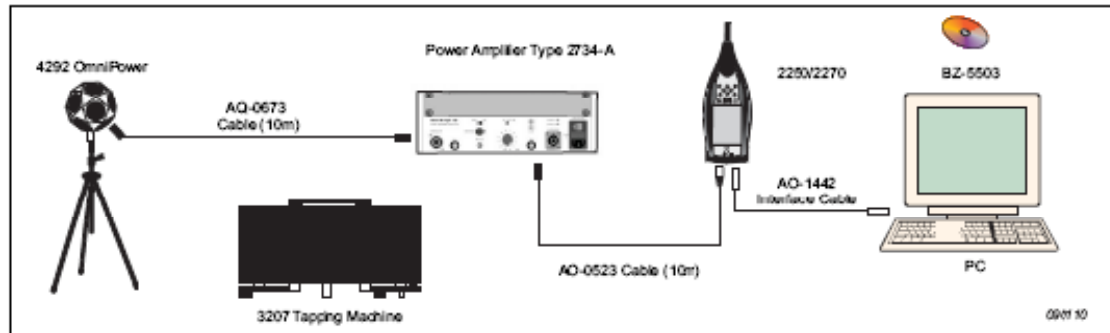
For the OmniPower tripod, Carrying Case KE-0364 (see Fig. 17, right) is equipped with both a shoulder strap and handles.

Fig. 17
Flight Case
KE-0449 (left)
and Carrying Case
KE-0364 (right)



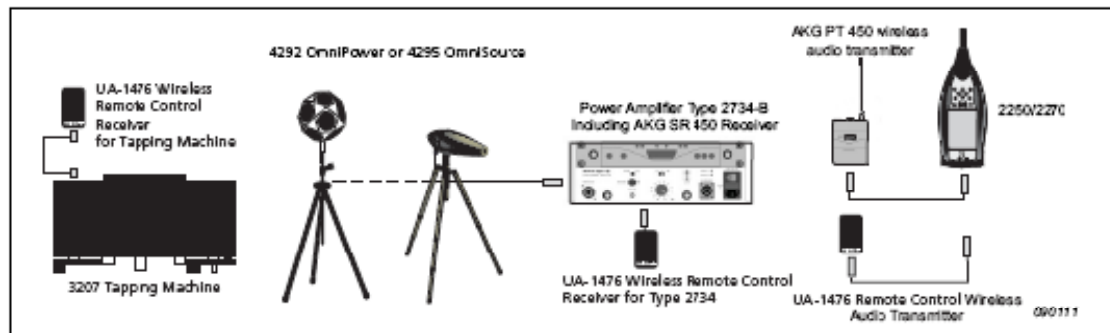
Complete Systems

Fig. 18 Complete system



The sound sources mentioned above belong to a range of complete measurement systems from Brüel & Kjær, including power amplifiers, sound-level analyzers, and PC-software for analyzing and documenting results.

Fig. 19 Sound sources with wireless remote control options



Hand-held Analyzer Types 2250 and 2270

Fig. 20
Hand-held Analyzer
Types 2250 and 2270



Types 2250 and 2270 are robust, hand-held instrument platforms designed to host a wide range of sound and vibration measurement applications. Their uses range from assessing environmental and workplace noise to industrial quality control and product development.

Easy to use, their robust, light and ergonomic design make them easy to grip, hold and operate with one hand. Their high-resolution colour touch screens show the instrument setup, status and data at a glance, and let you select what you want to see with the tap of a stylus. The "traffic light"

indicator, positioned centrally on the push button panel, shows you the current measurement status, even from a distance.

The hand-held analyzers are built for the tough environment of field measurements. They will work reliably in rain, dust, heat, frost, day or night, and can be placed on a tripod.

For documentation, you can add spoken or written comments to your measurements, and make sound recordings during any of the measurements. (Note that sound recording requires Sound Recording Option BZ-7226.)

Type 2250 is a single-channel analyzer, while Type 2270 is dual-channel and has additional features such as a built-in camera allowing you to attach photos to your measurements and a LAN interface.

The high precision hand-held analyzers offer a wide range of optional software application modules, including prominent applications such as Reverberation Time Software and Building Acoustics Software.

Reverberation Time and Building Acoustics

Reverberation Time

Reverberation time is an important feature of spaces where sound level, the intelligibility of speech, or perception of music is important. It is the time that it takes for a sound to decay by 60 dB. Usually, the time taken for the signal to drop 20 or 30 dB is measured and extrapolated to find the time that it would take the signal to dissipate by 60 dB.

Fig. 21
Reverberation Time measurement – measured using the interrupted noise method

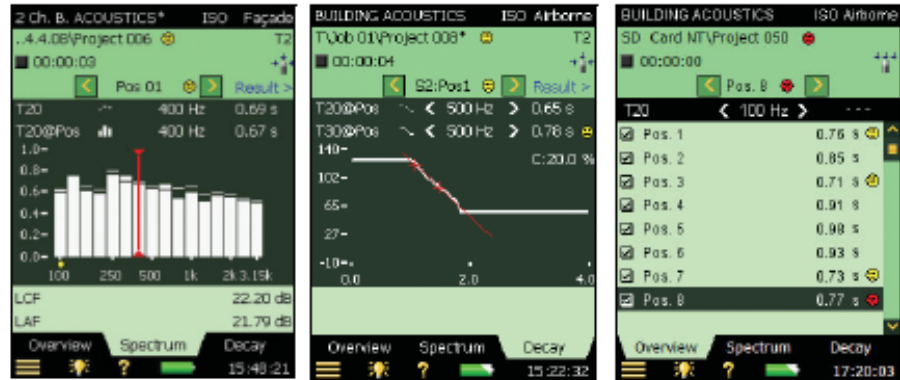


Reverberation time is measured, using an impulse or an interrupted noise, at several positions, which are then averaged together.

To measure reverberation time, simply press the Start/Pause push button on the hand-held analyzer and, if you are using impulse excitation, burst the balloon.

A yellow 'smiley' icon indicates that you may be able to improve the measurement at one (or more) frequency bands, a red smiley indicates that the measurement should be retaken. Tap the relevant smiley icon to read the explanation.

Fig. 22
Reverberation time spectrum (left); Reverberation decay curve (centre); and Overview of results (right)



Building Acoustics

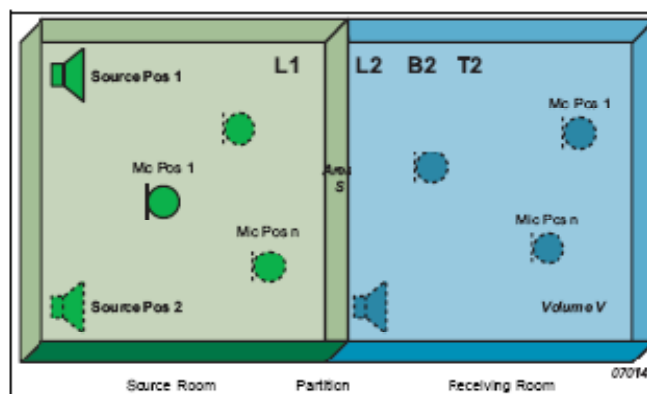
Building acoustics is the assessment of airborne, façade or impact sound insulation in buildings. The assessment is based on measured 1/1-octave or 1/3-octave spectra within the 50 – 5000 Hz range. Measurements may be serial (one frequency band at a time) or parallel (all bands simultaneously)

Airborne Sound Insulation

Fig. 23 shows a typical airborne task setup using a loudspeaker (emitting pink noise) and a number of microphone positions to measure the average source room spectrum L1, and the average receiving room spectrum L2. The average background noise spectrum B2 is measured to verify the true L2 spectrum. The average reverberation time spectrum T2 is measured, to correct for the amount of absorption in the receiving room. Finally the single number result (for example D_{nTn}) is calculated from the L1, L2, B2 and T2 spectra, and the result can then be compared with the minimum requirements stated in the building regulations.

Fig. 23
Sound source and microphone positions for measuring airborne sound insulation

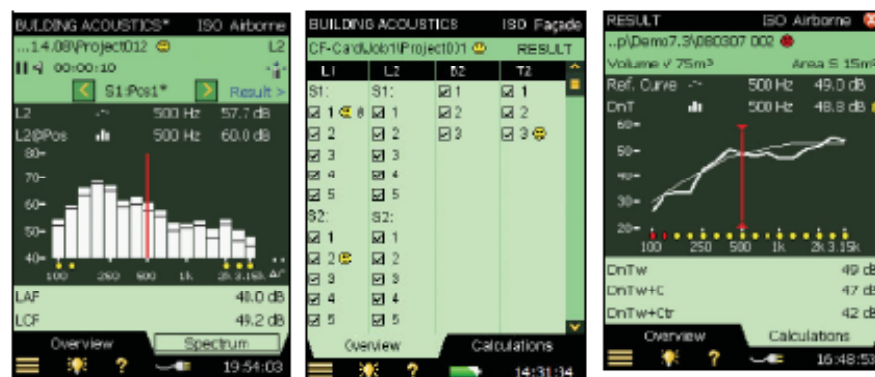
L1 = Source room level
L2 = Receiving room level
B2 = Background level
T2 = Reverberation Time



The sound level depends on the position in the rooms, so several microphone positions are used to measure the average of the source room level, L1, the average of the receiving room level L2 and the average of the background noise level B2. The average reverberation time T2 is also measured using several positions.

Examples of measurements and results are shown in Fig. 24.

Fig. 24
Examples of building acoustics measurements using Type 2250/2270: L2 average and L2 at one position (Left), Overview of measurements (Center) Final result (Right)



Façade Sound Insulation

Façade sound insulation is a variant of airborne sound insulation, with its own standards. The “source room” is the space outside the façade, and the sound source may be road traffic or a loudspeaker representing outdoor noise. When using traffic noise, the indoor and outdoor sound

levels must be measured simultaneously, requiring dual-channel measurements (Type 2270). The outdoor microphone positions are flush with the façade, or 2 m in front of it. Calculations are similar to those of airborne sound insulation, but take the pressure increase at the microphone positions into account.

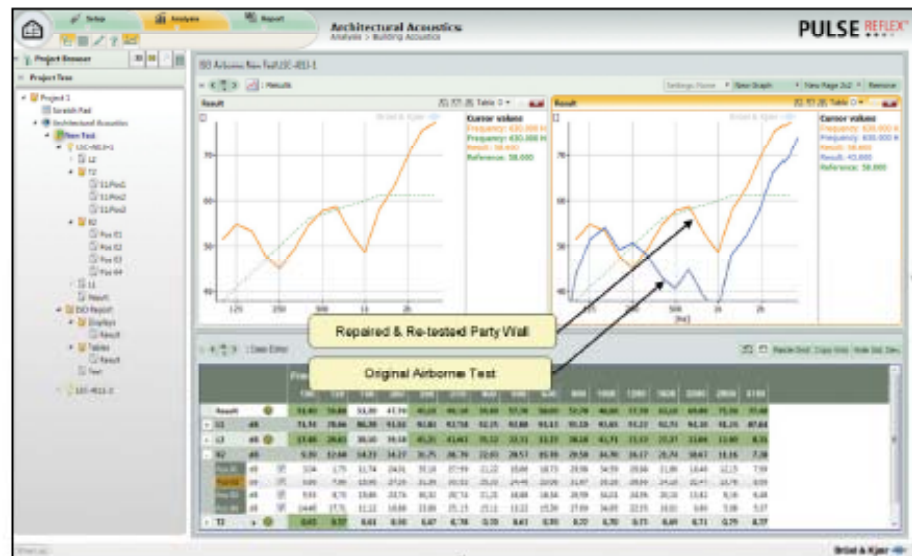
Impact Sound Insulation

Impact sound is typically caused by footsteps, and to measure impact sound insulation a standardised impact sound source (tapping machine) is placed in the source room. The receiving room levels are measured as for airborne sound insulation, with several positions of the tapping machine. Calculations are like those for airborne sound insulation, except the results represent absolute (not relative) levels.

PULSE Reflex™ Building Acoustics Type 8780

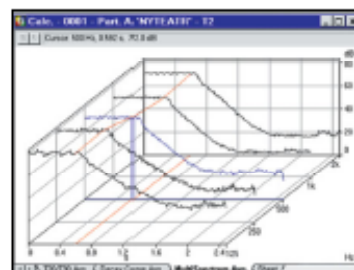
PULSE Reflex Building Acoustics Type 8780 is the software package for post-processing and reporting of building acoustics measurements made with Type 2250/2270. It is the first module in the PULSE Architectural Acoustics Suite, which will, in the future, provide a number of applications for all your needs. Measured data can be directly imported from Type 2250/2270 into Type 8780 for viewing, further analysis/re-analysis and reporting of data. In addition to being a post-processing tool, Type 8780 allows you to control Type 2250/2270 software upgrades and licensing of the Type 2250/2270 applications.

Fig. 25
Typical building acoustics project using Type 8780. Data are presented graphically and numerically with detailed data quality indications, using Type 2250/2270's smiley system



Qualifier™ Types 7830 and 7831

Fig. 26
3D multispectra, showing reverberation decay curves displayed with Type 7830 Qualifier software



Qualifier Type 7830 is a Windows®-compatible PC program that takes data from the building acoustics software and lets you store, view, modify, export and report your measurements. When inspecting the reverberation decay curves, you can graphically adjust the slope line or manually key in data. Reverberation decays can be displayed as 3D multispectra, providing a complete overview of the frequency dependent reverberation curves.

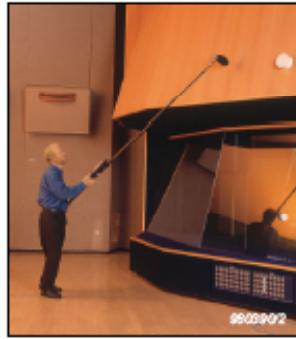
Reverberation time measurements can be averaged in two ways by:

- averaging of reverberation times (T20 and T30)
- averaging of decay curves (ensemble averaging)

Qualifier Light Type 7831 is like Type 7830, but for reverberation time only (matches BZ-7207).

Sound Intensity Software BZ-7205

Fig. 27
Mapping the sound reduction to find leakages between studio and control room



Building acoustic applications such as reduction indices and leakage detection benefit enormously from the sound intensity measurement technique, using Type 2260 Investigator with sound intensity kit and Intensity Software BZ-7205, as an alternative to a sound pressure-based measurement of the apparent sound insulation index R' for a given partition.

This measurement method allows the corrected intensity sound reduction index, $R_{I,C}$ to be measured. This gives extra information regarding the contribution of various flanking and leakage transmissions. In a traditional sound pressure-based measurement you get an apparent sound insulation index R' , which takes every type of transmission into account. However,

traditional measurements cannot identify individual transmission paths. But with this application, you can choose specific details of any particular segment of any given partition or surface. If a compound partition is to be studied (for example, a wall containing a window) the respective corrected intensity sound reduction index, $R_{I,C}$ for both the wall material and the window can be found.

Fig. 28
Type 2260 Investigator display screen showing the $R_{I,CW}$ in surface display

Meas., Results					
RI,CW	RI,C				
WALL/EAST:	37.0 dB				
RI,C1:	43.0 dB				
4					
3					
2	48	48	58	52	
1	43	43	43	53	
	1	2	3	4	

The single-number weighted and corrected intensity sound reduction index, $R_{I,CW}$ is automatically calculated for each segment and for the surface as a whole.

To create a sound field on one side of the wall (in the source room), you can use the internal white noise generator in Type 2260, or the generator built into Power Amplifier Type 2734, together with Type 2734 and OmniPower Sound Source Type 4292.

Specifications – OmniPower Sound Source Type 4292

STANDARDS

Conforms to the following:
 ISO 140-3
 ISO 3382
 DIN 52210

NOMINAL IMPEDANCE

6 Ω

POWER HANDLING

300 W continuous broadband
 1000 W short duration (duty cycle 1/10, on time 10 s)

OPERATING FREQUENCY RANGE

50–5000 Hz (1/3-octave band centre frequencies)

CONNECTION

Four-pin Neutrik® Speakon® socket, pins 1+ and 1-

SOUND POWER LEVEL

(with Power Amplifier Type 2734, bridge configuration, duty cycle 1/3, 100–3150 Hz pink-noise signal)
Broadband: 122 dB re 1 pW
Spectral: Min. 100 dB/1 pW in each 1/3-octave band

TRIPOD

Adjustable to give a speaker height of between 131 and 207 cm

FLOOR MOUNTING

Rubber feet provided for floor mounting

DIAMETER

Speaker Enclosure: 39 cm (15.35")

WEIGHT

Speaker Enclosure: 13.7 kg (30.2 lb.)
 Tripod: 2.3 kg (5.1 lb.)

Specifications – OmniSource Sound Source Type 4295

STANDARDS

Conforms to the following:
 ISO 140-3
 ISO 3382
 DIN 52210
 ISO 14257 (Draft)

OPERATING FREQUENCY RANGE

80–6300 Hz

NOMINAL IMPEDANCE

6 Ω

POWER HANDLING

50 W continuous

SOUND POWER LEVEL

(with Power Amplifier Type 2734-A or 2734-B, 80–6300 Hz pink-noise signal)

Broadband: 105 dB re 1 pW

Spectral: Min. 85 dB in each 1/3-octave band

CONNECTION

Four-pin Neutrik® Speakon® socket, pins 1+ and 1-

TRIPOD THREADS (LARGE TYPE)

One at rear end, one below centre of gravity

CARRYING CASE

Nylon with padded inlay, adjustable carrying strap

MECHANICAL SPECIFICATIONS

Material: Dense polyurethane plastic, painted black

Dimensions: $\varnothing 145 \times 560$ mm ($\varnothing 5.7 \times 22$ ")

Weight: 3.5 kg (7.7 lb.)

Compliance with Environmental Standards for Types 4292 and 4295

Temperature	IEC 60068-2-1 & IEC 60068-2-2: Environmental Testing. Cold and Dry Heat. Operating Temperature: +5 to +40°C (41 to 104°F) Storage Temperature: -25 to +70°C (-13 to 158°F) IEC 60068-2-14: Change of Temperature: -10 to +40°C (2 cycles, 1°C/min.)
Humidity	IEC 60068-2-78: Damp Heat: 93% RH (non-condensing at 40°C (104°F))
Mechanical	Non-operating: IEC 60068-2-6: Vibration: 0.3 mm, 20 m/s ² , 10–500 Hz IEC 60068-2-27: Shock: 1000 m/s ² IEC 60068-2-29: Bump: 1000 bumps at 250 m/s ²

Specifications – Tapping Machine Type 3207

STANDARDS

ISO 140
ISO 717
DIN 52210
BS 5821
ASTME 492

HAMMERS

Five in line, 100 mm between each hammer, single hammer weight 500±12 g

IMPACT FREQUENCY

Each hammer operates at 2Hz, tapping frequency for unit is 10±0.5Hz

IMPACT DYNAMICS

Equivalent free-fall height of hammers 40 mm, extra drop below impact plane at least 4 mm

REMOTE OPERATION

Socket: LEMO 4-pole

Pin 1: 0VDC, GND

Pin 2: Power supply for external unit, max. 24VDC, 1A

Pin 3: For "On": +5VDC (TTL-Level)

Pin 4: For "On": connect to Pin 1

Housing: Shield

REMOTE OPERATION WIRELESS CONTROL KIT UA-1476 (OPTIONAL)

Operating Frequency: 433.92MHz

Transmitter Unit:

– Connector: LEMO-coaxial socket

– Centre pin: +5VDC for "on"; Outer ring 0VDC

– Batteries: 2 x AAA/LR03/Micro 1.5V

– Dimensions: 105 x 58 x 18.5 mm (4.13 x 2.28 x 0.73")

– Weight: 90g

Receiver Unit

Connector: LEMO 4-pole plug with cable

For details of pin connections see "Remote Operation"

– Power supply: From the remote control socket

– Dimensions: 85 x 46 x 16 mm (3.35 x 1.81 x 0.63")

– Weight: 80g

BATTERY KIT UA-1477 (OPTIONAL)

Mounting Position: Internally in unit housing

Battery Life: 1.5 hours

Battery Type: Maintenance free 12V/2Ah Lead Acid battery

Charger Type: Same as Mains Adaptor (see below)

Charging Time: 24 hours for a completely discharged battery

ON/OFF SWITCH

3 Positions: Remote, Off, On

MAINS ADAPTOR

10.5–35VDC, min. 25W

Socket: LEMO coaxial (can also be used as charging socket)

Middle Pin: +10.5–35VDC, Outer ring: 0V

Mains Adaptor: Mains Adaptor ZG-0400

100–240V AC input, 24V DC output, max. 45W

Operating temperature max. +40°C

Can also be used to charge optional battery pack

SUPPORTS

3 extendable and height adjustable feet

DIMENSIONS

W x H x D: 480 x 273 x 155 mm (18.9 x 10.7 x 6.1")

(feet retracted)

W x H x D: 590 x 273 x 285 mm (23.2 x 10.7 x 11.2")


(feet extended)

Weight: 11.5 kg (25 lb.) with Mains Adaptor

MAINTENANCE REQUIREMENTS

After 24 hr operation or once a year (whichever comes first), lubricate with the supplied sewing machine oil according to instructions

Compliance with Regulations and Environmental Standards for Type 3207

	CE-mark indicates compliance with: EMC Directive, Low Voltage Directive and Machinery Directive Remote Control UA-1476: CE-mark means compliance with R&TTE Directive C-Tick mark indicates compliance with the EMC requirements of Australia and New Zealand
Safety	EN/IEC 61010–1 and UL 61010–1: Safety requirements for electrical equipment for measurement, control and laboratory use
EMC Emission	EN/IEC 61000–6–3: Generic emission standard for residential, commercial and light-industrial environments CISPR 22: Radio disturbance characteristics of information technology equipment. Class B limits. FCC Rules, Part 15: Complies with the limits for a Class B digital device This ISM device complies with Canadian ICES–001
EMC Immunity	EN/IEC 61000–6–2: Generic standards – Immunity for industrial environments EN/IEC 61326: Electrical equipment for measurement, control and laboratory use – EMC requirements Note: The above is only guaranteed using accessories listed in this Product Data Sheet.
Temperature	IEC 60068–2–1 & IEC 60068–2–2: Environmental testing. Cold and dry heat. Operating Temperature: 0 to +40°C (32 to 104°F) Storage Temperature: –25 to +70°C (–13 to 158°F)
Humidity	IEC 60068–2–78: Damp heat: 90% RH (non-condensing at 40°C (104°F))
Mechanical	Non-operating: IEC 60068–2–6: Vibration: 0.3 mm, 20 m/s ² , 10–500 Hz IEC 60068–2–27: Shock: 500 m/s ² , 6 directions IEC 60068–2–29: Bump: 1000 bumps at 250 m/s ²
Enclosure	IEC 60529: Protection provided by enclosures: IP 20

Specifications – Power Amplifier Types 2734-A and 2734-B

MAXIMUM OUTPUT POWER

(TA = 25°C, 1 kHz, 0.1% THD)

4 Ω: 500 W

6 Ω: 330 W

8 Ω: 250 W

CONTINUOUS OUTPUT POWER (1 kHz, 6 Ω)

With Air Filter: TA = 25°C: 260 W

Without Air Filter:

– TA = 25°C: 330 W

– TA = 35°C: 175 W

INPUT VOLTAGE

Nominal voltage @ Sensitivity =

0 dB: 0.3 V

–10 dB: 1 V

–20 dB: 3 V

Headroom at nominal input voltage

Balanced: 18 dB

Unbalanced @ Sensitivity =

0 dB: 17 dB

–10 dB: 15 dB

–20 dB: 12 dB

Common Mode Rejection (1 kHz): > 50 dB

Maximum DC Voltage: ±25 V

INPUT IMPEDANCE

1 kHz:

– Balanced: 20 kΩ ±1%

– Unbalanced: 10 kΩ ±1%

DC:

– Balanced: 220 kΩ ±1%

– Unbalanced: 110 kΩ ±1%

OUTPUT VOLTAGE

Line Output Peak Voltage: 9 V

Power Output Peak Voltage: 80 V

Power Output DC Voltage: 40 V

OUTPUT IMPEDANCE (1 kHz)

Line Output: 100 Ω

Line Output Load: ≥20 Ω

Power Output: 10 nΩ

Power Output Load: ≥2 Ω

FREQUENCY RESPONSE (20 Hz–20 kHz)

Line Output: +0, –1 dB

Power Output: ±1 dB

See also figure 1 below

SNR (MAX POWER 1 kHz)/(SILENCE 0...20 kHz)

Line Output: 101 dB

Power Output: 90 dB

THD+N (20 Hz–20 kHz)

Line Output: 1 kHz: < –78 dB

Power Output: 1–500 W, 4 Ω: < –80 dB

SENSITIVITY, ATTENUATION AND GAIN

Sensitivity: –20, –10, 0 dB

Sensitivity Error (no error @ 0 dB): ±0.1 dB

Attenuation: –30, –24, –18, –12, –8, –6, –5, –4, –3, –2, –1, 0 dB

Attenuation Error (no error @ 0 dB): ±0.1 dB

Total Gain (Sensitivity = Attenuation = 0 dB):

– Any Input to Line Output: 16 ±0.2 dB

– Any Input to Power Output: 43.1 ±0.4 dB

LEVEL INDICATOR

Trigger levels re power output clip level

Red LED: +3 dB

Yellow LED: 0 dB (Power Output clip indicator)

Green LED: –6 dB

Blue LED: –30 dB (Signal Present indicator)

FAN

Switch On Heatsink Temperature: 40°C

L_w at Min Speed: 25 dB re 1 μW

L_w at Max Speed: 52 dB re 1 μW

NOISE GENERATOR

Noise Types: white, pink

Frequency Range: 50–5000 Hz 1/3 octave bands

Crest Factor: 12 dB

Period Time: 22.5 s

Third Octave Spectral Error: ±0.3 dB

Line Output Voltage (Sensitivity = Attenuation = 0 dB): 2.16 V_{rms}

Switch Off: Equivalent RT in 1/3 octaves: <50 ms @ 50 Hz, <4ms @ 5 kHz

CONNECTORS

Balanced Input Socket: Neutrik® Combo XLR-type: 3-pin and ¼" jack

Unbalanced Input Socket: BNC

Unbalanced Line Output Socket: BNC

Power (Speaker) Output Socket: Neutrik® 4-pole Speakon® type

Mains Power Inlet: IEC type

CONTROLS

Generator Button: Toggling between On and Off

Generator Slide Switch: 2-state, White/Pink noise Sensitivity slide

switch: 3-state, –20, –10, 0 dB

Attenuation Rotary Knob: 12-state, –30, –24, –18, –12, –8, –6, –5, –4, –3, –2, –1, 0 dB

Mains Power Rocker Switch: 2-pole

STATUS INDICATORS

Protect Indicator: Red LED, power output over-current, overheat, overload or long-term high frequency

Power On Indicator: Green LED

MAINS POWER

Voltage Selector (Rear Panel): 230/115 V

Mains Voltage Range:

– @ 230 V: 200 - 240 V

– @ 115 V: 100 - 125 V

Mains Frequency Range: 45–65 Hz

Fuse: Wickmann/Littlefuse series 215 (or 181)

– @ 230 V: T 3.15 AH 250 V

– @ 115 V: T 6.3 AH 125 V

Maximum Power Consumption: 650 W

MECHANICAL

Weight (including mains cord in lid):

– Type 2734-A: 6.0 kg

– Type 2734-B: 7.0 kg

Dimensions W × H × D: 330 × 130 × 310 mm (13 × 5.1 × 12 ")

TRANSMITTER AKG PT 450 (OPTIONAL)

Specifications from manufacturer's technical data

Rf Carrier Frequency Ranges: 7 channels over 650–0165 MHz

Modulation: FM

Audio Bandwidth: 35 to 20000 Hz

THD (typical at rated deviation/1 kHz): <0.7%

S/N Ratio: 120 dB(A)

RF Output: 50 mW max. (ERP)

Battery Life:

1.5 V AA Dry Battery: 6 hours; 1.2 V NIMH, 2100 mAh AA size

Rechargeable Battery: 8 hrs

– Size: 60 × 73.5 × 30 mm (2.4 × 2.9 × 1.2")

– Net weight: 90 g (3.2 oz.)

RECEIVER AKG SR 450 (OPTIONAL)

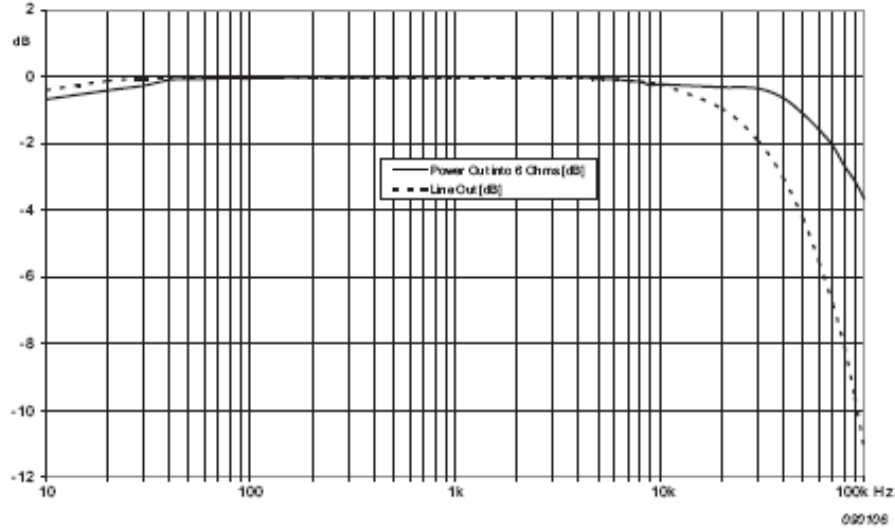
Specifications from manufacturer's technical data

RF Carrier Frequency Ranges: 7 channels over 650–865MHz
 Modulation: FM
 Audio Bandwidth: 35 to 20000Hz
 THD at 1kHz: <0.3%
 S/N Ratio: 120 dB(A)

Audio Outputs: Balanced XLR and unbalanced TS 1/4" jack,
 balanced level switchable to –30 or 0dBm

MECHANICAL
 Dimensions: 200 × 44 × 180 mm (7.8 × 1.7 × 7.4")
 Weight: 972g (2.2 lbs)

Fig. 1 Frequency Responses measured at a 0dB output power of 300W into 6Ω up to 20kHz and of 20W up from 20kHz



Compliance with Regulations and Environmental Standards for Type 2734

	CE-mark indicates compliance with: EMC Directive and Low Voltage Directive. C-Tick mark indicates compliance with the EMC requirements of Australia and New Zealand
Safety	EN/IEC 61010–1 and ANSI/UL 61010–1: Safety requirements for electrical equipment for measurement, control and laboratory use.
EMC Emission	EN/IEC 61000–6–4: Generic emission standard for industrial environments. CISPR 22: Radio disturbance characteristics of information technology equipment. Class A Limits. FCC Rules, Part 15: Complies with the limits for a Class A digital device
EMC Immunity	EN/IEC 61000–6–1: Generic standards - Immunity for residential, commercial and light-industrial environments. EN/IEC 61000–6–2: Generic standards - Immunity for industrial environments. EN/IEC 61326–1: Electrical equipment for measurement, control and laboratory use – EMC requirements Note 1: The above is only guaranteed using accessories included in this Product Data.
Temperature	IEC 60068–2–1 & IEC 60068–2–2: Environmental Testing. Cold and Dry Heat. Operating Temperature: 0 to +50°C (32 to 122°F) Storage Temperature: 0 to +70°C (32 to 158°F)
Humidity	IEC 60068–2–78: Damp Heat: 90% RH (non-condensing at 40°C (104°F))
Mechanical	Non-operating: IEC 60068–2–6: Vibration: 2 g _{rms} , 3 x 20 minutes IEC 60068–2–27: Bump: 1000 bumps at 10g, 6 directions IEC 60068–2–27: Shock: 70g, 6 directions
Enclosure	IEC 60529 (1989): Protection provided by enclosures: IP 20

Ordering Information

Type 4292	OmniPower Sound Source	Type 2250-J-001	Building Acoustics System including Type 2250-J, OmniPower Sound Source Type 4292 and Power Amplifier Type 2734-A
Type 4295	OmniSource Sound Source		
Type 3207	Tapping Machine		
ACCESSORIES INCLUDED WITH TYPE 4292			
UA-1690	Tripod	Type 2270-J-001	Building Acoustics System including Type 2270-J, OmniPower Sound Source Type 4292 and Power Amplifier Type 2734-A
ACCESSORIES INCLUDED WITH TYPE 3207			
ZG-0429	Mains adaptor (mains cable country dependent) 2 Gauges for drop height adjustment Oil canister for maintenance	Type 2270-K-001	Dual-channel Building Acoustics System including Type 2270-K, OmniPower Sound Source Type 4292 and Power Amplifier Type 2734-A
OPTIONAL ACCESSORIES			
Type 2734-A	Power Amplifier	BZ-7228-200	Building Acoustics Kit as per Type 2250-J-001, or Type 2270-J-001, excluding Hand-held Analyzer (for Types 2250 and 2270 users intending to upgrade to a full Building Acoustics measurement system)
Type 2734-B	Power Amplifier with built-in UL-0256 Wireless Audio System		
UL-0256	Wireless Audio System	BZ-7229-200	Dual-channel Building Acoustics Kit as per Type 2270-K-001, excluding Type 2270 (for Type 2270 users intending to upgrade to a full Dual-channel Building Acoustics measurement system)
KE-0392	Carrying Case for Type 4295		
KE-0449	Flight Case for Type 4292		
KE-0364	Carrying Case for Type 4292 Tripod (UA-1690)		
UA-0801	Lightweight Tripod		
AO-0523	Signal cable from Hand-held analyzer to Power Amplifier, 10 m (32.8 ft)	Type 8760	PULSE Reflex Building Acoustics Software
AO-0524	Signal cable from Hand-held Analyzer to BNC, 10 m (32.8 ft)	Type 7830	Qualifier PC Software for Building Acoustics reporting
AQ-0673	Speaker cable from Type 2734 to Types 4292, 4295 or equivalent, 10 m (32.8 ft)	Type 7831	Qualifier Light PC Software for reverberation time reporting
Type 2250-F	Hand-held Analyzer Type 2250 with Sound Level Meter Software BZ-7222 and Reverberation Time Software BZ-7227		
Type 2270-F	Hand-held Analyzer Type 2270 with Sound Level Meter Software BZ-7222 and Reverberation Time Software BZ-7227		
Type 2250-J	Hand-held Analyzer Type 2250 with Sound Level Meter Software BZ-7222 and Building Acoustics Software BZ-7228		
Type 2270-J	Hand-held Analyzer Type 2270 with Sound Level Meter Software BZ-7222 and Building Acoustics Software BZ-7228		
Type 2270-K	Hand-held Analyzer Type 2270 with Sound Level Meter Software BZ-7222 and Dual-channel Building Acoustics Software BZ-7229		
			For further information, see separate Product Data for the types mentioned above
			OPTIONAL ACCESSORIES FOR TYPE 3207
		AQ-0633	Remote Cable connecting Type 2260 Investigator to Type 3207, 10 m (32.8 ft)
		UA-1476	Wireless Remote Control (includes AQ-1439 Cable for Hand-held Analyzer Types 2250 and 2270)
		UA-1477	Battery Kit
		QB-0055	Replacement battery

BP 1689-20 200640



TRADEMARKS

Microsoft and Windows are registered trademarks of Microsoft Corporation in the United States and/or other countries - Investigator, OmniPower and OmniSource are trademarks of Brüel & Kjær Sound and Vibration Measurement A/S - Neutrik and Speakon are registered trademarks of Neutrik AG - IBM is a registered trademark of IBM Corporation in the United States and other countries

Brüel & Kjær reserves the right to change specifications and accessories without notice

HEADQUARTERS: Brüel & Kjær Sound & Vibration Measurement A/S · DK-2850 Naerum · Denmark
Telephone: +45 7741 2000 · Fax: +45 450 1405 · www.bksv.com · info@bksv.com

Local representatives and service organisations worldwide

Brüel & Kjær 



PRODUCT DATA

Audio Power Amplifier 100 W Stereo — Type 2716-C

Audio Power Amplifier Type 2716-C is a high-performance power amplifier optimised for sound and vibration applications. It can be used as a general-purpose power amplifier for electroacoustic applications.

USES

- Driver for loudspeakers, artificial mouths, etc.
- General-purpose audio power amplifier
- Power amplifier for audio analyzers

FEATURES

- Output-level meter
- Selectable gain
- Two balanced inputs
- Easy to install in a 19" rack



Description

Audio Power Amplifier Type 2716-C has two channels that can be used independently or jointly. Signals enter electronically balanced inputs, Input CH.A and Input CH.B, via XLR connectors. Output is approx. 300 W and is relatively independent of load.

Audio Power Amplifier Type 2716-C is compact and fits in a 19" rack. It has the same features and protection circuits normally found only in higher powered amplifiers.



Quiet Operation

Type 2716-C uses passive cooling during operation which removes the need for a cooling fan. The lack of a cooling fan, in turn, makes Type 2716-C very quiet during operation.

Extensive Protection

Power Amplifier Type 2716-C has circuits that protect it against short-circuits, DC, overheating, VHF and clipping (clip limiter may be switched off).

Compliance with Standards

 	CE-mark indicates compliance with: EMC Directive and Low Voltage Directive. C-Tick mark indicates compliance with the EMC requirements of Australia and New Zealand
Safety	EN/IEC 60065, Audio, video and similar electronic apparatus – Safety Requirements
EMC Emission	EN 55103-1, E3: EMC – Product family standard for audio, video, audiovisual and entertaining lighting control apparatus for professional use – Part 1: Emission
EMC Immunity	EN 55103-2, E3: EMC – Product family standard for audio, video, audiovisual and entertaining lighting control apparatus for professional use – Part 2: Immunity
Temperature	IEC 60068-2-1 & IEC 60068-2-2: Environmental Testing. Cold and Dry Heat. Operating Temperature: +5°C to +40°C (+41 to +104°F) Storage Temperature: -25 to +70°C (-13 to +158°F)
Humidity	IEC 60068-2-3: Damp Heat: 90% RH (non-condensing at 40°C (104°F))
Mechanical	Non-operating: IEC 60068-2-6: Vibration: 0.3mm, 20 m/s ² , 10–500 Hz IEC 60068-2-27: Shock: 1000 m/s ² IEC 60068-2-29: Bump: 1000 bumps at 250 m/s ²
Enclosure	IEC 60529: Protection provided by enclosures: IP20

Specifications – Audio Power Amplifier Type 2716-C

MAXIMUM OUTPUT POWER^a

Load	EIA @ 1 kHz and 1% THD
8 Ω stereo	110 W
4 Ω stereo	160 W
2 Ω stereo	200 W
8 Ω bridged	320 W
4 Ω bridged	400 W

SPEAKER PROTECTION

Short-circuit, DC, VHF a thermal protection is provided

FREQUENCY RESPONSE (8 Ω, 1 W)

20 Hz – 20 kHz: +0, -1 dB

a. Measured specifications for a 230 V AC. Continuous power (1 hour) is 1/3 of this

INPUTS AND OUTPUTS

Gain: 30 dB ± 1 dB
Input Attenuator: 0–30 dB in 6 dB ± 0.3 dB steps
Impedance: 20 kΩ
Common Mode Rejection: 50 dB @ 1 kHz
Slew Rate: 25 V/μs
Output Impedance: 0.03 Ω
Hum and Noise: More than 105 dB below max. power
Channel Separation: 70 dB @ 10 kHz
FRONT PANEL
Gain Controls: 2 –channels, A and B
Clip Indicator: 2 red LEDs, fast peak and slow release or shorted output
Protection Indicator: 2 yellow LEDs, 80°C at heat sink or 12 kHz at full power
Present Indicator: 2 green LEDs, -25 dB at input

On Indicator: 2 green LEDs, DC rail voltage for channel A and B

REAR PANEL

Input Connectors: Two XLR-type, 3-pin female (pin 2+) and 1/4" jack
Output Connectors: Two Neutrik®, 4-pin, Speakon® sockets
Link: Stereo – Link/Bridge A + B
Clip Limiter: On/Off

POWER REQUIREMENTS

Voltage Selector: 230 V/115 V

DIMENSIONS

W x H x D: 48.3 x 4.4 x 28.0 cm
(19 x 1.7 x 11 inches)

WEIGHT

7.5 kg (16.5 lb.)

Ordering Information

Type 2716-C-001 Audio power amplifier (no accessories)	Type 2716-C	Audio Power Amplifier with the following accessories: BNC to XLR cable, 3 m 2 Banana to Speakon® cable, 5 m	OPTIONAL ACCESSORIES AQ-0521 Bridging cable
	2 x WL-1324		
	2 x WL-1325		

TRADEMARKS

Neutrik and Speakon are registered trademarks of Neutrik AG

Brüel & Kjær reserves the right to change specifications and accessories without notice

HEADQUARTERS: DK-2850 Naerum - Denmark - Telephone: +45 4680 0500
Fax: +45 4680 1405 - www.bksv.com - info@bksv.com

Australia (+61) 2 9889 8888 - Austria (+43) 1 865 74 00 - Brazil (+55) 11 5188 8161
Canada (+1) 514 695 8225 - China (+86) 10 680 29908 - Czech Republic (+420) 2 6702 1100
Finland (+358) 9 755 950 - France (+33) 1 69 90 71 00 - Germany (+49) 421 17 87 0
Hong Kong (+852) 2548 7486 - Hungary (+36) 1 215 83 05 - Ireland (+353) 1 807 4063
Italy (+39) 02 57 96 061 - Japan (+81) 3 5715 5512 - Republic of Korea (+82) 2 3473 6635
Netherlands (+31) 318 55 9290 - Norway (+47) 68 77 11 55 - Poland (+48) 22 816 75 96
Portugal (+351) 21 4185 040 - Singapore (+65) 6377 4512 - Slovak Republic (+421) 25 445 0701
Spain (+34) 91 850 3820 - Sweden (+46) 33 225 622 - Switzerland (+41) 44 38 07 035
Taiwan (+886) 2 2502 7255 - United Kingdom (+44) 14 38 739 003 - USA (+1) 800 332 2040

Local representatives and service organisations worldwide

Brüel & Kjær 





PRODUCT DATA

Sound Calibrator — Type 4231

Sound Calibrator Type 4231 is a handy, portable sound source for calibration of sound level meters and other sound measurement equipment. The calibrator is very robust and stable, and conforms to EN/IEC 60942 Class LS and Class 1, and ANSI S1.40-1984.



USES AND FEATURES

USES

- Calibration of sound level meters and other sound measurement equipment

FEATURES

- Conforms to EN/IEC 60942 (2003) Class LS and Class 1, and ANSI S1.40-1984
- Robust, pocket-sized design with highly stable level and frequency
- Calibration accuracy ± 0.2 dB
- 94 dB SPL, or 114 dB SPL for calibration in noisy environments
- Extremely small influence of static pressure and temperature
- Sound pressure independent of microphone equivalent volume
- 1 kHz calibration frequency for correct calibration level independent of weighting networks
- Fits Brüel & Kjær 1" and 1/2" microphones (1/4" and 1/8" microphones with adaptor)
- Switches off automatically when removed from the microphone

Brüel & Kjær 

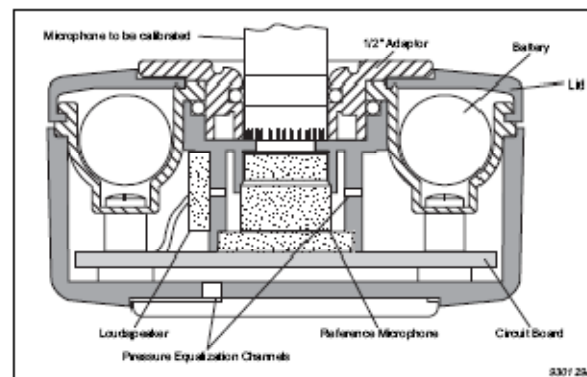
Sound Calibrator Type 4231

Sound Calibrator Type 4231 is a pocket-sized, battery operated sound source for quick and direct calibration of sound level meters and other sound measuring systems. It fits Brüel & Kjær 1" microphones and using the removable adaptor, 1/2" microphones. With optional adaptors, it can be used for 1/4" and 1/8" microphones as well.

The calibration frequency is 1000 Hz (the reference frequency for the standardised international weighting networks), so the same calibration value is obtained for all weighting networks (A, B, C, D and Linear). The calibration pressure of 94 ± 0.2 dB re $20 \mu\text{Pa}$ is equal to 1 Pa or 1 N/m^2 . The +20 dB level step gives 114 dB SPL, which is convenient for calibration in noisy environments, or for checking linearity.

The design of Type 4231 is based on a feed-back arrangement to ensure a highly stable sound pressure level and ease of use. The feed-back loop uses a condenser microphone (see Fig. 1), which is specially developed for this purpose.

Fig. 1
Cross-sectional view of Sound Calibrator Type 4231. The feed-back loop is based on a high-quality condenser microphone to ensure a very stable sound pressure level



This microphone is optimised to have extremely high stability and independence of variations in static pressure and temperature around the 1 kHz calibration frequency. The result of this is a user-friendly calibrator where exact fitting of the microphone is non critical and the effects of changes in temperature and static pressure are negligible.

Fig. 2
Type 4231 fitted to Hand-held Analyzer Type 2250. The calibrator's centre of gravity is positioned very close to the microphone, giving a stable set-up




The calibrator gives a continuous sound pressure level when fitted on a microphone (see Fig. 2) and activated.

The sensitivity of the sound measuring equipment can then be adjusted until it indicates the correct sound pressure level.

The calibrator is automatically switched off when removed from the microphone.

A leather protecting case, which does not need to be removed to use the calibrator, is supplied.

Compliance with Standards

	CE-mark indicates compliance with: EMC Directive and Low Voltage Directive. C-Tick mark indicates compliance with the EMC requirements of Australia and New Zealand.
Safety	EN/IEC 61010-1: Safety requirements for electrical equipment for measurement, control and laboratory use. ANSI/UL 61010-1: Safety requirements for electrical equipment for measurement, control and laboratory use.
EMC Emission	EN/IEC 61000-6-3: Generic emission standard for residential, commercial and light industrial environments. EN/IEC 61000-6-4: Generic emission standard for industrial environments. CISPR 22: Radio disturbance characteristics of information technology equipment. Class B Limits. FCC Rules, Part 15: Complies with the limits for a Class B digital device. EN/IEC 60942: Instrumentation Standard – Electroacoustics – Sound Calibrators.
EMC Immunity	EN/IEC 61000-6-1: Generic standards – Immunity for residential, commercial and light industrial environments. EN/IEC 61000-6-2: Generic standards – Immunity for industrial environments. EN/IEC 61326: Electrical equipment for measurement, control and laboratory use – EMC requirements. EN/IEC 60942: Instrumentation Standard – Electroacoustics – Sound Calibrators. Note: The above is only guaranteed using accessories listed in this Product Data sheet.
Temperature	IEC 60068-2-1 & IEC 60068-2-2: Environmental Testing. Cold and Dry Heat. Operating Temperature: -10 to +50°C (14 to 122°F) Storage Temperature: -25 to +70°C (-13 to +158°F)
Humidity	IEC 60068-2-78: Damp Heat: 90% RH (non-condensing at 40°C (104°F)).
Mechanical	Non-operating: IEC 60068-2-6: Vibration: 0.3 mm (10 to 58 Hz), 20 m/s ² (58–500 Hz) IEC 60068-2-27: Shock: 1000 m/s ² IEC 60068-2-29: Bump: 3000 bumps at 400 m/s ²
Enclosure	IEC 60528: Protection provided by enclosures: IP 50 with leather protection case.

Specifications – Sound Calibrator Type 4231

STANDARDS SATISFIED

EN/IEC 60942 (2003), Class LS and Class 1, Sound Calibrators
ANSI S1.40-1994, Specification for Acoustic Calibrators

SOUND PRESSURE LEVELS

94.0 dB ±0.2 dB (Principal SPL) or
114.0 dB ±0.2 dB re 20 µPa at reference conditions

FREQUENCY

1 kHz ±0.1%

SPECIFIED MICROPHONE

Size according to IEC 61094-4:

- 1" without adaptor
- 1/2" with adaptor UC-0210 (supplied)
- 1/4" with adaptor DP-0775 (optional)
- 1/8" with adaptor DP-0774 (optional)

EQUIVALENT FREE-FIELD LEVEL

(0° incidence, re Nominal Sound Pressure Level)
-0.15 dB for 1/2" Brüel & Kjær Microphones. See Type 4231 User Manual for other microphones

EQUIVALENT RANDOM INCIDENCE LEVEL

(re Nominal Sound Pressure Level)
+0.0 dB for 1", 1/2", 1/4" and 1/8" Brüel & Kjær Microphones

NOMINAL EFFECTIVE COUPLER VOLUME

>200 cm³ at reference conditions

DISTORTION

<1%

LEVEL STABILITY

Short-term: Better than 0.02 dB (as specified in IEC 60942)

One Year: Better than 0.05 dB ($\sigma = 98\%$)

Stabilization Time: <5 s

REFERENCE CONDITIONS

Temperature: 23°C ±3°C (73° ±5°F)

Pressure: 101 ±4 kPa

Humidity: 50%, -10% +15% RH

Effective Load Volume: 0.25 cm³

ENVIRONMENTAL CONDITIONS

Pressure: 65 to 106 kPa

Humidity: 10 to 90% RH (non-condensing)

Effective Load Volume: 0 to 1.5 cm³

INFLUENCE OF ENVIRONMENTAL CONDITIONS (Typical)

Temperature Coefficient: ±0.0015 dB/°C

Pressure Coefficient: +8 × 10⁻⁴ dB/kPa

Humidity Coefficient: 0.001 dB/%RH

POWER SUPPLY

Batteries: 2 × 1.5 V IEC Type LR6 ("AA" size)

Lifetime: Typically 200 hours continuous operation with alkaline batteries at 23°C (73°F)

Battery Check: When Type 4231 stops working continuously, and only operates when the On/Off button is held in, the batteries should be replaced

DIMENSIONS AND WEIGHT

(Without case)

Height: 40 mm (1.5")

Width: 72 mm (2.8")

Depth: 72 mm (2.8")

Weight: 150 g (0.33 lb.), including batteries

Note: All values are typical at 25°C (77°F), unless measurement uncertainty or tolerance field is specified. All uncertainty values are specified at 2 σ (i.e., expanded uncertainty using a coverage factor of 2)

Ordering Information

Type 4231 Sound Calibrator includes the following accessories:

KE-0317 Leather Case
QB-0013 2 Alkaline Batteries Type LR6
UC-0210 Adaptor for 1/2" microphones

Optional Accessories

DP-0775 Adaptor for 1/4" microphones
DP-0774 Adaptor for 1/8" microphones
DP-0887 Adaptor for Head and Torso Simulator Type 4128
DP-0888 Adaptor for Intensity Probe Sets Types 3545, 3548, 3583, 3584

Brüel & Kjær reserves the right to change specifications and accessories without notice

HEADQUARTERS: DK-2850 Naerum · Denmark · Telephone: +45 4580 0500
Fax: +45 4580 1405 · www.bksv.com · info@bksv.com

Australia (+61) 20880 8888 · Austria (+43) 1 865 74 00 · Brazil (+55) 11 5188 8161
Canada (+1) 514 695 4225 · China (+86) 10 580 29905 · Czech Republic (+420) 2 6702 1100
Finland (+358) 9 521 500 · France (+33) 1 69 90 71 00 · Germany (+49) 421 17 87 0
Hong Kong (+852) 2548 7486 · Hungary (+36) 1 215 83 05 · Iceland (+354) 1 807 4083
Italy (+39) 0257 58961 · Japan (+81) 3 5715 1512 · Republic of Korea (+82) 2 3473 0605
Netherlands (+31) 318 55 9290 · Norway (+47) 66 77 11 55 · Poland (+48) 22 816 75 56
Portugal (+351) 21 41 69 040 · Singapore (+65) 6377 4512 · Slovak Republic (+421) 25 443 0701
Spain (+34) 91 859 0820 · Sweden (+46) 33 225 622 · Switzerland (+41) 44 880 7035
Taiwan (+886) 2 2502 7255 · United Kingdom (+44) 14 38 739 000 · USA (+1) 800 332 2040

Local representatives and service organisations worldwide

Brüel & Kjær 



Reference C

C. Time Domain Test Signal Inputs

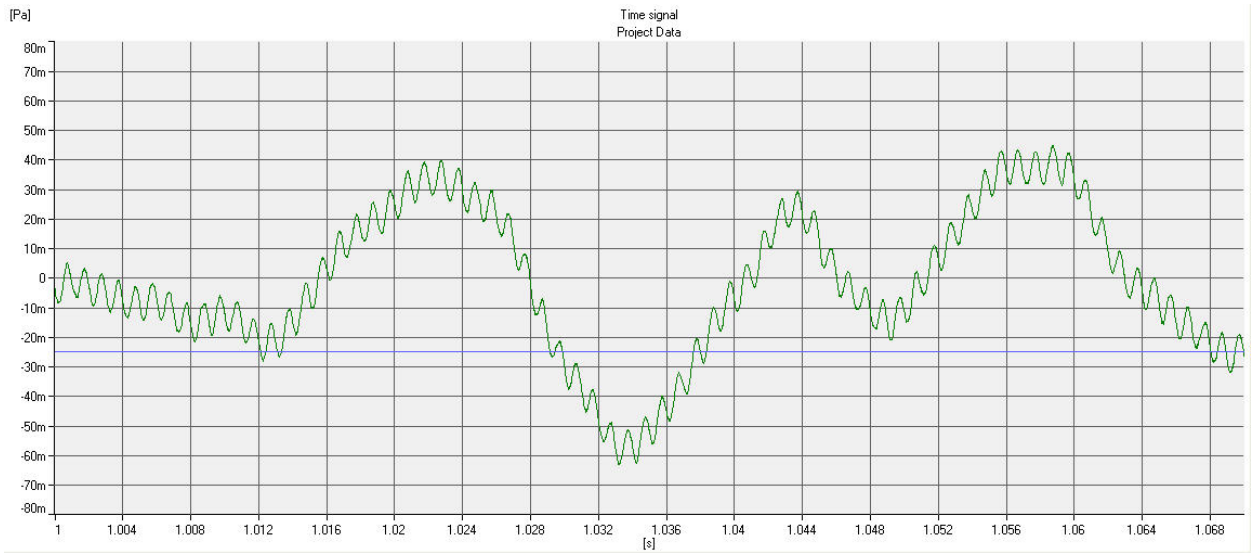


Exhibit C1 - 60 dB Steady Sinusoidal Test Signal with no Gaps

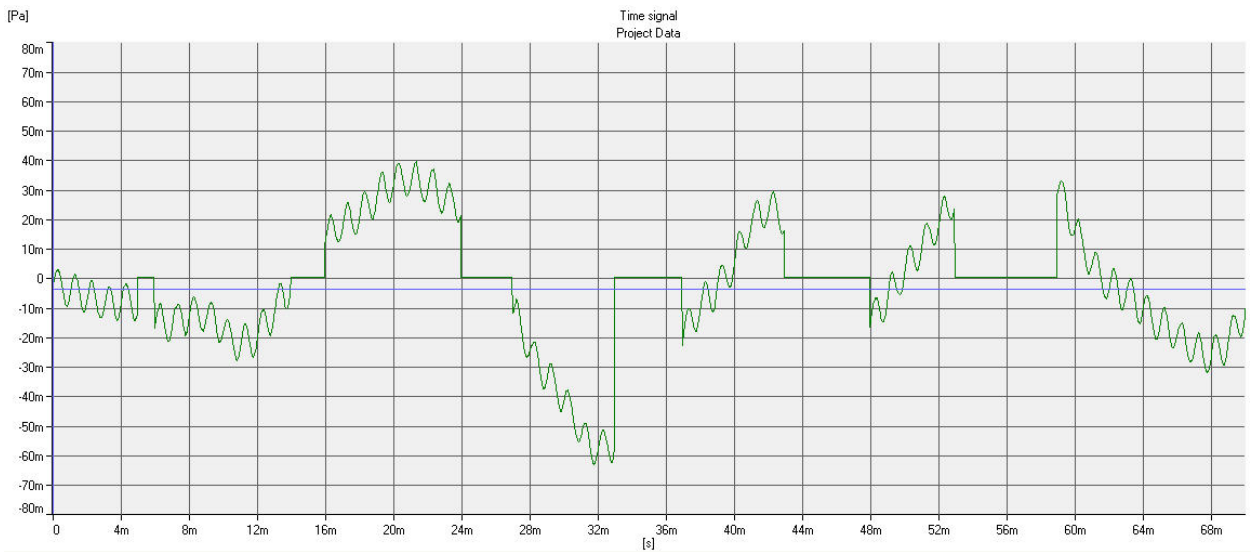


Exhibit C2 - 60 dB Steady Sinusoidal Test Signal with Gaps

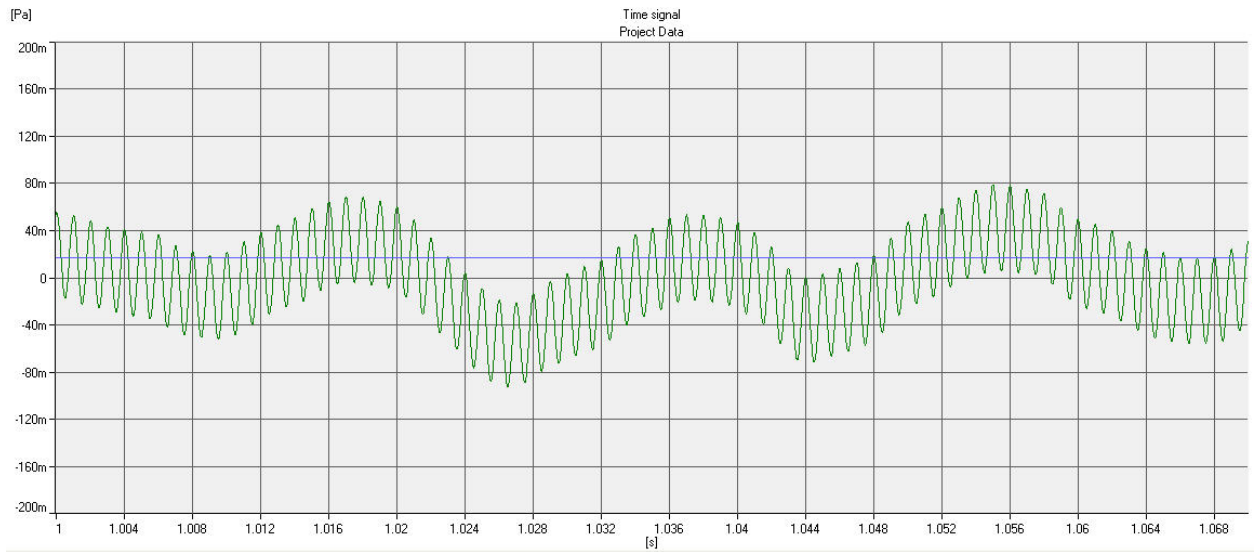


Exhibit C3 - 65 dB Steady Sinusoidal Test Signal with no Gaps

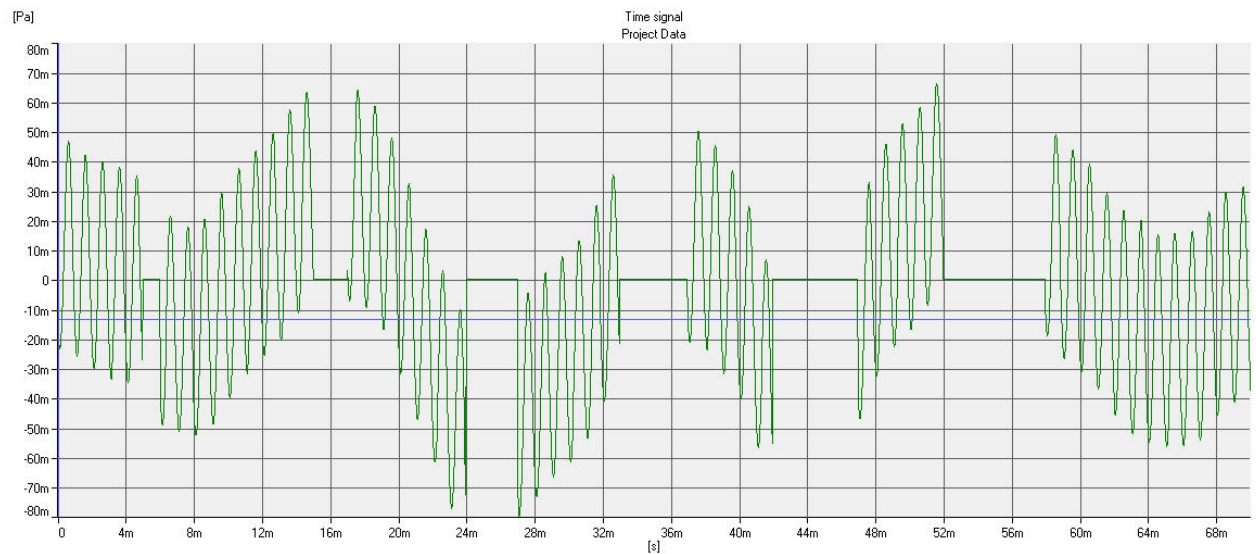


Exhibit C4 - 65 dB Steady Sinusoidal Test Signal with Gaps

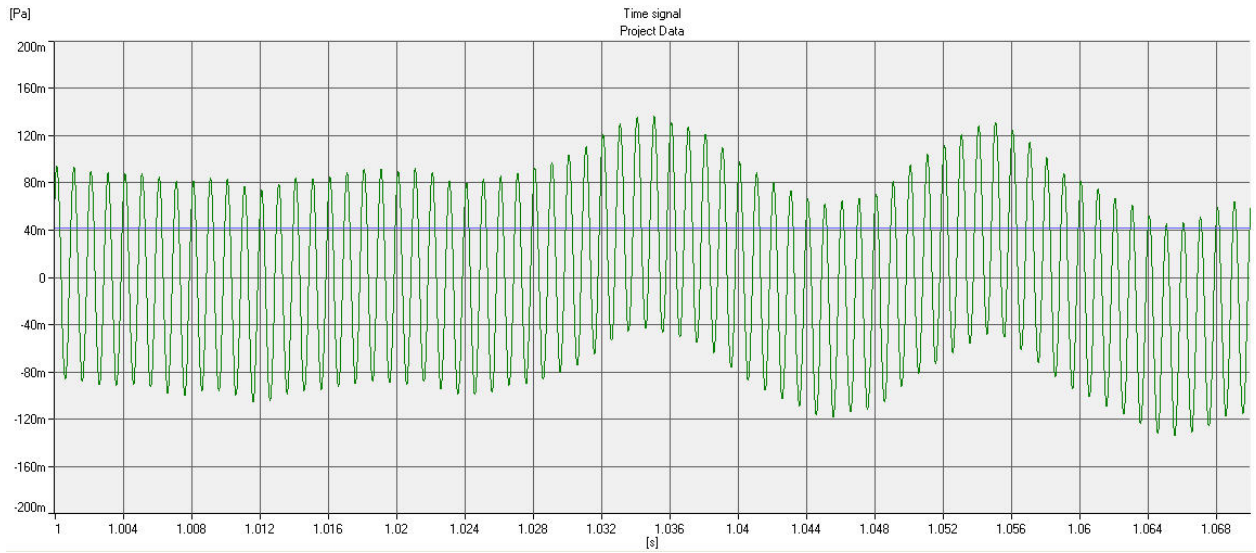


Exhibit C5 - 70 dB Steady Sinusoidal Test Signal with no Gaps

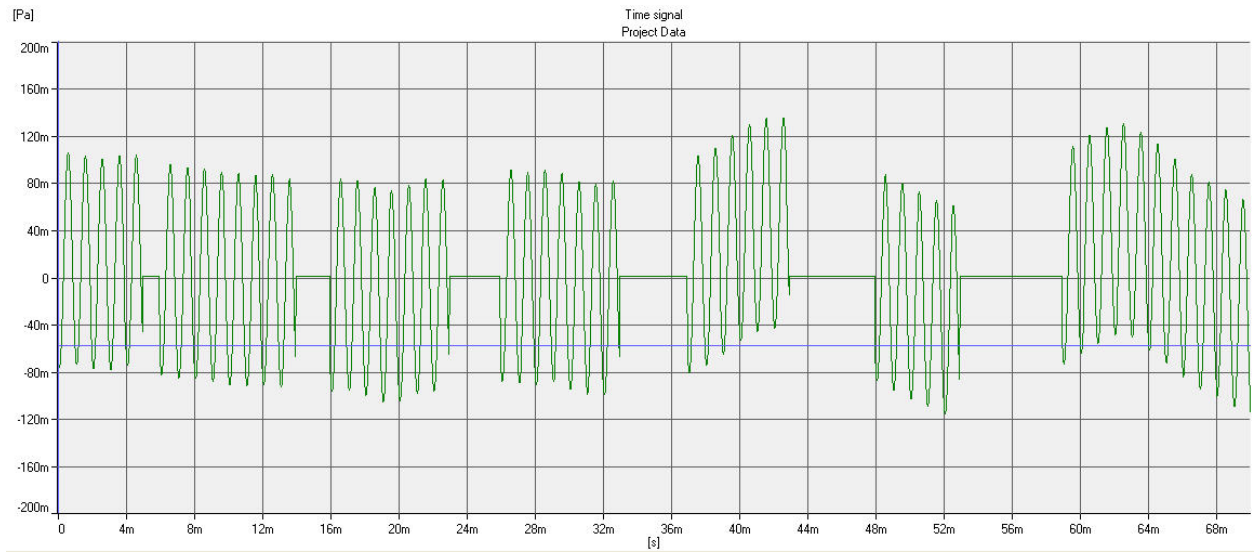


Exhibit C6 - 70 dB Steady Sinusoidal Test Signal with Gaps

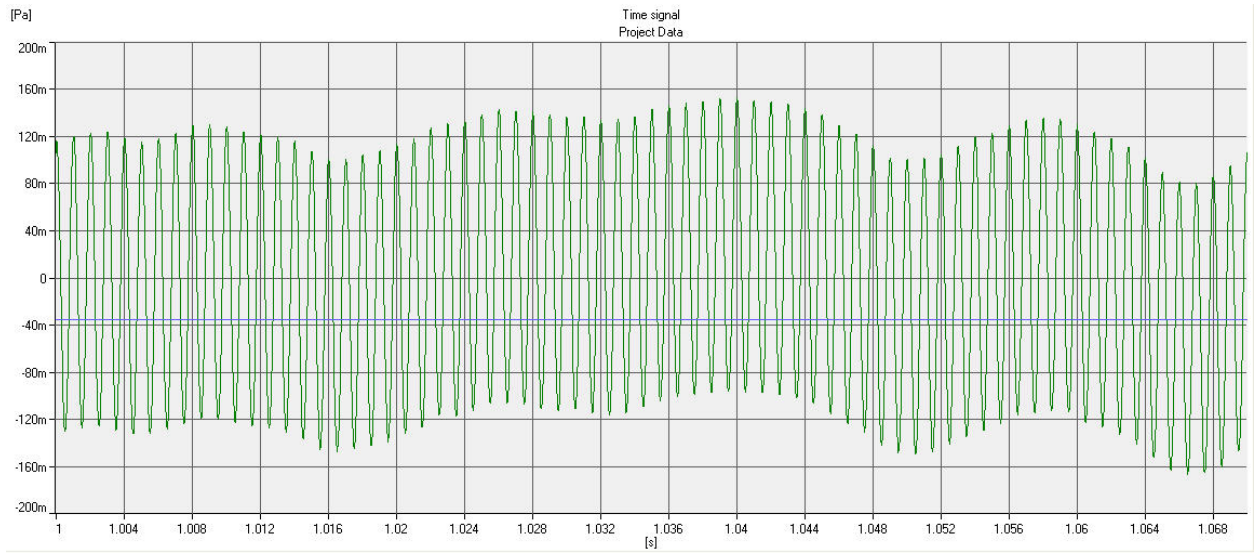


Exhibit C7 - 73 dB Steady Sinusoidal Test Signal with no Gaps

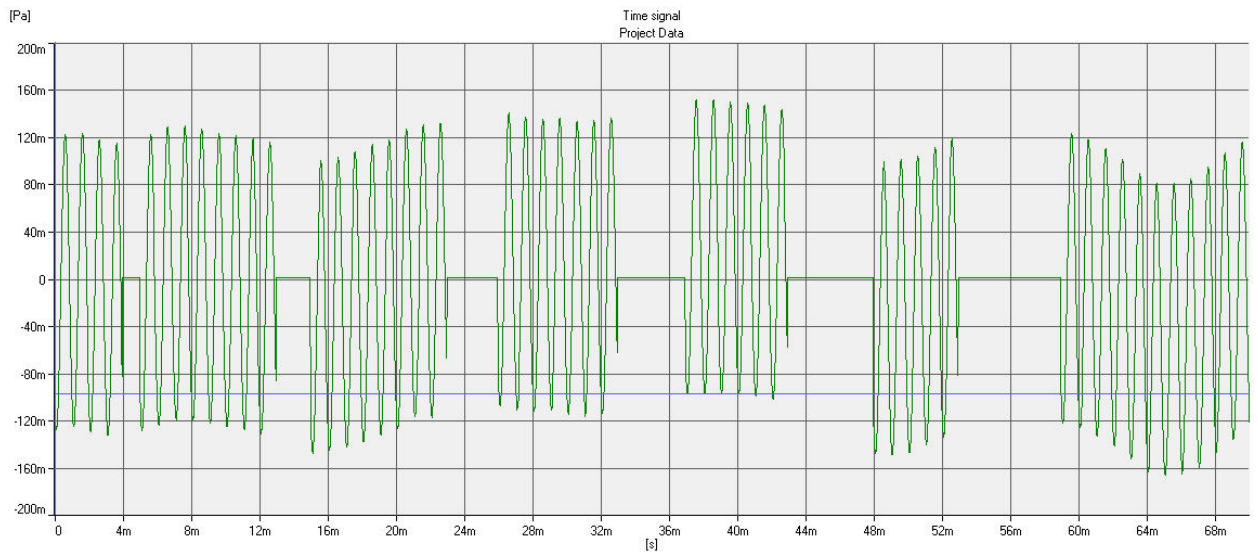


Exhibit C8 - 73 dB Steady Sinusoidal Test Signal with Gaps

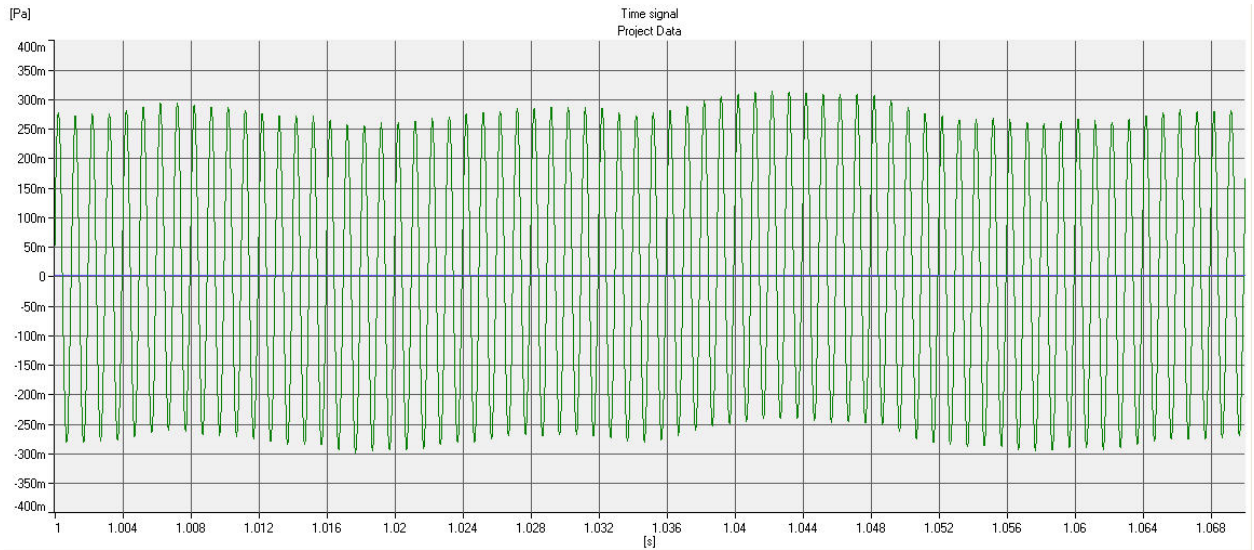


Exhibit C9 - 80 dB Steady Sinusoidal Test Signal with no Gaps

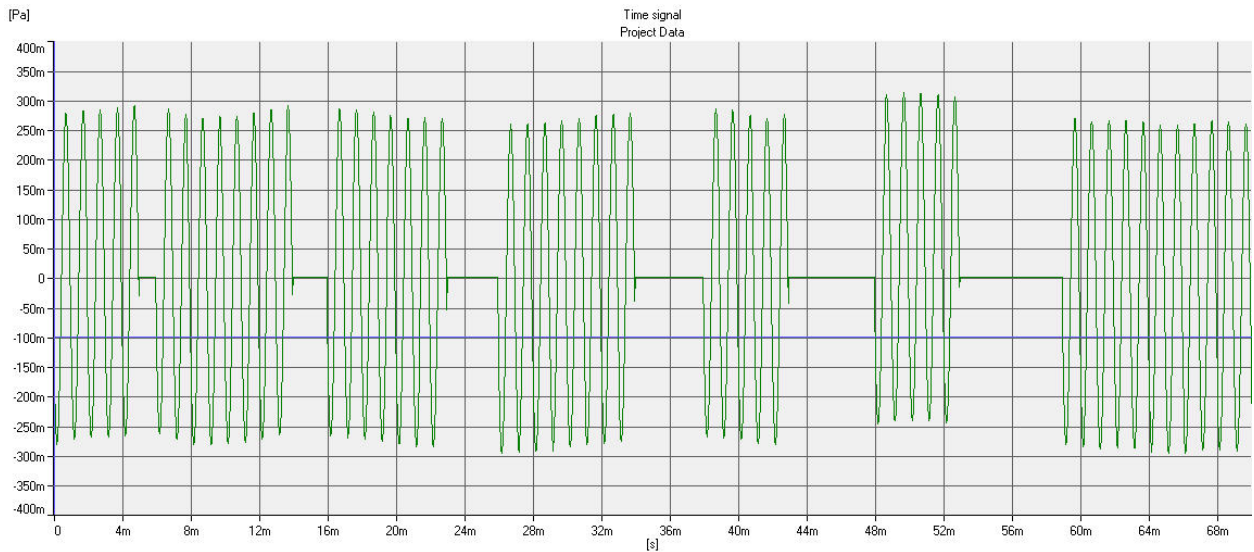


Exhibit C10 - 80 dB Steady Sinusoidal Test Signal with Gaps

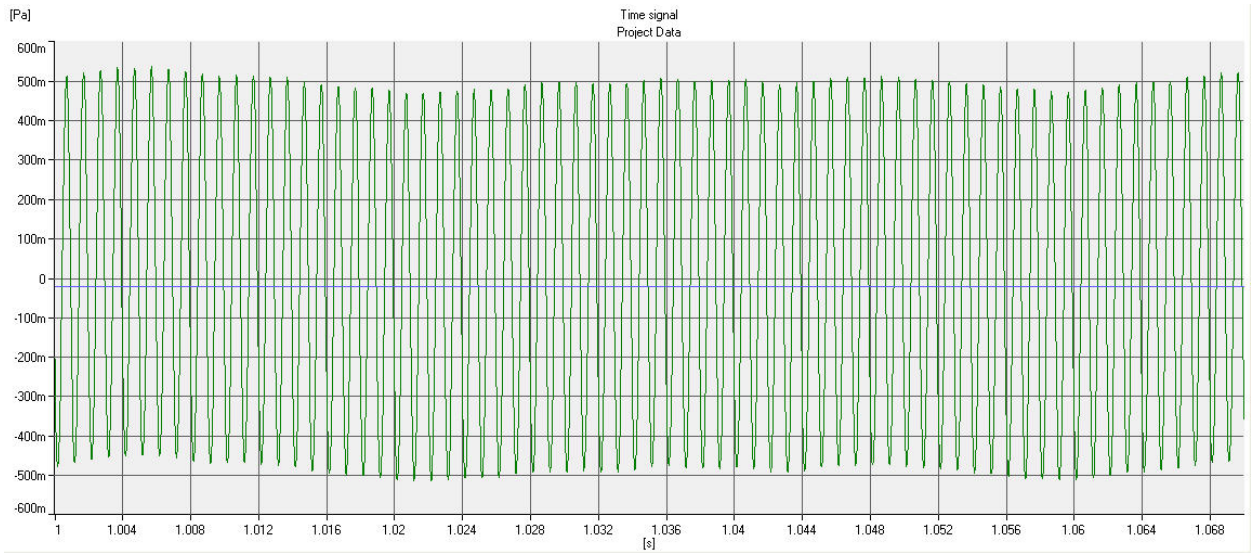


Exhibit C11 - 85 dB Steady Sinusoidal Test Signal with no Gaps

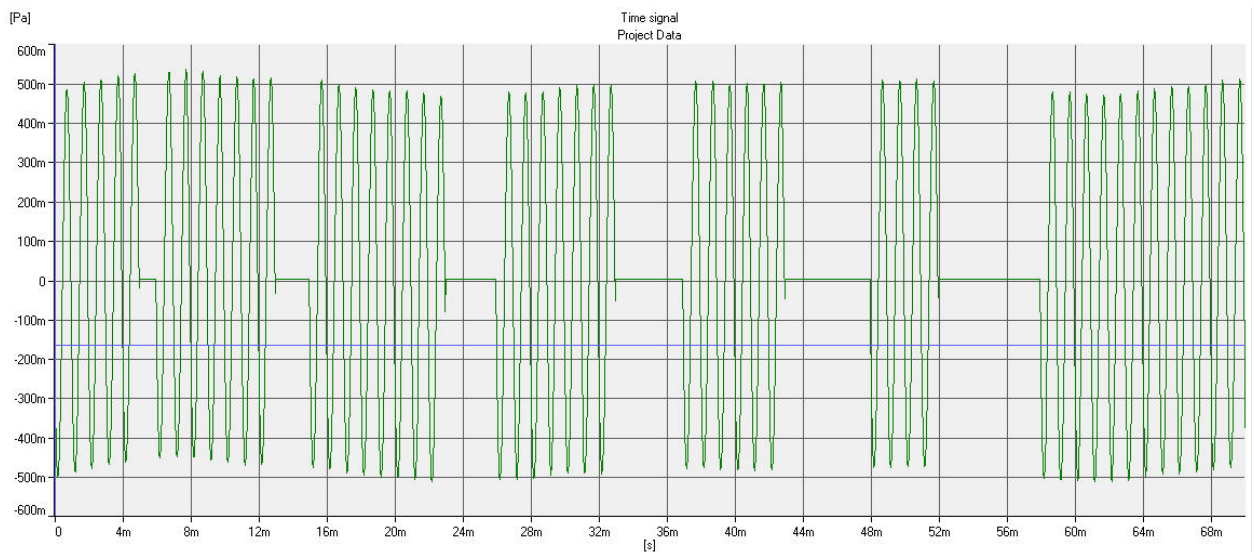


Exhibit C12 - 85 dB Steady Sinusoidal Test Signal with Gaps

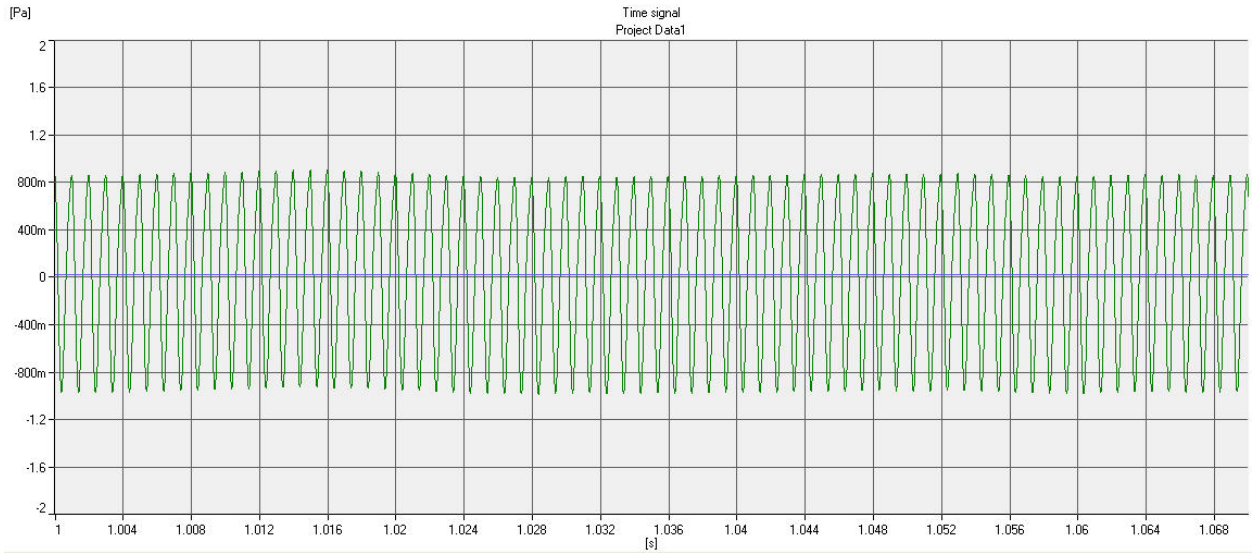


Exhibit C13 - 90 dB Steady Sinusoidal Test Signal with no Gaps

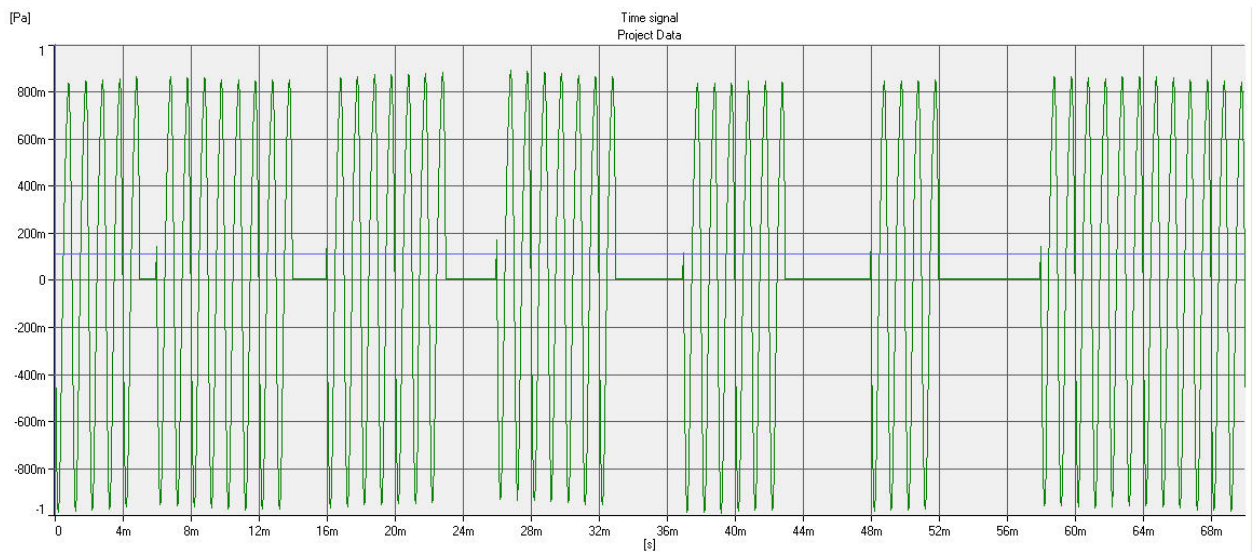


Exhibit C14 - 90 dB Steady Sinusoidal Test Signal with Gaps

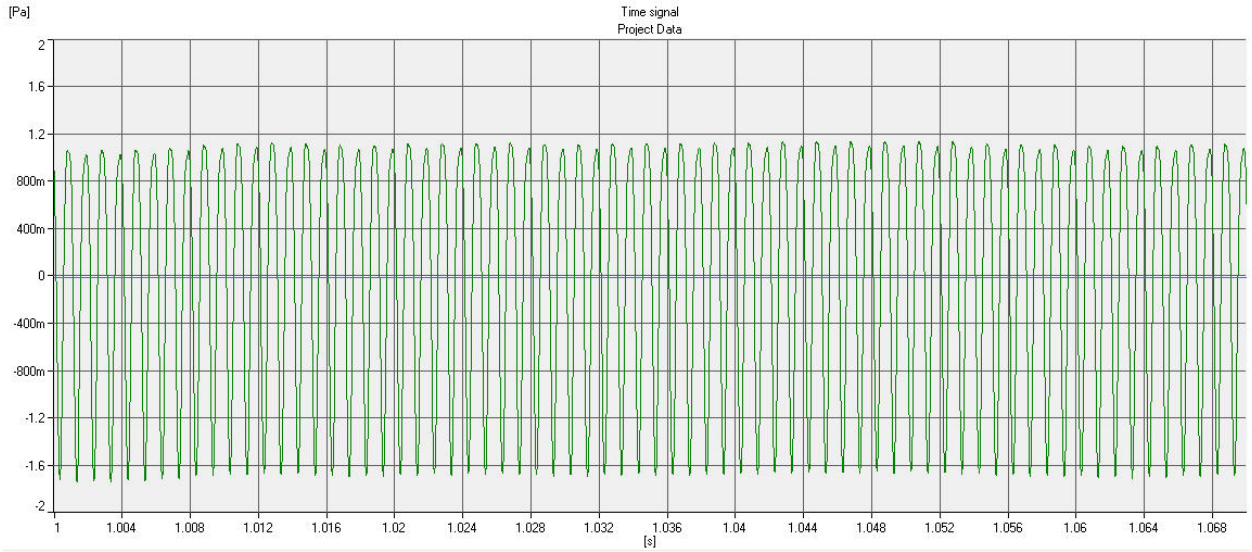


Exhibit C15 - 94 dB Steady Sinusoidal Test Signal with no Gaps

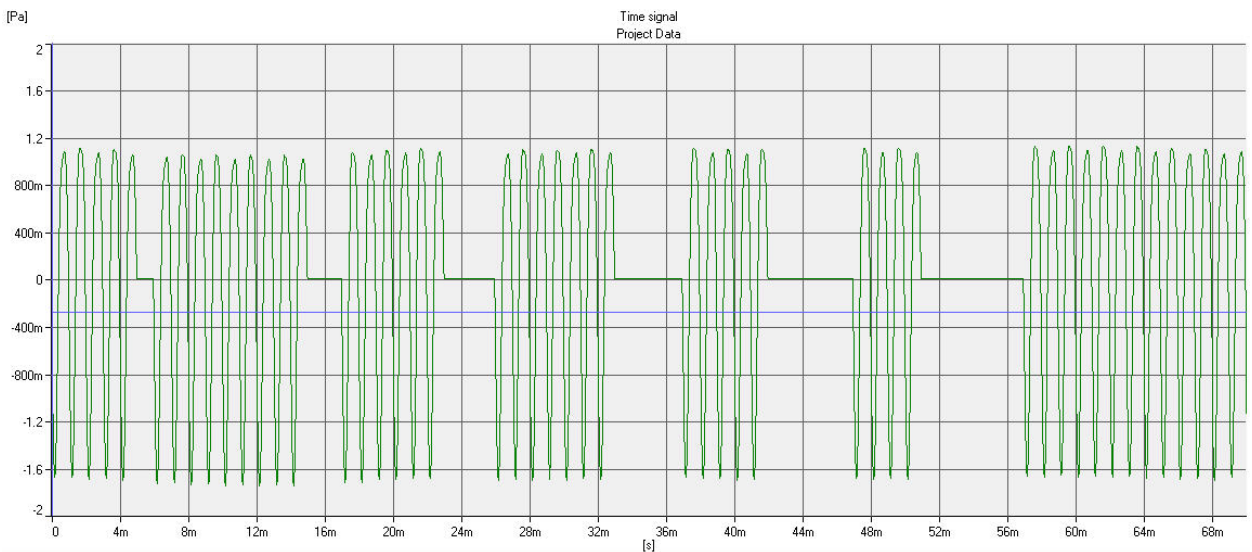


Exhibit C16 - 94 dB Steady Sinusoidal Test Signal with Gaps

Vita Auctoris

- 1978 Born in Windsor, Ontario.
- 1997 Received OSSGHD from F. J. Brennan High School.
- 2001 Received Degree of Bachelor of Applied Science from the University of Windsor, Windsor, Ontario.
- 2004 Received Degree of Master of Applied Science at the University of Windsor, Windsor, Ontario.
- 2009 Received Professional Engineer License from the Association of Professional Engineers Ontario
- 2010 Candidate for the Degree of Doctor of Philosophy at the University of Windsor, Windsor, Ontario